Università degli Studi del Piemonte Orientale

“Amedeo Avogadro”

Dipartimento di Scienze del Farmaco

Dottorato di Ricerca in Chemistry & Biology
XXXI cycle a.y. 2017-2018

Toward the development of small molecules for unconventional targets and diseases

Alessia Griglio

Supervised by Prof. Tracey Pirali

PhD program coordinator Prof. Guido Lingua

Università degli Studi del Piemonte Orientale

“Amedeo Avogadro”

Dipartimento di Scienze del Farmaco

Dottorato di Ricerca in Chemistry & Biology
XXXI cycle a.y. 2017-2018

Toward the development of small molecules for unconventional targets and diseases

Alessia Griglio

Supervised by Prof. Tracey Pirali

PhD program coordinator Prof. Guido Lingua

UNIVERSITÀ DEL PIEMONTE ORIENTALE
DOTTORATO DI RICERCA
IN CHEMISTRY & BIOLOGY

Via Duomo, 6
13100 – Vercelli (ITALY)

DECLARATION AND AUTHORISATION TO ANTIPLAGIARISM DETECTION

The undersigned Alessia Griglio student of the Chemistry & Biology Ph.D course (XXXI Cycle)

declares:

- to be aware that the University has adopted a web-based service to detect plagiarism through a software system called "Turnit.in",
- his/her Ph.D. thesis was submitted to Turnit.in scan and reasonably it resulted an original document, which correctly cites the literature;

acknowledges:

- his/her Ph.D. thesis can be verified by his/her Ph.D. tutor and/or Ph.D Coordinator in order to confirm its originality.

Date: 15/11/2018

Signature:

XY/tcs
Percorso del file

Contents

Preface 1
List of abbreviations 3
Chapter 1. Introduction 9
1.1. The Store-Operated Calcium Entry 11
1.1.1. The origin of the “capacitative calcium entry” hypothesis 11
1.1.2. Orai and STIM: the key players of the process 12
1.1.3. The pathophysiologic role of SOCE 13
1.1.4. Pharmacological modulation of SOCE over the years: an overview 15
1.1.5. References 18
1.2. Tryptophan catabolism 23
1.2.1. IDO1, IDO2 and TDO: a bird’s eye view 23
1.2.2. Targeting tryptophan metabolism for cancer immunotherapy 24
1.2.3. The landscape of IDO/TDO inhibitors 26
1.2.4. References 29
1.3. Hereditary multiple exostoses 33
1.3.1. Heparan sulfate structure and biosynthesis 33
1.3.2. Heparan sulfate functions in health and disease 34
1.3.3. Hereditary multiple exostoses: pathogenesis, clinical presentation and perspectives 36
1.3.4. References 38
Chapter 2. Outline of the thesis 39
2.1. Outline of the thesis 41
Chapter 3. Pyrtriazoles, a novel class of Store-Operated Calcium Entry modulators: discovery, biological profiling and *in vivo* proof-of-concept efficacy in SOCE-related diseases 43
3.1. Introduction 45
3.2. Aim of the work 48
3.3. Results and discussion 48
3.3.1. Chemistry 48
3.3.2. Biological evaluation 54

3.3.3. SAR study 57
3.3.4. Hydrolytic stability, metabolism and selectivity 58
3.3.5. *Ex vivo* evaluation of 23 and 31 on muscle biopsies from patients affected by TAM 60
3.3.6. *In vivo* evaluation of 31 in an animal model of acute pancreatitis 62
3.4. Conclusions 64
3.5. Experimental section 65
3.5.1. Chemistry 65
3.5.2. Appendix 89
3.6. References 91
Chapter 4. Synthesis, biological evaluation and molecular docking studies of Ugi and Passerini adducts as novel indoleamine 2,3-dioxygenase 1 inhibitors 93
4.1. Introduction 95
4.2. Aim of the work 96
4.3. Results and discussion 96
4.3.1. Chemistry 96
4.3.2. Biological evaluation 100
4.3.3. Enzymatic IDO1 inhibition and SAR study 103
4.3.4. Cellular IDO1 inhibitory activity 106
4.3.5. Molecular modeling 107
4.4. Conclusions 108
4.5. Experimental section 109
4.5.1. Chemistry 110
4.5.2. Appendix 126
4.6. References 127
Chapter 5. Benzimidazole derivatives as indoleamine 2,3-dioxygenase 1 inhibitors: *in silico*-driven synthesis, biological evaluation and structure-activity relationship stud 129
5.1. Introduction 131
5.2. Aim of the work 132
5.3. Results and discussion 132
5.3.1. Chemistry 132

5.3.2. Biological evaluation 136
5.3.3. Preliminary SAR study 139
5.4. Conclusions 141
5.5. Experimental section 142
5.5.1. Chemistry 142
5.5.2. Appendix 156
5.6. References 157
Chapter 6. Design, synthesis and evaluation of *N*-aryl-2-aminothiazole derivatives as potential leads for the treatment of hereditary multiple exostoses 159
6.1. Introduction 161
6.2. Aim of the work 162
6.3. Results and discussion 163
6.3.1. Chemistry 163
6.3.2. Biological evaluation 166
6.3.3. Physicochemical evaluation 170
6.4. Conclusions 170
6.5. Experimental section 171
6.5.1. Chemistry 171
6.5.2. X-ray crystallography 190
6.5.3. Physicochemical properties determination 195
6.5.4. Biological assay 196
6.5.5. Appendix 198
6.6. References 205
Chapter 7. Conclusions and outlook 207
7.1. Conclusions and outlook 209
Chapter 8. Publications 213

Preface

The work reported in this thesis is focused on three main projects that underpin my research activity during the PhD program. The topics discussed, despite unrelated each other, share a common feature: all of them regard unconventional and not yet drugged targets or diseases. Consequently, my effort has been the discovery of molecules of therapeutic relevance in order to satisfy current challenges in medicinal chemistry and improve the number of available candidates for addressing unmet medical need.

During the first two years and a half of my PhD I carried out my research activity at Università del Piemonte Orientale (UPO), where I primarily worked on the discovery of small molecules that targeting the Store-Operated Calcium Entry machinery and on the discovery of indoleamine 2,3-dioxygenase 1 inhibitors. Then, I moved to the University of California San Diego (UCSD) at Skaggs School of Pharmacy and Pharmaceutical Sciences where I had the opportunity to join for six months the Prof. C. Ballatore's research group, as a visiting PhD student. During this experience I worked on the development of heparan sulfate enhancers for the treatment of hereditary multiple exostoses.

Parts of this thesis have been reported in the literature and have been co-written by the author of this thesis:

- Riva, B. [#]; **Griglio, A.** [#]; Serafini, M.; Sanchez, C.; Aprile, S.; Di Paola, R.; Gugliandolo, E.; Alansary, D.; Biocotino, I.; Lim, D.; Grosa, G.; Galli, U.; Niemeyer, B.; Sorba, G.; Canonico, P.L.; Cuzzocrea, S.; Genazzani, A.; Pirali, T. Pyrtriazoles, a novel class of Store-Operated Calcium Entry modulators: discovery, biological profiling and in vivo proof-of-concept efficacy in acute pancreatitis. *J. Med. Chem.* **2018**, *61*, 9756-9783.

- **Griglio, A**.; Torre, E.; Serafini, M.; Bianchi, A.; Schmid, R.; Coda Zabetta, G.; Massarotti, A.; Sorba, G.; Pirali, T.; Fallarini, S. A multicomponent approach in the discovery of indoleamine 2,3-dioxygenase 1 inhibitors: synthesis, biological investigation and docking studies. *Bioorg. Med. Chem. Lett.* **2018**, *28*, 651-657.

List of abbreviations

2-APB	2-aminoethoxydiphenyl borate
4-PI	4-phenylimidazole
Å	angstrom
A375 cells	human melanoma cell lines
ADME	absorption, distribution, metabolism, excretion
AhR	aryl hydrocarbon receptor
Ala	alanine
Arg	arginine
ASCO	American Society of Clinical Oncology
BMP(s)	bone morphogenetic protein(s)
Boc	*tert*-butyloxycarbonyl
BTP2	bis(trifluoromethyl)pyrazole 2
$[Ca]^{2+}$	Ca^{2+} concentration
$CDCl_3$	deuterated chloroform
CD_3OD	deuterated methanol
$CHCl_3$	chloroform
CH_2Cl_2	dichloromethane
CH_3CN	acetonitrile
CHO cells	Chinese hamster ovary cells
$Cu(OAc)_2$	copper acetate
Cys	cysteine
δ	chemical shift
DCs	dendritic cells
DIPEA	*N*,*N*-diisopropylethylamine

DMAP	4-(Dimethylamino)pyridine
DMF	*N*,*N*-dimethylformamide
DMSO	dimethyl sulfoxide
DMSO-d_6	deuterated dimethyl sulfoxide
EC_{50}	half maximal effective concentration
EDCI	*N*-ethyl-*N*'-(3dimethylaminopropyl)carbodiimide hydrochloride
Et_2O	diethyl ether
EtOAc	ethyl acetate
EtOH	ethanol
ER	endoplasmic reticulum
FDA	Food and Drug Administration
FGF2	fibroblast growth factor 2
FGFs	fibroblast growth factors
Fura-2	fluorescent calcium indicator 2
GAG(s)	glycosaminoglycan(s)
GCN2	general control non-derepressible 2
GlcA	glucuronic acid
GlcNAc	*N*-acetyl-D-glucosamine
GLK1	glucokinase1
Gly	glycine
GoF	gain-of-function
Hek cells	human embryonic kidney cells
HME or MHE	hereditary multiple exostoses
HOBt	1-hydroxybenzotriazole
HPLC	high performance liquid chromatography
HRMS	high resolution mass spectrometry

HS	heparan sulfate
HSBP(s)	heparan sulfate binding protein(s)
HSPG(s)	heparan sulfate proteoglycan(s)
Hz	hertz
IC_{50}	half maximal inhibitory concentration
IDO1	indoleamine 2,3-dioxygenase 1
IDO2	indoleamine 2,3-dioxygenase 2
IdoA	iduronic acid
IFN-γ	interferon γ
IR	infrared
I_{SOC}	Store-Operated current
ITIMs	immunoreceptor tyrosine-based inhibitory motifs
J	coupling constant
KP	kynurenine pathway
Kyn	kynurenine
L-1MT	1-methyl-L-tryptophan
Leu	leucine
LMS9	mouse liver S9
L-Trp	L-tryptophan
LoF	loss-of-function
Lys	lysine
MDEB	methoxy diethylborinate
MeOH or CH_3OH	methanol
MHz	megahertz
MLM	mouse liver microsomes
MLS9	mouse liver S9 fractions
mM	millimolar
MO	multiple osteochondromas

m.p. or mp	melting point
MPO	myeloperoxidase
MTD	maximal tolerated dose
mTORC1	mammalian target of rapamycin complex 1
MTT	3-(4,5-dimethylthiazol-2-yl)-2,5diphenyltetrazolium bromide
nM	nanomolar
NMR	nuclear magnetic resonance
NADPH	nicotinamide adenine dinucleotide phosphate
NFK	*N*-formyl-L-kynurenine
OECD	Organisation for Economic Co-operation and Development
Orai	calcium release-activated calcium channel protein
Orai1	calcium release-activated calcium channel protein 1
Orai2	calcium release-activated calcium channel protein 2
Orai3	calcium release-activated calcium channel protein 3
Pd/C	palladium on carbon
$Pd(OAc)_2$	palladium acetate
$Pd(PPh_3)_2Cl_2$	bis(triphenylphosphine)palladium(II) dichloride
PE	petroleum ether
PEPT1	peptide transporter 1
PEPT2	peptide transporter 2

PG(s)	proteoglycan(s)
pH	$-\log_{10}[H^+]$
Phe	phenylalanine
pKa	$-\log_{10}Ka$
PK	pharmacokinetics
POAEE	palmitoleic acid ethyl ester
$POCl_3$	phosphorus oxychloride
PPh_3	triphenylphosphine
ppm	parts per million
Pyr(s)	pyrazole(s)
rhIDO1	recombinant human IDO1
r.t. or rt	room temperature
SAR	structure-activity relationship
satd. aq.	saturated aqueous
SCID	severe combined immunodeficiency
SEM	standard error of mean
Ser	serine
SHPs	tyrosine phosphatases
SOCE	Store-Operated Calcium Entry
SOCS 3	suppressor of cytokine signaling 3
SPR	structure property relationship
SR	sarcoplasmic reticulum
STIM	stromal interaction molecule
STIM1	stromal interaction molecule 1
STIM2	stromal interaction molecule 2
TAM	tubular aggregate myopathy
TBAF	tetra-*n*-butylammonium fluoride
***t*-BhQ**	*tert*-butylhydroquinone

TBTA	tris[(1-benzyl-*1H*-1,2,3-triazol-4-yl)methyl]amine
tBuBrettPhos	2-(Di-*tert*-butylphosphino)-2′,4′,6′-triisopropyl-3,6-dimethoxy-1,1′-biphenyl
***t*-BuOH**	*tert*-butanol
TDO	tryptophan 2,3-dioxygenase
TEA	triethylamine
TFA or CF_3COOH	trifluoroacetic acid
THF	tetrahydrofuran
TLC	thin-layer chromatography
Trityl	triphenylmethyl
Trp	tryptophan
TRPC	transient receptor potential canonical channels
TRPC3	transient receptor potential canonical 3
TRPM8	transient receptor potential melastatin 8
TRPV1	transient receptor potential vanilloid type 1
Tyr	tyrosine
UDPGA	uridine diphosphate glucuronic acid
Val	valine
VEGFs	vascular endothelial growth factors
VOCC	voltage-operated calcium channels
ν	frequency
µM	micromolar

Chapter 1

Introduction

1.1. The Store-Operated Calcium Entry

1.1.1. The origin of the "capacitative calcium entry" hypothesis

Calcium is an intracellular second messenger that plays a fundamental role in the human organism. The vast array of functions mediated by Ca^{2+} includes gene expression, cell proliferation, differentiation and apoptosis. Cytosolic $[Ca]^{2+}$ is very low (100-200 nM) compared to extracellular $[Ca]^{2+}$ (2-5 mM). Calcium is stored in intracellular organelles (endoplasmic reticulum, sarcoplasmic reticulum and Golgi apparatus) and in the presence of specific signals is able to diffuse through the cell membranes and enter the cytoplasm. Consequently, the increase of cytoplasmic $[Ca]^{2+}$ levels can be a result of two different mechanisms: the release of intracellular organelles-Ca^{2+} stores or the influx of extracellular $[Ca]^{2+}$ through $[Ca]^{2+}$ permeable ion channel located to the plasma membrane.[1]

The Store-Operated Calcium Entry (SOCE) is a unique mechanism that combines these two phenomena. Indeed, given that Ca^{2+}-pumps and exchangers are located on both plasma and intracellular organelles membranes to extrude Ca^{2+} from the cytosol, it would be expected that the intracellular organelle pool would be soon depleted. It was already back in 1986 that Jim Putney, a pioneer of the cross-talk between the endoplasmic reticulum (ER) and the plasma membrane, formalized the hypothesis that a phenomenon known as "capacitative calcium entry" would exist that allows entry through the plasma membrane to refill the depleted organelles.[2] The key experiment to exemplify capacitative calcium entry, or Store-Operated Ca^{2+} Entry (SOCE), as it is referred to nowadays, is depicted in Figure 1. In brief, emptying of the ER/SR store leads to opening of a plasma membrane channel through which Ca^{2+} can flow back in the cell. These two processes can be dissected by adding Ca^{2+} to the extracellular solution after the intracellular stores are depleted.

Nevertheless, the exact molecular mechanism behind this phenomenon has been elusive for a long time.

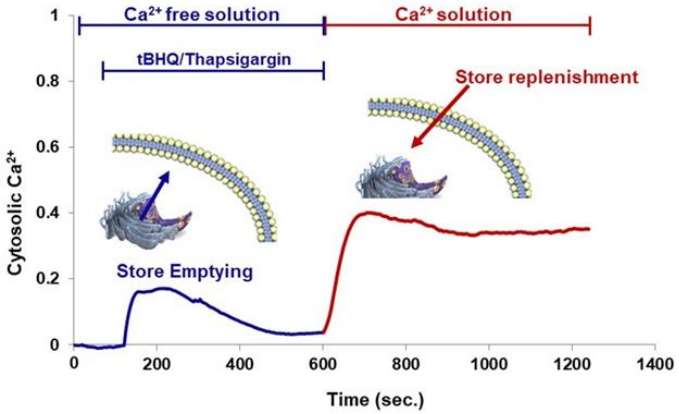

Figure 1. Representative trace of Store-Operated Calcium Entry (SOCE).

1.1.2. Orai and STIM: the key players of the process

During the last decade the principal components of SOCE were identified and consist of Ca^{2+}-sensors on the ER membrane (STIM proteins) and plasma membrane Ca^{2+}-channels (Orai channels).[3]

STIM proteins are single-span membrane proteins, highly conserved across species. Two members of the family have been described, STIM1 and STIM2, of which the former appears more expressed.[4]

Orai channels reside on the plasma membrane channel and three members of the family (Orai1, Orai2, and Orai3) have been identified, with Orai1 being the most abundant.[5] Structural information on Orai and STIM proteins is relatively scarce. Only the crystal structure of Orai1 from *Drosophila melanogaster*, which shares 73% sequence identity with human Orai1 within its transmembrane region, has been described at 3.35 Å resolution.[6]

Moreover, it is important to stress that other crucial proteins participate in the SOCE process, including the transient receptor potential canonical channels (TRPC).[7]

After the discovery of the key molecular components of SOCE mechanism intense efforts were pursued in order to understand how STIM and Orai interact each other. Now it is well known that emptying of calcium from the endoplasmic reticulum causes a conformational change in STIM. After oligomerization and translocation to the plasma membrane, STIM interacts with Orai and causes the opening of the channel with subsequent calcium influx and a current known as I_{SOC} (Figure 2).[8]

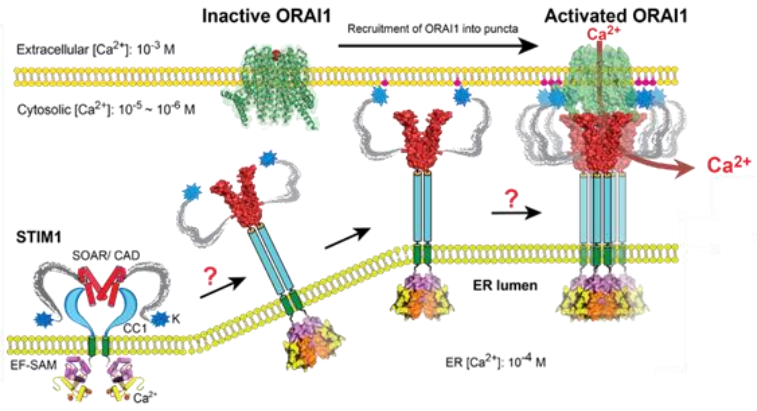

Figure 2. Scheme illustrating the mechanism and the molecular choreography of SOCE. Taken from Ma, G. *et al*. *Nat. Commun.* **2015**, *6*, 1-14.

1.1.3. The pathophysiologic role of SOCE

Capacitative calcium entry, mediating the I_{SOC} current,[9] is not solely a replenishment mechanism, but also encodes cellular signals *per se*, regulating cytokine production, gene expression, cell growth, proliferation, differentiation and even cell death. Therefore, dysfunctions in this cellular event are implicated in a vast range of human disorders including allergy,[10] thrombosis,[11] cancer,[12] inflammatory bowel disease[13] and acute pancreatitis[14], pointing to SOCE as a druggable target for developing novel therapies.

The Store-Operated Ca^{2+} Entry is an important Ca^{2+} influx pathway in many non-excitable cells (immune cells, platelets and skeletal muscles) while it plays a minor role in other cell types.

Among the several diseases characterized by a hyperactivation of SOCE mentioned before there is acute pancreatitis. This disease is caused by the intracellular premature activation of pancreatic pro-enzymes, packaged into zymogen granules inside the acinar cells. Briefly, what happens is that excessive Ca^{2+} release from intracellular stores is followed by excessive entry of Ca^{2+} from the interstitial fluid and subsequent pro-enzymes activation which results in necrosis and inflammation. Recently, Gerasimenko *et al.* have shown that the pharmacological blockage of SOCE *in vitro* protects against palmitoleic acid ethyl ester (POAEE)-induced necrosis of pancreatic acinar cells.[14] Yet, it has been reported that GSK-7975A and CM128 were protective in three separate models of chemically-induced acute pancreatitis demonstrating that the use of SOCE inhibitors could be a potential strategy to treat this disease which is life-threating and currently lacks effective treatment.[15]

Importantly, very recently, mutations in genes encoding STIM or Orai proteins have been related with the development of rare genetic disorders. In particular, loss-of-function genes mutations (LoF) cause a form of severe combined immunodeficiency (SCID). By contrast, gain-of-function mutations (GoF) are responsible for other three rare diseases: tubular aggregate myopathy (TAM), York platelet syndrome and Stormorken syndrome.[16] TAM can be re-conducted to GoF mutations in either STIM1 and Orai1, and is clinically characterized by variable combinations of myalgias, cramps and muscle stiffness.[17] York platelet syndrome sees blood dyscrasias as the main phenotype and has, so far, only been associated to STIM1 mutations.[18] Importantly, families with these disorders have been described in Italy.[19] While the mutations have different clinical presentations, quality of life of patients is always severely hampered. Lastly, Stormorken syndrome is a mixture of

the first two diseases and associates the myopathic signs described for TAM to mild bleeding tendency due to platelet dysfunction.[20] All the described disorders related to gain-of-function and loss-of-function mutations are currently without therapy and therefore a pharmacological modulation of SOCE mechanism can be a potential tool to treat these rare diseases.

1.1.4. Pharmacological modulation of SOCE over the years: an overview

As mentioned above, aberrant activity of SOCE has been associated with a wide range of human diseases including immune deficiency, neurodegeneration, muscular and cardiovascular disorders as well as cancer progression and rare genetic diseases.

Specific pharmacological manipulation of SOCE has been challenging over the years. For a long time, non-selective agents such as 2-APB,[21] CAI [22] and SKF-9636514 [23] have been the primary experimental tools to modulate SOCE. Over the years, much interest has been directed at a series of 3,5-bistrifluoromethyl pyrazole derivatives, disclosed by Abbott in 2000.[24] Specifically, BTP2 (Pyr2, YM-58483) is a potent inhibitor, but it has pleiotropic effects on both Orai and TRPC channels.[25] Subsequently, other pyrazoles, identified as Pyrs, have been reported. Among them Pyr3, a previously suggested selective inhibitor of TRPC3,[26] was shown to inhibit both TRPC3- and Orai1-mediated Ca^{2+} entry. By contrast, two compounds, Pyr6 and Pyr10, are able to distinguish to a certain degree Orai and TRPC-mediated Ca^{2+} entry.[27] While the initial interest was mainly the discovery of experimental tools to gain insights into the role played by SOCE, drug development programs in this direction are currently underway.[28] In this context, second-generation agents have been described with different characteristics in terms of mechanism of action and selectivity profile, including Synta66,[29] RO2959,[30] GSK-7975A[31] and the Amgen antibody mAb 2C1.1[32] (Figure 3).

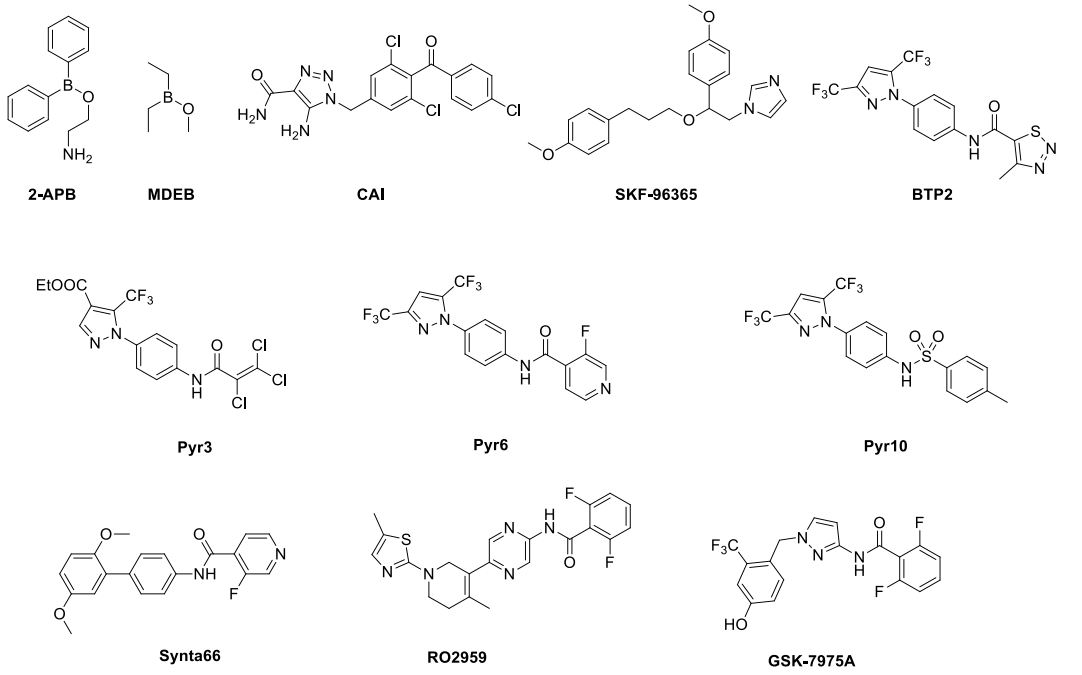

Figure 3. Chemical structures of SOCE modulators.

A growing number of small molecules have been developed so far; however, a key limitation in the search for SOCE modulators has been to identify molecules that display selectivity together with potency and lack of toxicity. As a result, to date, only few compounds have achieved human clinical trials: CM2489 and CM4620 developed by CalciMedica, RP3128 and RP4010 discovered by Rhizen Pharmaceutical and PRCL-02 from PRCL Research Inc. (Table 1). Unfortunately, none of them has reached regulatory approval and the advent of novel modulators would certainly increase the chances of clinical benefit.

Interestingly, *in silico* screening of an FDA-approved drug library has recently led to the discovery of five compounds that can potentially serve as leads for future development of SOCE inhibitors.[28d]

Name	Structure	Company	Phase	Pathology	Note
CM2489	Undisclosed	CalciMedica	1	Moderate to severe plaque psoriasis	-
CM4620	Undisclosed	CalciMedica	2	Acute pancreatitis	-
RP3128	Undisclosed	Rhizen Pharmaceuticals	I/IIa	Asthma	Terminated due to recruitment delays
RP4010	Undisclosed	Rhizen Pharmaceuticals	I/Ib	Relapsed or refractory non-Hodgkin's lymphoma	-
PRCL-02	Undisclosed	PRCL Research Inc.	1	Plaque psoriasis	-

Table 1. SOCE inhibitors in clinical trials.

Finally, it is important to stress that most of the reported inhibitors in the literature (IC_{50} < 10 μM) display an amide moiety as a common feature in their chemical structure. This suggests the hypothesis that the amide linkage could represent a pharmacophore for SOCE modulation. Moreover, as it has been speculated that the inhibitor GSK-7975A interacts with Orai1, many of the promising molecules discovered so far that possess the amide moiety may act in a similar way. Nevertheless, further investigations are necessary in order to investigate the exact mechanism of action of known SOCE inhibitors.[28d]

Besides negative modulators, SOCE potentiating agents have been reported. 2-APB is a well-known, though not so selective, effector of SOCE, but it may either enhance or inhibit the current depending on concentrations,[33] while MDEB, another borinate compound, has only a potentiating ability on I_{SOC} (Figure 3).[34]

In summary, none of the SOCE modulators available today has widely exceeded the selectivity issue and has been approved for clinical purposes; consequently, the quest for new and selective agents remains mandatory.

1.1.5. References

1. Prakriya, M.; Lewis, R.S. Store-operated calcium channels. *Physiol. Rev.* **2015**, *95*, 1383-1436.
2. Putney, J. W. A model for receptor-regulated calcium entry. *Cell Calcium.* **1986**, *7*, 1-12.
3. a. Lewis, R.S. The molecular choreography of a store-operated calcium channel. *Nature.* **2007**, *446*, 284-287.
   b. Prakriya, M. The molecular physiology of CRAC channels. *Immunol. Rev.* **2009**, *231*, 88-98.
   c. Soboloff, J.; Rothberg, B.S.; Madesh, M.; Gill, D.L. STIM proteins: dynamic calcium signal transducers. *Nat. Rev. Molecular Cell Biol.* **2012**, *13*, 549-565.
4. a. Liou, J.; Kim, M.L.; Heo, W.D.; Jones, J.T.; Myers, J.W.; Ferrel, J.E.; Meyer, T. STIM is a Ca^{2+} sensor essential for Ca^{2+}-store-depletion-triggered Ca^{2+} influx. *Curr. Biol.* **2005**, *15*, 1235–1241.
   b. Roos, J.; Di Gregorio, P.; Yeromin, A.V.; Ohlsen,K.; Lioudyno, M.; Zhang, S.; Safrina, O.; Kozak, J.A.; Wagner, S.L.; Cahalan, M.D.; Veliçelebi, G.; Stauderman, K.A. STIM1, an essential and conserved component of store-operated Ca^{2+} channel function. *J. Cell Biol.* **2005**, *169*, 435–445.
5. a. Vig, M.; Peinelt, C.; Beck, A.; Koomoa, D.L.; Rabah, D.; Koblan-Huberson, M.; Kraft, S.; Turner, H.; Fleig, A.; Penner, R.; Kinet, J.P. CRACM1 is a plasma membrane protein essential for store-operated Ca^{2+} entry. *Science.* **2006**, *312*, 1220–1223.
   b. Zhang, S.L.; Yeromin, A.V.; Zhang, X.H.-F.; Yu, Y.; Safrina, O.; Penna, A.; Roos, J.; Stauderman, K.A.; Cahalan, M.D. Genome-wide RNAi screen of Ca^{2+} influx identifies genes that regulate Ca^{2+} release-activated Ca^{2+} channel activity. *Proc. Natl Acad. Sci. USA.* **2006,** *103*, 9357–9362.
6. Hou, X.; Pedi, L.; Diver, M.M.; Long, S.B. Crystal structure of the calcium release–activated calcium channel Orai, *Nature*. **2012**, *338*, 1308-1313.
7. a. Cheng K.T.; Ong, H.L.; Liu, X.; Ambudkar, I.S. Contribution and regulation of TRPC channels in store-operated Ca^{2+} entry. *Curr. Top Membr.* **2013**, *71*, 149-179.
   b. Cheng, K.T.; Ong, H.L.; Liu, X.; Ambudkar, I.S.; Ong, H.L.; Amudkar, I.S. Molecular determinants of TRPC1 regulation within ER-PM junctions. *Cell Calcium*. **2015**, *58*, 376-386.
8. Ma, G.; Wei, M.; He, L.; Liu, C.; Wu, B.; Zhang, S.L.; Jing, J.; Liang, X.; Senes, A.; Tan, P.; Li, S.; Sun, A.; Bi, Y.; Zhong, L.; Si, H.; Shen, H.; Y.; Li, M.; Lee, M.S.; Zhou, W.; Wang, J.; Wang, Y.; Zhou, Y. Inside-out Ca^{2+} signalling prompted by STIM1 conformational switch. *Nat. Commun.* **2015**, *6*, 7826-7840.
9. Hoth, M.; Penner, R. Depletion of intracellular calcium stores activates a calcium current in mast cells. *Nature*. **1992**, *355*, 353-356.

10. Peters-Golden, M.; Gleason, M.M.; Togias, A. Cysteinyl leukotrienes: multi-factorial mediators in allergic rhinitis. *Clin. Exp. Allergy.* **2006**, *36*, 689-703.
11. Braun, A.; Varga-Szabo, D.; Kleinschnitz, C.; Pleines, I.; Bender, M.; Austinat, M.; Bösl, M.; Stoll, G.; Nieswandt, B. Orai1 (CRACM1) is the platelet SOC channel essential for pathological thrombus formation. *Blood.* **2008,** *113*, 2056-2063.
12. a. Yang, S.; Zhang, J. J.; Huang, X-Y. Orai1 and STIM1 are critical for breast tumor cell migration and metastasis. *Cancer Cell.* **2016**, *138*, 2067-2077,
b. Xie, J.; Pan, H.; Yao, J.; Zhou, Y.; Han, W. SOCE and cancer: recent progress and new perspectives. *Int. J. Cancer.* **2016**, *138*, 2067-2077.
13. Feske, S. Calcium signalling in lymphocyte activation and disease. *Nat. Rev. Immunol.* **2007**, *7*, 690-702.
14. Gerasimenko, J. V.; Gryshchenko, O.; Ferdek, P. E.; Stapleton, E.; Hébert, T. O.; Bychkova, S.; Peng, S.; Begg, M.; Gerasimenko, O. V.; Petersen, O. H. Ca^{2+} release-activated Ca^{2+} channel blockade as a potential tool in antipancreatitis therapy. *Proc. Natl. Acad. Sci. USA.* **2013**, *110*, 13186-13191.
15. Wen, L.; Voronina, S.; Javed, M. A.; Awais, M.; Szatmary, P.; Latawiec, D.; Chvanov, M.; Collier, D.; Huang, W.; Barrett, J.; Begg, M.; Stauderman, K.; Roos, J.; Grigoryev, S.; Ramos, S.; Rogers, E.; Whitten, J. Velicelebi, G.; Dunn, M.; Tepikin, A.V.; Criddle, D.N.; Sutton, R. Inhibitors of ORAI1 prevent cytosolic calcium-associated injury of human pancreatic acinar cells and acute pancreatitis in 3 mouse models. *Gastroenterology.* **2015**, *149*, 481-492.
16. Lacruz, R.S.; Feske, S. Diseases caused by mutations in Orai1 and STIM1. *N. Y. Acad. Sci.* **2015,** *1356*, 45-79.
17. V.; Wiley, G.; Kousi, M.; Ong, E-C.; Lehmann, T.; Nicholl, D.J.; Suri, M.; Shahrizaila, N.; Katsanis, N.; Gaffney, P.M.; Wierenga, K.J., Tsiokasa, L. Activating mutations in STIM1 and Orai1 cause overlapping syndromes of tubular myopathy and congenital miosis. *Procl. Natl. Acad. Sci USA.* **2014**, *111*, 4197-4202.
b. Bohm, J.; Chevessier, F.; Maues De Paula, A.; Koch, C.; Attarian, S.; Feger, C.; Hantai, D.; Laforet, P.; Ghorab, K.; Vallat, J.-M.; Fardeau, M.; Figarella-Branger, D.; Pouget, J.; Romero, N.B.; Koch, M.; Ebel, C.; Levy, N.; Krahn, M.; Eymard, B.; Bartoli, M.; Laporte, J. Constitutive activation of the calcium sensor STIM1 causes tubular-aggregate myopathy. *Am. J. Hum. Genet.* **2013**, *92*, 271-278.
c. Endo, J.; Noguchi, S.; Hara, Y.; Hayashi, Y.K.; Motomura, K.; Miyatake, S.; Murakami, N.; Tanaka, S.; Yamashita, S.; Kizu, R.; Bamba, M.; Goto, Y.; Matsumoto, N.; Nonaka, I.; Nishino, I. Dominant mutations in ORAI1 cause tubular aggregate myopathy with hypocalcemia via constitutive activation of store-operated Ca^{2+} channels. *Human Molecular Genetics*, **2015**, *4*, 637-648.
18. Markello, T.; Chen, D.; Kwan, J.Y.; Horkayne-Szakaly, I.; Morrison, A.; Simakova, O.; Maric, I.; Lozier, J.; Cullinane, A.R.; Kilo,T.; Meister, L.;

Pakzad, K.; Bone, W.; Chainani, S.; Lee, E.; Links, A.; Boerkoel, C.; Fischer, R.; Toro, C.; White, J.G.; Gahl, W.A.; Gunay-Aygun, M. York platelet syndrome is a CRAC channelopathy due to gain-of-function mutations in STIM1. *Mol. Genet. Metab*. **2015**, *114*, 474-482.

19. Tasca, G.; D'amico, A.; Monforte, M.; Nadaj-Pakleza, A.; Vialle, M.; Fattori, F.; Vissing, J.; Ricci, E.; Bertini, E. Muscle imaging in patients with tubular aggregate myopathy caused by mutations in STIM1. *Neuromuscul. Disord***. 2015**, *25*, 898-903.
20. a. Stormorken, H.; Sjaastad, O.; Langslet, A.; Sulg, I.; Egge, K.; Diderichsen, J. A new syndrome: trombocytopathia, muscle fatigue. Asplenia, miosis, migraine, dyslexia and ichthyosis. *Clin. Genet.* **1985,** *28*,367-374.
    b. Misceo, D.; Holmgren, A.; Louch, W.E.; Holme, P.A.; Mizobuchi, M.; Morales, R.J.; De Paula, A.M.; Stray-Pedersen, A.; Lyle, R.; Dalhus, B.; Christensen, J.; Stormorken, H.; Tjønnfjord, G.E.; Frengen, E. A dominant STIM1 mutation causes Stormorken syndrome, *Hum. Mutat.* **2014**, *35*, 556-564.
21. a. Maruyama, T.; Toshiya, K.; Shinjii, N.; Tomio, K.; Katsuhiko, M. 2APB, 2-aminoethoxydiphenyl borate, a membrane-penetrable modulator of Ins (1,4,5)P_3-induced Ca^{2+} release. *J. Biochem.* **1997**, *122*, 498-505.
    b. Prakriya, M.; Lewis, R. S. Potentiation and Inhibition of Ca^{2+} Channels by 2-aminoethyldiphenyl borate (2-APB) occurs independently of IP_3 receptors. *J. Physiol*. **2001**, *536*, 3-19.
    c. Hu, H-Z.; Gu, Q.; Wang, C.; Colton, C.K.; Tang, J.; Kinoshita-Kawada, M.; Lee, L-Y.; Wood, J.D.; Zhu, M.X. 2-aminoethyldiphenyl borate is a common activator of TRPV1, TRPV2, and TRPV3. *J. Biol. Chem*. **2004**, *279*, 35741-35748.
    d. Chokshi, R.; Fruasaha, P.; Kozak, J. A. 2-aminoethyl diphenyl borinate (2-APB) inhibits TRPM7 channels through an intracellular acidification mechanism. *Channels.* **2012**, *6*, 362-369.
22. Kohn, E.C.; Liotta, L.A. L651582: A novel antiproliferative and antimetastasis agent. *J. Natl. Cancer Inst.* **1990**, *82*, 60-64.
23. a. Merrit, J.E.; Armstrong, W.P.; Benham, C.D.; Hallam, T.J.; Jacob, R.; Jaxa-Chamiec, A.; Leigh, B.K.; McCarthy, S.A.; Moores, K.E.; Rink., T.J. SKF-96365, a novel inhibitor of receptor-mediated calcium entry. *J. Biochem*. **1990**, *271*, 515-522.
    b. Singh, A.; Hildebrand, M.E.; Garcia, E.; Snutch, T.P. The transient receptor potential channel antagonist SKF96365 is a potent blocker of low-voltage T-type calcium channels. *Br. J. Pharmacol.* **2010**, *160*, 1464-1475.
24. Djuric, S.W.; BaMaung, N.Y.; Basha, A.; Liu, H.; Luly, J.R.; Madar, D.J.; Scioyyi, R.J.; Tu, N.P.; Wagenaar, F.L.; Zhoun, X.; Ballaron, S.; Bauch, J.; Chen, Y-W.; Chiou, X.G.; Fey, T.; Gauvin, D.; Gubbins, E.; Hsieh, G.C.; Marsh, K.C.; Mollison, K.W.; Pong, M.; Shaughnessy, T.K.; Sheets, M.P.; Smith, M.; Trevillyan, J.M.; Warrior, U.; Wegner, C.D.; Carter, G.W. 3,5-

bis(trifluoromethyl)pyrazoles: a novel class of NFAT transcription factor regulator. *J. Med. Chem.* **2000**, *43*, 2975-2981.

25. Takezawa, R.; Cheng, H.; Beck, A.; Ishikawa, J.; Launay, P.; Kubota, H.; Kinet, J.P.; Fleig, A., Yamada, T.; Penner, R. A pyrazole derivative potently inhibits lymphocyte Ca^{2+} influx and cytokine production by facilitating transient receptor potential melastatin 4 channel activity. *Mol. Pharmacol*. **2006**, *69*, 1413-1420.
26. Kiyonaka, S.; Kato, K.; Nishida, M.; Mio, K.; Numaga, T.; Sawaguchi, Y.; Yoshida, T.; Wakamori, M.; Mori, E.; Numata, M.; Ishii, M.; Takemoto, H.; Ojida, A.; Watanabe, K.; Uemura, A.; Kurose, H.; Morii, T.; Kobayashi, T.; Sato, Y.; Sato, C.; Hamachi, I.; Moria, Y. Selective and direct inhibition of TRPC3 channels underlies biological activities of a pyrazole compound. *Proc. Natl. Acad. Sci. USA.* **2009**, *106*, 5400-5405.
27. Schleifer, H.; Doleschal, B.; Lichtenegger, M.; Oppenrieder, R.; Derler, I.; Frischauf, I.; Glasnov, T. N.; Kappe, C. O.; Romanin, C.; Groschner, K. Novel pyrazole compounds for pharmacological discrimination between receptor-operated and store-operated Ca^{2+} entry pathways. *Br. J. Pharmacol.* **2012**, *167*, 1712-1722.
28. a. Sweeney, Z. K.; Minatti, A.; Button, D. C.; Patrick, S. Ca^{2+} release-activated Ca^{2+} channel inhibitors. *Pharm. Pat. Anal*. **2009**, *3*, 171-182.
    b. Pevarello, P.; Cainarca, S.; Liberati, C.; Tarroni, P.; Piscitelli, F.; Severi, E. Small-molecule inhibitors of Store-Operated Calcium Entry. *Chem. Med. Chem.* **2014**, *4*, 706-718.
    c. Tia, C.; Du, L.; Zhou, Y.; Li, M. Store-operated CRAC channel inhibitors: opportunities and challenges. *Future Med. Chem*. **2016**, *8*, 817-832.
    d. Stauderman, K.A. CRAC channels as targets for drug discovery and development. *Cell Calcium*. **2018**, *74*, 147-159.
29. Di Sabatino, A.; Rovedatti, L.; Kaur, R.; Spencer, J.P.; Brown, J.T.; Morisset, V.D.; Biancheri, P.; Leakey, N.A.B.; Wilde, J.I.; Scott, L. Corazza, G.R.; Lee, K.; Sengupta, N.; Knowles, C.H.; Gunthorpe, M.J.; McLean, P.G.; MacDonald, T.T.; Kruidenier, L. Targeting gut T cell Ca^{2+} release-activated Ca^{2+} channels inhibits T cell cytokine production and T-Box transcription factor T-Bet in inflammatory bowel disease. *J. Immunol*. **2009**, *183*, 3454-3462.
30. Chen, G.; Panicker, S.; Lau, K.Y.; Apparsundaram, S.; Patel, V. A.; Chen, S. L.; Soto, R.; Jung, J. K. C.; Ravindran, P.; Okuhara, D,; Bohnertd, G.; Che, Q.; Rao, P.E.; Allard, J.D.; Badi, L.; Bitter, H-M.; Nunn, P.A.; Narula, S.K.; DeMartino, J.A. Characterization of a novel CRAC inhibitor that potently blocks human T cell activation and effector functions. *Mol. Immunol*. **2013**, *54*, 355-367.
31. Derler, I.; Schindl, R.; Fritsch, R.; Heftberger, P.; Riedl, M.C.; Begg, M.; House, D.; Romanin, C. The action of selective CRAC channel blockers is affected by the Orai pore geometry. *Cell Calcium*. **2013**, *53*, 139-151.

32. Lin, F.F.; Elliot, R.; Colombero A.; Gaida, K.; Kelley, L.; Moksa, A.; HO, S.Y.; Bykova, E.; Wong, M.; Rathanaswami, P.; Hu, S.; Sullivan, J.K.; Nguyen, H.Q.; MvBride, H.J. Generation and characterization of fully human monoclonal antibodies against human Orai1 for autoimmune disease. J. *Pharmacol. Exp. Ther.* **2013**, *345*, 225-238.
33. Diver, J.M.; Sage, S.O.; Rosado, J.A. The inositol trisphosphate receptor antagonist 2-aminoethoxydiphenylborate (2-APB) blocks Ca^{2+} entry channels in human patelets: cautions for its use in studying Ca^{2+} influx. *Cell Calcium.* **2001**, *30*, 323-329.
34. Djillani, A.; Doignon, I.; Luyten, T.; Lamkhioued, B.; Gangloff, S. C.; Parys, J. B.; Nüße, O.; Chomienne, C.; Dellis, O. Potentiation of the Store-Operated Calcium Entry (SOCE) induces phytohemagglutinin-activated Jurkat T cell apoptosis. *Cell Calcium*. **2015**, *58*, 171-85.

1.2. Tryptophan catabolism

1.2.1. IDO1, IDO2 and TDO: a bird's eye view

Tryptophan (Trp) is an essential amino acid that plays an important role in protein synthesis and in neurotransmitter serotonin and neurohormone melatonin biosynthesis. The major route for Trp catabolism in humans is represented by the kynurenine pathway (KP). In this context, the first and rate-limiting step consists of the oxidation of L-tryptophan (L-Trp) to *N*-formyl-L-kynurenine (NFK) which is catalysed by three different enzymes belonging to dioxygenases family: indoleamine 2,3-dioxygenase 1 (IDO1), indoleamine 2,3-dioxygenase 2 (IDO2) and tryptophan 2,3-dioxygenase (TDO).

IDO1, the well-known member, is an intracellular heme-containing enzyme expressed in a vast array of tissues including brain, placenta, stomach, liver, gut, lung and cells within the immune system. It recognizes a broad range of substrates (i.e. L-tryptophan, D-tryptophan, tryptamine, melatonin, serotonin) and it is functionally active as monomer. [1]

IDO2 has been recently discovered and share 43% homology at the amino acid level with its isoform IDO1. Nevertheless, its physiological role remains unclear.[1-2]

TDO functions as an homotetramer and it is predominately expressed in the liver although it has also been found in the brain. Its functions include the regulation of systemic Trp levels as well as liver Kyn levels. In contrast to IDO1, TDO is enantiomer specific, indeed it only catalyzes L-Trp.[3]

1.2.2. Targeting tryptophan metabolism for cancer immunotherapy

The tryptophan to kynurenine catabolic pathway plays a pivotal role in both innate and adaptive immunity control. IDO's immunoregulatory effects are mainly mediated by dendritic cells (DCs) and involve both Trp deprivation and Kyn production, which act on $IDO1^+$ DCs, thus rendering an otherwise stimulatory DCs capable of regulatory effects, as well as on T lymphocytes. As a result, $IDO1^+$ DCs mediate multiple effects on T cells, including inhibition of proliferation, apoptosis, and differentiation towards a regulatory phenotype.[4] More in detail, Trp deprivation promotes activation of the kinase general control non-derepressible 2 (GCN2) which causes inhibition of T-effector cells proliferation. Moreover, reduction of Trp levels leads to blockage of master amino acid-sensing kinase (GLK1) and suppression of mammalian target of rapamycin complex 1 (mTORC1) with subsequent increase of T-effector cells apoptosis. On the other side, increased kynurenines lead to aryl hydrocarbon receptor (AhR) activation, a transcription factor involved in cancer progression, and increase in immunosuppressive T-regulatory cells (Figure 1).[5]

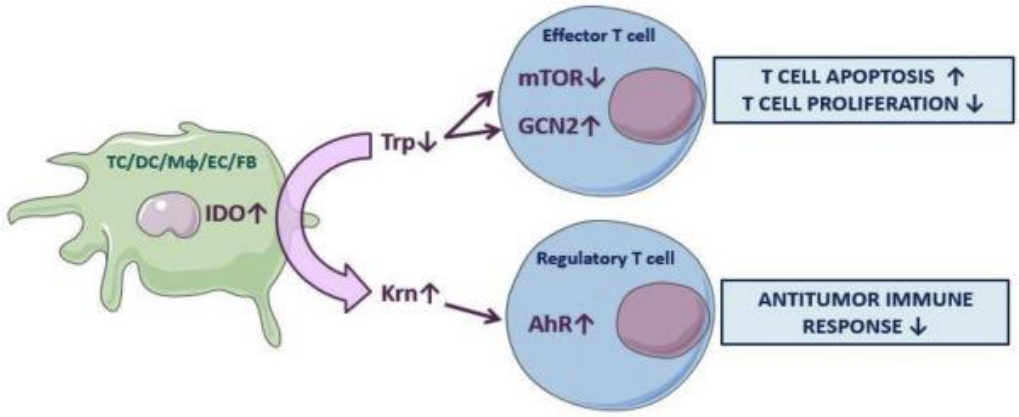

Figure 1. Schematic representation of the mechanisms by which IDO1 mediates immune escape in tumour microenvironment. Taken from Brochez, L. *et al. Eur. J. Cancer.* **2017**, *76*, 167-182.

Actually, IDO1 does not merely degrade Trp and produce Kyn, but it also acts as a signal-transducing molecule.[6] In particular, its signalling function relies on the presence of two immunoreceptor tyrosine-based inhibitory motifs (ITIMs). When phosphorylated, ITIMs act as docking sites for distinct molecular partners, that can either prolong IDO1's half-life, promoting long-term immunoregulatory effects (tyrosine phosphatases, SHPs), or reduce IDO1's half-life (SOCS3 protein), favouring inflammatory responses.[7]

There is a growing body of evidence supporting that IDO1 plays a crucial role in pathological immune escape.[3,8] Notably, in cancer, IDO1 contributes to immunosuppression in tumour microenvironment and its overexpression is correlated with tumour progression, invasiveness and reduced overall survival.[3] Indeed, IDO1 has been shown to be highly expressed in tumours and *Ido1* knock-out tumour-bearing mice, compared with wild type mice, have lower levels of spontaneous metastasis, smaller tumour volume and increased survival time. Most importantly, high expression of IDO1 is associated with poor prognosis in various human tumours.[9] It has been largely demonstrated in animal models that IDO1 inhibition can break an acquired immune tolerance, significantly increasing the immunological responses induced by various chemotherapeutic drugs and immunotherapeutic agents.[10]

Additionally, scientific evidences that demonstrate TDO overexpression in many cancers (i.e. melanomas, brain and breast tumours) have been recently emerging. Indeed, *in vitro* and *in vivo* studies underline the role played by TDO in promoting tumour cell survival and in immune escape mechanism. Most significantly, tumour cells can catabolize Trp *via* TDO instead or in addition to IDO1, suggesting that specific inhibition of IDO1 may not be adequate to counteract a decrease in tryptophan levels.

Accumulating proofs indicate that IDO2 mediates autoimmune responses as it is expressed in B cells and has a role in modulating autoantibody production. Moreover, despite the relationship between IDO2 and cancer has not yet extensively

studied, the association between pancreatic adenocarcinoma and gastrointestinal cancer and IDO2 overexpression together with IDO1 and TDO has been reported.[5b, 11]

1.2.3. The landscape of IDO/TDO inhibitors

As mentioned above, IDO1, IDO2 and TDO are emerging as druggable targets in cancer immunotherapy as there is a growing body of evidence supporting their crucial role in oncological immune escape.[3,8] As a result, it is not surprising that the well-known enzyme IDO1 has been center-stage as a druggable target in the last 10 years with great hopes. Indeed, it has been largely demonstrated that IDO1 inhibition can break an acquired immune tolerance, synergizing with chemotherapy, radiotherapy or other immunotherapeutic agents.[10e]

In 2006 the X-ray crystal structure of human IDO1 complexed with 4-PI (a weak IDO1 inhibitor) has been solved by Sugimoto *et al.* suggesting the existence of two hydrophobic pockets, named pocket A and pocket B, in the catalytic site of the enzyme (Figure 2).

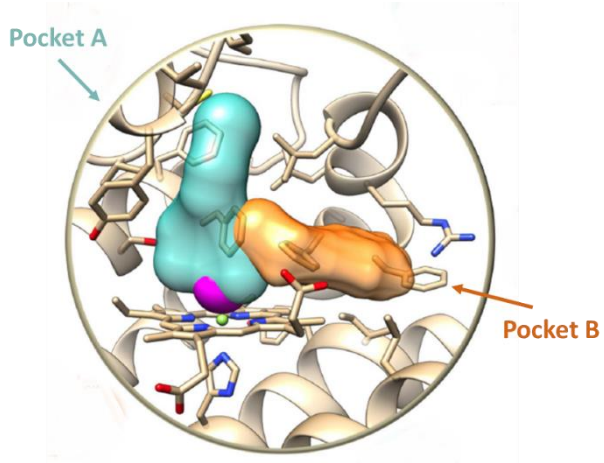

Figure 2. Depiction of the IDO1 active site (PDB code 4PKS): pocket A (turquois), pocket B (orange) and the iron binding site (magenta). Taken from Röhrig, U.F. *et al. J. Med. Chem.* **2015,** *58,* 9421.9437.

Since then, several other papers have provided additional structures of the enzyme in complex with inhibitors.[12] Nevertheless, among the thousands of compounds reported in the scientific and patent literature as IDO inhibitors, only five molecules to date have reached human clinical trials and no IDO1 inhibitor has been approved, confirming that the translation from bench to bedside in IDO inhibition is proving to be a big challenge.[13] Besides indoximod [14], epacadostat [15] and GDC-0919 [16] (structure not disclosed), very recently PF-06840003 [17] and BMS-986205 [18] (structure not disclosed) have entered clinical trials (Figure 3). Unfortunately, the recent report at the 2018 ASCO Annual Meeting revealed that epacadostat failed to show a clinical benefit in combination to pembrolizumab in unresectable or metastatic melanoma.[19] In this respect, two nodal points can be associated on the reason of the failure: first, the difficulty in the identification of good markers to stratify patients that will respond better from IDO inhibition; secondly, recent data have shown that IDO2 and TDO mediate natural and acquired resistance to IDO1 inhibitors.

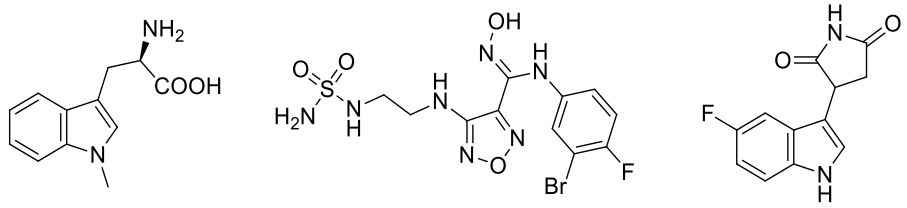

indoximod epacadostat PF-06840003

Figure 3. Chemical structures of IDO1 inhibitors entered onto clinical trial.

While IDO1 inhibition has been deeply explored, TDO inhibitors pipeline has been investigated to a far lesser extent. The indole LM10, a TDO inhibitor developed in 2011 by Dolusi *et al.*, displayed a good anti-tumour activity in a preclinical model together with good solubility and good bioavailability. [20] However, further investigations are required before undergoing clinical trials (Figure 4). The crystal structure of human TDO (hTDO) has been recently elucidated making *in silico*-guided design of novel inhibitors reliable.[21] Indeed, two additional molecules were

developed between 2015 and 2016 and include *N*1-benzyl-1H-naphtho[2,3-d][1,2,3]triazole-4,9-diones **1** disclosed by Wu *et al.* and a 3-(indol-3-yl)pyridine compound (structure not disclosed) developed by Pfizer, with an IC_{50} of 30 nM and 27 nM, respectively (Figure 4).[22-23]

Little is still known about targeting the newcomer enzyme, IDO2. In 2012 during a screening of a small library of molecules already approved by the Food and Drug Administration (FDA) tenatoprazole drug demonstrated to be highly selective for IDO2 inhibition while no effect at ≥ 100 μM for IDO1 or TDO has been seen (Figure 4).[24]

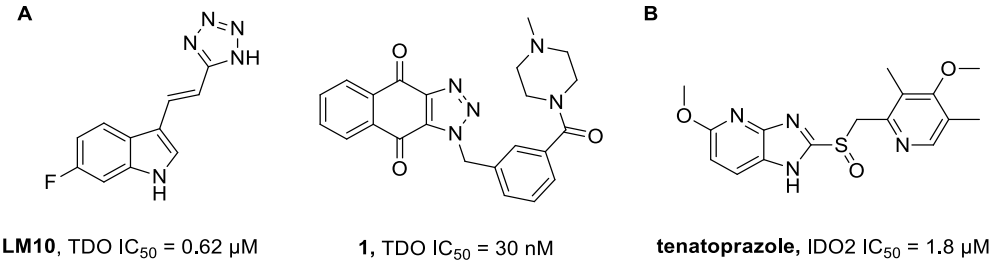

Figure 4. (**A**) Chemical structures of most promising TDO inhibitors. (**B**) Chemical structure of tenatoprazole drug.

Inhibition of IDO2, alongside increasing the efficacy and durability of IDO/TDO inhibition in tumours that over-express the enzyme, would also reduce autoimmune side-effects associated with immunotherapy, as this enzyme supports autoantibody production in B cells.[25] However, intense efforts need to be pursued in both the searching for TDO and IDO2 inhibitors.

Interestingly, dual IDO1/TDO inhibitors are appearing in the landscape as shown by compound RG70099 developed by Roche.[26] Overall, evidences clearly suggest that combi-IDO/TDO inhibitors may represent a promising strategy in order to limit acquired resistance to IDO1 blockade and reduce autoimmune side effects of immunotherapy.

1.2.4. References

1. Dounay, A.B.; Tuttle, J.B.; Verhoest, P.R. Challenges and opportunities in the discovery of new therapeutics targeting the kynurenine pathway. *J. Med. Chem.* **2015**, *58*, 8762-8782.
2. Fatokun, A.A.; Hunt, N.H.; Ball, H.J. Indoleamine 2,3 dioxygenase 2 (IDO2) and the kynurenine pathway: characteristics and potential roles in health and disease, *Amino Acids* **2013**, *45*, 1319-1329.
3. Platten, M.; Wick, W.; Van den Eynde, B.J. Tryptophan catabolism in cancer; beyond IDO and tryptophan depletion. *Cancer Res.* **2012,** *72*, 5435-5439.
4. Grohmann, U.; Fallarino, F.; Puccetti, P. Tolerance, DCs and tryptophan: much about IDO. *Trends Immunol.* **2003**, *24*, 242-248.
5. a. Moon, Y.W.; Hajjar, J.; Hwu, P.; Naing, A. Targeting the indoleamine 2,3-dioxygenase pathway in cancer. *J. for ImmunoTherapy of Cancer* **2015**, 3-51.
   b. Platten, M.; Doeberitz, N.V.K.; Oezen, I.; Wick, W.;Ochs, K. Cancer immunotherapy by targeting IDO1/TDO and their downstream effectors, *Frontiers in immunology* **2015**, *5*, 1-7.
6. a. Pallotta, M.T.; Orabona, C.; Volpi, C.; Vacca, C.; Belladonna, M.L.; Bianchi, R.; Servillo, G.; Brunacci, C.; Calvitti, M.; Bicciato, S.; Mazza, E.M.; Boon, L.; Grassi, F.; Fioretti, M.C.; Fallarino, F.; Puccetti, P.; Grohmann, U. Indoleamine 2,3-dioxygenase is a signaling protein in long-term tolerance by dendritic cells. *Nat Immunol.* **2011**, *12*, 870-878.
   b. Orabona C.; Pallotta, M.T.; Volpi, C.; Fallarino, F.; Vacca, C.; Bianchi, R.; Belladonna, M.L.; Fioretti, M.C.; Grohmann, U.; Puccetti, P. SOCS3 drives proteasomal degradation of indoleamine 2,3-dioxygenase (IDO) and antagonizes IDO-dependent tolerogenesis. *Proc Natl Acad Sci USA.* **2008**, *105*, 20828-20833.
7. a. Orabona C.; Pallotta, M.T.; Grohmann, U. Different partners, opposite outcomes: a new perspective of the immunobiology of indoleamine 2,3-dioxygenase. *Mol Med.* **2012**, *18*, 834-42.
   b. Albini, E.; Rosini, V.; Gargaro, M.; Mondanelli, G.; Belladonna, M.L.; Pallotta, M.T.; Volpi, C.; Fallarino, F.; Macchiarulo, A.; Antognelli, C.; Bianchi, R.; Vacca, C.; Puccetti, P.; Grohmann, U.; Orabona, C. Distinct roles of immunoreceptor tyrosine-based motifs in immunosuppressive indoleamine 2,3-dioxygenase 1. *J Cell Mol Med.* **2017**, *21*, 165-176.
8. a. Prendergast, G. C.; Smith, C.; Thomas, S.; Mandik-Nayak, L.; Laury-Kleintop, L.; Metz, R.; Muller, A. J. Indoleamine 2,3-dioxygenase pathways of pathgenic inflammation and immune escape in cancer. *Cancer Immunol. Immunother.* **2014**, 63, 721-735.
   b. Gostner, J. M.; Becker, K.; Uberall, F.; Fuchs, D. The potential of targeting indoleamine 2,3-dioxygenase for cancer treatment. *Expert Opin. Ther. Targets*. **2015**, 19, 606-615.

9. Godin-Ethier, J.; Hanafi, L. A.; Piccirillo, C. A.; Lapointe, R. Indoleamine 2,3-dioxygenase expression in human cancers: clinical and immunologic perspectives. *Clin. Cancer Res.* **2011**, *17*, 6985-6991.
10. a. Muller, A. J.; DuHadaway, J. B.; Donover, P. S.; Sutanto-Ward, E.; Prendergast, *G. C.* Inhibition of indoleamine 2,3-dioxygenase, an immunoregulatory target of the cancer suppression gene Bin1, potentiates cancer chemotherapy. *Nat Med.* **2005**, *11*, 312-319.
b. Huang, T. T.; Yen, M. C.; Lin, C. C.; Weng, T. Y.; Chen, Y. L.; Lin, C. M.; Lai, M. D. Skin delivery of short hairpin RNA of indoleamine 2,3 dioxygenase induces antitumor immunity against orthotopic and metastatic liver cancer. *Cancer Sci.* **2011**, *102*, 2214-2220.
c. Holmgaard, R.B.; Zamarin, D.; Munn, D. H.; Wolchok, J. D.; Allison, J. P. Indoleamine 2,3-dioxygenase is a critical resistance mechanism in antitumor T cell immunotherapy targeting CTLA-4. *J Exp Med.* **2013**, *210*, 1389-1402.
d. Spranger, S.; Koblish, H. K.; Horton, B.; Scherle, P. A.; Newton, R.; Gajewski, T. F. Mechanism of tumor rejection with doublets of CTLA-4, PD-1/PD-L1, or IDO blockade involves restored IL-2 production and proliferation of CD8+ T cells directly within the tumor microenvironment. *J Immunother Cancer*. **2014**, 2:3.
e. Brochez, L.; Chevolte, I.; Kruse, V. The rationale of indoleamine 2,3-dioxygenase inhibition for cancer therapy. *Eur. J. Cancer.* **2017**, *76*, 167-182.
11. Muller, A.; Manfredi, M.G.; Zakharia, Y.; Prednergast, G.C. Inhibiting IDO pathways to treat cancer: lessons from the ECHO-301 trial and beyond. *Semin Immunopathol.* **2018**, 1-8.
12. Sugimoto, H.; Oda, S.; Otsuki, T.; Hino, T.; Yoshida, T.; Shiro, Y. Crystal structure of human indoleamine 2,3 dioxygenase: catalytic mechanism of O_2 incorporation by a heme-containing dioxygenase. *Proc. Natl. Acad. Sci. USA.* **2006**, *103*, 2611-2616.
13. Prendergast, G.C.; Malachowski, W.P.; DuHadaway, J.B.; Muller, A.J. Discovery of IDO1 Inhibitors: From Bench to Bedside. *Cancer Res.* **2017**, *77*, 6795-6811.
14. a. Cady S.G.; Sono, M. 1-Methyl-DL-tryptophan, beta-(3-benzofuranyl)-DL-alanine (the oxygen analog of tryptophan), and beta-[3-benzo(b)thienyl]-DL-alanine (the sulfur analog of tryptophan) are competitive inhibitors for indoleamine 2,3-dioxygenase. *Arch Biochem Biophys*. **1991**, *291*, 326-333.
b. Metz, R.; DuHadaway, J.; Kamasani, U.; Laury-Kleintop, L.; Muller, A.J.; Prendergast, G.C. Novel tryptophan catabolic enzyme IDO2 is the preferred biochemical target of the antitumor indoleamine 2,3-dioxygenase inhibitory compound d-1-Methyl-Tryptophan. *Cancer Res.* **2007**, *67*, 792-801.
15. A. Yue, E. W.; Sparks, R.; Polam, P.; Modi, D.; Douty, B.; Wayland, B.; Glass, B.; Takvorian, A.; Glenn, J.; Zhu, W.; Bower, M.; Liu, X.; Leffet, L.; Wang, Q.; Bowman, K. J.; Hansbury, M. J.; Wei, M.; Li, y.; Wynn, R.; Burn, T. C.; Koblish, H. K.; Fridman, J. S.; Emm, T.; Scherle, P. A.; Metcalf, B.; Combs,

A. P. INCB24360 (epacadostat), a highly potent and selective indoleamine-2,3-dioxygenase 1 (IDO1) inhibitor for immunooncology. *ACS Med. Chem. Lett.* **2017**, *8*, 486-491.
b. Combs A, Yue E, Sparks R, et al. Patent WO2010/005958; **2010**

16. Crunkhorn, S. Deal watch: Genetech dives deeper into the next waves of cancer immunotherapies. *Nat. Rev. Drug Discovery*. **2014**, *13*, 879
17. Tumang, J.; Gomes, B.; Wythes, M.; Crosignani, S.; Bingham, P.; Bottemanne, P.; Cannelle, H.; Cauwenberghs, S.; Chaplin, J.; Dalvie, D.; Denies, S.; De Maeseneire, C.; Folger, P.; Frederix, K.; Guo, J.; Hardwick, J.; Hook, K.; Jessen, K.; Kindt, E.; Letellier, M-C.; Liao, K-H.; Li, W.; Maegley, K.; Marillier, R.; Miller, N.; Murray, B.; Pirson, R.; Preillon, J.; Rabolli, V.; Ray, C.; Scales, S.; Srirangam, J.; Solowiej, J.; Streiner, N.; Torti, V.; Tsaparikos, K.; Vicini, P.; Driessens, G.; Kraus, M. PF-06840003: a highly selective IDO-1 inhibitor that shows good in vivo efficacy in combination with immune checkpoint inhibitors. *AACR* **2016**, Abstract number 4863.
18. Siul, L. L.; Gelmon, K.; Chu, Q.; Pachynski, R.; Alese, O.; Basciano, P.; Walker, J.; Mitra, P.; Zhu, L.; Phillips, P.; Hunt, J.; Desai, J. BMS-986205, an optimized indoleamine 2,3-dioxygenase 1 (IDO1) inhibitor, is well tolerated with potent pharmacodynamic (PD) activity, alone and in combination with nivolumab (nivo) in advanced cancers in a phase 1/2a trial. *AACR* **2017**, poster number 6774.
19. Long, G.V.; Dummer, R.; Hamid, O.; Gajewski, T.; Caglevic, C.; Dalle, S.; Arance, A.; Carlino, M.S.; Grob, J-J.; Kim, T.M.; Demidov, L.V.; Robert, C.; Larkin, J.M.G.; Anderson, J.; Maleski, J.E.; Jones, M.M.; Diede, S.J.; Mitchell, T.C. Epacadostat (E) plus pembrolizumab (P) versus pembrolizumab alone in patients (pts) with unresectable or metastatic melanoma: Results of the phase 3 ECHO-301/KEYNOTE-252 study. *Journal of Clinical Oncology*. **2018** 36:15_suppl, 108-108.
20. a. Yu, C-P.; Song, Y-L.; Zhu, Z-M.; Huang, B. Targeting TDO in cancer immunotherapy. *Med. Oncol.* **2017**, 34:73.
b. Dolusic, E.; Larrieu, P.; Moineaux, L.; Stroobant, V.; Pilotte, L.; Colau, D.; Pochet, L.; Vanden Eynde, B.; Masereel, B.; Wouters, J.; Frederick, R. Tryptophan 2,3-dioxygenase (TDO) inhibitors. 3-(2-(Pyridyl)ethenyl)indoles as potential anticancer immunomodulators. *J. Med. Chem.* **2011**, *54*, 5320–5334.
21. Lewis-Ballester, A.; Forouhar, F.; Kim, S-M.; Lew, S.; Wang, Y.; Karkashon, S.; Seetharaman, J.; Batabyal, D.; Chiang, B.; Hussain, M.; Correia, M. A.; Yeh, S.; Tong, L. Molecular basis for catalysis and substrate-mediated cellular stabilization of human tryptophan 2,3-dioxygenase. *Scientific Reports* **2016**, *6*, 35169.
22. Wu, J-S.; Lin, S-Y; Liao,F-Y.; Hsiao, W-C.; Lee,L-C.; Peng, Y-H.; Hsieh, C-L.; Wu, M-H.; Song, J-S.; Yueh, A.; Chen,C-H.; Yeh, S-H.; Liu, C-Y.; Lin, S-Y.; Yeh, T-K.; Hsu, J. T.-A.; Shih, C.; Ueng, S-H,; Hung, M-S.; Wu, S-Y.

Identification if substituted naphthotriazolediones as novel tryptophan 2,3-dioxygenase (TDO) inhibitors through structure-based virtual screening. *J. Med. Chem.* **2015**, *58*, 7807-7819.

23. Ninkovic, S.; Crosignani, S.; McAlpine, I. J. et al. Patent US 2016/0272628A1; **2016**.
24. Bakmiwewa, S.M.; Fatokun, A.A.; Tran, A.; Payne R.J.; Hunt, N.H.; Ball, H.J. Identification of selective inhibitors of indoleamine 2,3-dioxygenase 2. *Bioorg. Med. ChemLett.* **2012**, *22*, 7641, 7646.
25. Merlo, L.M.; DuHadaway, J. B.; Grabler, S.; Prendergast, G. C.; Muller, A. J.; Mandik-Nayak, L. IDO2 modulates T cell-dependent autoimmune responses through a B cell-intrinsic mechanism. *J. Immunol*. **2016**, *196*, 4487-4497.
26. Gyülvészi, G.; Fischer, C.; Mirolo, M.; Stern, M.; Green, L.; Nopora,A.; Ceppi, M.; Wang, H.; Bürgi, B.; Staempfli, A.; Muster, W.; Müller, L.; Van Waterschoot, R.; Gloge, A.; Sade, H.; Klaman, I; Hölzlwimmer, G.; Surya, A.; Banerjee, M.; Shrivastava, R.; Middya, S.; Yadav, D.; Basu, S.; Meneses-Lorente, G.; Lugli, S.; Acuña, G. RG70099: A novel, highly potent dual IDO1/TDO inhibitor to reverse metabolic suppression of immune cells in the tumor micro-environment, *AACR **2016***.

1.3. Hereditary multiple exostoses

1.3.1. Heparan sulfate structure and biosynthesis

Heparan sulfate (HS) is a glycosaminoglycan (GAG) present in cell surface and extracellular matrix heparan sulfate proteoglycans (HSPGs). The HSPG family includes membrane-anchored proteoglycans syndecans and glypicans, the secreted extracellular matrix proteoglycans agrin, perlecan and type XVIII collagen and the secretory vesicle proteoglycan serglycin. Proteoglycans (PGs) consist of a core protein, and one or more glycosaminoglycans (GAGs) side chains attached to specific serine residues. GAGs are long unbranched negatively charged heteropolysaccharides that consist of alternating residues of an uronic acid and an amino sugar. The amino sugar can be *N*-acetylated or *N*-sulfated glucosamine (heparan sulfate) or *N*-acetylgalactosamine (chondroitin/dermatan sulfate) while the uronic acid consist of glucuronic (GlcA) or iduronic acid (IdoA).[1] The first step in HS synthesis is the formation of a linkage tetrasaccharide which is composed of a xylose, two galactose residues and glucuronic acid. Then chain polymerization begins with *N*-acetyl-D-glucosamine (GlcNAc) addition and proceeds with sequential and addition of glucuronic acid (GlcA) and GlcNAc carried out by an enzyme complex composed of Ext1 and Ext2. Xylose addiction to a serine residue in the PG core is carried out in the endoplasmic reticulum while the following steps in HS biosynthesis take place in the Golgi apparatus. The first GlcNAc residue is added to the linkage tetrasaccharide by Extl3. The nascent HS chains then undergo a series of structural modification including sulfation at different position and glucuronic acid epimerization leading to chains characterized by high structural complexity and biological specificity (Figure 1).[2]

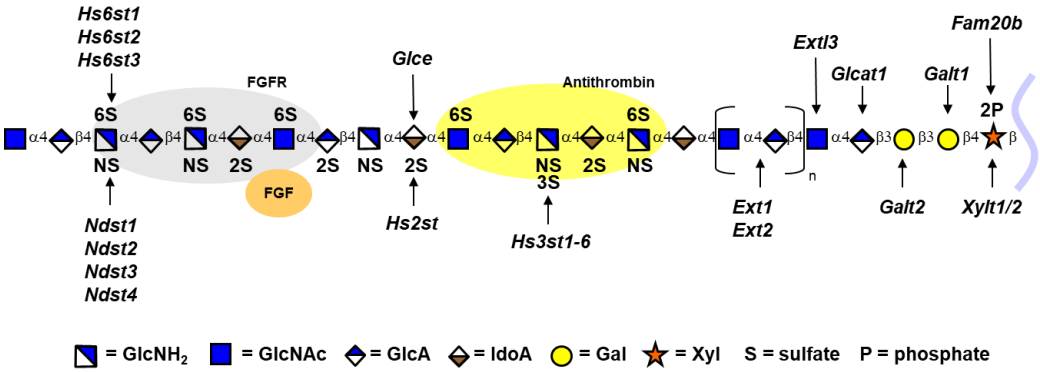

Figure 1. Heparan sulfate structure and assembly. Taken from Sarrazin, S. *et al. Cold Spring Harb Perspect Biol.* **2011**, *3*, 1-33.

1.3.2. Heparan sulfate functions in health and disease

HS plays an essential role in regulating cellular functions such as cell growth, adhesion, angiogenesis, and blood coagulation by binding to a large number of proteins, including growth factors, signaling proteins, integral membrane receptors, chemokines, and extracellular matrix proteins. At least 300 heparan sulfate binding proteins (HSBPs) have been identified so far with differences in terms of affinity, specificity and function.

Perlecan, agrin and type XIII collagen present in the matrix of basement membranes help define matrix structure and organisation and provide a substratum for cell migration. It has been reported that HSPGs are found in secretory vesicles where they control several activities including the maintenance of the active state of proteases and the packaging of granular contents. Again, granule proteoglycans regulate biological functions such as coagulation, wound repair and host defence after vesicles secretion. Moreover, they can protect cytokines, grown factors and chemokines against proteolysis by binding to them. HSPGs present in the cell surface can act as receptors regulating distribution and activity of its ligand and as coreceptors by modifying the activation threshold or the duration of signalling by different tyrosine kinase-type growth factor receptors (Figure 2). These various

activities depend on recognition of the HS chains through HS-binding domains present in the various protein ligands, including fibroblast growth factors (FGFs), vascular endothelial growth factors (VEGFs), bone morphogenetic proteins (BMPs). Finally, they cooperate with different cell adhesion receptors by facilitating a plethora of function ranging from cell-cell interactions to cell motility.[1]

It has been reported that HSPGs are involved in pathological conditions. Changes in HS composition have been associated with tumour cell transformation and invasiveness. Furthermore, HS has also been implicated in the development of neurodegenerative diseases (i.e. prion, Alzheimer's, and Parkinson's disease). Viruses and bacteria possess HSBPs consistent with the known role that these complex polysaccharides play in infection.[2a,3] Finally, a decrease in HS levels has been related to the development of hereditary multiple exostoses (HME), a rare genetic pediatric disorder.[4] The pathology of this disease will be described in detail in the next paragraph.

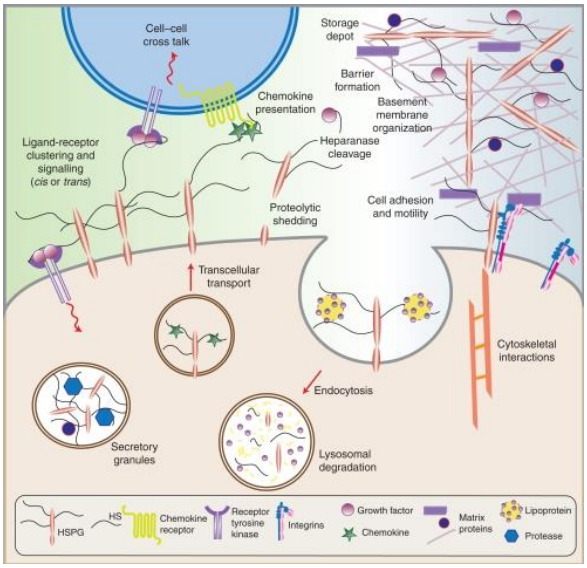

Figure 2. Pictorial representation of the vast array of functions mediated by HSPGs. Taken from Sarrazin, S. *et al. Cold Spring Harb Perspect Biol.* **2011**, *3*, 1-33.

1.3.3. Hereditary multiple exostoses: pathogenesis, clinical presentation and perspectives

Hereditary multiple exostoses, also known as multiple osteochondromas (MO), is an autosomal dominant disorder that results from heterozygous loss-of-function mutations in *EXT1* or *EXT2*. 1 in every 50,000 children worldwide are affected by this relatively rare pediatric disease.[5] Heterozygosity diminishes the capacity of cells to make heparan sulfate. Indeed, EXT deficiency causes truncation of the HS chains and consequent decrease in HS levels in plasma and various tissues. HME is characterized by the formation of multiple bony spurs or lumps, known as exostoses or osteochondromas, next to long bones, ribs and vertebrae and other skeletal elements. Patients with HME present shortened stature, bowing and shortening of forearm elements, changes in angulations of the knee and fingers, and limb-length inequalities. Because of their multiple locations, considerable size and great number, the exostoses cause several complications with the advance of the disease. These include joint ankylosis, skeletal deformities, impingement of muscle, blood vessels and nerves and conversion to malignant chondrosarcoma especially during adulthood (2-3%).[6] Matsumoto *et al.* demonstrated that another common complication of the disease is represented by scoliosis.[7]

Currently, the most common treatment for HME patients consists of surgical removal of osteochondromas which results in the correction of major skeletal defects. In some cases osteochondromas are impossible to resect because of dangerous or delicate localization within the body. Symptomatic pain that appears in patients is controlled by the use of palliative drugs.[8] At present no pharmacological treatment has been developed for reducing the number or growth of exostoses.

Nevertheless, it has been recently demonstrated that chondrogenesis requires bone morphogenetic protein (BMP) signalling and that *Ext1*-mutant mice display enhanced BMP signalling that leads to osteochondromagenesis.[9]

Promisingly, Sinha and co-workers showed that the use of LDN-193189, a BMP signalling antagonist, effectively reduced osteochondroma growth in *Ext1*-mutant mice[10] providing a therapeutic approach for MHE (Figure 3).

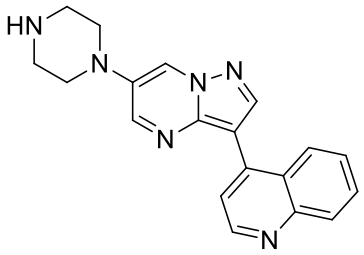

LDN-193189

Figure 3. Chemical structure of BMP antagonist LDN-193189.

In summary, further efforts are needed in order to identify novel approaches to develop drugs for treating the disease.

1.3.4. References

1. a. Sarrazin, S.; Lamanna, W.C., Esko, J. Heparan Sulfate Proteoglycans. *Cold Spring Harb Perspect Biol.* **2011**, *3*, 1-33.
   b. Esko, J.D.; Kimata, K.; Lindahl, U. Proteoglycans and sulfated glycosaminoglycans. In: Varki, A.; Cummings, R.D.; Esko, J.D. et al. editors. Essentials of Glycobiology. 2nd edition. Cold Spring Harbor (NY): Cold Spring Harbor Laboratory Press. **2009**. Chapter 16.
2. a. Multhaupt, H.A.B.; Couchmanm, J.R. Heparan Sulfate biosynthesis methods for investigation of the heparanosome. *J Histochem Cytochem*. **2012**, *60*, 908–915.
   b. Schwartz, N.B.; Smalheiser, N.R. Biosynthesis of Glycosaminoglycans and Proteoglycans. In: Margolis, R.U.; Margolis, R.K. (eds) Neurobiology of Glycoconjugates. Springer, **1989**. Boston, MA.
3. a. Weiss, R.J.; Esko, J.; Tor, Y. Targeting heparin and heparan sulfate protein interactions. *Org. Biomol. Chem.* **2017**, *15*, 5656-5668.
   b. Lindahl, U.; Kjellén, L. Pathophysiology of heparan sulfate: many diseases, few drugs. *Journal of internal medicine.* **2013**, *273*, 555-571.
4. Huegel, J.; Sgariglia, F.; Enomoto-Ivamoto, M.; Koyama, E.; Dormans, J.P.; Pacifi, M. Heparan sulfate in skeletal development, growth, and pathology: the case of hereditary multiple exostoses. *Dev. Dyn.* **2013**, *242*, 1021-1032.
5. Pacifi, M. The pathogenic roles of heparan sulfate in hereditary multiple exostoses. *Matrix Biol.* **2018**, *71-72*, 28-39.
6. a. Pacifi, M. Hereditary multiple exostoses: new insights into pathogenesis clinical complications and potential treatments. *Curr Osteoporos Rep*, **2017**, *15*, 142-152.
   b. Beltrami, G.; Ristori, G.; Scoccianti, G.; Tamburini, A.; Capanna, R. Hereditary multiple exostoses: a review of clinical appearance and metabolic pattern. *Clinical cases in mineral and bone metabolism.* **2016**, *13*, 110-118.
7. Matsumoto, Y.; Matsumoto, K.; Harimaya, K. Scoliosis in patients with hereditary multiple exostoses. *Eur Spine J.* **2015,** *24*, 1568-1573.
8. Phan, A.Q.; Pacifi, M.; Esko, J.D. Advances in the pathogenesis and possible treatments for multiple hereditary exostoses from the 2016 international MHE conference. *Connective tissue research*. **2018**, *59*, 85-98.
9. Inubushi, T.; Nozawa, S.; Matsumoto, K.; Irie, F.; Yamaguchi, Y. Aberrant perichondrial BMP signaling mediates multiple osteochondromagenesis in mice. *JCI Insight*, **2017,** *2*, 1-14.
10. Sinha, S.; Mundy, C.; Bechtold, T.; Sgariglia, F.; Ibrahim, M.M.; Billings, P.C.; Crrol, K.; Koyama, E.; Jones, K.B.; Pacifi, M. Unsuspected osteochondroma-like outgrowths in the cranial base of hereditary multiple exostoses patients and modeling and treatment with a BMP antagonist in mice. *PLos Genetics*. **2017**, *13*, 1-26.

Chapter 2

Outline of the thesis

2.1. Outline of the thesis

This thesis illustrates three different projects on which I focused my research activity during the PhD program: the development of Store-Operated Calcium Entry modulators, the discovery of indoleamine 2,3-dioxygenase 1 inhibitors for anticancer therapy and the search for small molecules enhancers of heparan sulphate as candidate therapeutics for the treatment of hereditary multiple exostoses.

Chapter 3 describes the discovery, by a click chemistry approach, of a new class of molecule able to fine-tune the Store-Operated Calcium Entry mechanism. Interestingly, both enhancers and inhibitors of the process have been reported.

Chapter 4 presents an isocyanide-based multicomponent approach to the rapid and versatile generation of imidazothiazole compounds as IDO1 inhibitors.

Chapter 5 introduces the discovery, by a virtual screening approach, of a novel scaffold for IDO1 inhibition and the *in silico*-driven synthesis of a series of structurally related analogues.

Chapter 6 reports my research activity in the development of HS enhancers that took place at University of California San Diego (UCSD) under the supervision of Prof. Carlo Ballatore. Specifically, it illustrates the design, synthesis, structure activity relationship (SAR) study and physicochemical properties evaluation of *N*-aryl-2-aminothiazoles as potential leads for the treatment of HME disease.

Finally, Chapter 7 sums up and highlights future developments in each field.

Chapter 3

Pyrtriazoles, a novel class of Store-Operated Calcium Entry modulators: discovery, biological profiling and *in vivo* proof-of-concept efficacy in SOCE-related diseases

3.1. Introduction

As mentioned in Chapter 1.1.4., alteration of the SOCE machinery is related to the development of a vast array of diseases ranging from cancer to rare diseases. Therefore, this cellular event has been suggested to be druggable target for developing novel therapies.[1] However, despite the increasing number of molecules discovered so far, only few compounds have progressed to the clinic and none of them has obtained the FDA approval, primarily owing to their drawbacks in terms specificity and selectivity.[2] It follows that there is a need to increase the range of available compounds.

A rational design of SOCE modulators is at present complicated since structural information on Orai and STIM proteins is very poor (See Chapter 1.1.2).[3] In this context, Prof. Pirali's research group started from the observation that the arylamide substructure appears to be an essential pharmacophoric feature for SOCE modulation and almost all the inhibitors reported in the literature share this structural redundancy.[2] Thus, before I started the PhD program, a click chemistry approach had been pursued in order to investigate whether the arylamide displayed by known SOCE modulators could be isosterically replaced by the 1,4-disubstituted 1,2,3-triazole ring. To this aim, starting from known pyrazole derivatives, namely BTP2 and Pyr compounds, they isosterically substituted the amide moiety with the triazole ring (Figure 1).[4-7] Giving that the trifluoromethyl groups in the C3 and C5 positions of the pyrazole ring or, alternatively, the ethyl carboxylate group in the C4 position are necessary for the inhibitory activity they were kept fixed, while the portion beared by the triazole ring, which appears to contribute to selectivity, was extensively varied. A library of seventy-nine candidates was designed, synthesized and biologically evaluated for their ability to modulate SOCE (Figure 1). Within this series, a *hit compound*, namely **1S**, was identified as a promising inhibitor of SOCE. Strikingly, two enhancers of the process (**2T** and **3G**, Figure 1) were discovered,

affording experimental tools to further explore the (patho)physiological role of capacitative calcium entry. Yet, they represent the first SOCE enhancers that do not display a borinate substructure (See Chapter 1.1.4).[8]

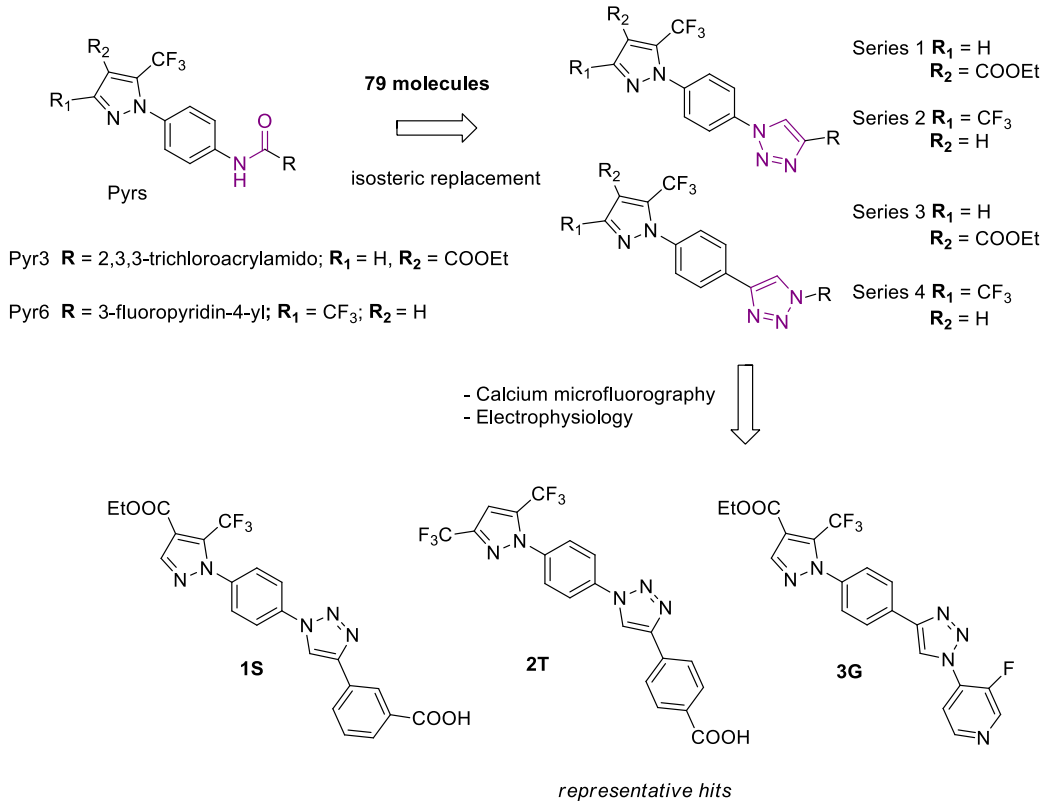

Figure 1. Scheme representing the strategy performed for the discovery of SOCE modulators and the chemical structures of SOCE inhibitor **1S** and enhancers **2T** and **3G**.

However, Prof. Pirali's laboratory decided to focus its attention on the *hit* **1S**, as inhibitors have immediate therapeutic applications. Thanks to the collaboration with Prof. Genazzani's group, compound **1S** activity was evaluated. **1S** displays an IC_{50} value for inhibition of SOCE of 0.6 ± 0.1 μM in Hek cells compared to 0.5 ± 0.1 of Pyr3 and 0.3 ± 0.1 of Pyr6, the reference substances (Figure 2A). Cytotoxicity was measured evaluating viability of cells after 24 h treatment via the MTT assay. Viability of cells treated with Pyr3 at 10 μM was 28.6 ± 0.4%, compared to 70.3 ± 5.8% of Pyr6 and 84.0 ± 1.0% of **1S** (Figure 2B). Gratifyingly, compound **1S** is the

less cytotoxic and affects cell viability at concentration 100-fold the IC_{50} for SOCE inhibition.

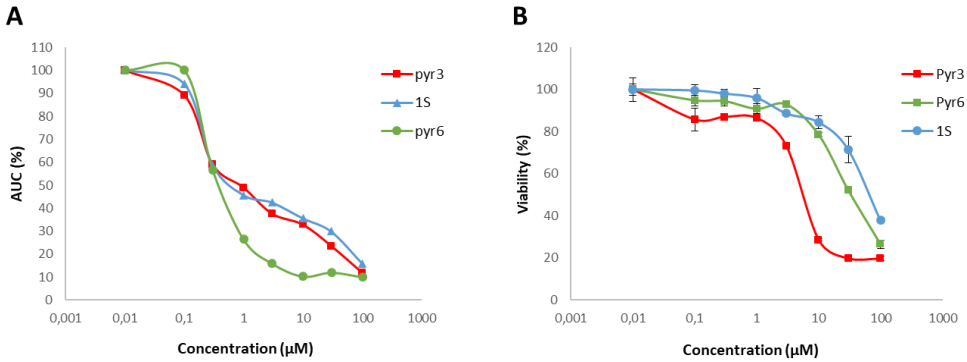

Figure 2 (**A**) Concentration-response curves of **1S**, Pyr3 and Pyr6 in Hek cell line;(**B**) MTT assay of Pyr3, Pyr6 and **1S**.

As it has been reported that Pyrs may also affect other channels, Genazzani's laboratory tested the activity of **1S** on voltage-operated channels, TRPV1 and TRPM8 channels that have been shown previously to be affected by SOCE inhibitors. Promisingly, it does not have an effect on voltage-dependent channels, although it inhibits TRPV1 channels.

Finally, given that the ester group in **1S** might be susceptible to hydrolysis, they decided to examine whether the corresponding carboxylic acid **61** retained activity. To this aim, during the research experience as a PhD student in Prof. Pirali's laboratory, I synthesized compound **61**. Unfortunately, it is not active, demonstrating that the ester group is necessary for the inhibition of SOCE (Figure 3).

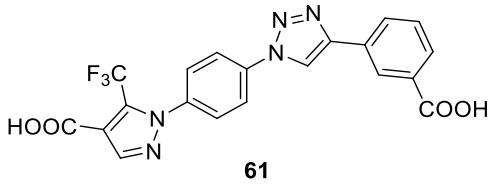

Residual SOCE activity (% of control) in Hek cells > 90%

Figure 3. Chemical structure of 1S corresponding carboxylic acid **61**.

Therefore, in collaboration with Prof. Grosa, we decided to investigate the hydrolytic stability of **1S** in mouse plasma. The residual substrate after 30 minutes of 0% confirms that the ethyl ester underwent fast hydrolysis. Consequently, this result suggests that **1S** might not be good *lead compound* for systemic use.

3.2. Aim of the work

In order to improve the hydrolytic stability of the *hit compound* **1S** and eventually increase its potency and selectivity during my PhD I have performed a focused SAR study. Toward this aim, three portions of the molecule have been switched: the central triazole ring core, the ethyl ester group in the C4 position of the pyrazole ring and the carboxylic moiety on the terminal aryl ring. All the synthesized molecules have been evaluated as SOCE inhibitors. Moreover, the selectivity of selected compounds and the hydrolytic and metabolic stability have been investigated. Finally, efficacy in two different diseases characterized by aberrant SOCE activity, TAM and acute pancreatitis, has been proven.

3.3. Results and discussion

3.3.1. Chemistry

First of all, in order to investigate whether the triazole ring behaved merely as an isostere of the amide group or played a role in the interaction with the SOCE machinery, **1S** analogues displaying both the direct (**6**) and inverse (**12**) amide were synthesized, according to Scheme 1.

The synthesis of the pyrazolic precursors **3** and **9** was accomplished following the route depicted in Scheme 1. The carboxylic acid **3** was obtained by condensing the commercially available oxobutyrate **4** with 4-hydrazinylbenzoic acid **5** (Scheme 1A). Amine **9**, instead, was synthesized in two steps: condensation reaction followed by reduction of the aromatic nitro group (Scheme 1B).

Then the amines (**2** and **9**) and the carboxylic acids (**3** and **8**) were coupled, while protecting and deprotecting the additional carboxylic group.

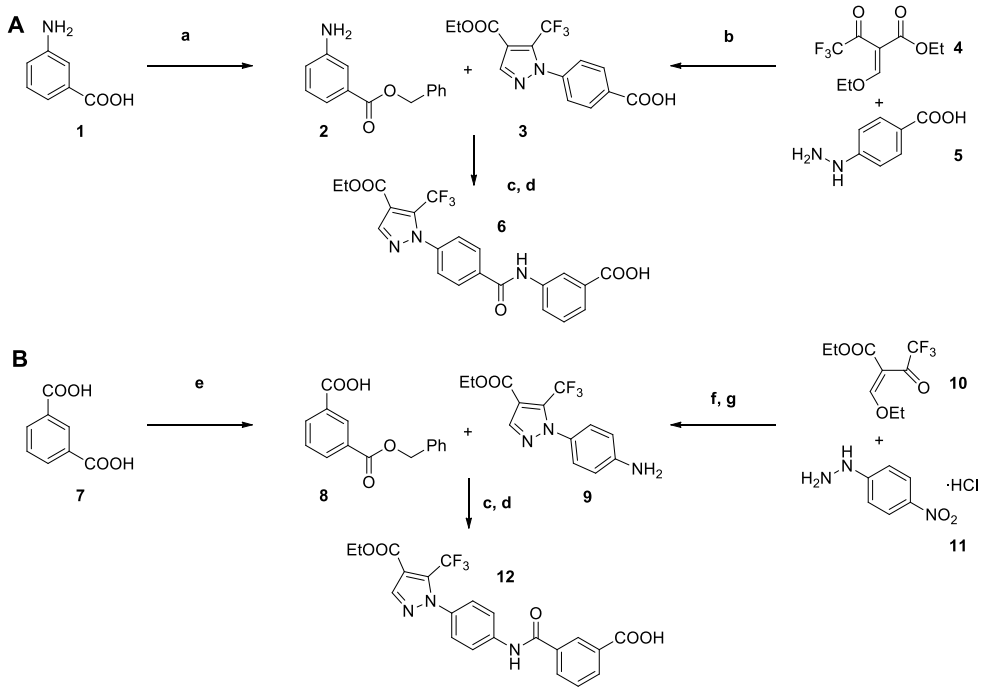

Scheme 1. Modification of the triazole moiety of compound **1S**, direct and inverse amides. (**a**) K_2CO_3, benzyl bromide, dry DMF, rt, 16 h, 47%; (**b**) EtOH, THF, rt, 3 h, 93%; (**c**) EDCI, DIPEA, DMAP, dry CH_2Cl_2, rt, 16 h, 84-94%; (**d**) H_2, 5% Pd/C, MeOH, rt, 1 h, 55-72%; (**e**) TEA, benzyl bromide, DMF, MeOH, H_2O, rt-100 °C, 16 h, 36%; (**f**) DMF, reflux, 2 h, 96%; (**g**) H_2, 5% Pd/C, EtOAc, rt, 2 h, 94%.

The corresponding 1,5-disubstituted triazole (**14**) has also been synthesized using a ruthenium-based catalyst (Scheme 2). To this aim, the required azide **13** was obtained by diazotation-azidation of aniline **9**.

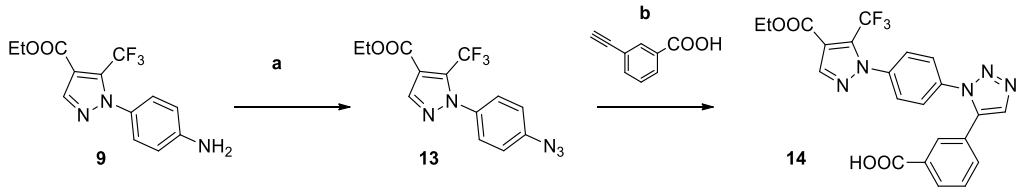

Scheme 2. Modification of the triazole moiety of compound **1S**, 1,5-disubstituted triazole. (**a**) $NaNO_2$, NaN_3, HCl, H_2O, rt, 1 h, 78%; (**b**) Cp*RuCl(cod), microwaves, DMF, 90 °C, 10 min, 39%;

Then, the ethyl ester portion of **1S** was modified. In particular, intermediate **15** was transesterified (**16**, **17**), reduced to amine (**18**, **19**), converted into azide (**20**, **21**) and clicked with commercially available 3-ethynylbenzoic acid to give the final methyl ester **22** and isopropyl ester **23** (Scheme 3).

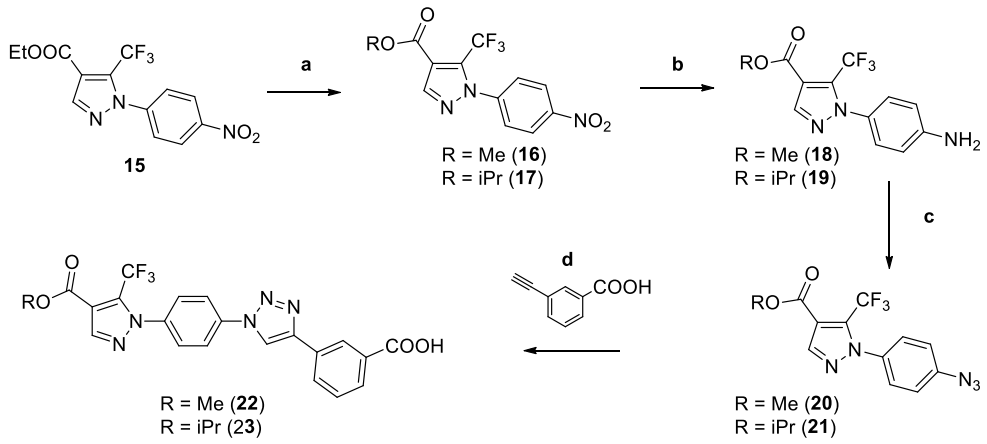

Scheme 3. Modification of the ester moiety of compound **1S**, methyl and isopropyl esters. (**a**) Conc. H_2SO_4, MeOH or 2-propanol, reflux, 32 h, 81-90%; (**b**) H_2, 5% Pd/C, EtOAc, rt, 2 h, 91-94%; (**c**) $NaNO_2$, NaN_3, HCl, H_2O, rt, 3 h, 62-87%; (**d**) Sodium ascorbate, $CuSO_4$•$5H_2O$, *t*-BuOH, H_2O, rt, 16 h, 54-55%.

Alternatively, intermediate **13** was hydrolized to **24**, coupled with different alcohols (**25**-**30**) and clicked with 3-ethynylbenzoic acid, leading to a series of structurally different esters (**31**-**36**) (Scheme 4).

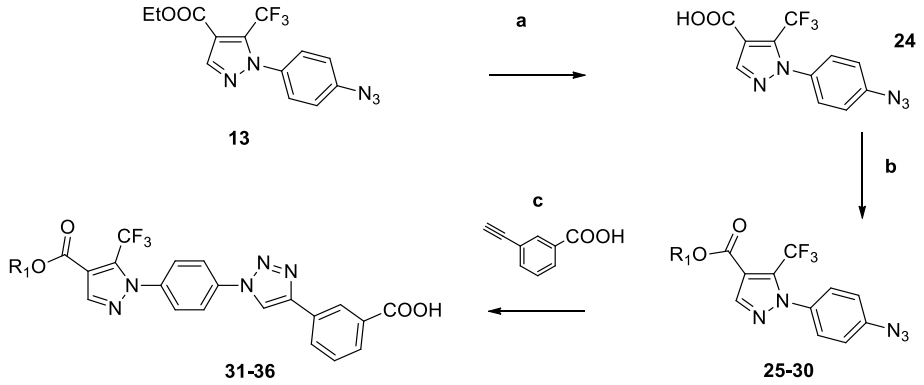

Scheme 4. Modification of the ester moiety of compound **1S**, second series of esters.
(**a**) NaOH, H_2O, acetone, rt, 3 h, 60%; (**b**) EDCI, DMAP, TEA, dry CH_2Cl_2, rt, 16 h, 47-68%; (**c**) Sodium ascorbate, $CuSO_4$•$5H_2O$, *t*-BuOH, H_2O, rt, 16 h, 53-80%.

Moreover, the ethyl ester of intermediate **9** was reduced in the presence of $LiAlH_4$, converted into azide **37** and clicked with 3-ethynylbenzoic acid to give the final primary alcohol **38** (Scheme 5A).

Yet, intermediate **24** was coupled with isopropylamine and then clicked with 3-ethynylbenzoic acid, yielding the secondary amide **40** (Scheme 5B).

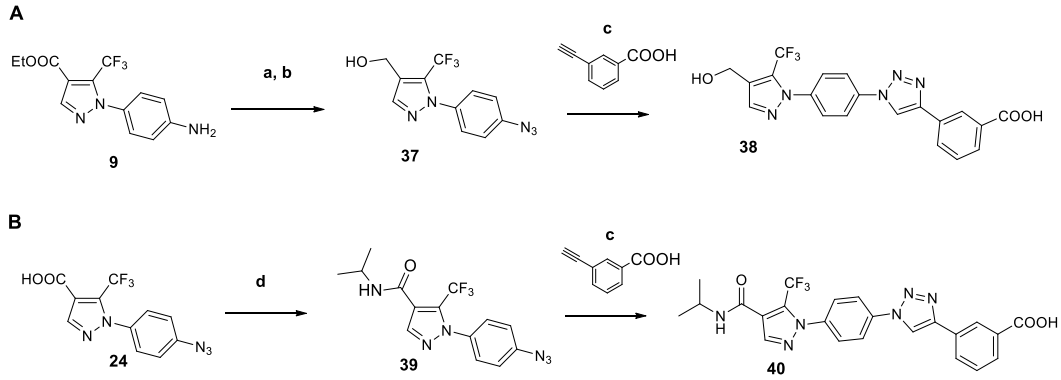

Scheme 5. Modification of the ester moiety of compound **1S**, primary alcohol and secondary amide.
(**a**) $LiAlH_4$, dry THF, rt, 6 h, 80%; (**b**) $NaNO_2$, NaN_3, HCl, H_2O, rt, 3 h, 92%; (**c**) Sodium ascorbate, $CuSO_4$•$5H_2O$, *t*-BuOH, H_2O, rt, 16 h, 83-87%; %; (**d**) Isopropylamine, EDCI, HOBt, TEA, dry CH_2Cl_2, rt, 16 h, 59%.

The ethyl ester of compound **1S** was reacted with aqueous ammonia to give the primary amide **41** (Scheme 6).

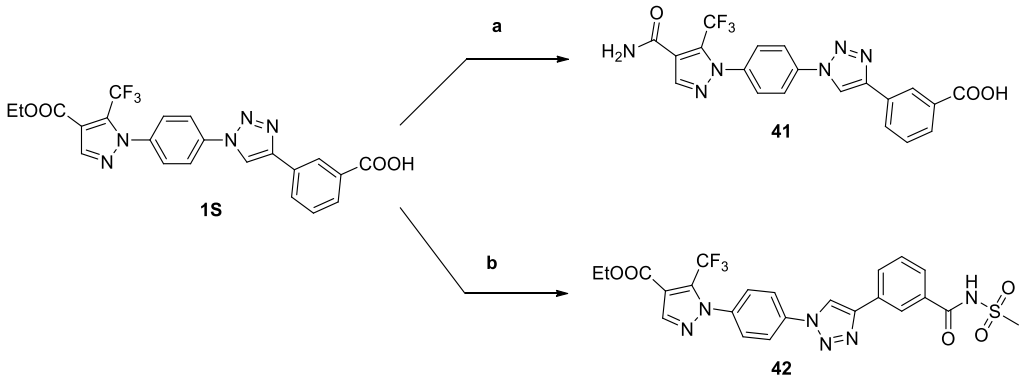

Scheme 6. Synthesis of compounds **41** and **42**.
(**a**) Conc. NH_4OH, 90 °C, 3 h, 63%; (**b**) Methansulfonamide, EDCI, TEA, DMAP, dry CH_2Cl_2, rt, 16 h, 71%.

Last, we investigated whether the carboxylic moiety of compound **1S** was tolerant to substitution with acyl methansulfonamide **42** (Scheme 6), methyl ester **55**, methyl ketone **56**, primary amide **57**, primary alcohol **58**, sulfonamide **59** and hydroxamic acid **60** (Scheme 7). To this aim, the corresponding alkynes **44**, **46**, **48**, **50**, **52** were prepared by a Sonogashira coupling and deprotection (Scheme 8 A-E) while alkyne **54** was synthesize by coupling reaction using *O*-(trimethylsilyl)hydroxylamine and deprotection (Scheme 8F).

While the described compounds have been patented [9] other promising analogues have been synthesized, but they are not disclosed in this thesis for patentability reason.

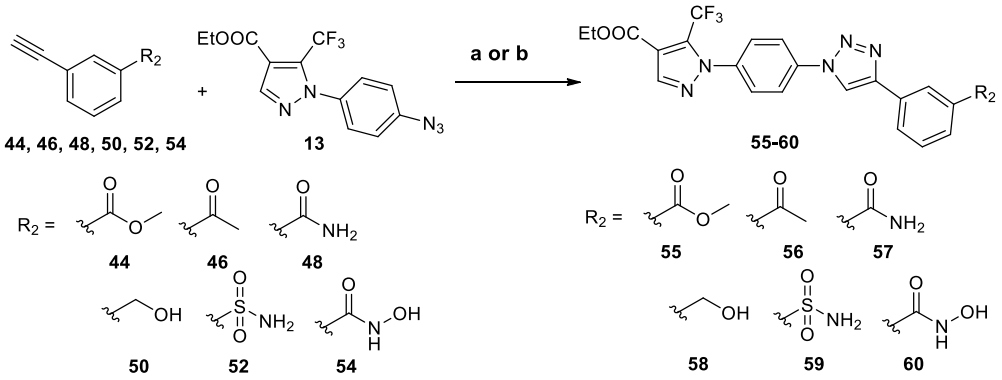

Scheme 7. Modification of the carboxylic moiety of compound **1S**.
(**a**) Sodium ascorbate, $CuSO_4$•5H2O, t-BuOH, H_2O, rt, 16 h, 42-80%. (**b**) TBTA, $Cu(OAc)_2$, sodium ascorbate, THF, H_2O, rt, 16 h, 42%.

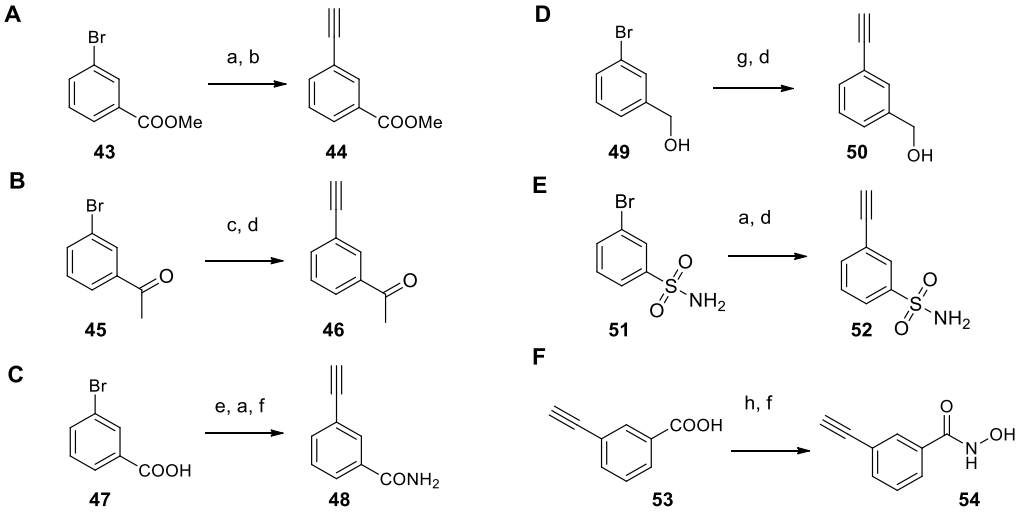

Scheme 8. Synthesis of alkynes.

(**a**) Ethynyltrimethylsilane, DIPEA, CuI, $Pd(PPh_3)_2Cl_2$, toluene, 100 °C, 6 h, 48- 99%; (**b**) TBAF, CH_3COOH, THF, 0 °C, 1 h, 98%; (c) ethynyltrimethylsilane, TEA, CuI, $Pd(PPh_3)_2Cl_2$, THF, 50 °C, 6 h, 98%; (d) K_2CO_3, MeOH, rt, 30 min-1 h, 49-98%; (**e**) Oxalyl chloride, conc. NH_4OH, THF, DMF, rt, 30 min, 98%.(**f**) TBAF, THF, 0 °C, 30 min – 1h, 70-79%; (**g**) ethynyltrimethylsilane, PPh_3, $Pd(OAc)_2$, TEA, 94 °C, 1 h, 65%; (**h**) *O*-(Trimethylsilyl)hydroxylamine, TEA, EDCI, dry CH_2Cl_2, rt, 4 h.

3.3.2. Biological evaluation

The synthesized analogues were screened in the laboratory of Prof. Genazzani for activity on Store-Operated Ca^{2+} Entry in Hek cells, *via* calcium imaging experiments using Fura-2 as a fluorimetric dye. In brief, a multi-plate reader approach was employed in which intracellular stores of Hek cells were emptied with *t*-BhQ (50 µM) in the presence of the compounds (at 10 µM). Calcium was then re-added to the extracellular medium and intracellular levels determined. The results are displayed in Table 1. These included their effect at a concentration of 10 µM, cell viability via the MTT assay at 10 µM and determination of the IC_{50s} for the inhibition of SOCE for the most active compounds in Hek cells. Pyr3 and Pyr6 were used as reference substances.

Cpd	Structure	Residual SOCE activity (% of control)	% viability @ 10 µM	SOCE inhibition IC_{50} (µM)
Pyr3	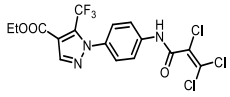	8.9 ± 0.6	28.6 ± 0.4	0.5 ± 0.1
Pyr6	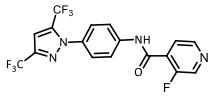	10.3 ± 3.0	70.3 ± 5.8	0.3 ± 0.1
1S	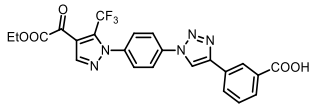	12.8 ± 2.2	84.0 ± 1.0	0.6 ± 0.1
6	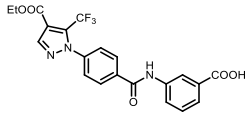	> 90%	ND	ND
12	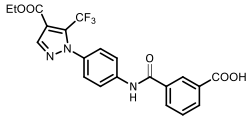	63.5 ± 3.2	65.9 ± 5.3	ND

Cpd	Structure	Residual SOCE activity (% of control)	% viability @ 10 µM	SOCE inhibition IC_{50} (µM)
14	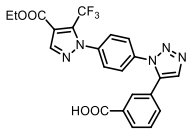	> 90%	ND	ND
22	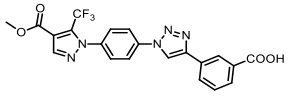	7.9 ± 1.8	69.2 ± 2.5	ND
23	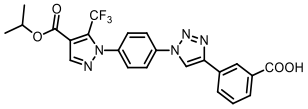	3.5 ± 0.3	87.2 ± 5.8	3.1 ± 1.3
31	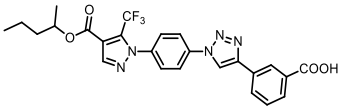	17.5 ± 1.6	93.6 ±4.6	4.4 ± 1.2
32	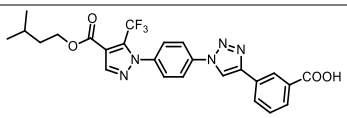	> 90%	ND	ND
33	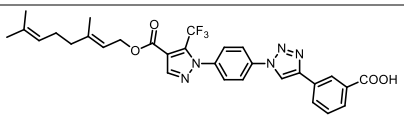	> 90%	ND	ND
34	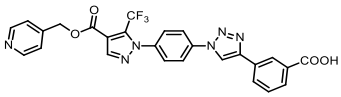	> 90%	ND	ND
35	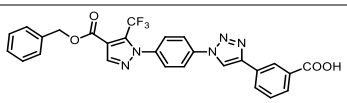	10.5 ± 1.4	82.2 ± 4.3	ND
36	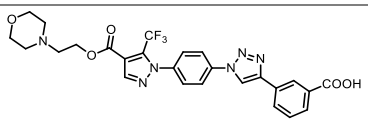	> 90%	ND	ND
38	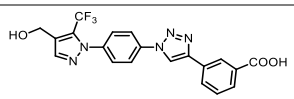	> 90%	ND	ND

Cpd	Structure	Residual SOCE activity (% of control)	% viability @ 10 µM	SOCE inhibition IC_{50} (µM)
40	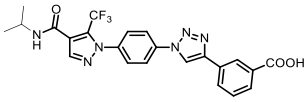	> 90%	ND	ND
41	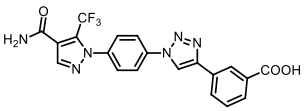	> 90%	ND	ND
42	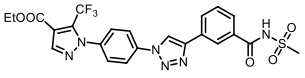	> 90%	ND	ND
55	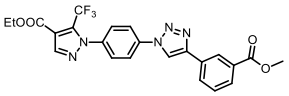	> 90%	ND	ND
56	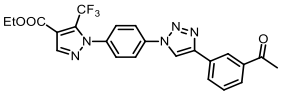	> 90%	ND	ND
57	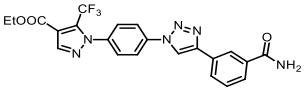	72.1 ± 2.5	ND	ND
58	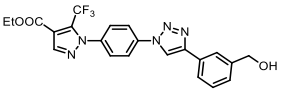	> 90%	ND	ND
59	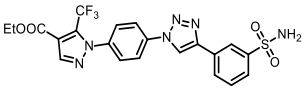	83.6 ± 4.1	ND	ND
60	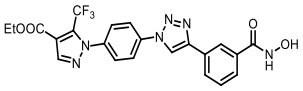	6.4 ± 5.7	67.5 ± 5.0	ND

Table 1. Effect of **1S** analogues on Store-Operated Ca^{2+} Entry, IC_{50} values and cytotoxicity in Hek cells. ND = not determined

3.3.3. SAR study

From the data obtained, the first observation is that the triazole ring does not merely behave as an isostere of the amide group but plays a pivotal role in the modulation of SOCE. Indeed, when substituted with both its direct and the inverse amide (**6** and **12**), a decrease in activity surprisingly occurs, validating this series of compounds as an entirely novel class of SOCE modulators. Moreover, the 1,4-disubstituted triazole ring can not be replaced with the 1,5-disubstituted analogue **14**.

Second, the methyl ester **22** and the isopropyl ester **23** are more active compared to the ethyl ester **1S**, the pentan-2-yl ester **31** inhibits SOCE to the same extent, while the other synthesized esters (**32-36**) lose the ability to act on SOCE. Furthermore, the ethyl ester can not be replaced by a primary alcohol (**38**) or by an amide (**40**, **41**).

Finally, the carboxylic group moiety is not tolerant to the substitution with other functionalities (**42**, **55-59**), except for the hydroxamic acid **60**, which is endowed with remarkable activity, but significantly affects cell viability at 10 µM.

A summary of the SAR is reported in the Figure below.

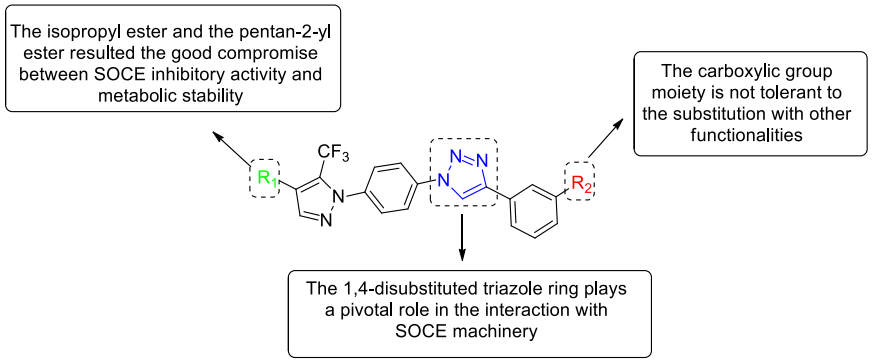

Figure 4. Summary of the SAR study of Pyrtriazole compounds.

3.3.4. Hydrolytic stability, metabolism and selectivity

Given that the ester group in **1S** was susceptible to hydrolysis and the corresponding carboxylic acid resulted inactive, we decided to investigate the hydrolytic stability of **1S** esters, selected according to their activity on SOCE (**22**, **23, 31**, **35**), in mouse plasma. As it can be seen (Table 2) the short linear esters (**1S** and **22**) and the (benzyloxy)carbonyl **35** underwent fast hydrolysis, suggesting that they might not be good *lead compounds* for systemic use. Conversely, the branched esters **23** and **31** showed an overall good stability in plasma, with a residual substrate after 30 minutes of 87.7 and 97.8%, respectively.

Cpd	structure	Plasma stability (residual substrate)
1S	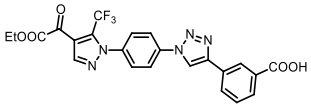	0%
Pyr3	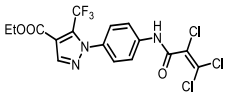	20.4%
22	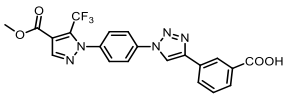	6.5%
23	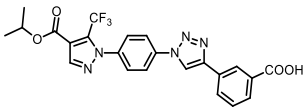	87.7%
31	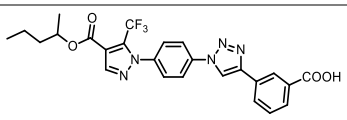	97.8%
35	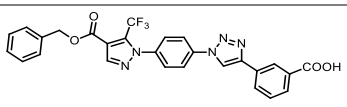	0%

Table 2. Hydrolytic stability of selected **1S** analogues in plasma mouse.

Given that the plasma stability of Pyr3 was poor (20.4% residual substrate after 30 min), **23** and **31** appeared as major improvements in this respect.

Therefore, we decided to evaluate their metabolism in mouse liver homogenates. In mouse liver S9 fractions (MLS9), their hydrolytic stability was confirmed with the residual substrate after 1 hour being 81.3% and 73.7% for **23** and **31**, respectively. We next investigated the *in vitro* oxidative metabolism of the two compounds by performing incubations in the presence of NADPH. Alternatively, given the presence of a carboxyl acid moiety, the formation of acylglucuronide metabolites was assessed by incubating the compounds in mouse liver microsomes (MLM) activated by UDPGA. Overall, hydrolysis of the ester function was the main metabolic pathway in liver metabolism, as no significant differences in residual substrate were observed in the presence or absence of NADPH or UDPGA. However, minute amounts of other metabolites (<1%) were detected and characterized by mass spectrometry analysis. Compound **31** underwent oxidative hydroxylation at the pentan-2-yl chain, giving the metabolite **31-OH** (Figure 5). Moreover, both the carboxyl functions of compounds **23** and **31** were susceptible to the formation of acylglucuronide metabolites (**23-G** and **31-G**; Figure 5). Finally, no traces of glucuronide conjugates of metabolite **61** were detected in the incubations.

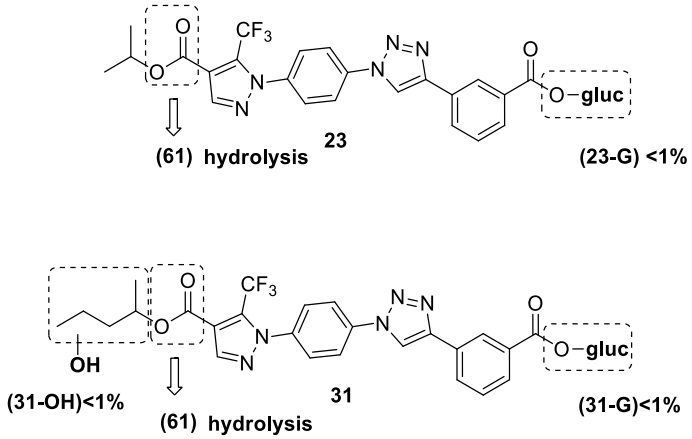

Figure 5. *In vitro* metabolic pathways for compounds **23** and **31**.

Last, the selectivity of **23** and **31** in respect to voltage-operated calcium channels, TRPV1 and TRPM8 channels has been evaluated. Gratifyingly, as it can be observed in Figure 6, neither **23** or **31** had an effect on these channels. This therefore makes these two compounds stand out compared to Pyr3 and Pyr6, in terms of selectivity stability and cytotoxicity.

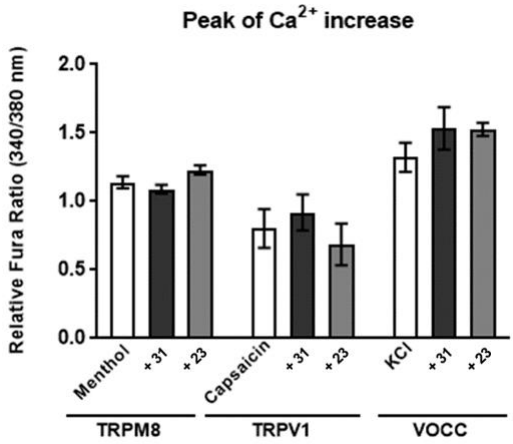

Figure 6. Characterization of the selected compounds. Histograms show the effect of **23** or **31** on the peak amplitude in primary cultures of mouse cerebellar granule cells and in Hek cells over-expressing TRPV1 or TRPM8. Values are mean ± SEM of 600 cells from 30 plates on four separate experimental days.

3.3.5. *Ex vivo* evaluation of 23 and 31 on muscle biopsies from patients affected by TAM

Based on the data obtained about compound **23** in human embryonic kidney Hek cells (cell model used for the screening of all compounds reported, Figure 7A), we evaluated the effect of this molecules in *in vitro* and *ex vivo* models of TAM.

TAM is a rare genetic disease in which either Orai or STIM are mutated with gain of-fuction mutations and lead to an increased Ca^{2+}-entry mainly in muscle and platelets (See Chapter 1.1.3).

To support this hypothesis, by calcium imaging approach, we demonstrated, that **23** (10 μM) was able to restore Ca^{2+} entry to control levels both in a Hek cells

transfected with an Orai1 gain-of-function mutation (Hek Orai1 C290G, Figure 7B) and in cells transfected with non-mutated protein (not shown). Moreover, to further support the possibility that the modulation of this mechanism may represent an efficient pharmacological approach in TAM disease, we decided to investigate whether **23** could counter-act the effect of the same Orai1 mutation (C290G) in a muscle biopsy from a patient affected by tubular aggregate myopathy. As it can be observed in Figure 7C, in the patient biopsy, Ca^{2+}-entry triggered by store depletion was significantly increased compared to Ca^{2+}-entry in a control patient not affected by the disorder. Treatment with 10 µM **23** led to a significant decrease of SOCE, reaching levels similar to the unaffected patient. Furthermore, the same protocol described above was performed for compound **31** (not shown), since compounds **23** and **31** display similar potency and stability. Promisingly, also compound **31** proved to be effective both in *in vitro* and *ex vivo* models of TAM. These data, as a whole, represent the proof-of-concept that symptoms from GoF mutations of STIM or Orai can be corrected *via* this pharmacological approach.

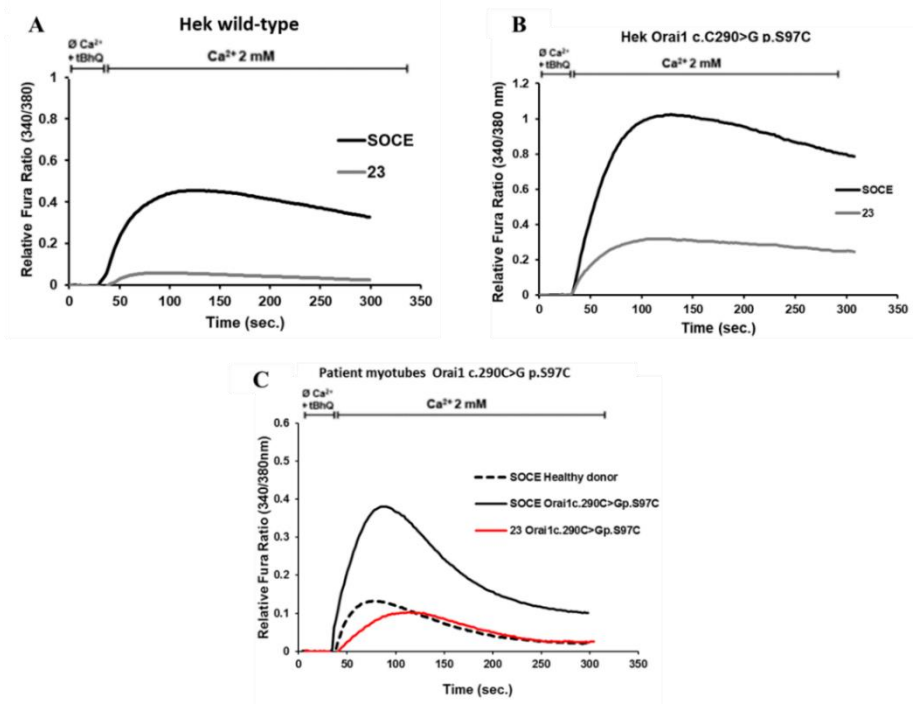

Figure 7. (**A**) Effect of **23** on Hek wild-type cells; (**B**) effect of **23** on mutated embryonic kidney (Hek Orai1 C290G) cells (**C**) effect of **23** on a muscle biopsy from a patient bearing the Orai1 C290G mutation.

3.3.6. *In vivo* evaluation of 31 in an animal model of acute pancreatitis

Besides evaluating our SOCE inhibitors in the aforementioned genetic diseases, in collaboration with Prof. Cuzzocrea, we opted to verify the potential use of **31** in acute pancreatitis.

First, to verify its tolerability, we investigated its toxicity after a single dose (40 mg/Kg) for 14 days, monitoring mortality, body weight, clinical signs of distress and histological alterations of major organs (brain, heart, liver, lung, kidney, lung, stomach and ileum) in accordance to the OECD guideline for acute toxicity. None of the 6 treated animals showed any alterations.

We next performed a pharmacokinetic analysis to further characterize the compound. The half-life of **31** was 1.3 hours, with a C_{max} of 640 μg/L after 1 hour. The clearance was 17 L/h/Kg, with a volume of distribution of 32 L/Kg. Despite the surprisingly high volume of distribution, the plasma concentrations reached (approx. 1.2 μM) led us to believe that it might have exerted a therapeutic effect and decided therefore to perform proof-of-principle *in vivo* experiment. It has been demonstrated that GSK-7975A and CM128 were protective against POAEE-induced necrosis of pancreatic acinar cells in three separate models of chemically-induced acute pancreatitis, including the model that uses cerulein. Indeed, a clinical trial has been initiated on CM4620, another SOCE inhibitor. Given that this is an acute disorder, we reasoned that **31**, with a half-life of hours, might have been suitable. **31** was given twice (40 mg/Kg, n = 10) by intraperitoneal injection, 30 and 150 minutes after the first cerulein injection. As shown in Figure 8, the histological scores were significantly ameliorated by treatment with **31**. This was evident in the

haematoxylin/eosin stainings, when evaluating oedema and inflammation and when determining neutrophil infiltration via MPO staining.

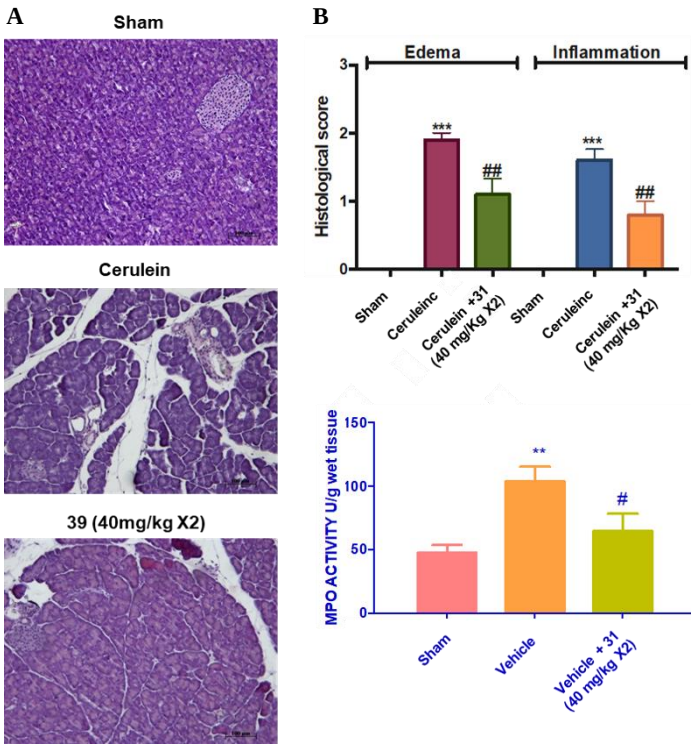

Figure 8. Evaluation of compound **31** in a model of acute pancreatitis**.**
(**A**) H&E sections of pancreatic tissues were assessed at 200X magnification over ten separate fields for severity of pancreatitis. (**B**) Evaluation of edema, inflammatory infiltration and apoptosis was performed with a three point scoring system (edema-0: absent or rare, 1: in the interlobular space, 2: in the intralobular space, 3: the isolated-island shape of pancreatic acinus; inflammation-0: absent, 1: mild (infiltration in ducts), 2: moderate (infiltration in parenchyma < 50%), 3: severe (infiltration in parenchyma > 50%); parenchyma apoptosis-0: absent, 1: focal (<5%), 2: and/or sublobular (<20%), 3: and/or lobular (>20%)). Analysis were performed in a blinded manner. (**C**) MPO activity.
Data represent the mean ± standard error of the mean (SEM) of 10 mice for each group. ***p < 0.001; **p < 0.05 versus Sham; ##p < 0.05; #p < 0.5 versus cerulein.

3.4. Conclusions

In conclusion, we have discovered a novel class of agents that are able to modulate Store-Operated Ca^{2+} Entry and starting from a promising *hit* we have performed a SAR study. While almost all the SOCE inhibitors reported to date share an arylamide moiety, the modulators described by us display a 1,4-diaryl-*1H*-1,2,3-triazole ring.

We selected two structural analogues (**23** and **31**), according to SOCE inhibition, cytotoxicity and extent of hydrolysis, for further investigations on metabolic stability and selectivity. These analogues display IC_{50s} in the low micromolar range and are specific on SOCE compared to the channels evaluated in the present study (voltage-operated, TRPV1 and TRPM8). Moreover, these compounds appeared suitable as *lead compounds* for systemic use as they were relatively stable. Indeed, slow hydrolysis of the ester function was the main metabolic pathway both in mouse plasma and liver, with minute formation of the oxidative (**23**) or glucuronidated (**23** and **31**) metabolites. The *ex vivo* experiments demonstrated that **23** and **31** may have a value in the therapy of tubular aggregate myopathy, a disease characterized by gain-of-function mutations in either STIM or Orai. This conclusion has promped our lab to develop *via* a commercial service (PolyGene Transgenics, CH) a knock-in animal model (KI-STIM1^{I115}) that bears one of the most frequent mutations in Italy, STIM1 (I115F). The characterization showed that the litters are viable and heterozygous animals (tested at 1 and 3, 6 and 12 months) display muscle weakness, as observed in rotarod and treadmill tests. Furthermore, the murine muscles exhibit contraction and relaxation defects as well as dystrophic features, and functional investigations display an increased Ca^{2+} influx in myotubes. Once concluded the characterization of this transgenic mouse model, one of our best negative modulators will be evaluated *in vivo*, to further strengthen the possibility that Pyrtriazoles have the potential to become a viable strategy in the treatment of TAM.

On the other hand, the *in vivo* study performed on **31** showed that half-life was 1.3 hours and a twice-administration of the compound significantly ameliorated cerulein-induced pancreatitis, in the absence of signs of toxicity. Yet, the high volume of distribution and the short half-life *in vivo* might suggest that further refinements are necessary and indeed these are already being investigated by our research group.

Overall, the described compounds hold great promise to both get insights into the biological role of SOCE and pave the way for the treatment of human disorders arising from imbalanced calcium homeostasis.

3.5. Experimental section

General Methods. Commercially available reagents and solvents were used as purchased without further purification. When needed, solvents were distilled and stored on molecular sieves. Column chromatography was performed on silica gel Merck Kieselgel 70-230 mesh ASTM. Thin layer chromatography (TLC) was carried out on 5 cm × 20 cm plates with a layer thickness of 0.25 mm (Merck silica gel 60 F254). When necessary, TLC plates were visualized with aqueous $KMnO_4$ or with aqueous Pancaldi solution. Melting points were determined in open glass capillary with a Stuart scientific SMP3 apparatus. All the target compounds were checked by IR (FT-IR Thermo-Nicolet Avatar), ^{1}H and ^{13}C NMR (Jeol ECP 300 MHz), and mass spectrometry (Thermo Finningan LCQ-deca XP-plus) equipped with an ESI source and an ion trap detector. Chemical shifts are reported in parts per million (ppm).

3.5.1. Chemistry

Benzyl 3-aminobenzoate, (2).

3-Aminobenzoic acid (1.00 g, 7.29 mmol) was dissolved in dry DMF (20 mL). Then anhydrous K_2CO_3 (1.11 g, 8.15 mmol) was added followed by dropwise addition of

benzyl bromide (0.87 mL, 7.29 mmol). The resulting mixture was stirred at room temperature for 16 h, then diluted with aqueous saturated Na_2CO_3 solution and extracted with ethyl acetate (x3). The combined organic phases were washed with brine, dried over sodium sulfate and concentrated. The crude material was purified by column chromatography using petroleum ether/ethyl acetate 98:2 and then petroleum ether/ethyl acetate 9:1 as eluent to give compound **2** (777 mg, 3.42 mmol, 47%) as a pale yellow oil. ^{1}H NMR (300 MHz, $CDCl_3$): δ = 7.55 (d, *J* = 7.7 Hz, 1H), 7.50-7.35 (m, 6H), 7.21 (t, *J* = 7.7 Hz, 1H), 6.84 (d, *J* = 7.7 Hz, 1H), 5.38 (br s, 2H), 3.91 (s, 2H). MS (ESI): *m/z*: 228 $[M + H]^+$.

4-(4-(Ethoxycarbonyl)-5-(trifluoromethyl)-1H-pyrazol-1-yl)benzoic acid, (3).

To a solution of 4-hydrazinylbenzoic acid (1 g, 6.58 mmol) in EtOH (10 mL), THF (2 mL) was added and the reaction mixture was cooled at -8 °C under nitrogen atmosphere. Then (*E*)-ethyl 2-(ethoxymethylene)-4,4,4-trifluoro-3-oxobutanoate (1.28 mL, 6.58 mmol) was added dropwise. After stirring at room temperature for 3 h the mixture was filtered under vacuum and rinsed with heptane to give compound **3** (2 g, 6.10 mmol, 93%) as a dark white solid. ^{1}H NMR (300 MHz, DMSO-d_6): δ = 8.36 (s, 1H), 8.14 (d, *J* = 7.5 Hz, 2H), 7.71 (d, *J* = 7.5 Hz, 2H), 4.36 (q, *J* = 7.1 Hz, 2H), 1.33 (t, *J* = 7.1 Hz, 3H). MS (ESI): *m/z*: 329 $[M + H]^+$.

3-(4-(4-(Ethoxycarbonyl)-5-(trifluoromethyl)-1H-pyrazol-1-yl)benzamido)benzoic acid, (6).

Step 1: To a solution of compound **2** (0.53 g, 2.33 mmol) in dry CH_2Cl_2 (13 mL), EDCI (0.73 g, 3.61 mmol), DIPEA (0.74 g, 5.74 mmol), DMAP (23.4 mg, 0.19 mmol) and compound **3** (0.63 g, 1.91 mmol) were added in order. The reaction was stirred at room temperature for 16 h. Then, CH_2Cl_2 is added and the organic phase was washed with 3N HCl (x4), dried over sodium sulfate and evaporated to afford ethyl 1-(4-((3-((benzyloxy)carbonyl)phenyl)carbamoyl)phenyl)-5-(trifluoromethyl)-1*H*-pyrazole-4-carboxylate (1.18 mg, 2.19 mmol, 94%) as a white solid. ^{1}H NMR (300 MHz, $CDCl_3$): δ = 8.46 (s, 1H), 8.14-8.03 (m, 3H), 8.00 (d, *J* =

8.3 Hz, 2H), 7.84 (d, *J* = 7.7 Hz, 1H), 7.46 (d, *J* = 8.3 Hz, 2H), 7.42-7.29 (m, 5H), 5.32 (s, 2H), 4.39 (q, *J* = 7.1 Hz, 2H), 1.37 (t, *J* = 7.1 Hz, 3H). MS (ESI): *m/z*: 536 $[M - H]^-$.

Step 2: Ethyl 1-(4-((3-((benzyloxy)carbonyl)phenyl)carbamoyl)phenyl)-5-(trifluoromethyl)-1*H*-pyrazole-4-carboxylate (500 mg, 0.93 mmol), Pd/C (5 wt%, 150 mg, 0.07 mmol of Pd) and MeOH (5 mL) were added in order under hydrogen atmosphere and the resulting mixture was stirred for 1 h at room temperature. Then, the reaction was filtered under vacuo over a pad of celite, rinsed with ethyl acetate and evaporated. The crude material was subjected to column chromatography using petroleum ether/ethyl acetate 4:6, petroleum ether/ethyl acetate 2:8 and ethyl acetate (+0.1% HCOOH) to give compound **6** (228 mg, 0.51 mmol, 55%) as a white solid. mp 281-282 °C dec. ^{1}H NMR (300 MHz, CD_3OD): δ = 8.39 (s, 1H), 8.20 (s, 1H), 8.13 (d, *J* = 8.1 Hz, 2H), 7.99 (d, *J* = 7.9 Hz, 1H), 7.83 (d, *J* = 7.9 Hz, 1H), 7.65 (d, *J* = 8.1 Hz, 2H), 7.49 (t, *J* = 7.9 Hz, 1H), 4.38 (q, *J* = 7.1 Hz, 2H), 1.38 (t, *J* = 7.1 Hz, 3H). ^{13}C NMR (75 MHz, DMSO-d_6): δ = 167.7, 165.2, 160.3, 143.0, 141.8, 139.8, 136.8, 132.5 (q, *J* = 38.2 Hz), 132.0, 129.5, 129.4, 126.8, 125.0, 124.9, 121.3, 119.7 (q, *J* = 260.3 Hz), 117.1, 61.7, 14.5. IR (KBr): $\tilde{\nu}$ = 3271, 2990, 2663, 2534, 1661, 1242, 1137, 709, 564 cm^{-1}. MS (ESI): *m/z* 448 $[M + H]^+$.

3-((Benzyloxy)carbonyl)benzoic acid, (8).

To a solution of isophthalic acid (1.66 g, 10 mmol) in MeOH (20 mL) and water (2 mL) TEA (1.40 mL, 10.1 mmol) was added. The reaction was stirred at room temperature overnight. Then, DMF (25 mL) was added followed by dropwise addiction of benzyl bromide (1.31 mL, 11 mmol) and the resulting mixture was heated at 100 °C for 16 h. Aqueous saturated $NaHCO_3$ solution was added and the reaction was extracted with ethyl acetate (x2). The collected organic phases were washed with brine, dried over sodium sulfate and evaporated. The crude material was purified by column chromatography using petroleum ether/ethyl acetate 7:3 and petroleum ether/ethyl acetate 6:4 (+0.1% HCOOH) as eluent to give compound **8**

(922 mg, 3.60 mmol, 36%) as a white solid. ^{1}H NMR (300 MHz, $CDCl_3$): δ = 8.80 (s, 1H), 8.42-8.30 (m, 2H), 7.57 (t, *J* = 5.2 Hz, 1H), 7.49-7.34 (m, 5H), 5.46 (s, 2H). MS (ESI): *m/z*: 257 $[M + H]^+$.

Ethyl 1-(4-aminophenyl)-5-(trifluoromethyl)-1H-pyrazole-4-carboxylate, (9).

Ethyl acetate (30 mL), Pd/C (5 wt%, 0.9 g) and compound **62** (3.00 g, 9.12 mmol) were added in order under hydrogen atmosphere. After stirring at room temperature for 2 h the resulting mixture was filtered under vacuo over a pad of celite, rinsed with ethyl acetate and evaporated to give compound **9** (2.56 g, 8.57 mmol, 94%) as a yellow solid. ^{1}H NMR (300 MHz; $CDCl_3$): δ = 8.06 (s, 1H), 7.17 (d, *J* = 8.5 Hz, 2H), 6.72 (d, *J* = 8.5 Hz, 2H), 4.37 (q, *J* = 7.1 Hz, 2H), 3.19 (br s, 2H), 1.39 (t, *J* = 7.1 Hz, 3H). MS (ESI): *m/z*: 300 $[M + H]^+$.

3-((4-(4-(Ethoxycarbonyl)-5-(trifluoromethyl)-1H-pyrazol-1-yl)phenyl)carbamoyl)benzoic acid, (12).

Step 1: Ethyl 1-(4-(3-((benzyloxy)carbonyl)benzamido)phenyl)-5-(trifluoromethyl)-1*H*-pyrazole-4-carboxylate was synthesized as previously reported for the preparation of compound **6** in step 1, starting from compound **8** (350 mg, 1.17 mmol) and compound **9 (**290 mg, 0.97 mmol). The crude material was purified by column chromatography using petroleum ether/ethyl acetate 9:1, petroleum ether/ethyl acetate 8:2 and petroleum ether/ethyl acetate 7:3 as eluent yielding ethyl 1-(4-(3-((benzyloxy)carbonyl)benzamido)phenyl)-5-(trifluoromethyl)-1*H*-pyrazole-4-carboxylate (527 mg, 0.98 mmol, 84%) as a yellow solid. ^{1}H NMR (300 MHz, $CDCl_3$): δ = 9.01 (s, 1H), 8.50 (s, 1H), 8.26-8.01 (m, 3H), 8.00 (d, *J* = 8.3 Hz, 2H), 7.51-7.23 (m, 7H), 5.30 (s, 2H), 4.31 (q, *J* = 7.1 Hz, 2H), 1.35 (t, *J* = 7.1 Hz, 3H). MS (ESI): *m/z*: 538 $[M + H]^+$.

Step 2: The title compound was synthesized as previously reported for the preparation of compound **6** in step 2, starting from ethyl 1-(4-(3-((benzyloxy)carbonyl)benzamido)phenyl)-5-(trifluoromethyl)-1*H*-pyrazole-4-carboxylate (165 mg, 0.31 mmol). The crude material was subjected to column

chromatography using petroleum ether/ethyl acetate 4:6, petroleum ether/ethyl acetate 2:8 and petroleum ether/ethyl acetate 9:1 (+ 0.1% HCOOH) to give compound **12** (98 mg, 0.22 mmol, 72%) as a white solid. mp 269.5-270.5 °C dec. ^{1}H NMR (300 MHz, CD_3OD): δ = 8.62 (s, 1H), 8.25-8.23 (m, 2H), 8.16 (s, 1H),7.95 (d, *J* = 8.9 Hz, 2H), 7.65 (t, *J* = 7.6 Hz, 1H), 7.47 (d, *J* = 8.9 Hz, 2H), 4.37 (q, *J* = 7.4 Hz, 2H), 1.38 (t, *J* = 7.1 Hz, 3H). ^{13}C NMR (75 MHz, DMSO-d_6): δ = 167.4, 165.7, 160.9, 142.6, 141.1, 135.6, 134.7, 133.0, 132.6, 132.1 (q, *J* = 38.2 Hz), 131.8, 129.5, 129.1, 127.1, 121.1, 120.4 (q, *J* = 276.4 Hz), 116.6, 61.6, 14.5. IR (KBr): $\tilde{\nu}$ = 3335, 1655, 1540, 1243, 1136, 845, 736 cm^{-1}. MS (ESI): *m/z* 448 $[M + H]^+$.

Ethyl 1-(4-azidophenyl)-5-(trifluoromethyl)-1H-pyrazole-4-carboxylate, (13).

To a suspension of compound **9** (2.60 g, 8.70 mmol) in water (40.7 mL) 37% HCl aqueous solution (3.3 mL) was added. The resulting mixture was cooled at 0 °C and a solution of $NaNO_2$ (0.57 g, 8.26 mmol) in water (3.9 mL) was added. After 10 min a solution of NaN_3 (0.64 g, 9.85 mmol) in water (3.9 mL) was added and the reaction was left to reach room temperature and stirred for 1 h. The mixture was worked up by dilution with ethyl acetate and washing with water (x1). The organic layer was dried over sodium sulfate and evaporated yielding compound **13** (2.20 g, 6.77 mmol, 78%) as a pale red oil. ^{1}H NMR (300 MHz, $CDCl_3$): δ = 8.08 (s, 1H), 7.39 (d, *J* = 8.5 Hz, 2H), 7.11 (d, *J* = 8.5 Hz, 2H), 4.35 (q, *J* = 7.1 Hz, 2H), 1.37 (t, *J* = 7.1 Hz, 3H). ^{13}C NMR (75 MHz, $CDCl_3$): δ = 160.9, 142.6, 141.9, 135.9, 133.6 (q, J = 39.0 Hz), 127.4, 119.6, 119.1 (q, J = 269.1 Hz), 116.9, 61.4, 14.1. IR (KBr) $\tilde{\nu}$ = 3406, 3221, 2987, 2415, 2096, 1713, 1560, 1510, 1355, 1286, 1148, 971, 848, 558, 404 cm^{-1}.

3-(1-(4-(4-(Ethoxycarbonyl)-5-(trifluoromethyl)-1H-pyrazol-1-yl)phenyl)-1H-1,2,3-triazol-5-yl)benzoic acid, (14).

To a solution of compound **13** (100 mg, 0.31 mmol) and commercially available 3-ethynylbenzoic acid (44.9 mg, 0.31 mmol) in DMF (1.7 mL) Cp*RuCl(cod) (11.7 mg, 0.1 mmol) was added. The reaction tube was flushed with nitrogen, capped and

heated at 90 ºC for 10 min in microwave (CEM Discover SP) to give compound **14** (57 mg, 0.12 mmol, 39%) as an amorphous yellow solid. ^{1}H NMR (300 MHz, $CDCl_3$): δ = 8.25 (s, 1H), 8.05-7.98 (m, 2H), 7.54-7.43 (m, 3H), 7.28-7.26 (m, 2H), 6.85 (d, *J* = 7.9 Hz, 2H), 4.37 (q, *J* = 7.3 Hz, 2H), 1.35 (t, *J* = 7.3 Hz, 3H). ^{13}C NMR (75 MHz, DMSO-d_6): δ = 169.5, 165.4, 144.2, 139.7, 134.9 (q, *J* = 41.2 Hz), 133.7 (2C), 132.0, 131.8, 131.4, 131.0, 129.8, 129.3, 126.7, 121.5, 119.8, 118.7 (q, *J* = 280.8 Hz), 114.5, 62.6, 14.2. IR (neat): $\tilde{\nu}$ = 3281, 2920, 2851, 1719, 1684, 1296, 1246, 1150, 1039, 753, 679 cm^{-1}. MS (ESI): *m/z* 472 $[M + H]^+$.

***Ethyl 1-(4-nitrophenyl)-5-(trifluoromethyl)-1H-pyrazole-4-carboxylate,* (15).**

To a solution of (4-nitrophenyl) hydrazine hydrochloride (1.99 g, 10.5 mmol) in DMF (20 mL) compound **10** (2.15 mL, 11.04 mmol) was added. The resulting mixture was stirred at reflux for 2 h. Then, diethyl ether was added and the organic layer was washed with water (x2), dried over sodium sulfate and evaporated to give compound **15** (3.32 g, 10.08 mmol, 96%) as a deep yellow solid. ^{1}H NMR (300 MHz; $CDCl_3$): δ = 8.39 (d, *J* = 8.8 Hz, 2H), 8.16 (s,1H), 7.66 (d, *J* = 8.8 Hz, 2H), 4.38 (q, *J* = 7.1 Hz, 2H), 1.38 (t, *J* = 7.1 Hz, 3H). MS (ESI): *m/z*: 330 $[M + H]^+$.

Methyl 1-(4-nitrophenyl)-5-(trifluoromethyl)-1H-pyrazole-4-carboxylate, (16).

Compound **15** (500 mg, 1.52 mmol) was solubilized in MeOH (15 mL) and concentrated H_2SO_4 (950 µL) was added dropwise. The mixture was stirred at reflux for 16 h, then volatile was removed under vacuo. Ethyl acetate was added and the organic phase was washed with aqueous saturated $NaHCO_3$ solution (x1), dried over sodium sulfate and evaporated, affording compound **16** (388 mg, 1.23 mmol, 81%) as a yellow solid. ^{1}H NMR (300 MHz, $CDCl_3$): δ = 8.38 (d, *J* = 8.8 Hz, 2H), 8.16 (s, 1H), 7.65 (d, *J* = 8.8 Hz, 2H), 3.89 (s, 3H). MS (ESI): *m/z* 316 $[M + H]^+$.

Isopropyl 1-(4-nitrophenyl)-5-(trifluoromethyl)-1H-pyrazole-4-carboxylate, (17).

The title compound was synthesized as previously reported for the preparation of compound **16**, starting from compound **15** (516 mg, 1.57 mmol) and using 2-

propanol as solvent (15 mL). After evaporation, compound **17** was collected (484 mg, 1.41 mmol, 90%) as a yellow oil. ^{1}H NMR (300 MHz; $CDCl_3$): δ = 8.35 (d, *J* = 8.8 Hz, 2H), 8.12 (s, 1H), 7.63 (d, *J* = 8.8 Hz, 2H), 5.21 (ept, *J* = 6.3 Hz, 1H), 1.31 (d, *J* = 6.3 Hz, 6H). MS (ESI): *m/z*: 344 $[M + H]^+$.

Methyl 1-(4-aminophenyl)-5-(trifluoromethyl)-1H-pyrazole-4-carboxylate, (18).

The title compound was synthesized as previously reported for the preparation of compound **9**, starting from compound **16** (354 mg, 1.11 mmol). The crude material was filtered under vacuo over a pad of celite, rinsed with ethyl acetate and evaporated to give compound **18** (297 mg, 1.04 mmol, 94%) as a pale yellow solid. ^{1}H NMR (300 MHz; $CDCl_3$): δ = 8.06 (s, 1H), 7.16 (d, *J* = 8.4 Hz, 2H), 6.70 (d, *J* = 8.4 Hz, 2H), 3.89 (s, 3H). MS (ESI): *m/z*: 286 $[M + H]^+$.

Isopropyl 1-(4-aminophenyl)-5-(trifluoromethyl)-1H-pyrazole-4-carboxylate, (19).

The title compound was synthesized as previously reported for the preparation of compound **9**, starting from compound **17** (486 mg, 1.42 mmol). The crude material was filtered under vacuo over a pad of celite, rinsed with ethyl acetate and evaporated to give compound **19** (404 mg, 1.29 mmol, 91%) as a yellow oil. ^{1}H NMR (300 MHz; $CDCl_3$): δ = 8.00 (s, 1H), 7.06 (d, *J* = 6.7 Hz, 2H), 6.61 (d, *J* = 6.7 Hz, 2H), 5.15 (ept, *J* = 6.1 Hz, 1H), 4.78 (br s, 2H), 1.26 (d, *J* = 6.1 Hz, 6H). MS (ESI): *m/z*: 314 $[M + H]^+$.

Methyl 1-(4-azidophenyl)-5-(trifluoromethyl)-1H-pyrazole-4-carboxylate, (20).

The title compound was synthesized as previously reported for the preparation of compound **13**, starting from compound **18** (276 mg, 0.97 mmol). After evaporation, compound **20** was recovered (261 mg, 0.84 mmol, 87%) as a yellow oil. ^{1}H NMR (300 MHz, CDCl3): δ = 8.05 (s, 1H), 7.36 (d, *J* = 8.3 Hz, 2H), 7.08 (d, *J* = 8.3 Hz, 2H), 3.85(s, 3H).

Isopropyl 1-(4-azidophenyl)-5-(trifluoromethyl)-1H-pyrazole-4-carboxylate, (21).

The title compound was synthesized as previously reported for the preparation of compound **13**, starting from compound **19** (362 mg, 1.16 mmol). The crude material was purified by column chromatography using petroleum ether/ethyl acetate 8:2 as eluent, yielding compound **21** (224 mg, 0.72 mmol, 62%) as a yellow oil. ^{1}H NMR (300 MHz, $CDCl_3$): δ = 8.07 (s, 1H), 7.38 (d, *J* = 8.5 Hz, 2H), 7.11 (d, *J* = 8.5 Hz, 2H), 5.22 (ept, *J* = 6.0 Hz, 1H), 1.34 (d, *J* = 6.0 Hz, 6H).

1-(4-Azidophenyl)-5-(trifluoromethyl)-1H-pyrazole-4-carboxylic acid, (24).

To a solution of compound **13** (1.00 g, 3.07 mmol) in THF (10 mL) and water (10 mL) NaOH (0.25 g, 6.15 mmol) was added and the resulting mixture was stirred at room temperature for 8 h. Then, ethyl acetate was added and the organic phase was washed with 3N HCl (x1) and brine (x1), dried over sodium sulfate and evaporated, yielding compound **24** (0.55 g, 1.84 mmol, 60%) as a white solid. ^{1}H NMR (300 MHz, $CDCl_3$): δ = 8.20 (s, 1H), 7.43 (d, *J* = 8.8 Hz, 2H), 7.15 (d, *J* = 8.8 Hz, 2H). MS (ESI): *m/z* 298 $[M + H]^+$.

General procedure for the synthesis of compounds 25-30

To a solution of compound **24** (131 mg, 0.44 mmol) in dry CH_2Cl_2 (2.88 mL) EDCI (92 mg, 0.48 mmol), TEA (67 µL, 0.48 mmol), DMAP (5.37 mg, 0.05 mmol) and the corresponding alcohol (1.1 eq) were added in order. The resulting mixture was stirred at room temperature for 16 h. CH_2Cl_2 was added and the organic phase was washed with 3N HCl (x3), dried over sodium sulfate and evaporated. Purification by column chromatography using petroleum ether/ethyl acetate 98:2, petroleum ether/ethyl acetate 95:5 as eluent yielded compounds **25-30.**

Characterization of compounds 25-30.

Pentan-2-yl 1-(4-azidophenyl)-5-(trifluoromethyl)-1H-pyrazole-4-carboxylate, (25).

White solid; yield 47% (76 mg, 0.21 mmol); mp 129-130 °C dec. ^{1}H NMR (300 MHz, $CDCl_3$): δ = 8.07 (s, 1H), 7.38 (d, *J* = 8.5 Hz, 2H), 7.11 (d, *J* = 8.5 Hz, 2H), 5.14 (sex, *J* = 6.3 Hz, 1H), 1.78-1.63 (m, 1H), 1.52-1.60 (m,1H), 1.36-1.18 (m, 5H), 0.92 (t, *J* = 7.2 Hz, 3H).

Isopentyl 1-(4-azidophenyl)-5-(trifluoromethyl)-1H-pyrazole-4-carboxylate, (26).

Yellow oil; yield 68% (110 mg, 0.30 mmol). ^{1}H NMR (300 MHz, $CDCl_3$): δ = 8.09 (s, 1H), 7.40 (d, *J* = 8.0 Hz, 2H), 7.13 (d, *J* = 8.0 Hz, 2H), 4.34 (t, *J* = 6.6 Hz, 2H), 1.72-1.63 (m, 3H), 0.96 (d, *J* = 6.6 Hz, 6H).

(E)-3,7-Dimethylocta-2,6-dien-1-yl 1-(4-azidophenyl)-5-(trifluoromethyl)-1H-pyrazole-4-carboxylate, (27)

Yellow oil; yield 48% (91 mg, 0.21 mmol). ^{1}H NMR (300 MHz, $CDCl_3$): δ = 8.10 (s, 1H), 7.40 (d, *J* = 8.2 Hz, 2H), 7.13 (d, *J* = 8.2 Hz, 2H), 5.44 (t, *J* = 6.9 Hz, 1H), 5.08 (t, *J* = 6.9 Hz, 1H), 4.82 (d, *J* = 6.9 Hz, 2H), 2.11-2.08 (m, 4H), 1.80 (s, 3H), 1.67 (s, 3H), 1.60 (s, 3H).

Pyridin-4-ylmethyl 1-(4-azidophenyl)-5-(trifluoromethyl)-1H-pyrazole-4-carboxylate, (28).

White solid; yield 48% (82 mg, 0.21 mmol); mp 149-150 °C. ^{1}H NMR (300 MHz, $CDCl_3$): δ = 8.60 (d, *J* = 5.8 Hz, 2H), 8.14 (s, 1H), 7.37 (d, *J* = 8.8 Hz 2H), 7.29 (d, *J* = 5.8 Hz, 2H), 7.11 (d, *J* = 8.8, 2H), 5.33 (s, 2H).

Benzyl 1-(4-azidophenyl)-5-(trifluoromethyl)-1H-pyrazole-4-carboxylate, (29).

White solid; yield 60% (101 mg, 0.26 mmol); mp 136-137 °C. ^{1}H NMR (300 MHz, $CDCl_3$): δ = 8.13 (s, 1H), 7.60-7.23 (m, 7H), 7.13 (d, *J* = 8.5 Hz, 2H), 5.36 (s, 2H).

2-Morpholinoethyl 1-(4-azidophenyl)-5-(trifluoromethyl)-1H-pyrazole-4-carboxylate, (30).

Yellow oil; yield 55% (98 mg, 0.24 mmol). ^{1}H NMR (300 MHz, $CDCl_3$): δ = 8.09 (s, 1H), 7.40 (d, *J* = 8.5 Hz, 2H), 7.13 (d, *J* = 8.5 Hz, 2H), 4.43 (t, *J* = 5.8 Hz, 2H), 3.82 (t, *J* = 4.11 Hz, 4H), 2.73 (t, *J* = 5.8 Hz, 2H), 2.55 (t, J = 4.11 Hz, 4H).

(1-(4-Azidophenyl)-5-(trifluoromethyl)-1H-pyrazol-4-yl)methanol, (37).

Step 1: To a solution of compound **9** (166 mg; 0.55 mmol) in dry THF (4 mL) $LiAlH_4$ (20.9 mg, 0.55 mmol) was added at 0 °C and under nitrogen atmosphere. The reaction was left to reach room temperature. After 6 h the reaction was quenched with ethyl acetate and then with saturated aqueous solution of sodium sulfate. The mixture was filtered over a pad of celite and rinsed with ethyl acetate. The organic phase was washed with water and dried over sodium sulfate and evaporated. The crude material was purified with chromatography column using petroleum ether/ethyl acetate 7:3 as eluent to give (1-(4-aminophenyl)-5-(trifluoromethyl)-1*H*-pyrazol-4-yl)methanol (113.3 mg, 0.44 mmol, 80%) as a yellow solid. ^{1}H NMR (300 MHz, $CDCl_3$): δ = 7.69 (s, 1H), 7.17 (d, *J* = 7.9 Hz, 2H), 6.69 (d, *J* = 7.9 Hz, 2H), 4.73 (s, 2H). MS (ESI): *m/z* 258 $[M + H]^+$.

Step 2: The title compound was synthesized as previously reported for the preparation of compound **13**, starting from (1-(4-aminophenyl)-5-(trifluoromethyl)-1*H*-pyrazol-4-yl)methanol (107 mg, 0.42 mmol). After evaporation, compound **37** was recovered (109.4 mg, 0.39 mmol, 92%) as a yellow oil. ^{1}H NMR (300 MHz, $CDCl_3$): δ = 7.74 (s, 1H), 7.40 (d, *J* = 7.1 Hz, 2H), 7.10 (d, *J* = 7.1 Hz, 2H), 4.72 (s, 2H).

1-(4-Azidophenyl)-N-isopropyl-5-(trifluoromethyl)-1H-pyrazole-4-carboxamide, (39).

To a solution of compound **24** (407.5 mg, 1.37 mmol) in dry CH_2Cl_2 (4 mL) EDCI (315.6 mg, 1.65 mmol), TEA (420 µL, 3.02 mmol), HOBt (222.5 mg, 1.65 mmol)

and isopropyl amine (141 µL, 1.65 mmol) were added in order. The resulting mixture was stirred at room temperature for 16 h. CH_2Cl_2 was added and the organic phase was washed with aqueous saturated NH_4Cl solution (x1), dried over sodium sulfate and evaporated. Purification by column chromatography using petroleum ether/ethyl acetate 8:2 and petroleum ether/ethyl acetate 7:3 as eluents yielded compound **39** (272 mg, 0.80 mmol, 59%) as a white solid. ^{1}H NMR (300 MHz, CD_3OD): δ = 7.93 (s, 1H), 7.49 (d, *J* = 8.5 Hz, 2H), 7.24 (d, *J* = 8.5 Hz, 2H), 4.14 (ept, *J* = 6.3 Hz, 1H), 1.23 (d, *J* = 6.3 Hz, 6H).

3-(1-(4-(4-Carbamoyl-5-(trifluoromethyl)-1H-pyrazol-1-yl)phenyl)-1H-1,2,3-triazol-4-yl)benzoic acid, (41).

Compound **1S** (50 mg, 0.10 mmol) was suspended in 33% aqueous ammonium hydroxide solution (1.4 mL) in a screw-capped tube. The reaction was stirred at 90 °C for 3 h. Then, the solvent was removed under vacuo and the crude material was subjected to column chromatography using ethyl acetate as eluent to give compound **41** (28 mg, 0.06 mmol, 63%) as a white solid. mp 160-161 °C dec. ^{1}H NMR (300 MHz, CD_3OD): δ = 9.11 (br s, 1H), 8.17 (d, *J* = 8.5 Hz, 2H), 8.12 (s, 1H), 8.07 (s, 1H), 7.95 (d, *J* = 8.5 Hz, 2H), 7.75 (d, *J* = 7.1 Hz ,1H), 7.69 (d, *J* = 7.1 Hz, 1H), 7.59 (s, 1H), 7.35 (t, *J* = 7.1 Hz, 1H). ^{13}C NMR (75 MHz, DMSO-d_6): δ = 172.3, 163.0, 147.4, 143.1, 138.1, 136.2, 134.7 (q, *J* = 38.6 Hz), 132.3, 131.0, 130.0, 129.1, 128.8, 128.7, 128.6, 126.7, 121.2, 121.1, 118.7 (q, *J* = 259.6 Hz). IR (neat): $\tilde{\nu}$ = 3188, 2853, 2634, 1913, 1577, 1421, 1133, 1035, 973, 846, 754 719, 658, 532, 505 cm^{-1}. MS (ESI): *m/z* 443 $[M + H]^+$.

Ethyl 1-(4-(4-(3-((methylsulfonyl)carbamoyl)phenyl)-1H-1,2,3-triazol-1-yl)phenyl)-5-(trifluoromethyl)-1H-pyrazole-4-carboxylate, (42).

To a solution of compound **1S** (100 mg, 0.21 mmol) in dry CH_2Cl_2 (2 mL), EDCI (80 mg, 0.42 mmol), TEA (87 µL, 0.63 mmol), DMAP (2.4 mg, 0.02 mmol) and methansulfonamide (40 mg, 0.42 mmol) were added in order under nitrogen. The reaction was stirred at room temperature for 16 h. Then, CH_2Cl_2 is added and the

organic phase was washed with aq. sat. NH_4Cl, dried over sodium sulfate and evaporated. The crude material was purified by column chromatography using ethyl acetate and ethyl acetate/methanol 9:1 as eluents to afford compound **42** (82 mg, 0.15 mmol, 71%) as a white solid. mp 209-210 °C. ^{1}H NMR (300 MHz, CD_3OD): δ = 9.02 (s, 1H), 8.57 (s, 1H), 8.21-8.14 (m, 3H), 8.03 (d, *J* = 7.9 Hz, 2H), 7.73 (d, *J* = 7.9 Hz, 2H), 7.45 (t, *J* = 8.2 Hz, 1H), 4.36 (q, *J* = 6.6 Hz, 2H), 1.38 (t, *J* = 6.6 Hz, 3H). ^{13}C NMR (75 MHz, acetone-d_6): δ = 173.9, 160.5, 148.1, 142.5, 139.1, 138.1, 133.1 (q, *J* = 40.3 Hz), 130.5, 129.9, 129.8, 128.9, 128.1, 127.8, 126.7, 120.6, 119.3, 118.4 (q, *J* = 281 Hz), 117.1, 61.1, 40.3, 13.6. IR (KBr): $\tilde{\nu}$ = 3093, 2982, 1731, 1649, 1523, 1357, 1243, 1148, 959, 848 cm^{-1}. MS (ESI): *m/z* 549 $[M + H]^+$.

Methyl 3-ethynylbenzoate, (44).

Step 1: To a solution of methyl 3-bromobenzoate (2 g, 9.30 mmol) in toluene (50 mL) DIPEA (6.5 mL, 37.2 mmol), CuI (0.32 g, 1.67 mmol), $Pd(PPh_3)_2Cl_2$ (0.39 g, 0.56 mmol) and ethynyltrimethylsilane (5.25 mL, 37.2 mmol) were added in a Schlenk apparatus. The reaction was stirred at reflux for 6 h under nitrogen atmosphere. Then, the mixture was filtered over a pad of celite and rinsed with ethyl acetate. The organic phase was washed with water (x1), dried over sodium sulfate and evaporated. The crude material was purified by column chromatography using petroleum ether and petroleum ether/ethyl acetate 95:5 as eluents to give methyl 3-((trimethylsilyl)ethynyl)benzoate as a brown oil (1.95 g, 8.30 mmol, 89%). ^{1}H NMR (300 MHz; $CDCl_3$): δ = 8.10 (s, 1H), 7.93 (d, *J* = 7.7 Hz, 1H), 7.59 (d, *J* = 7.7 Hz, 1H), 7.32 (t, *J* = 7.7 Hz, 1H), 3.88 (s, 3H), 0.22 (s, 9H).

Step 2: Methyl 3-((trimethylsilyl)ethynyl)benzoate (0.60 g, 2.55 mmol) was dissolved in THF (6 mL). The mixture was cooled at 0 °C and CH_3COOH (175 µL, 3.06 mmol) and TBAF (3.06 mL, 3.06 mmol) were added. The reaction was stirred at 0 °C for 1 h. The volatile was removed under vacuo, ethyl acetate was added and the organic layer was washed with water (x1). After drying over sodium sulfate and evaporation of the solvent, the crude material was purified by column

chromatography using petroleum ether and petroleum ether/ethyl acetate 95:5 as eluents to give compound **44** (0.40 g, 2.50 mmol, 98%) as a yellow oil. ^{1}H NMR (300 MHz, $CDCl_3$): δ = 8.17 (s, 1 H), 7.96 (d, *J* = 6.5 Hz, 1H), 7.67 (d, *J* = 6.5 Hz, 1H), 7.40 (t, *J* = 6.5 Hz, 1H), 3.92 (s, 3H), 3.12 (s, 1H). MS (ESI): *m/z*: 161 $[M + H]^+$.

1-(3-Ethynylphenyl)ethanone, (46).

Step 1: To a solution of 1-(3-bromophenyl)ethanone (2 g, 10.05 mmol) in THF (20 mL) TEA (2.1 mL, 15.07 mmol), CuI (7.62 mg, 0.04 mmol), $Pd(PPh_3)_2Cl_2$ (141.08 mg, 0.20 mmol) and ethynyltrimethylsilane (2.78 mL, 20.09 mmol) were added in a Schlenk apparatus. The reaction was stirred at 50 °C for 6 h under nitrogen atmosphere. Then, the mixture was filtered under vacuo and rinsed with ethyl acetate. The volatile was then removed under vacuo and the crude material was purified by column chromatography using petroleum ether/ethyl acetate 98:2 as eluents to give 1-(3-((trimethylsilyl)ethynyl)phenyl)ethanone as a brown oil (2.13 g, 9.85 mmol, 98%). ^{1}H NMR (300 MHz; $CDCl_3$): δ = 7.96 (s, 1H), 7.78 (d, *J* = 7.7 Hz, 1H), 7.56 (d, *J* = 7.7 Hz, 1H), 7.28 (t, *J* = 7.7 Hz, 1H), 3.02 (s, 3H), 0.24 (s, 9H).

Step 2: 1-(3-((Trimethylsilyl)ethynyl)phenyl)ethanone (1.84 g, 8.52 mmol) was dissolved in MeOH (18 mL) and K_2CO_3 (2.96 g, 21.4 mmol) was added. The reaction was stirred for 1 h. The volatile was removed under vacuo, ethyl acetate was added and the organic layer was washed with water (x1). After drying over sodium sulfate and evaporation of the solvent, the crude material was purified by column chromatography using petroleum ether/ethyl acetate 95:5 as eluent to give compound **46** (1.20 g, 8.33 mmol, 98%) as a yellow solid. ^{1}H NMR (300 MHz, $CDCl_3$): δ = 8.01 (s, 1H), 7.88 (d, *J* = 7.6 Hz, 1H), 7.61 (d, *J* = 7.6 Hz, 1H), 7.37 (t, *J* = 7.6 Hz, 1H), 3.13 (s, 1H), 2.56 (s, 3H). MS (ESI): *m/z*: 145 $[M + H]^+$.

3-Bromobenzamide, (62).

3-Bromobenzoic acid (2 g, 9.95 mmol) was dissolved in THF (20 mL) and oxalyl chloride (1.74 mL, 19.90 mmol) and DMF (62 µL) were added. After stirring at room

temperature for 2 h, conc. NH_4OH (12 mL) was added. The reaction was stirred for additional 30 min and then was evaporated, affording compound **62** (2.11 g, 9.75 mmol, 98%) as a white solid. ^{1}H NMR (300 MHz; CD_3OD): δ = 8.04 (s, 1H) 7.84 (d, *J* = 7.6 Hz, 1H), 7.70 (d, *J* = 7.6 Hz, 1H), 7.39 (t, *J* = 7.6 Hz, 1H).

3-Ethynylbenzamide, (48).

Step 1: 3-((Trimethylsilyl)ethynyl)benzamide was synthesized as previously reported for the preparation of compound **44** in **step 1**, starting from compound **47** (1.30 g, 6.02 mmol). The crude material was subjected to chromatography column using petroleum ether/ethyl acetate 7:3 and petroleum ether/ethyl acetate 5:5 as eluents, yielding 3-((trimethylsilyl)ethynyl)benzamide (0.63 g, 2.91 mmol, 48%) as a brown oil. ^{1}H NMR (300 MHz; $CDCl_3$): δ = 7.88 (s, 1H), 7.76 (d, *J* = 7.9 Hz, 1H), 7.60 (d, *J* = 7.9 Hz, 1H), 7.42 (t, *J* = 7.9 Hz, 1H), 0.26 (s, 9H).

Step 2: 3-((Trimethylsilyl)ethynyl)benzamide (0.63 g, 2.89 mmol) was dissolved in THF (13 mL). The mixture was cooled at 0 °C and TBAF (3.47 mL, 3.47 mmol) was added. The reaction was stirred at 0 °C for 30 min. The volatile was removed under vacuo, water was added and the aqueous layer was extracted with ethyl acetate (x3). The organic phase was dried over sodium sulfate and evaporated. The crude material was purified by column chromatography using petroleum ether/ethyl acetate 5:5 as eluent to give compound **48** (0.33 g, 2.25 mmol, 79%) as a yellow solid. ^{1}H NMR (300 MHz, $CDCl_3$): δ = 7.91 (s, 1 H), 7.80 (d, *J* = 7.7 Hz, 1H), 7.64 (d, *J* = 7.7 Hz, 1H), 7.43 (t, *J* = 7.7 Hz, 1H), 3.13 (s, 1H). MS (ESI): *m/z*: 146 $[M + H]^+$.

(3-Ethynylphenyl)methanol, (50).

Step 1: In a Schlenk apparatus (3-bromophenyl)methanol (1.5 g, 8.02 mmol), TEA (7.5 mL), PPh_3 (42.02 mg, 0.16 mmol), $Pd(OAc)_2$ (18.01 mg, 0.08 mmol) and ethynyltrimethylsilane (2.23 mL, 16.04 mmol) were added. The reaction was stirred at 94 °C for 1 h under nitrogen atmosphere. Then, the mixture was filtered under vacuo and rinsed with ethyl acetate. The organic phase was washed with water (3x) and dried over sodium sulfate. The volatile was then removed under vacuo and the

crude material was purified by column chromatography using petroleum ether/ethyl acetate 95:5 and petroleum ether/ethyl acetate 9:1 as eluents to give (3-((trimethylsilyl)ethynyl)phenyl)methanol as a brown oil (1.07 g, 5.25 mmol, 65%). ^{1}H NMR (300 MHz; $CDCl_3$): δ = 7.96 (s, 1H), 7.26 (d, *J* = 7.2 Hz, 1H), 7.18 (d, *J* = 7.2 Hz, 1H), 6.98 (t, *J* = 7.2 Hz, 1H), 4.50 (s, 2H), 0.21 (s, 9H).

Step 2: The title compound was synthesized as previously reported for the preparation of compound **46** in **step 2**, starting from (3-((trimethylsilyl)ethynyl)phenyl)methanol (1.07 g, 5.25 mmol). The crude material was subjected to chromatography column using petroleum ether/ethyl acetate 95:5 and petroleum ether/ethyl acetate 9:1 as eluents, yielding compound **50** (0.34 g, 2.52 mmol, 49%) as a yellow oil. ^{1}H NMR (300 MHz, $CDCl_3$): δ = 7.42 (s, 1H), 7.32 (d, *J* = 6.2 Hz, 1H), 7.22-7.11 (m, 2H), 4.56 (s, 2H), 3.01 (s, 1H). MS (ESI): *m/z*: 133 $[M + H]^+$.

3-Ethynylbenzenesulfonamide, (52).

Step 1: 3-((Trimethylsilyl)ethynyl)benzenesulfonamide was synthesized as previously reported for the preparation of compound **44** in **step 1**, starting from compound **51** (0.50 g, 2.12 mmol). The crude material was subjected to chromatography column using petroleum ether/ethyl acetate 95:5 and petroleum ether/ethyl acetate 8:2 as eluents, yielding 3-((trimethylsilyl)ethynyl)benzenesulfonamide (0.53 g, 2.09 mmol, 99%) as a brown oil. ^{1}H NMR (300 MHz; $CDCl_3$): δ = 8.02 (s, 1H), 7.85 (d, *J* = 7.6 Hz, 1H), 7.64 (d, *J* = 7.6 Hz, 1H), 7.46 (t, *J* = 7.6 Hz, 1H), 0.25 (s, 9H).

Step 2: The title compound was synthesized as previously reported for the preparation of compound **46** in **step 2**, starting from 3-((trimethylsilyl)ethynyl)benzenesulfonamide (0.53 g, 2.11 mmol). After evaporation, ethyl acetate wad added and the organic phase was washed with HCl 3N, dried over sodium sulfate and evaporated. The crude material was subjected to chromatography column using petroleum ether/ethyl acetate 7:3 as eluent, yielding

compound **52** (0.34 g, 1.88 mmol, 89%) as a yellow oil. ^{1}H NMR (300 MHz; CD_3OD): δ = 8.03 (s, 1 H), 7.87 (d, *J* = 7.7 Hz, 1H), 7.67 (d, *J* = 7.7 Hz, 1H), 7.53 (t, *J* = 7.7 Hz, 1H), 3.67 (s, 1H). MS (ESI): *m/z*: 182 $[M + H]^+$.

3-Ethynyl-N-hydroxybenzamide, (54).

To a solution of 3-ethynylbenzoic acid (99 mg, 0.68 mmol) in dry CH_2Cl_2 (1 mL), TEA (94 µL, 0.68 mmol), EDCI (143 mg, 0.68 mmol) and *O*-(trimethylsilyl)hydroxylamine (99.6 mg, 0.68 mmol) were added in order under nitrogen atmosphere. After 4 h, the reaction was finished. The volatile was removed under vacuo and the crude material was dissolved in THF (3.2 mL). The mixture was cooled at 0 °C and TBAF (0.68 mL, 0.68 mmol) was added. The reaction was stirred for 1 h at 0 °C and then ethyl acetate was added. The organic phase was washed with HCl 3N (1x), dried over sodium sulfate and evaporated. The crude material was purified by column chromatography using ethyl acetate and ethyl acetate/methanol 8:2 as eluents, yielding compound **54** (76.6 mg, 0.48 mmol, 70%) as a white solid. ^{1}H NMR (300 MHz; CD_3OD): δ = 7.84 (s, 1H), 7.73 (d, *J* = 7.7 Hz, 1H), 7.59 (d, *J* = 7.7 Hz, 1H), 7.44 (t, *J* = 7.7 Hz, 1H), 3.56 (s, 1H). MS (ESI): *m/z*: 162 $[M + H]^+$.

General procedure for the preparation of compounds 22-23, 31-36, 38, 40, 55-59.

To a suspension of azide (0.29 mmol, 1 eq) in water (570 µL) and *t*-BuOH (570 µL) alkyne (0.29 mmol, 1 eq) was added. Then, 30 µL of aqueous solution of sodium ascorbate 1M and copper sulfate pentahydrate (0.0029 mmol, 0.01 eq) were added and the mixture was maintained under vigorous stirring overnight. Ice was added and the precipitate was filtered and rinsed with water and heptane. Purification by silica gel column chromatography afforded compounds **22-23**, **31-36**, **38**, **40, 55-59**.

3-(1-(4-(4-(Methoxycarbonyl)-5-(trifluoromethyl)-1H-pyrazol-1-yl)phenyl)-1H-1,2,3-triazol-4-yl)benzoic acid, (22).

The title compound was synthesized following the general procedure, starting from compound **20** (260 mg, 0.84 mmol) and 3-ethynylbenzoic acid (123 mg, 0.84 mmol). The crude material was purified by column chromatography using petroleum ether/ethyl acetate 4:6 and petroleum ether/ethyl acetate 1:9 as eluents to afford compound **22** (210 mg, 0.46 mmol, 55%) as a white solid. mp 228-229 °C dec. ^{1}H NMR (300 MHz, DMSO-d_6): δ = 9.57 (s, 1H), 8.56 (s, 1H), 8.33 (s, 1H), 8.26-8.19 (m, 3H), 7.97 (d, *J* = 6.9 Hz, 1H), 7.84 (d, *J* = 8.4 Hz, 2H), 7.62 (t, *J* = 6.9 Hz, 1H), 3.86 (s, 3H). ^{13}C NMR (75 MHz, DMSO-d_6): δ = 161.2 (2C), 147.5, 143.0, 139.1, 138.1 (2C), 132.4 (q, *J* = 39.5 Hz), 130.9, 129.8, 129.7, 128.5, 126.8, 121.2 (2C), 120.9, 119.4 (q, *J* = 268.3 Hz), 116.6, 52.9. IR (KBr): $\tilde{\nu}$ = 3511, 2958, 1724, 1688, 1524, 1261, 1039, 846, 759, 554 cm^{-1}. MS (ESI): *m/z* 458 $[M + H]^+$.

3-(1-(4-(4-(Isopropoxycarbonyl)-5-(trifluoromethyl)-1H-pyrazol-1-yl)phenyl)-1H-1,2,3-triazol-4-yl)benzoic acid, (23).

The title compound was synthesized following the general procedure, starting from compound **21** (83 mg, 0.24 mmol) and 3-ethynylbenzoic acid (35.8 mg, 0.24 mmol). The crude material was purified by column chromatography using petroleum ether/ethyl acetate 6:4 and petroleum ether/ethyl acetate 4:6 as eluents to afford compound **23** (63 mg, 0.13 mmol, 54%) as a white solid. mp 250-251 °C dec. ^{1}H NMR (300 MHz, DMSO-d_6): δ = 9.58 (s, 1H), 8.55 (s, 1H), 8.33 (s, 1H), 8.27-8.05 (m, 3H), 7.97 (d, *J* = 7.6 Hz, 1H), 7.85 (d, *J* = 8.4 Hz, 2H), 7.64 (t, *J* = 7.6 Hz, 1H), 5.15 (ept, *J* = 6.3 Hz, 1H), 1.32 (t, *J* = 6.0 Hz, 6H). ^{13}C NMR (75 MHz, DMSO-d_6): δ = 167.4, 159.9, 146.9, 142.4, 138.7, 137.5, 131.6 (q, *J* = 39.3 Hz), 130.3, 129.3, 129.2, 129.1, 128.0 (2C), 126.2, 120.7 (2C), 118.8 (q, *J* = 244.3 Hz), 116.8, 69.4, 22.0. IR (KBr): $\tilde{\nu}$ = 3479, 2924, 1716, 1689, 1524, 1298, 1149, 1033, 845, 759 cm^{-1}. MS (ESI): *m/z* 486 $[M + H]^+$.

3-(1-(4-(4-((Pentan-2-yloxy)carbonyl)-5-(trifluoromethyl)-1H-pyrazol-1-yl)phenyl)-1H-1,2,3-triazol-4-yl)benzoic acid, (31).

The title compound was synthesized following the general procedure, starting from compound **25** (66.6 mg, 0.18 mmol) 3-ethynylbenzoic acid (26.5 mg, 0.18 mmol). The crude material was purified by column chromatography using petroleum ether/ethyl acetate 8:2 and petroleum ether/ethyl acetate 5:5 as eluents to afford compound **31** (72 mg, 0.14 mmol, 80%) as a white solid. mp 198-199 °C. ^{1}H NMR (300 MHz, $CDCl_3$) δ = 8.60 (s, 1H), 8.40 (s, 1H), 8.28 (d, *J* = 7.3 Hz, 1H), 8.15 (d, *J* = 7.6 Hz, 2H), 8.00 (d, *J* = 7.6 Hz, 2H), 7.77-7.57 (m, 3H), 5.19 (sex, *J* = 4.2 Hz, 1H), 1.82-1.67 (m, 1H), 1.67-1.53 (m, 1H), 1.51-1.40 (m, 1H), 1.35 (d, *J* = 6.0 Hz, 3H), 1.30-1.22 (m, 1H), 0.96 (t, *J* = 7.0 Hz, 3H). ^{13}C NMR (75 MHz, DMSO-d_6) δ = 167.6, 160.6, 147.4, 143.0, 139.3, 138.0, 132.6 (q, *J* = 40 Hz), 132.3, 131.0, 130.0, 129.7, 128.6, 126.7, 121.3, 121.2, 121.1, 119.3 (q, *J* = 269.0 Hz), 117.3, 72.2, 37.9, 20.2, 18.6 14.3. IR (KBr): $\tilde{\nu}$ = 2960, 2873, 2670, 1716, 1523, 1249, 1033, 845, 759, 683 cm^{-1}. IR (KBr): $\tilde{\nu}$ = 2960, 2873, 2670, 1716, 1523, 1249, 1033, 845, 759, 683 cm^{-1}. MS (ESI): *m/z* 514 $[M + H]^+$

3-(1-(4-(4-((Isopentyloxy)carbonyl)-5-(trifluoromethyl)-1H-pyrazol-1-yl)phenyl)-1H-1,2,3-triazol-4-yl)benzoic acid, (32).

The title compound was synthesized following the general procedure, starting from compound **26** (80.4 mg, 0.22 mmol) and 3-ethynylbenzoic acid (32.1 mg, 0.22 mmol). The crude material was purified by column chromatography using petroleum ether/ethyl acetate 7:3 and petroleum ether/ethyl acetate 4:6 as eluents to afford compound **32** (66 mg, 0.13 mmol, 58%) as a white solid. mp 217-218 °C. ^{1}H NMR (300 MHz, acetone-d_6): δ = 9.29 (s, 1H), 8.65 (s, 1H), 8.27-8.22 (m, 4H), 8.02 (d, *J* = 7.1 Hz, 1H), 7.85 (d, *J* = 8.2 Hz, 2H), 7.62 (t, *J* = 7.1 Hz, 1H), 4.36 (t, *J* = 6.1 Hz, 2H), 1.82-1.77 (m, 1H), 1.65 (q, *J* = 6.1 Hz, 2H), 0.95 (d, *J* = 6.1 Hz, 6H). ^{13}C NMR (75 MHz, DMSO-d_6): δ = 167.6, 160.9, 147.3, 143.0, 139.2, 138.0, 132.5, 132.2 (q, *J* = 36 Hz), 130.9, 130.2, 129.7, 128.6, 126.7, 121.2 (2C), 121.0, 119.2 (q, *J* = 250.0

Hz), 116.9, 64.1, 37.4, 25.0, 22.8. IR (KBr): $\tilde{\nu}$ = 2958, 2873, 1732, 1689, 1524, 1299, 1252, 1151, 1033, 845, 759 cm^{-1}. MS (ESI): *m/z* 514 $[M + H]^+$.

(E)-3-(1-(4-(4-(((3,7-Dimethylocta-2,6-dien-1-yl)oxy)carbonyl)-5-(trifluoromethyl)-1H-pyrazol-1-yl)phenyl)-1H-1,2,3-triazol-4-yl)benzoic acid, (33).

The title compound was synthesized following the general procedure, starting from compound **27** (53 mg, 0.12 mmol) and 3-ethynylbenzoic acid (17.9 mg, 0.12 mmol). The crude material was purified by column chromatography using petroleum ether/ethyl acetate 3:7 and petroleum ether/ethyl acetate 1:9 as eluents to afford compound **33** (38 mg, 0.06 mmol, 54%) as a white solid. mp 198-199 °C. ^{1}H NMR (300 MHz, acetone-d_6): δ = 9.30 (s, 1H), 8.66 (s, 1H), 8.28-8.25 (m, 3H), 8.21 (s, 1H), 8.07 (d, *J* = 7.4 Hz, 1H), 7.85 (d, *J* = 8.5 Hz, 2H), 7.65 (t, *J* = 7.4 Hz, 1H), 5.49 (t, *J* = 7.1 Hz, 1H), 5.12 (t, *J* = 7.1 Hz, 1H), 4.85 (d, *J* = 7.1 Hz, 2H), 2.13-2.04 (m, 4H), 1.79 (s, 3H), 1.65 (s, 3H), 1.60 (s, 3H). ^{13}C NMR (75 MHz, acetone-d_6): δ = 166.6, 160.4, 147.5, 142.7, 142.5, 139.4, 138.2, 132.3 (q, *J* = 40.1 Hz), 131.5, 131.4, 131.1, 129.9, 129.4, 129.3, 128.0, 126.8, 123.8, 120.1, 119.6, 119.4 (q, *J* = 279.4 Hz), 118.3, 117.1, 61.7, 39.4, 26.4, 25.6, 16.9, 15.7. IR (KBr): $\tilde{\nu}$ = 3554, 3141, 2986, 1637, 1616, 1524, 1384, 1230, 968, 844 cm^{-1}. MS (ESI): *m/z* 580 $[M + H]^+$.

3-(1-(4-(4-((Pyridin-4-ylmethoxy)carbonyl)-5-(trifluoromethyl)-1H-pyrazol-1-yl)phenyl)-1H-1,2,3-triazol-4-yl)benzoic acid, (34).

The title compound was synthesized following the general procedure, starting from compound **28** (81 mg, 0.21 mmol) and 3-ethynylbenzoic acid (30.5 mg, 0.21 mmol). The crude material was purified by column chromatography using petroleum ether/ethyl acetate 6:4 and petroleum ether/ethyl acetate 4:6 as eluents to afford compound **34** (63 mg, 0.12 mmol, 56%) as a white solid. mp 169-170 °C. ^{1}H NMR (300 MHz, CD_3OD): δ = 9.60 (br s, 1H), 8.73-8.49 (m, 5H), 8.30-8.16 (m, 3H), 8.08-7.68 (m, 5H), 7.47 (s, 1H), 5.43 (s, 2H). ^{13}C NMR (75 MHz, DMSO-d_6): δ = 172.1, 162.4, 147.9, 147.6, 140.8, 139.3, 137.8, 134.8, 133.3 (q, *J* = 39.2 Hz), 133.0, 130.9,

130.8, 129.7, 129.5, 128.7, 128.3, 126.7, 125.4, 121.3, 120.9, 119.6 (q, J = 265.3 Hz), 70.5. IR (KBr): $\tilde{\nu}$ = 3086, 2924, 2131, 1718, 1522, 1294, 1239, 1142, 808, 758 cm^{-1}. MS (ESI): *m/z* 535 $[M + H]^+$.

3-(1-(4-(4-((Benzyloxy)carbonyl)-5-(trifluoromethyl)-1H-pyrazol-1-yl)phenyl)-1H-1,2,3-triazol-4-yl)benzoic acid, (35).

The title compound was synthesized following the general procedure, starting from compound **29** (45.2 mg, 0.12 mmol) and 3-ethynylbenzoic acid (17 mg, 0.12 mmol). The crude material was purified by column chromatography using petroleum ether/ethyl acetate 5:5 and petroleum ether/ethyl acetate 2:8 as eluents to afford compound **35** (42 mg, 0.08 mmol, 65%) as a white solid. mp 196-197 °C dec. ^{1}H NMR (300 MHz, CD_3OD): δ = 9.61 (br s, 1H), 8.55 (s, 1H), 8.44 (s, 1H), 8.21 (d, J = 8.6 Hz, 2H), 7.97 (d, J = 7.8 Hz, 1H), 7.88 (d, J = 8.6 Hz, 2H), 7.67 (t, J = 7.8 Hz, 1H), 7.50-7.38 (m, 7H), 5.38 (s, 2H). ^{13}C NMR (75 MHz, DMSO-d_6): δ = 167.6, 160.7, 147.3, 143.1, 134.3 (q, J = 39.3 Hz), 139.2, 138.1, 136.2, 132.3, 131.0, 130.0, 129.7, 129.1 (2C), 128.8 (2C), 128.7, 128.6, 126.7, 121.2, 119.7 (q, J = 269 Hz), 116.6, 67.1. IR (KBr): $\tilde{\nu}$ = 3092, 2933, 2131, 1721, 1522, 1298, 971, 850, 561 cm^{-1}. MS (ESI): *m/z* 534 $[M + H]^+$.

3-(1-(4-(4-((2-Morpholinoethoxy)carbonyl)-5-(trifluoromethyl)-1H-pyrazol-1-yl)phenyl)-1H-1,2,3-triazol-4-yl)benzoic acid, (36).

The title compound was synthesized following the general procedure, starting from compound **30** (40.3 mg, 0.10 mmol) and 3-ethynylbenzoic acid (14.4 mg, 0.10 mmol). The crude material was purified by column chromatography using petroleum ether/ethyl acetate 2:8 and ethyl acetate/methanol 9:1 as eluents to afford compound **36** (29 mg, 0.05 mmol, 53%) as a yellow solid. mp 196-197 °C dec. ^{1}H NMR (300 MHz, DMSO-d_6): δ = 8.40 (d, J = 7.6 Hz, 2H), 8.26 (s, 1H), 8.18 (s, 1H), 8.04 (s, 1H), 7.52 (t, J = 7.6 Hz, 1H), 7.80 (d, J = 8.3 Hz, 2H), 7.39 (d, J = 8.3Hz, 2H), 4.54 (t, J = 5.8 Hz, 2H), 3.85-3.82 (m, 4H), 2.98 (t, J = 5.8 Hz, 2H), 2.84-2.80 (m, 4H). ^{13}C NMR (75 MHz, DMSO-d_6): δ = 161.3, 158.7, 148.1, 145.6, 144.3, 144.2, 142.1,

132.1 (q, *J* = 39.2 Hz), 131.3, 129.7, 128.1, 127.0, 125.4, 124.3, 121.6, 119.3 (q, *J* = 269.1 Hz), 116.2, 114.6, 68.1, 60.4, 55.8, 55.3. IR (KBr): $\tilde{\nu}$ = 2923, 2360, 2124, 2092, 1725, 1512, 1299, 1226, 1143, 1037, 974 cm^{-1}. MS (ESI): *m/z* 557 $[M + H]^+$.

3-(1-(4-(4-(Hydroxymethyl)-5-(trifluoromethyl)-1H-pyrazol-1-yl)phenyl)-1H-1,2,3-triazol-4-yl)benzoic acid, (38).

The title compound was synthesized following the general procedure, starting from compound **37** (104.4 mg, 0.37 mmol) and 3-ethynylbenzoic acid (53.8 mg, 0.37 mmol). The crude material was purified by column chromatography using petroleum ether/ethyl acetate 4:6 and petroleum ether/ethyl acetate 2:8 as eluents to afford compound **38** (132 mg, 0.31 mmol, 83%) as a white solid. mp 225-226°C. ^{1}H NMR (300 MHz, acetone-d_6): δ = 9.27 (s, 1H), 8.65 (s, 1H), 8.29-8.21 (m, 3H), 8.05 (d, *J* = 7.7 Hz, 1H), 7.87 (s, 1H), 7.77 (d, *J* = 8.5 Hz, 2H), 7.65 (t, *J* = 7.7 Hz, 1H), 4.75 (s, 2H). ^{13}C NMR (75 MHz, DMSO-d_6): δ = 167.6, 147.3, 141.3, 139.3, 137.5, 132.2, 131.0, 130.0, 129.7, 128.2, 127.2 (q, *J* = 37.7 Hz), 126.8, 126.7, 121.3 (2C), 121.2 (q, *J* = 207.5 Hz), 121.0, 53.9. IR (KBr): $\tilde{\nu}$ = 3223, 3123, 2893, 2669, 1689, 1524, 1306, 1140, 845, 759 cm^{-1}. MS (ESI): *m/z* 430 $[M + H]^+$.

3-(1-(4-(4-(Isopropylcarbamoyl)-5-(trifluoromethyl)-1H-pyrazol-1-yl)phenyl)-1H-1,2,3-triazol-4-yl)benzoic acid, (40).

The title compound was synthesized following the general procedure, starting from compound **39** (150 mg, 0.44 mmol) and 3-ethynylbenzoic acid (65 mg, 0.44 mmol). The crude material was purified by column chromatography using petroleum ether/ethyl acetate 3:7 and ethyl acetate as eluents to afford compound **40** (185 mg, 0.38 mmol, 87%) as a white solid. mp 237-238 °C. ^{1}H NMR (300 MHz, DMSO-d_6): δ = 9.52 (s, 1H), 8.56 (s, 1H), 8.36 (d, *J* = 7.4 Hz, 1H), 8.22 (d, *J* = 8.6 Hz, 2H), 8.15 (s, 1H), 7.98 (d, *J* = 7.4 Hz, 1H), 7.78 (d, *J* = 8.6 Hz, 2H), 7.60 (t, *J* = 7.4 Hz, 1H), 4.04 (ept, *J* = 6.3 Hz, 1H), 1.18 (s, 3H), 1.16 (s, 3H). ^{13}C NMR (75 MHz, DMSO-d_6): δ =.168.8 (2C), 159.8, 147.7, 140.3, 139.1, 137.8, 134.7, 130.6, 129.8 (q, *J* = 42.6 Hz), 129.7, 129.6, 129.1, 126.7, 122.7, 121.3, 120.7, 118.1 (q, *J* = 263.8 Hz),

41.6, 22.7. IR (KBr): $\tilde{\nu}$ = 2972, 2876, 1689, 1647, 1522, 1456, 1398, 1297, 1148, 847, 815 cm^{-1}. MS (ESI): *m/z* 485 $[M + H]^+$.

Ethyl 1-(4-(4-(3-(methoxycarbonyl)phenyl)-1H-1,2,3-triazol-1-yl)phenyl)-5-(trifluoromethyl)-1H-pyrazole-4-carboxylate, (55).

The title compound was synthesized following the general procedure, starting from compound **13** (94 mg, 0.29 mmol) and alkyne **44** (46 mg, 0.29 mmol). The crude material was purified by column chromatography using petroleum ether/ethyl acetate 7:3 and petroleum ether/ethyl acetate 5:5 as eluents to afford compound **55** as a yellow solid (83 mg, 0.17 mmol, 59%). mp 160-161 °C. ^{1}H NMR (300 MHz, DMSO-d_6): δ = 9.61 (s, 1H), 8.55 (s, 1H), 8.37 (s, 1H), 8.31-8.10 (m, 3H), 7.99 (d, *J* = 7.7 Hz, 1H), 7.84 (d, *J* = 6.1 Hz, 2H), 7.69 (t, *J* = 7.7 Hz, 1H), 4.34 (q, *J* = 7.1 Hz, 2H), 3.92 (s, 3H), 1.32 (t, *J* = 7.0 Hz, 3H). ^{13}C NMR (75 MHz, DMSO-d_6): δ = 166.5, 160.9, 147.1, 143.0, 139.2, 138.0, 132.5 (q, *J* = 39.1 Hz), 131.2, 131.1, 130.5, 130.3, 129.5, 128.6, 126.4, 121.2 (2C), 117.0, 115.3 (q, *J* = 269.1 Hz), 61.7, 52.9, 14.5. IR (KBr): $\tilde{\nu}$ = 3139, 2987, 1712, 1525, 1289, 1238, 971, 850 cm^{-1}. MS (ESI): *m/z* 486 $[M + H]^+$.

Ethyl 1-(4-(1-(3-acetylphenyl)-1H-1,2,3-triazol-4-yl)phenyl)-5-(trifluoromethyl)-1H-pyrazole-4-carboxylate, (56).

The title compound was synthesized following the general procedure, starting from compound **13** (150 mg, 0.46 mmol) and alkyne **46** (66 mg, 0.46 mmol). The crude material was purified by column chromatography using petroleum ether/ethyl acetate 8:2 and petroleum ether/ethyl acetate 7:3 as eluents to afford compound **56** as a yellow solid (173 mg, 0.37 mmol, 80%). mp 213-214 °C. ^{1}H NMR (300 MHz, DMSO-d_6): δ = 9.61 (s, 1H), 8.51 (s, 1H), 8.37 (s, 1H), 8.27-8.17 (m, 3H), 8.00 (d, *J* = 7.7 Hz, 1H), 7.88 (d, *J* = 8.5 Hz, 2H), 7.69 (t, *J* = 7.7 Hz, 1H), 4.34 (q, *J* = 6.9 Hz, 2H), 2.68 (s, 3H), 1.32 (t, *J* = 7.1 Hz, 3H). ^{13}C NMR (75 MHz, DMSO-d_6): δ = 198.4, 160.9, 147.4, 143.0, 139.2, 138.1, 138.0, 134.0 (q, *J* = 38.9 Hz), 131.1, 130.3, 130.2, 128.8, 128.6, 126.2 (q, *J* = 252 Hz), 125.4, 121.3, 121.2, 118.5, 61.7, 27.4,

14.5. IR KBr): $\tilde{\nu}$ = 3137, 2914, 1718, 1677, 1524, 1238, 1158, 1076, 1036, 968, 852 cm^{-1}. MS (ESI): *m/z* 470 $[M + H]^+$.

Ethyl 1-(4-(4-(3-carbamoylphenyl)-1H-1,2,3-triazol-1-yl)phenyl)-5-(trifluoromethyl)-1H-pyrazole-4-carboxylate, (57).

The title compound was synthesized following the general procedure, starting from compound **13** (94.2 mg, 0.29 mmol) and alkyne **48** (42.1 mg, 0.29 mmol). The crude material was purified by column chromatography using petroleum ether/ethyl acetate 5:5 and petroleum ether/ethyl acetate 2:8 as eluents to afford compound **57** as a yellow solid (89 mg, 0.19 mmol, 65%). mp 213.5-214.5 °C. ^{1}H NMR (300 MHz, DMSO-d_6): δ = 9.51 (s, 1H), 8.49 (s, 1H), 8.35 (s, 1H), 8.20 (d, *J* = 8.8 Hz, 2H), 8.10 (d, *J* = 7.5 Hz, 1H), 7.98-7.80 (m, 3H), 7.59 (t, *J* = 7.5 Hz, 1H), 7.51 (br s, 2H), 4.32 (q, *J* = 6.9 Hz, 2H), 1.30 (t, *J* = 6.9 Hz, 3H). ^{13}C NMR (75 MHz, DMSO-d_6): δ = 168.2, 160.8, 147.7, 143.0, 139.2, 138.1, 135.7, 132.3 (q, *J* = 38.9 Hz), 130.7, 129.6, 128.5 (2C), 127.8, 125.3, 121.2, 120.9, 117.0, 116.8 (q, *J* = 269.2 Hz), 61.7, 14.5. IR (KBr): $\tilde{\nu}$ = 3436, 3130, 1690, 1557, 1523, 1257, 1039, 781, 682 cm^{-1}. MS (ESI): *m/z* 471 $[M + H]^+$.

Ethyl 1-(4-(1-(3-(hydroxymethyl)phenyl)-1H-1,2,3-triazol-4-yl)phenyl)-5-(trifluoromethyl)-1H-pyrazole-4-carboxylate, (58).

The title compound was synthesized following the general procedure, starting from compound **13** (315 mg, 0.97 mmol) and alkyne **50** (128 mg, 0.97 mmol). The crude material was purified by column chromatography using petroleum ether/ethyl acetate 5:5 and petroleum ether/ethyl acetate 2:8 as eluents to afford compound **58** as a yellow solid (201 mg, 0.44 mmol, 45%). mp 200.5-201.5 °C. ^{1}H NMR (300 MHz, DMSO.d_6): δ = 9.45 (s, 1H), 8.37 (s, 1H), 8.19 (d, *J* = 7.2 Hz, 2H), 7.95 (s, 1H), 7.91-7.80 (m, 3H), 7.45 (t, *J* = 6.9 Hz, 1H), 7.33 (d, *J* = 6.9 Hz, 1H), 4.59 (s, 2H), 4.31 (t, *J* = 6.6 Hz, 2H), 1.32 (q, *J* = 6.9 Hz, 3H). ^{13}C NMR (75 MHz, acetone-d_6): δ = 171.1, 145.1, 144.3, 134.5, 134.1, 132.2 (q, *J* = 40.7 Hz), 132.0, 131.9, 129.1 (2C), 125.5, 124.6 (q, *J* = 274 Hz), 123.7, 120.6, 116.5, 115.2, 110.7, 62.3, 61.4,

13.7. IR (KBr): $\tilde{\nu}$ = 3415, 2989, 2870, 1719, 1525, 1248, 1154, 1038, 977, 853 cm^{-1}. MS (ESI): *m/z* 458 $[M + H]^+$.

Ethyl 1-(4-(4-(3-sulfamoylphenyl)-1H-1,2,3-triazol-1-yl)phenyl)-5-(trifluoromethyl)-1H-pyrazole-4-carboxylate, (59).

The title compound was synthesized following the general procedure, starting from compound **13** (94.2 mg, 0.29 mmol) and alkyne **52** (52.6 mg, 0.29 mmol). The crude material was purified by column chromatography using petroleum ether/ethyl acetate 8:2 and petroleum ether/ethyl acetate 5:5 as eluents to afford compound **59** as a yellow solid (76 mg, 0.15 mmol, 52%). mp 208.5-209.5 °C. ^{1}H NMR (300 MHz, DMSO-d_6): δ = 9.61 (s, 1H), 8.46 (s, 1H), 8.38 (s, 1H), 8.22 (d, *J* = 8.8 Hz, 2H), 8.15 (d, *J* = 7.7 Hz, 1H), 7.89-7.81 (m, 3H), 7.74 (t, *J* = 7.7 Hz, 1H), 7.51 (br s, 2H), 4.34 (q, *J* = 6.9 Hz, 2H), 1.32 (t, *J* = 7.1 Hz, 3H). ^{13}C NMR (75 MHz, DMSO-d_6): δ = 160.8, 147.0, 145.6, 143.0, 139.3, 138.0, 132.0 (q, *J* = 38.9 Hz), 131.3, 130.5, 129.1, 128.5, 126.0, 122.9, 121.3 (2C), 119.5 (q, *J* = 269 Hz), 117.0, 61.7, 14.5. IR (KBr): $\tilde{\nu}$ = 3263, 2985, 1722, 1694, 1526, 1257, 1037, 849, 596 cm^{-1}. MS (ESI): *m/z* 507 $[M + H]^+$.

Ethyl 1-(4-(4-(3-(hydroxycarbamoyl)phenyl)-1H-1,2,3-triazol-1-yl)phenyl)-5-(trifluoromethyl)-1H-pyrazole-4-carboxylate, (60).

To a solution of $Cu(OAc)_2$ (2.63 mg, 0.0145 mmol, 0.05 eq) in THF (26 µL) TBTA (4.09 mg, 0.0077 mmol, 0.05 eq) was added and the resulting mixture was stirred at room temperature for 30 min. A solution of compound **13** (94.27 mg, 0.29 mmol, 1 eq) in THF (0.05 mL), a solution of compound **54** (46.69 mg, 0.29 mmol, 1 eq) in THF (0.05 mL) and a solution of sodium ascorbate (5.94 mg, 0.03 mmol, 0.1 eq) solubilized in the minimum amount of water were added. The reaction was stirred at room temperature overnight. The precipitate was filtered and rinsed with water (x2) and diethyl ether (x2) to give a solid. The crude material was purified by column chromatography using petroleum ether/ethyl acetate 5:5 as eluent to afford compound **60** as an amorphous white solid (90 mg, 0.18 mmol, 42%). ^{1}H NMR (300

MHz, CD_3OD): δ = 9.17 (s, 1H), 8.61 (s, 1H), 8.22 (s, 1H), 8.18 (d, *J* = 8.2 Hz, 2H), 7.75 (d, *J* = 8.2 Hz, 2H), 7.61 (t, *J* = 8.8 Hz, 1H), 7.49 (d, *J* = 8.8 Hz, 1H), 7.25 (d, *J* = 8.8 Hz, 1H), 4.37 (q, *J* = 7.1 Hz, 2H), 1.38 (t, *J* = 7.1 Hz, 3H). ^{13}C NMR (75 MHz, DMSO-d_6): δ = 169.8, 163.2, 148.2, 143.5, 139.6, 134.9, 133.7 (q, *J* = 40.0 Hz), 133.0, 131.8, 130.9, 130.4, 129.5, 128.9, 127.5, 126.2, 119.8, 118.2 (q, *J* = 278 Hz), 116.8, 60.9, 15.7. IR (KBr): $\tilde{\nu}$ = 3554, 3473, 3413, 2924, 1778, 1737, 1617, 1523, 969, 845 cm^{-1}. MS (ESI): *m/z* 487 $[M + H]^+$.

3.5.2. Appendix

^{1}H NMR (DMSO-d_6) of compound **23**

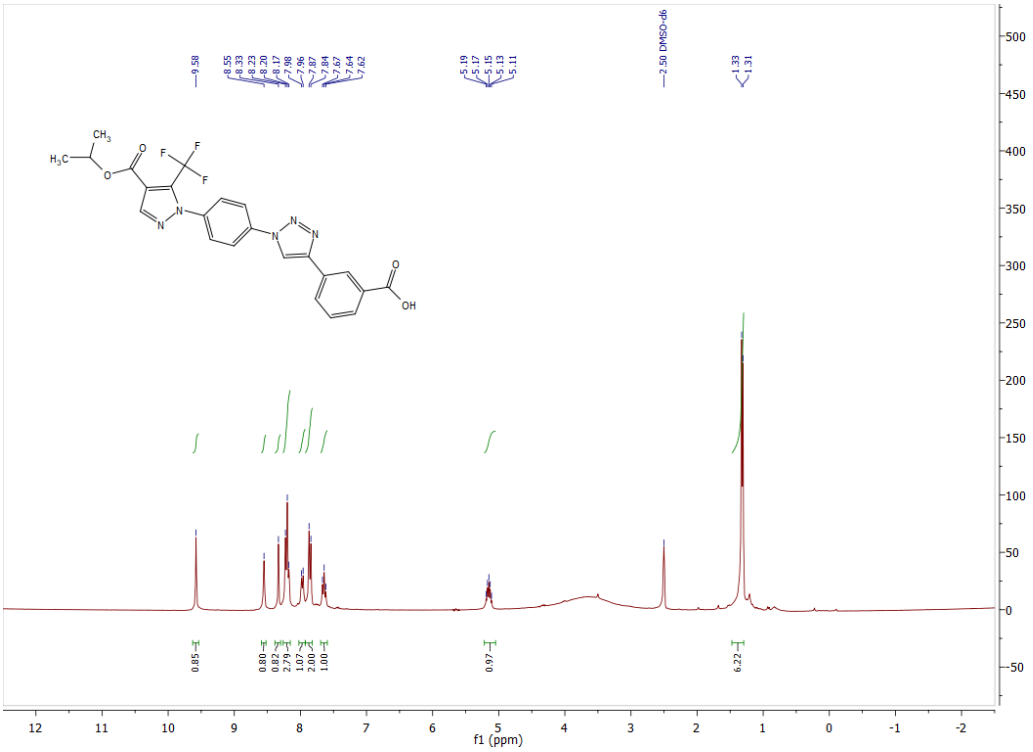

^{1}H NMR ($CDCl_3$) of compound **31**

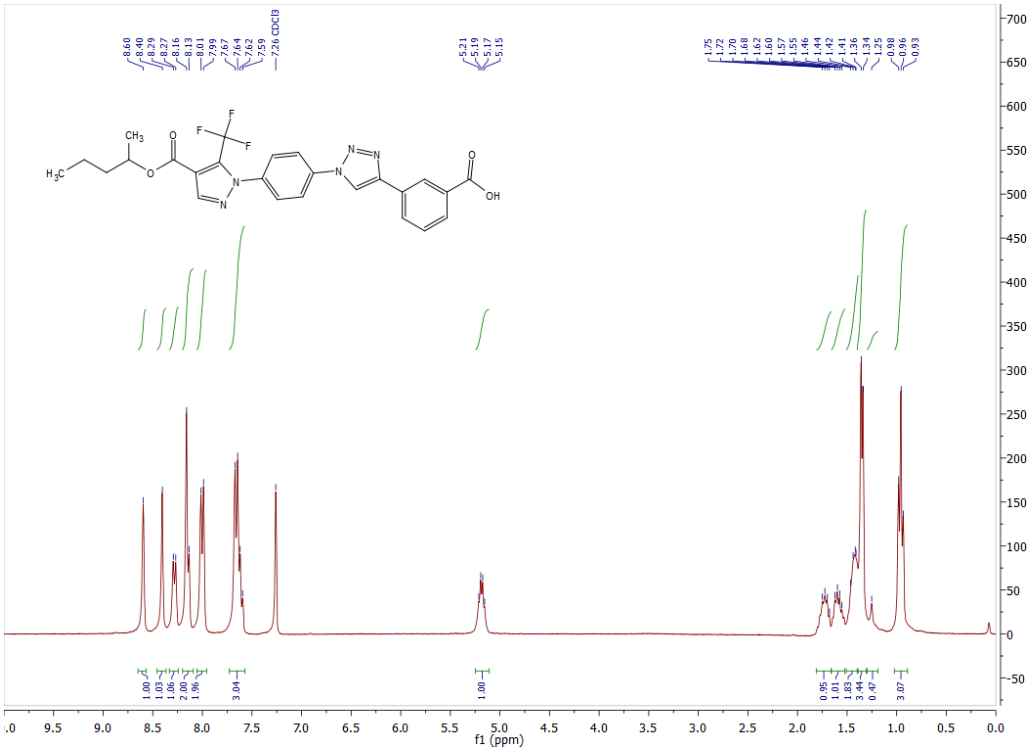

3.6. References

1. a. Parekh, A.B.; Store Operated CRAC channels: function in health and disease. *Nat. Rev. Drug Discov.* **2010,** *9*, 339-410.
   b. Feske, S. CRAC channelopathies. *Plufgers Arch.* **2010,** *460*, 417-435.
   c. Groschner, K.; Graier, W.F.; Romanin, C. Advances in experimental medicine and biology. In *Store-Operated Ca^{2+} Entry (SOCE) Pathways – Emerging signalling concepts in human (patho)physiology*, *2nd* Ed. Groschner, K.; Graier, W.; Romanin, C. Eds.; Springer: Berlin, **2017**, pp 993.
2. Stauderman, K.A. CRAC channels as targets for drug discovery and development. Cell Calcium. **2018**, *74*, 147-159.
3. Hou, X.; Pedi, L.; Diver, M.M.; Long, S.B. Crystal structure of the calcium release–activated calcium channel Orai, *Nature.* **2012**, *338*, 1308-1313.
4. Djuric, S.W.; BaMaung, N.Y.; Basha, A.; Liu, H.; Luly, J.R.; Madar, D.J.; Scioyyi, R.J.; Tu, N.P.; Wagenaar, F.L.; Zhoun, X.; Ballaron, S.; Bauch, J.; Chen, Y-W.; Chiou, X.G.; Fey, T.; Gauvin, D.; Gubbins, E.; Hsieh, G.C.; Marsh, K.C.; Mollison, K.W.; Pong, M.; Shaughnessy, T.K.; Sheets, M.P.; Smith, M.; Trevillyan, J.M.; Warrior, U.; Wegner, C.D.; Carter, G.W. 3,5-bis(trifluoromethyl)pyrazoles: a novel class of NFAT transcription factor regulator. *J. Med. Chem*. **2000**, *43*, 2975-2981.
5. Takezawa, R.; Cheng, H.; Beck, A.; Ishikawa, J.; Launay, P.; Kubota, H.; Kinet, J.P.; Fleig, A., Yamada, T.; Penner, R. A pyrazole derivative potently inhibits lymphocyte Ca^{2+} influx and cytokine production by facilitating transient receptor potential melastatin 4 channel activity. *Mol. Pharmacol*. **2006**, *69*, 1413-1420.
6. Kiyonaka, S.; Kato, K.; Nishida, M.; Mio, K.; Numaga, T.; Sawaguchi, Y.; Yoshida, T.; Wakamori, M.; Mori, E.; Numata, M.; Ishii, M.; Takemoto, H.; Ojida, A.; Watanabe, K.; Uemura, A.; Kurose, H.; Morii, T.; Kobayashi, T.; Sato, Y.; Sato, C.; Hamachi, I.; Moria, Y. Selective and direct inhibition of TRPC3 channels underlies biological activities of a pyrazole compound. *Proc. Natl. Acad. Sci. USA.* **2009**, *106*, 5400-5405.
7. Schleifer, H.; Doleschal, B.; Lichtenegger, M.; Oppenrieder, R.; Derler, I.; Frischauf, I.; Glasnov, T. N.; Kappe, C. O.; Romanin, C.; Groschner, K. Novel Pyrazole Compounds for Pharmacological Discrimination Between Receptor-Operated and Store-Operated Ca^{2+} Entry Pathways. *Br. J. Pharmacol*. **2012,** *167*, 1712-1722.
8. Djillani, A.; Doignon, I.; Luyten, T.; Lamkhioued, B.; Gangloff, S. C.; Parys, J. B.; Nüße, O.; Chomienne, C.; Dellis, O. Potentiation of the Store-Operated Calcium Entry (SOCE) Induces Phytohemagglutinin-Activated Jurkat T Cell Apoptosis. *Cell Calcium*. **2015**, *58*, 171-85.
9. Pirali, T.; Riva, B.; Genazzani, A.A. Modulators of SOCE, compositions and use thereof. WO 2017/212414 A1. Dec 14, **2017**

Chapter 4

Synthesis, biological evaluation and molecular docking studies of Ugi and Passerini adducts as novel indoleamine 2,3-dioxygenase 1 inhibitors

4.1. Introduction

As stated in Chapter 1.2.3, the key catabolic enzyme for tryptophan to kynurenines, indoleamine 2,3-dioxygenase 1 (IDO1), has been center-stage as a druggable target for cancer immunotherapy in the last 10 years with great hopes. However, among the thousands of compounds reported in the scientific and patent literature as IDO inhibitors, to date only five molecules have reached human clinical trials, confirming that the translation of *in vitro* to *in vivo* IDO inhibition is a big challenge.[1] Moreover, epacadostat has recently failed to show a clinical benefit in combination to pembrolizumab in unresectable or metastatic melanoma.[2] Thus, additional and continued efforts to identify new inhibitors with improved properties are needed.

In 2014 the imidazothiazole compounds **1** and **2** were reported by Tojo *et al.* (Figure 1A)[3] displaying IC_{50} values of 1.9 μM and 77 nM, respectively, in an enzyme-based assay. The crystal structure of the complex IDO1/**1** was described (Figure 1B), demonstrating that the nitrogen of the imidazole ring is bound to the heme iron and the tolyl group is located in pocket A of the active site. Interestingly, a shift of Phe226 occurs and the resulting induced fit in pocket B allows for the allocation of the *p*-chlorophenyl ring adjacent to Phe226. In contrast, **2** showed an improved inhibitory activity: indeed, the rigid urea moiety allows the *p*-cyanophenyl group to interact with both Phe226 (π-π interaction) and Arg231 (electrostatic interaction). Surprisingly, despite the promising inhibitory activity on the purified enzyme, no inhibition was detectable when Dr. Fallarini's research group tested compound **2** in a cell-based assay at concentration of 10 μM.

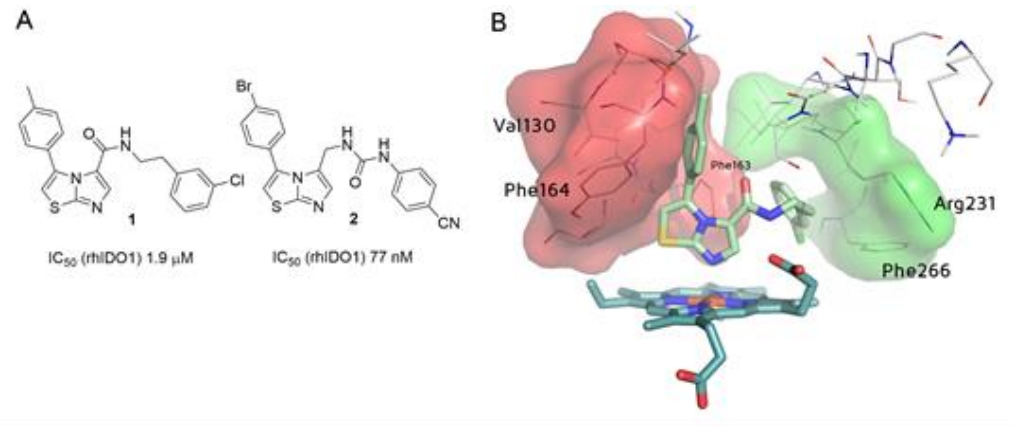

Figure 1. (**A**) Structure of imidazothiazole compounds **1** and **2**. (**B**) Compound **1** bound to IDO1 (PDB code: 4PK6). Heme is depicted as cyan sticks and compound **1** as pale green sticks. Red surface: pocket A; green surface: pocket B.

4.2. Aim of the work

The peculiar profile of this class of molecules described above prompted us to investigate the synthesis and the biological evaluation of a range of imidazothiazoles compounds displaying a modified side chain, with the aim of both finding new analogues with an improved cellular activity against IDO1 and probing interactions with the active site aminoacids. Therefore, during my PhD I carried out the synthesis and the characterization of this class of molecules (See Chemistry section 4.5.1.).

4.3. Results and discussion

4.3.1. Chemistry

For the synthesis of a first series of compounds we exploited the Ugi multicomponent reaction,[4] which allows for the rapid and versatile generation of imidazothiazoles displaying different α-acylaminoamides in the side chain.

Starting from the required amine **3** described in literature,[3] the isocyanide **5** was prepared by formylation with ethyl formate followed by dehydration in the presence of phosphorous oxychloride and triethylamine (Scheme 1).

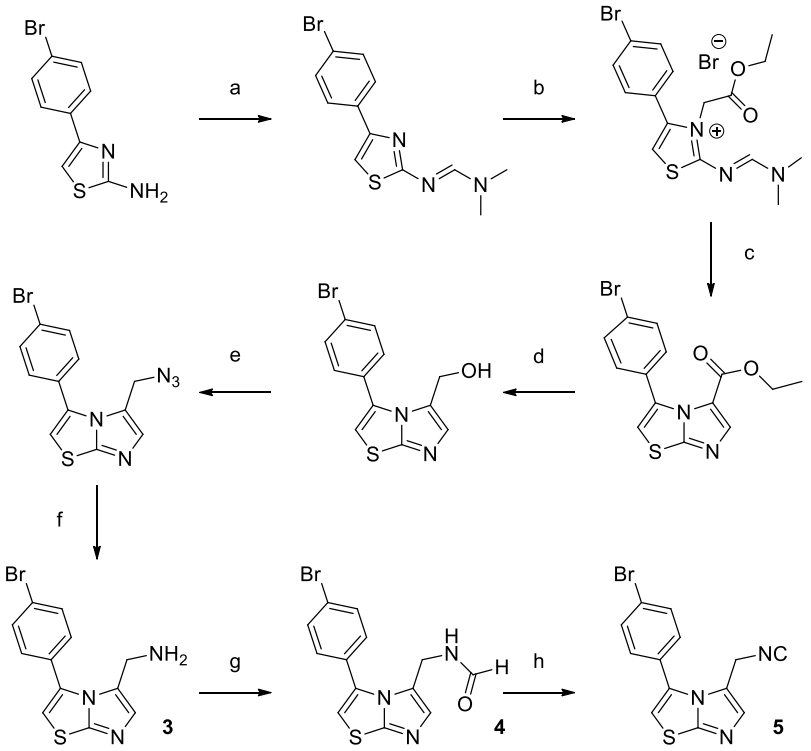

Scheme 1. Isocyanide synthetic pathway.
(**a**) DMF-DMA, DMF, 80 °C, 99%; (**b**) ethyl bromoacetate, 80 °C, 76%; (**c**) DBU, DMF, 60 °C, 99%; (**d**) $LiAlH_4$, dry THF, 0 °C, 81%; (**e**) DPPA, DBU, DMF, 60 °C, 67%; (**f**) PPh_3, H_2O, THF, 45 °C, 96%; (**g**) HCOOEt, reflux, 99%; (**h**) $POCl_3$, TEA, dry CH_2Cl_2, -30 °C, 77%.

With the isocyanide **5** in our hand, we performed the Ugi reaction with aqueous methylamine as the amine component and formalin as the carbonyl partner, in order to minimize the steric hindrance in the side chain and allow for the penetration in the deep and tight pocket B of IDO active site. As a proof of principle, acetic acid, different substituted benzoic acids and phenylacetic acid were used (Scheme 2). Products **6a-g** precipitated from the reaction mixture as white solids and were obtained simply by filtration.

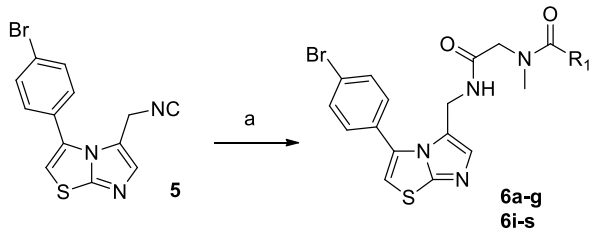

R1 = methyl (**6a**)	4-hydroxybenzyl (**6k**)
phenyl (**6b**)	3-hydroxybenzyl (**6l**)
4-cyanophenyl (**6c**)	2-hydroxybenzyl (**6m**)
4-nitrophenyl (**6d**)	4-nitrobenzyl (**6n**)
4-methoxyphenyl (**6e**)	3-nitrobenzyl (**6o**)
3-methoxyphenyl (**6f**)	2-nitrobenzyl (**6p**)
benzyl (**6g**)	4-chlorobenzyl (**6q**)
4-cyanobenzyl (**6i**)	3-chlorobenzyl (**6r**)
3-cyanobenzyl (**6j**)	2-chlorobenzyl (**6s**)

Scheme 2. Synthesis of U-4CR analogues.
(**a**) 37% aqueous formaldehyde solution, 40% aqueous methylamine solution, R_1-COOH, CH_3OH, rt, 24-61%.

As phenylacetic acid gave the best enzymatic inhibitory activity (see Biological evaluation section 4.3.2.), we decided to evaluate whether the substitution of the methyl on the nitrogen of **6g** with a hydrogen would have improved the inhibitory activity. It is well known how difficult is to use ammonia in the Ugi reaction, especially when coupled with the highly reactive formaldehyde as the carbonyl compound, due to a number of possible side reactions.[5] Indeed, when 33% aqueous ammonium hydroxide was used, no product was afforded, even when the less nucleophilic 2,2,2-trifluoroethanol[6] was employed as solvent instead of methanol. Even the use of 2,4-dimethoxybenzylamine as ammonia equivalent and the subsequent removal of 2,4-dimethoxybenzyl group under acidic conditions proved to be unsuccessful.[7] Thus, the reaction was carried out with ammonium chloride as a nitrogen source[8] in the presence or absence of triethylamine as a base to access **6h**, but the yield was very low under all the experimental conditions used (10-12%). Therefore, tritylamine was used as an ammonia surrogate,[9] followed by deprotection with trifluoroacetic acid, leading to **6h** in high yield (Scheme 3).

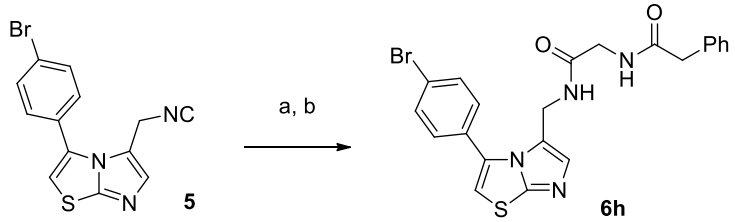

Scheme 3. Synthesis of compound **6h**.(**a**) Tritylamine, phenylacetic acid, paraformaldehyde, methanol, 40 °C, 93%; (**b**) TFA, CH_2Cl_2, 0 °C, 84%.

A drop in inhibitory activity occurred (see Biological evaluation section 4.3.2.), hence the methylamine was kept fixed and different substituents at different positions of the benzylic ring were explored. As the active site of IDO1, despite its marked hydrophobic nature, features a number of sites capable of hydrogen-bonding to inhibitors, moieties such as cyano and hydroxy were introduced, together with nitro and chlorine, able to affect the electronic properties. Compounds **6i**, **6k** and **6n-p** precipitated from the reaction mixture and were isolated in high purity (Scheme 2), while **6j**, **6l**, **6m** and **6q-s** were purified by column chromatography.

Next, we investigated whether the substitution of the *N*-methyl group with oxygen at the linker site might lead to an improvement in inhibitory activity. To this aim, Passerini reaction was performed[10] and the isocyanide **5** was reacted with aqueous formaldehyde and functionalized phenyl acetic acids to afford compounds with different α-acyloxyamides in the side chain, **7a-l** (Scheme 4).

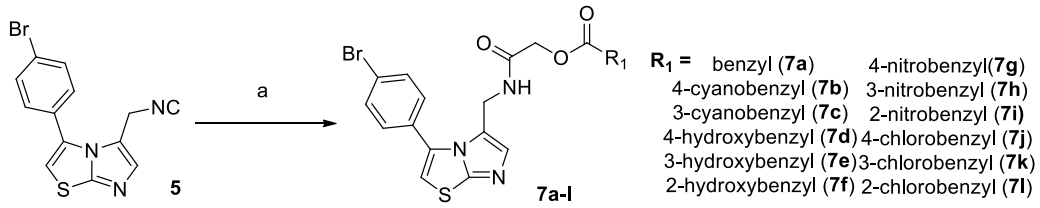

Scheme 4. Synthesis of P-3CR analogues.
(**a**) 37% aqueous formaldehyde solution, R_1-COOH, CH_2Cl_2, reflux, 35-87%.

Finally, Passerini product **7a** was hydrolyzed to access α-hydroxyamide **7m** and test whether the presence of a shorter side-chain with a free hydroxyl group might affect the inhibitory activity (Scheme 5).

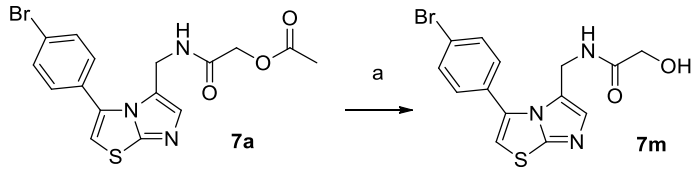

Scheme 5. Synthesis of compound **7m**.
(a) NaOH, H_2O/acetone, rt, 70%.

As the synthesized products displayed low cellular activity in the cell-based assay (see Biological evaluation section 4.3.2.), in an attempt to increase cell permeability, we investigated whether the introduction of a dipeptide structure in the side chain would retain the inhibitory activity on the enzyme, allowing for cell penetration. Indeed, a dipeptide structure might be recognized by peptide transporters such as PEPT1 and PEPT2.[11] To this aim, two Boc-protected aminoacids, namely Boc-phenylglycine and Boc-4-hydroxyphenylglycine, were reacted in the Ugi reaction with isocyanide **5**, tritylamine and paraformaldehyde. Subsequent deprotection with TFA removed both Boc and trityl protecting groups (Scheme 6), affording compounds **8a** and **8b**.

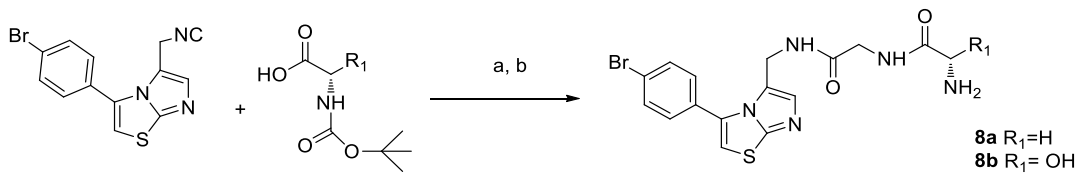

Scheme 6. Synthesis of compounds **8a** and **8b**.
(**a**) Boc-protected aminoacid, tritylamine, paraformaldehyde, CH_3OH, 40 °C, 43-88%; (**b**) TFA, CH_2Cl_2, 0 °C, 34-39%.

4.3.2. Biological evaluation

The synthesized molecules have been tested in the laboratory of Dr. Fallarini.

The measurement of cell viability is mandatory when reporting cellular IDO1 inhibitory activity, because the observed reduction of tryptophan degradation could simply be an effect of cytotoxicity. Thus, we decided to first investigate the

cytotoxicity of all the synthesized compounds on A375 cell line. Cells were treated (48 h) with each compound (10 µM) and cell viability was measured by MTT assay. As reported in Table 1, compounds **6c**, **6e**, **6m** and **6-s** affected cell viability. In particular, **6q** and **6s** were the most cytotoxic, inducing a reduction of cell viability of -29% and -36%, respectively.

The ability of the synthesized compounds to inhibit human IDO1 was first analyzed by a cell-free assay using a purified recombinant human IDO1 (rhIDO1) enzyme. Each compound (1 µM) was added to the reaction buffer and the rhIDO1 conversion of L-Trp to L-Kyn determined spectrophotometrically using p-dimethylaminobenzaldehyde. Under these conditions, the IC_{50} value of **2** was consistent with previous data in literature[3]. For all the synthesized compounds displaying an inhibition above 60% the IC_{50} value was determined.

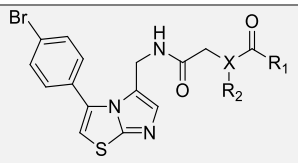

Cpd	X	R_1	R_2	Cell viability (%) at 10 µM ±SEM	Enzymatic assay inhibition (%) @ 1 µM	Enzymatic IC_{50} (µM)	IDO cellular assay inhibition (%) @ 10 µM
1-methyl-L-tryptophan (L-1MT)				100±8	-	-	38
2				99±3	97	0.08	0
6a	N	methyl	methyl	98±5	21		
6b	N	phenyl	methyl	96±4	50		6.9
6c	N	4-cyanophenyl	methyl	87±2	47		
6d	N	4-nitrophenyl	methyl	100±6	45		
6e	N	4-methoxyphenyl	methyl	82±8	49		

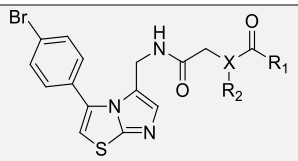

Cpd	X	R_1	R_2	Cell viability (%) at 10 µM ±SEM	Enzymatic assay inhibition (%) @ 1 µM	Enzymatic IC_{50} (µM)	IDO cellular assay inhibition (%) @ 10 µM
6f	N	3-methoxyphenyl	methyl	98±5	48		
6g	N	benzyl	methyl	100±4	62	0.69	2.5
6h	N	benzyl	H	100±8	46		
6i	N	4-cyanobenzyl	methyl	92±7	18		
6j	N	3-cyanobenzyl	methyl	90±9	0		
6k	N	4-hydroxybenzyl	methyl	91±11	55		0
6l	N	3-hydroxybenzyl	methyl	100±2	63	0.45	0
6m	N	2-hydroxybenzyl	methyl	88±14	0		
6n	N	4-nitrobenzyl	methyl	100±3	66	0.81	24
6o	N	3-nitrobenzyl	methyl	93±5	65	0.63	8
6p	N	2-nitrobenzyl	methyl	92±12	67	0.73	11
6q	N	4-chlorobenzyl	methyl	64±4	51		
6r	N	3-chlorobenzyl	methyl	83±7	39		
6s	N	2-chlorobenzyl	methyl	71±12	41		
7a	O	benzyl	-	98±6	72	0.58	0
7b	O	4-cyanobenzyl	-	100±3	69	0.34	0
7c	O	3-cyanobenzyl	-	97±5	29		
7d	O	4-hydroxybenzyl	-	100±4	89	0.20	4

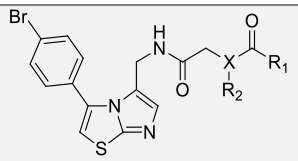

Cpd	X	R_1	R_2	Cell viability (%) at 10 µM ±SEM	Enzymatic assay inhibition (%) @ 1 µM	Enzymatic IC_{50} (µM)	IDO cellular assay inhibition (%) @ 10 µM
7e	O	3-hydroxybenzyl	-	100±3	59		14
7f	O	2-hydroxybenzyl	-	100±3	73	0.87	0
7g	O	4-nitrobenzyl	-	100±7	39		
7h	O	3-nitrobenzyl	-	100±5	50		0
7i	O	2-nitrobenzyl	-	100±10	41		
7j	O	4-chlorobenzyl	-	100±3	32		
7k	O	3-chlorobenzyl	-	100±6	39		
7l	O	2-chlorobenzyl	-	100±3	46		
7m	OH	-	-	97±8	48		
8a	N	(S)-2-amino-2-phenyl	H	96±7	10		
8b	N	(S)-2-amino-2-(4-hydroxyphenyl)	H	100±5	0		

Table 2. Structure and biological profile of imidazothiazole compounds.

4.3.3. Enzymatic IDO1 inhibition and SAR study

Structure-activity studies of the α-acylaminoamides have fully explored the chemical space around this structure (Table 1). First, acetic acid, benzoic acid and phenylacetic acid were used in the Ugi reaction to access **6a**, **6b** and **6g**. While the

inhibitory activity was low when a methyl group was present (**6a**, 21% of inhibition at 1 μM), the introduction of a phenyl in **6b** or a benzyl in **6g** improved the inhibition effect (50% and 62%, respectively), with an IC_{50} value for compound **6g** equal to 0.69 μM. The introduction of different substituents on the phenyl ring (**6c-f**) did not produce any improvement of the activity.

As the benzylic substructure displayed the highest inhibitory activity, the substitution of the N-Me in **6g** with a NH in 6h was investigated. The decrease in lipophilicity produced a decrease in inhibitory activity (46%).

Keeping the N-Me group fixed, the effect of different substituents on the benzyl ring was investigated (**6i-s**). The cyano group produced a complete loss of activity when present at position 3' (**6j**, 0%) and 4' (**6i**, 18%). The same occurred when the hydroxyl moiety was introduced at position 2' (**6m**, 0%). On the contrary, the hydroxyl group at position 3' gave rise to the most active compound of this series, **6l**, with an IC_{50} value of 0.45 μM, while its presence at position 4' gave the compound **6k** displaying an inhibitory activity of 55%. The presence of a nitro group produced a progressive increase in activity by moving the substituent from position 4' (**6n**, IC_{50} = 0.81 μM) to either position 2' (**6p**, IC_{50} = 0.73 μM) or 3' (**6o**, IC_{50} = 0.63 μM). The presence of a chlorine at different positions on the benzylic ring did not produce any improvement of activity (**6q-s**), which was settled between 39 and and 51%.

In parallel with Passerini reactions, α-acyloxyamides **7a-l** were synthesized and, in general, they showed a better inhibitory activity compared to the corresponding α-acylaminoamides **7i-s**, revealing that the different bond angles between -O- and -N- at the linker site, together with the different flexibility of the side chain, largely altered the location of the benzylic ring and its substituent and positively affected the interaction with the enzyme aminoacids. This is confirmed by comparison of the non-substituted compound **7a** (IC_{50} = 0.58 μM) with the corresponding analogue **6g** (IC_{50} = 0.69 μM).

Analogously, the influence of different substituents on the benzyl ring was studied. Electron-withdrawing groups such as nitro and chlorine gave rise, at any position, to a loss of activity (**7g-l**) with a percentage of inhibition lower than 50%. Cyano group, when present at position 3', did not produce a remarkable effect on IDO1 inhibition (**7c**, 29%), while when displayed at position 4' produced a significant increase in activity (**7b**, 69%, IC_{50} = 0.34 µM). Even the polar hydroxyl group when present at position 4' increased inhibitory potency, giving rise to the most potent compound of this class of imidazothiazoles (**7d**, 89%, IC_{50} = 0.20 µM) (Figure 2), with a slight loss of activity when moved to either position 3' (**7e**, 59%) or 2' (**7f**, 73%, IC_{50} = 0.87 µM).

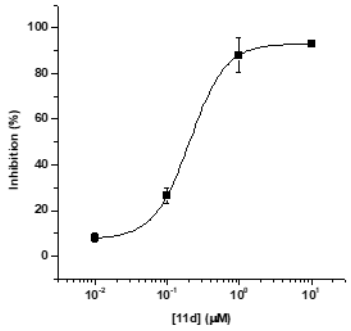

Figure 2. Concentration-response curve for compound **7d** in IDO1 inhibition enzymatic assay.

The presence of a α-hydroxyamide moiety in the side-chain was shown to maintain a moderate inhibitory activity (**7m**, 48%).

A final round of SAR revealed that the introduction of an additional primary amino group at the α-position of the amide is detrimental for inhibitory activity both in **8a** (10%) and **8b** (0%) and this experimental evidence is consistent with the pronounced hydrophobic nature of the IDO1 active site. Therefore, these two products did not proceed further in the cell-based assay, despite the presence of the dipeptide substructure.

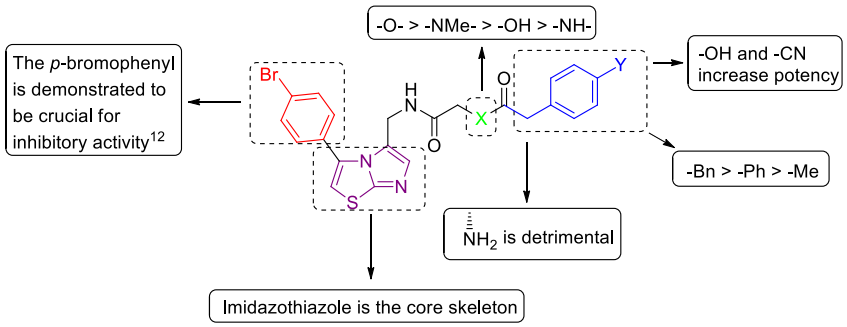

Figure 3. Graphical representation of SARs relative to the side chain.

Compounds that showed an inhibition value greater than 50% in the enzymatic assay were then evaluated in a cell-based assay, except for **6q** which resulted cytotoxic at 10 µM.

4.3.4. Cellular IDO1 inhibitory activity

The ability of selected compounds to inhibit human IDO1 activity was determined in an *in vitro* cell-based assay, to evaluate their inhibitory effect together with their ability to permeate the cell membrane. The human melanoma A375 cell line was selected for the cellular assay because does not express either IDO1 gene or protein under normal culture condition, but efficiently up regulates IDO1 expression and enhances L-Kyn level in response to IFN-γ treatment. A375 cells were stimulated with IFN-γ (500U/mL), incubated in the presence of each selected compound (10 µM) for 48 h and enzymatic activity of IDO determined by measuring the formation of the L-Kyn product by high-performance liquid chromatography (HPLC) method. IDO1 inhibitor L-1MT was used as positive control in this system and showed a percentage of inhibition of 38%. Results are shown in Table 1. The synthesized compounds proved to be inactive when tested in the cell-based assay, except for compounds **6n**, **6p** and **7e,** which displayed a percentage of inhibition higher than 10% at 10 µM. **6n** was the most potent inhibitor, leading to a 24% of activity,

comparable to L-1MT. In all cases, a significant discrepancy between the enzymatic and the cellular inhibition was observed. cLogP values (calculated by ACDlab software) of the synthesized compounds are between 3.80 and 5.50, ruling out that a low hydrophobicity is the reason for the poor cellular activity. Similarly, pKa values referred to the basic imidazole nitrogen (calculated by ACDlab software) are around 4.5, leading to such a low degree of protonation at physiological pH that cannot explain the low cell penetration. Alternative reasons for poor performance of the inhibitors in the cell-based assay could be that compounds are poorly soluble in the cell–based assay conditions and have the tendency to precipitate. It is also possible that they get transported out of the cell or bind to serum proteins in the cell growth medium, although this is currently speculative.

4.3.5. Molecular modeling

In collaboration with the computational chemist Dr. Massarotti, molecular modeling was used to understand the potential pose of the most promising imidazothiazoles **7d** and **6n** in the IDO1 binding site. Docking studies were carried out using the software OMEGA2[12] and FRED[13], showing that the two structures lay with a partially different orientation than compound **1** (Figure 1). The *p*-bromophenyl ring of both **7d** and **6n** is accommodated in the hydrophobic pocket A (Tyr126, Cys129, Val130, Phe163 and Phe164), while the imidazothiazole core is able to form a strong nitrogen–iron bond with the heme group (Figure 4A, 4B). The side chain of **7d** and **6n** extends in proximity to pocket B (Phe226 and Arg231) and one carbonyl group is found to be forming a hydrogen bond with Arg231. The benzyl group protrudes into a different pocket (Leu234, Ser235, Gly236, Lys238, Ala260, Gly261 and Gly262), named C, which is located in the most external part of the IDO binding site (Figure 4C). In particular, the aromatic ring interacts with Gly261 in both the compounds, the hydroxyl group of **7d** donates a H-bond interaction to the

carbonyl moiety of Lys238, while the nitro group of **6n** accepts a H-bond interaction with the nitrogen of the same backbone residue.

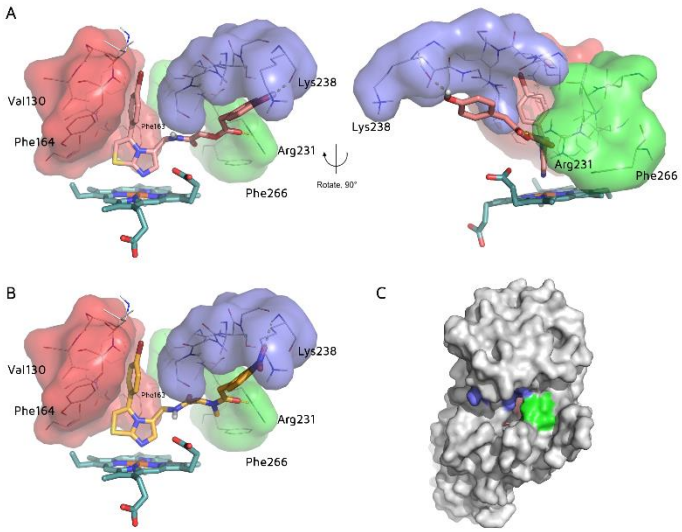

Figure 4. Docking poses of compounds **7d** (**A**) and **6n** (**B**). Structures are depicted as pink and orange sticks, respectively, while heme is depicted as cyan sticks. Red surface: pocket A; green surface: pocket B; blue surface: pocket C. Visualization of A-B-C pockets on protein surface (**C**).

4.4. Conclusions

In summary, starting from a common isocyanide intermediate, we have prepared a range of imidazothiazoles by a straightforward multicomponent approach. Iterative cycles of synthesis and testing resulted in the rapid identification of **7d** with an IC_{50} value in the enzyme-based assay of 200 nM. The computational study suggests that **7d** is characterized by a unique binding mode. The coordination formed between the imidazole nitrogen and the heme iron, the hydrophobic interaction of the *p*-bromophenyl ring in pocket A and the hydrogen bonds with Arg231 in pocket B and Lys238 in pocket C are the major interactions between **7d** and IDO1. The hydrogen bond with Lys238 appears to confer increased potency to this class of inhibitors and explains the higher activity associated with both **7d** and **6n**. While compound **7d**

doesn't display significant inhibitory activity in A375 cells, **6n** shows a full biocompatibility and a 24% of IDO1 inhibition at 10 μM, together with an enzymatic IC_{50} of 810 nM. Overall, the information acquired in this study provides a new direction for future design of IDO1 inhibitors. Indeed, we have demonstrated that an isocyanide based-multicomponent approach represents a straightforward and versatile access to IDO1 inhibitors displaying a densely-functionalized side-chain. This allows for the construction of a network of interactions with both the heme group and the residues located in three different pockets of the active site. Building on these findings, further studies aimed at developing compounds with an improved cellular inhibitory activity led us to the identification of a novel promising class of compounds that targets IDO1. This discovery will be illustrated in detail in the following Chapter.

4.5. Experimental section

General Methods. Commercially available reagents and solvents were purchased from Sigma-Aldrich and Alfa Aesar and used without further purification. When needed, solvents were distilled and stored on molecular sieves. Melting points were determined in an open glass capillary with a Stuart scientific SMP3 apparatus. All the target compounds were checked by using IR (FT-IR Thermo-Nicolet Avatar), ^{1}H and ^{13}C APT (Jeol ECP 300 MHz), and mass spectrometry (Thermo Finningan LCQ-deca XP-plus) devices equipped with an ESI source and an ion trap detector. Chemical shifts (δ) are reported in parts per million (ppm) and coupling costants (*J*) are expressed in Hz. Column chromatography was performed on silica gel Merck Kieselgel 70-230 mesh ASTM. Thin layer chromatography (TLC) was carried out on 5 cm x 20 cm plates with a layer thickness of 0.25 mm (Merck silica gel 60). The spots were visualized by ultraviolet light (wavelengths 254 and 366 nm) and, when necessary, with Dragendorff reagent and $KMnO_4$. The purity of the targets

compounds (>95%) was determined via elemental analysis and was within ±0.4% of the calculated value.

4.5.1. Chemistry

N-((3-(4-Bromophenyl)imidazo[2,1-b]thiazol-5-yl)methyl)formamide, (4).

The amine **3** (1 eq, 13.6 mmol) was dissolved in ethyl formate (84 mL) and the resulting mixture was heated at reflux for 3 hours. When the reaction was finished, the volatile was removed under reduced pressure to give *N*-((3-(4-bromophenyl)imidazo[2,1-b]thiazol-5-yl)methyl)formamide 4. The crude material was used in the next step without further purification. White solid. Yield: 99%.

3-(4-Bromophenyl)-5-(isocyanomethyl)imidazo[2,1-b]thiazole, (5).

To a solution of N-((3-(4-bromophenyl)imidazo[2,1-b]thiazol-5-yl)methyl)formamide 4 (1 eq, 10.5 mmol) in dry CH_2Cl_2 (33.3 mL), TEA (5 eq, 6.90 mL) was added. The reaction was cooled to - 30 °C and a solution of $POCl_3$ (1.5 eq, 1.36 mL) in dry CH_2Cl_2 (11 mL) was added dropwise. After stirring for 2 hours, a saturated aqueous solution of $NaHCO_3$ was added and the mixture was allowed to reach room temperature. CH_2Cl_2 was added and the organic phase was washed with a saturated aqueous solution of $NaHCO_3$ (x 2), dried over sodium sulfate and evaporated. The crude material was purified by chromatography column using PE/$CHCl_3$ 1:9 as eluent yielding 3-(4-bromophenyl)-5-(isocyanomethyl)imidazo[2,1-b]thiazole **5**. Yellow-white solid. Yield: 77%. mp 128.3-129.3 °C. ν_{max} cm^{-1} 3093, 2972, 2906, 2142, 1574, 1455, 1430, 1146, 841, 757, 539. ^{1}H NMR (300 MHz, DMSO-d_6): δ = 7.75 (d, *J* = 7.8 Hz, 2H), 7.64 (d, *J* = 7.8 Hz, 2H), 7.34 (s, 2H), 4.73 (s, 2H). ^{13}C NMR (75 MHz, DMSO-d_6): δ = 157.9, 151.7, 136.1, 131.7, 131.2, 129.7, 128.0, 118.8, 111.6, 110.9, 36.2.

General procedure for the synthesis of compounds 6a-g and 6i-s.

37% aqueous formaldehyde solution (3 eq) was dissolved in CH_3OH, then 40% aqueous methylamine solution (2 eq) was added under vigorous stirring. After 30

minutes carbossilic acid (1 eq) and isocyanide 5 (1 eq) were added in order. The reaction mixture was left to react. In some cases (**6a**, **6b**, **6c**, **6d**, **6e**, **6f**, **6g**, **6i**, **6k**, **6n**, **6o**, **6p**) product precipitates and the precipitated white solid was collected by filtration using a Buchner funnel and rinsed with ethyl acetate. In case that no precipitation was observed (**6j**, **6l**, **6m**, **6q**, **6r**, **6s**), CH_3OH was evaporated and the reaction was worked up by diluition with ethyl acetate and washing with a saturated aqueous solution of Na_2CO_3 (except for the compounds **6l** and **6m** which were washed with a saturated aqueous solution of $NaHCO_3$). The organic layer was dried over sodium sulfate and evaporated. The crude material was purified by chromatography column.

N-((3-(4-Bromophenyl)imidazo[2,1-b]thiazol-5-yl)methyl)-2-(N-methylacetamido)acetamide, (6a).

White solid. Yield: 55%. mp 250-250.5 °C dec. Found: C, 48.52; H, 4.15; N, 13.27. $C_{17}H_{17}BrN_4O_2S$ requires C, 48.46; H, 4.07; N, 13.30. ν_{max} cm^{-1} 3310, 3082, 2931, 1920, 1645, 1450, 1072, 1013, 609. ^{1}H NMR (300 MHz, DMSO-d_6): δ = 8.05 (s, 1H), 7.91 (s, 1H), 7.69 (d, *J* = 7.7 Hz, 2H), 7.55 (d, *J* = 7.7 Hz, 2H), 7.21 (br s, 1H), 3.99 (s, 2H), 3.67 (s, 2H), 2.90 (s, 3H), 1.98 (s, 3H). ^{13}C NMR (75 MHz, DMSO-d_6, referred to the main rotamer): δ = 170.9, 168.3, 155.1, 132.3, 132.1, 132.0, 131.8, 129.2, 123.8, 115.5, 111.7, 50.2, 37.6, 34.4, 21.7. MS (ESI) m/z 445 $[M+H]^+$.

N-(2-(((3-(4-Bromophenyl)imidazo[2,1-b]thiazol-5-yl)methyl)amino)-2-oxoethyl)-N-methylbenzamide, (6b).

White solid. Yield: 52%. mp 249-250 °C. Found: C, 54.84; H, 4.02; N, 11.57. $C_{22}H_{19}BrN_4O_2S$ requires C, 54.66; H, 3.96; N, 11.59. ν_{max} cm^{-1} 3277, 3056, 2933, 1645, 1629, 1547, 1456, 821, 696. ^{1}H NMR (300 MHz, DMSO-d_6): δ = 8.05 (s, 1H), 7.68 (d, *J* = 10.7 Hz, 2H), 7.55 (m, 2H), 7.42 (m, 4H), 7.25 (m, 2H), 4.04 (s, 2H), 3.61 (s, 2H), 2.48 (s, 3H). ^{13}C NMR (75 MHz, DMSO-d_6): δ = 170.2, 167.7, 149.9, 136.8, 135.0, 133.0, 132.2, 132.0 (2C), 131.2, 129.0, 127.3, 124.7, 123.6, 111.6, 52.8, 38.4, 35.2. MS (ESI) m/z 485 $[M+H]^+$.

N-(2-(((3-(4-Bromophenyl)imidazo[2,1-b]thiazol-5-yl)methyl)amino)-2-oxoethyl)-4-cyano-N-methylbenzamide, (6c).

White solid. Yield: 55%. mp 243-244 °C dec. Found: C, 54.25; H, 3.56; N, 13.85. $C_{23}H_{18}BrN_5O_2S$ requires C, 54.34; H, 3.57; N, 13.78. ν_{max} cm^{-1} 3282, 2940, 2230, 1643, 1548, 1455, 843, 817. ^{1}H NMR (300 MHz, DMSO-d_6): δ = 8.09 (s, 1H), 7.91 (d, *J* = 8.8 Hz, 2H), 7.59 (m, 6H), 7.21 (s, 1H), 3.86 (s, 2H), 3.36 (s, 2H), 2.82 (s, 3H). ^{13}C NMR (75 MHz, DMSO-d_6, referred to the main rotamer): δ = 170.1, 167.5, 149.9, 141.3, 134.7, 133.1, 132.2, 132.1, 131.9, 129.2, 128.4, 128.1, 124.0, 123.8, 118.9, 112.7, 53.4, 50.0, 34.3. MS (ESI) m/z 510 $[M+H]^+$.

N-(2-(((3-(4-Bromophenyl)imidazo[2,1-b]thiazol-5-yl)methyl)amino)-2-oxoethyl)-N-methyl-4-nitrobenzamide, (6d).

White solid. Yield: 24%. mp 245-246 °C dec. Found: C, 50.15; H, 3.47; N, 13.22. $C_{22}H_{18}BrN_5O_4S$ requires C, 50.01; H, 3.43; N, 13.25. ν_{max} cm^{-1} 3281, 3084, 2930, 2353, 1644, 1544, 1072, 1013. ^{1}H NMR (300 MHz, DMSO-d_6): δ = 8.28 (d, *J* = 8.5 Hz, 2H), 7.66 (d, *J* = 8.0 Hz, 2H), 7.60 (d, *J* = 8.0 Hz, 2H), 7.42 (d, *J* = 8.5 Hz, 2H), 7.26 (s, 1H), 6.73 (s, 1H), 3.98 (s, 2H), 3.47 (s, 2H), 3.00 (s, 3H). ^{13}C NMR (75 MHz, DMSO- d_6): δ = 169.9, 169.3, 167.4, 149.9, 148.4, 143.1, 142.8, 134.7, 132.0 (2C), 129.2, 128.8, 128.6, 124.3, 123.8, 53.3, 49.9, 34.3. MS (ESI) m/z 530 $[M+H]^+$.

N-(2-(((3-(4-Bromophenyl)imidazo[2,1-b]thiazol-5-yl)methyl)amino)-2-oxoethyl)-4-methoxy-N-methylbenzamide, (6e).

White solid. Yield: 25%. mp 248-249 °C dec. Found: C, 54.01; H, 4.17; N, 10.88. $C_{23}H_{21}BrN_4O_3S$ requires C, 53.81; H, 4.12; N, 10.91. ν_{max} cm^{-1} 3272, 3066, 2836, 2365, 1640, 1541, 1455, 1257, 839, 763. ^{1}H NMR (300 MHz, DMSO-d_6): δ = 8.13 (s, 1H), 8.03 (br s, 1H), 7.92 (d, *J* = 8.3 Hz, 2H), 7.78 (d, *J* = 8.9 Hz, 2H), 7.66 (d, *J* = 8.9 Hz, 2H), 7.33 (s, 1H), 7.17 (d, *J* = 8.3 Hz, 2H), 4.58 (s, 2H), 4.08 (s, 2H), 3.83 (s, 3H), 3.47 (s, 3H). ^{13}C NMR (75 MHz, DMSO- d_6): δ = 168.0, 160.8, 149.9, 134.5,

132.3, 132.0, 131.8 (2C), 129.3, 129.1, 128.9, 124.4, 123.8, 114.0, 111.6, 77.2, 55.6, 35.3, 34.4. MS (ESI) m/z 515 $[M+H]^+$.

N-(2-(((3-(4-Bromophenyl)imidazo[2,1-b]thiazol-5-yl)methyl)amino)-2-oxoethyl)-3-methoxy-N-methylbenzamide, (6f).

White solid. Yield: 56%. mp 247-248 °C dec. Found: C, 53.97; H, 4.21; N, 10.85. $C_{23}H_{21}BrN_4O_3S$ requires C, 53.81; H, 4.12; N, 10.91. ν_{max} cm^{-1} 3274, 3064, 2937, 2835, 1646, 1625, 1456, 1241, 785, 697. ^{1}H NMR (300 MHz, DMSO-*d*$_6$): δ = 8.05 (s, 1H), 7.68 (m, 2H), 7.57 (d, *J* = 9.3 Hz, 2H), 7.32 (m, 2H), 7.21 (m, 3H), 4.04 (s, 2H), 3.78 (s, 3H), 3.61 (s, 2H), 2.84 (s, 3H). ^{13}C NMR (75 MHz, DMSO-*d*$_6$): δ = 169.7, 167.8, 159.5, 149.8, 138.1, 134.6, 132.1 (2C), 130.1, 129.1, 123.8, 119.2, 115.7, 112.8, 112.4, 111.8, 105.4, 55.7, 53.6, 49.9, 34.4. MS (ESI) m/z 537 $[M+H]^+$.

N-(2-(((3-(4-Bromophenyl)imidazo[2,1-b]thiazol-5-yl)methyl)amino)-2-oxoethyl)-N-methyl-2-phenylacetamide, (6g).

White solid. Yield: 39%. mp 194-195 °C. Found: C, 55.40; H, 4.18; N, 11.34. $C_{23}H_{21}BrN_4O_2S$ requires C, 55.54; H, 4.26; N, 11.26. ν_{max} cm^{-1} 3289, 3027, 2922, 2358, 1733, 1539, 1398, 1242, 929, 817. ^{1}H NMR (300 MHz, DMSO-*d*$_6$): δ = 8.08 (s, 1H), 7.93 (br s, 1H), 7.70 (d, *J* = 7.7 Hz, 2H), 7.56 (t, *J* = 8.2 Hz, 2H), 7.21 (m, 6H), 3.99 (s, 2H), 3.71 (s, 2H), 3.28 (s, 3H), 2.96 (s, 2H). ^{13}C NMR (75 MHz, DMSO-*d*$_6$, referred to the main rotamer): δ = 171.4, 168.2, 136.1, 134.5, 132.2, 132.0, 131.8, 129.7, 129.6, 128.7, 128.6, 126.7, 124.4, 123.8, 111.6, 50.4, 37.3, 34.9, 34.4. MS (ESI) m/z 499 $[M+H]^+$.

N-(2-(((3-(4-Bromophenyl)imidazo[2,1-b]thiazol-5-yl)methyl)amino)-2-oxoethyl)-2-(4-cyanophenyl)-N-methylacetamide, 6i.

White solid. Yield: 42%. mp 240-241 °C. Found: C, 55.30; H, 3.92; N, 13.35. $C_{24}H_{20}BrN_5O_2S$ requires C, 55.18; H, 3.86; N, 13.41. ν_{max} cm^{-1} 3297, 2939, 2362, 2229, 1644, 1541, 1458, 1014, 816. ^{1}H NMR (300 MHz, DMSO-*d*$_6$, referred to the main rotamer): δ = 8.12 (s, 1H), 7.96 (br s, 1H), 7.76 (d, *J* = 7.7 Hz, 2H), 7.69 (d, *J*

= 7.9 Hz, 2H), 7.56 (d, *J* = 7.7 Hz, 2H), 7.41 (d, *J* = 7.9 Hz, 2H), 7.22 (s, 1H), 3.99 (s, 2H), 3.84 (s, 2H), 3.71 (s, 2H), 2.97 (s, 3H). ^{13}C NMR (75 MHz, DMSO-d_6, referred to the main rotamer): δ = 170.5, 167.8, 149.7, 142.4, 134.6, 132.5, 132.4, 132.1, 132.0, 131.9, 131.1, 124.5, 123.8, 119.4, 111.7, 109.8, 52.4, 50.6, 37.4, 34.5. MS (ESI) m/z 523 $[M+H]^+$.

N-(2-(((3-(4-Bromophenyl)imidazo[2,1-b]thiazol-5-yl)methyl)amino)-2-oxoethyl)-2-(3-cyanophenyl)-N-methylacetamide, (6j).

White solid. Yield: 61%. Chromatography: PE/EtOAc 1/9. mp 67-69 °C. Found: C, 55.32; H, 3.91; N, 13.32. $C_{24}H_{20}BrN_5O_2S$ requires C, 55.18; H, 3.86; N, 13.41. ν_{max} cm^{-1} 3248, 3077, 2878, 2231, 1673, 1451, 1214, 1152, 1011. ^{1}H NMR (300 MHz, DMSO-d_6): δ = 7.61 (d, *J* = 6.6 Hz, 2H), 7.43 (m, 6H), 7.26 (s, 1H), 6.48 (s, 1H), 4.41 (s, 2H), 3.80 (s, 2H), 3.71 (s, 2H), 3.08 (s, 3H). ^{13}C NMR (75 MHz, DMSO-d_6): δ = 170.9, 167.9, 150.6, 136.0, 134.7, 133.9, 132.9, 132.5 (2C), 132.3, 132.0, 130.8, 129.5, 128.4, 124.6, 123.3, 118.7, 112.7, 52.1, 39.7, 37.5, 34.3. MS (ESI) m/z 523 $[M+H]^+$.

N-(2-(((3-(4-Bromophenyl)imidazo[2,1-b]thiazol-5-yl)methyl)amino)-2-oxoethyl)-2-(4-hydroxyphenyl)-N-methylacetamide, (6k).

White solid. Yield: 41%. mp 214-216 °C. Found: C, 54.02; H, 4.15; N, 10.77. $C_{23}H_{21}BrN_4O_3S$ requires C, 53.81; H, 4.12; N, 10.91. ν_{max} cm^{-1} 3320, 3085, 3007, 2927, 1645, 1520, 1455, 1409, 1281, 804. ^{1}H NMR (300 MHz, DMSO-d_6, referred to the main rotamer): δ = 9.17 (br s, 1H), 8.87 (br s, 1H), 7.75-7.63 (m, 2H), 7.62-7.42 (m, 2H), 7.16-7.23 (m, 2H), 7.00-6.96 (m, 2H), 6.71-6.59 (m, 2H), 3.99 (s, 2H), 3.70 (s, 2H), 3.56 (d, *J* = 4.4 Hz, 2H), 2.92 (s, 3H). ^{13}C NMR (75 MHz, DMSO-d_6, referred to the main rotamer): δ = 171.7, 168.2, 156.4, 149.7, 134.6, 132.1, 131.9, 130.5, 129.9, 129.2, 126.2, 124.4, 123.8, 115.6, 111.7, 52.3, 50.4, 37.4, 35.0. MS (ESI) m/z 514 $[M+H]^+$.

N-(2-(((3-(4-Bromophenyl)imidazo[2,1-b]thiazol-5-yl)methyl)amino)-2-oxoethyl)-2-(3-hydroxyphenyl)-N-methylacetamide, (6l).

White solid. Yield: 48%. Chromatography: PE/EtOAc 1/9. mp 204-206 °C. Found: C, 54.03; H, 4.18; N, 10.87. $C_{23}H_{21}BrN_4O_3S$ requires C, 53.81; H, 4.12; N, 10.91. ν_{max} cm^{-1} 3284, 3109, 2935, 1641, 1534, 1458, 1406, 1262, 820, 774. ^{1}H NMR (300 MHz, DMSO-*d*$_6$, referred to the main rotamer): δ = 9.32 (br s, 1H), 7.96 (br s, 1H), 7.69 (d, *J* = 8.3 Hz, 2H), 7.64-7.46 (m, 3H), 7.21 (d, *J* = 8.3 Hz, 2H), 7.06 (s, 1H), 6.62 (s, 1H), 6.58 (s, 1H), 3.99 (s, 2H), 3.70 (d, *J* = 5.0 Hz, 2H), 3.60 (s, 2H), 2.93 (s, 3H). ^{13}C NMR (75 MHz, DMSO-*d*$_6$, referred to the main rotamer): δ = 171.3, 168.2, 157.8, 149.7, 137.4, 134.6, 132.1, 131.9, 129.9, 129.7, 129.1, 124.4, 123.8, 120.2, 116.5, 113.9, 111.7, 52.3, 50.4, 37.5, 35.0. MS (ESI) m/z 514 $[M+H]^+$.

N-(2-(((3-(4-Bromophenyl)imidazo[2,1-b]thiazol-5-yl)methyl)amino)-2-oxoethyl)-2-(2-hydroxyphenyl)-N-methylacetamide, (6m).

White solid. Yield: 40%. Chromatography: PE/EtOAc 1/9. mp 82-84 °C. Found: C, 53.67; H, 4.10; N, 10.93. $C_{23}H_{21}BrN_4O_3S$ requires C, 53.81; H, 4.12; N, 10.91. ν_{max} cm^{-1} 3272, 3060, 2925, 1800, 1666, 1595, 1455, 1398, 1246, 754. ^{1}H NMR (300 MHz, DMSO-*d*$_6$, referred to the main rotamer): δ = 7.59 (d, *J* 7.7 Hz, 2H), 7.48 (s, 1H), 7.27 (d, *J* = 7.7 Hz, 2H), 7.18-7.00 (m, 2H), 6.83 (d, *J* = 8.2 Hz, 2H), 6.60 (s, 1H), 6.40 (br s, 1H), 4.09 (s, 2H), 3.84 (s, 2H), 3.70 (s, 2H), 3.21 (s, 3H). ^{13}C NMR (75 MHz, DMSO-*d*$_6$, referred to the main rotamer): δ = 173.8, 155.9, 134.2, 133.2, 132.3, 132.1, 130.9, 129.4, 129.0, 128.1, 124.7, 123.4, 121.3, 120.4, 120.1, 117.3, 110.7, 60.5, 52.2, 36.3, 14.3. MS (ESI) m/z 514 $[M+H]^+$.

N-(2-(((3-(4-Bromophenyl)imidazo[2,1-b]thiazol-5-yl)methyl)amino)-2-oxoethyl)-N-methyl-2-(4-nitrophenyl)acetamide, (6n).

White solid. Yield: 43%. mp 205-207 °C. Found: C, 50.77; H, 3.70; N, 12.97. $C_{23}H_{20}BrN_5O_4S$ requires C, 50.93; H, 3.72; N, 12.91. ν_{max} cm^{-1} 3295, 3105, 3047, 2945, 1647, 1523, 1452, 1348, 1112, 819. ^{1}H NMR (300 MHz, DMSO-*d*$_6$): δ = 8.16

(d, *J* = 8.5 Hz, 2H), 7.98 (br s, 1H), 7.69 (d, *J* = 6.7 Hz, 2H), 7.57 (d, *J* = 8.5 Hz, 2H), 7.51 (d, *J* = 6.7 Hz, 2H), 7.20 (s, 1H), 7.17 (s, 1H), 3.91 (s, 2H), 3.83 (s, 2H), 3.76 (d, *J* = 4.4 Hz, 2H), 3.00 (s, 3H). ^{13}C NMR (75 MHz, DMSO-*d*$_6$): δ = 170.4, 168.2, 146.8, 144.7, 133.3, 132.2, 131.9, 131.4, 130.3, 129.9, 129.2, 129.1, 124.4, 123.8, 123.7, 52.3, 50.6, 37.4, 34.7. MS (ESI) m/z 543 $[M+H]^+$.

N-(2-(((3-(4-Bromophenyl)imidazo[2,1-b]thiazol-5-yl)methyl)amino)-2-oxoethyl)-N-methyl-2-(3-nitrophenyl)acetamide, (6o).

White solid. Yield: 46%. mp 191-193 °C. Found: C, 51.04; H, 3.80; N, 12.88. $C_{23}H_{20}BrN_5O_4S$ requires C, 50.93; H, 3.72; N, 12.91. ν_{max} cm^{-1} 3291, 3089, 3047, 2924, 1642, 1522, 1455, 1343, 807, 739. ^{1}H NMR (300 MHz, DMSO-*d*$_6$, referred to the main rotamer): δ = 8.11 (s, 1H), 8.05 (br s, 1H), 7.69 (d, *J* = 6.6 Hz, 2H), 7.64-7.55 (m, 5H), 7.22 (s, 1H), 7.17 (s, 1H), 3.93 (s, 2H), 3.84 (s, 2H), 3.75 (d, *J* 5.5 Hz, 2H), 3.02 (s, 3H). ^{13}C NMR (75 MHz, DMSO-*d*$_6$, referred to the main rotamer): δ = 170.7, 168.1, 149.7, 148.1, 138.9, 137.1, 134.6, 132.1, 132.0, 131.9, 130.0, 129.9, 129.1, 124.9, 123.8, 121.9, 111.8, 52.3, 50.6, 37.3, 35.1. MS (ESI) m/z 543 $[M+H]^+$.

N-(2-(((3-(4-Bromophenyl)imidazo[2,1-b]thiazol-5-yl)methyl)amino)-2-oxoethyl)-N-methyl-2-(2-nitrophenyl)acetamide, (6p).

White solid. Yield: 40%. mp 200-202 °C dec. Found: C, 50.77; H, 3.68; N, 12.95. $C_{23}H_{20}BrN_5O_4S$ requires C, 50.93; H, 3.72; N, 12.91. ν_{max} cm^{-1} 3296, 3086, 3051, 2933, 1643, 1542, 1519, 1456, 1341, 738. ^{1}H NMR (300 MHz, DMSO-*d*$_6$, referred to the main rotamer): δ = 8.01 (s, 1H), 7.87 (br s,1H), 7.79-7.43 (m, 6H), 7.36 (s, 1H), 7.27-7.08 (m, 2H), 4.13 (s, 2H), 3.98 (s, 2H), 3.70 (s, 2H), 3.04 (s, 3H). ^{13}C NMR (75 MHz, DMSO-*d*$_6$, referred to the main rotamer): δ = 169.7, 168.0, 149.8, 134.6, 133.8, 132.2, 132.1, 131.9, 131.8, 129.9, 129.1, 128.7, 125.0, 124.4, 123.8, 111.7, 111.0, 52.2, 50.5, 38.5, 37.1. MS (ESI) m/z 543 $[M+H]^+$.

N-(2-(((3-(4-Bromophenyl)imidazo[2,1-b]thiazol-5-yl)methyl)amino)-2-oxoethyl)-2-(4-chlorophenyl)-N-methylacetamide, (6q).

Yellow-white solid. Yield: 60%. Chromatography: PE/EtOAc 1/9. mp 78-80 °C. Found: C, 52.10; H, 3.85; N, 10.51. $C_{23}H_{20}BrClN_4O_2S$ requires C, 51.94; H, 3.79; N, 10.53. ν_{max} cm^{-1} 3290, 3050, 2925, 1650, 1537, 1455, 1291, 1014, 810, 744. ^{1}H NMR (300 MHz, $CDCl_3$, referred to the main rotamer): δ = 7.61 (d, *J* = 8.0 Hz, 2H), 7.56-7.44 (m, 2H), 7.32 (d, *J* = 8.0 Hz, 2H), 7.24 (d, *J* = 8.3 Hz, 2H), 7.11 (s, 1H), 6.63 (s, 1H), 6.38 (br s,1H), 4.13 (s, 2H), 3.79 (s, 2H), 3.65 (s, 2H), 3.05 (s, 3H). ^{13}C NMR (75 MHz, $CDCl_3$, referred to the main rotamer): δ = 171.7, 168.1, 150.4, 134.6, 132.9, 132.2, 130.8, 130.4, 129.4, 129.0, 128.9, 124.6, 123.5, 110.8, 110.2, 52.0, 39.8, 37.5, 34.2. MS (ESI) m/z 532 $[M+H]^+$.

N-(2-(((3-(4-Bromophenyl)imidazo[2,1-b]thiazol-5-yl)methyl)amino)-2-oxoethyl)-2-(3-chlorophenyl)-N-methylacetamide, (6r).

Yellow-white solid. Yield: 56%. Chromatography: PE/EtOAc 1/9. mp 183-185 °C. Found: C, 51.86; H, 3.73; N, 10.59. $C_{23}H_{20}BrClN_4O_2S$ requires C, 51.94; H, 3.79; N, 10.53. ν_{max} cm^{-1} 3276, 3211, 3058, 2926, 1683, 1654, 1534, 1458, 1399, 774. ^{1}H NMR (300 MHz, $CDCl_3$, referred to the main rotamer): δ = 7.59 (d, *J* = 8.3 Hz, 2H), 7.46 (s, 1H), 7.32 (d, *J* 8.3 Hz, 2H), 7.16 (d, *J* = 4.4 Hz, 1H), 7.12 (m, 2H), 7.01 (s, 1H), 6.73 (br s, 1H), 6.59 (s, 1H), 4.10 (d, *J* = 3.8 Hz, 2H), 3.77 (s, 2H), 3.61 (s, 2H), 3.02 (s, 3H). ^{13}C NMR (75 MHz, $CDCl_3$, referred to the main rotamer): δ = 170.8, 168.2, 138.9, 133.3, 132.1, 132.0, 130.4, 129.9, 129.1, 128.7, 128.6, 126.8, 124.5, 123.8, 111.8, 111.1, 52.4, 50.6, 37.4, 35.1. MS (ESI) m/z 532 $[M+H]^+$.

N-(2-(((3-(4-Bromophenyl)imidazo[2,1-b]thiazol-5-yl)methyl)amino)-2-oxoethyl)-2-(2-chlorophenyl)-N-methylacetamide, (6s).

Yellow solid. Yield: 61%. Chromatography: PE/EtOAc 1/9. mp 192-194 °C. Found: C, 52.03; H, 4.01; N, 10.46. $C_{23}H_{20}BrClN_4O_2S$ requires C, 51.94; H, 3.79; N, 10.53. ν_{max} cm^{-1} 3285, 3055, 2925, 1648, 1541, 1458, 1400, 1243, 820, 750. ^{1}H NMR (300

MHz, DMSO-d_6, referred to the main rotamer): δ = 7.61 (d, *J* 8.3 Hz, 2H), 7.52-7.43 (m, 2H), 7.31 (d, *J* = 8.3 Hz, 2H), 7.26 (s, 1H), 7.24-7.14 (m, 2H), 6.63 (s, 1H), 6.35 (br s, 1H), 4.13 (d, *J* = 5.0 Hz, 2H), 3.85 (s, 2H), 3.78 (s, 2H), 3.11 (s, 3H). ^{13}C NMR (75 MHz, DMSO-d_6, referred to the main rotamer): δ = 170.3, 169.2, 134.7, 134.2, 132.5, 132.2, 132.1, 131.9, 129.9, 129.4, 129.1, 128.9, 127.5, 124.5, 123.8, 111.7, 111.0, 52.3, 50.6, 38.0, 35.1. MS (ESI) m/z 532 $[M+H]^+$.

Synthesis of N-((3-(4-Bromophenyl)imidazo[2,1-b]thiazol-5-yl)methyl)-2-(2-phenylacetamido)acetamide, (6h).

To a solution of paraformaldehyde (1 eq, 0.63 mmol) in CH_3OH (1.25 mL), tritylamine (1 eq) was added and the reaction was heated at 40 °C and left to react for 40 minutes under vigorous stirring. After, phenylacetic acid (1 eq) and isocyanide **5** (1 eq) were added and the mixture was allowed to reach room temperature and stirred for 15 hours. The volatile was removed under reduced pressure, ethyl acetate was added and the organic phase was washed with a saturated aqueous solution of Na_2CO_3, dried over sodium sulfate and evaporated to give *N*-(2-(((3-(4-bromophenyl)imidazo[2,1-b]thiazol-5-yl)methyl)amino)-2-oxoethyl)-2-phenyl-N-tritylacetamide as a yellow solid which was used in the next step without further purification. The residue was dissolved in CH_2Cl_2 (2 mL), the reaction was cooled to 0°C and CF_3COOH (2 mL) was added. After 30 minutes at 0°C and 4 hours at room temperature NaOH 2M was added upon pH 7-8 and the mixture was extracted with ethyl acetate (x 1), dried over sodium sulfate and evaporated. The crude material was purified by chromatography column using PE/EtOAc 1/9 as eluent. Yellow-white solid. Yield: 78%. mp 178-180 °C. Found: C, 54.78; H, 3.97; N, 11.52. $C_{22}H_{19}BrN_4O_2S$ requires C, 54.66; H, 3.96; N, 11.59. ν_{max} cm^{-1} 3288, 3190, 2921, 1748, 1662, 1544, 1450, 1139, 1008, 702. ^{1}H NMR (300 MHz, $CDCl_3$, referred to the main rotamer): δ = 7.57 (d, *J* = 8.5 Hz, 2H), 7.40-7.18 (m, 7H), 7.08 (s, 1H), 6.61 (s, 1H), 6.59 (br s, 1H), 6.48 (br s, 1H), 4.11 (d, *J* = 4.4 Hz, 2H), 3.61 (d, *J* = 4.7 Hz, 2H), 3.51 (s, 2H). ^{13}C NMR (75 MHz, $CDCl_3$, referred to the main rotamer): δ =

169.5, 166.3, 150.4, 138.8, 134.5, 132.3, 132.1, 130.7, 130.3 (2C), 128.2, 124.6, 118.6, 111.2, 110.8, 49.4, 30.6, 17.6. MS (ESI) m/z 485 $[M+H]^+$.

General procedure for the synthesis of compounds 7a-l.

To a solution of 3-(4-bromophenyl)-5-(isocyanomethyl)imidazo[2,1-b]thiazole **5** (1 eq) in dry CH_2Cl_2, 37% aqueous formaldehyde solution (5 eq) and carbossilic acid (1 eq) were added and the resulting mixture was stirred at reflux. When the reaction was finished, the organic phase was washed with a saturated aqueous solution of Na_2CO_3 (except for the compounds **7d**, **7e** and **7f** which were washed with a saturated aqueous solution of $NaHCO_3$), dried over sodium sulfate and evaporated. Ethyl acetate was added to the crude material and the precipitated white solid was collected by filtration using a Buchner funnel and rinsed with ethyl acetate. In case that no precipitation occurs (**7a**, **7c**, **7d**, **7g**, **7i**), the crude material was purified by chromatography column.

2-(((3-(4-Bromophenyl)imidazo[2,1-b]thiazol-5-yl)methyl)amino)-2-oxoethyl 2-phenylacetate, (7a).

White solid. Yield: 41%. Chromatography: PE/EtOAc 5/5. mp 102-104 °C. Found: C, 54.69; H, 3.81; N, 8.63. $C_{22}H_{18}BrN_3O_3S$ requires C, 54.55; H, 3.75; N, 8.68. ν_{max} cm^{-1} 3288, 3190, 2921, 1748, 1662, 1544, 1450, 1139, 1008, 702. ^1H NMR (300 MHz, $CDCl_3$): δ = 7.50 (d, *J* 8.0 Hz, 2H), 7.14 (d, *J* = 4.7 Hz, 2H), 7.11-7.03 (m, 6H), 6.60 (s, 1H), 5.75 (br s, 1H), 4.30 (s, 2H), 4.07 (d, *J* = 4.4 Hz, 2H), 3.61 (s, 2H). ^{13}C NMR (75 MHz, $CDCl_3$): δ = 169.5, 166.1, 153.0, 135.2, 133.4, 132.2, 132.0, 130.6, 129.0, 128.8, 128.1, 127.6, 124.7, 122.3, 110.8, 62.3, 41.4, 34.1. MS (ESI) m/z 486 $[M+H]^+$.

2-(((3-(4-Bromophenyl)imidazo[2,1-b]thiazol-5-yl)methyl)amino)-2-oxoethyl 2-(4-cyanophenyl)acetate, (7b).

White solid. Yield: 74%. mp 196-198 °C. Found: C, 54.37; H, 3.40; N, 10.95. $C_{23}H_{17}BrN_4O_3S$ requires C, 54.23; H, 3.36; N, 11.00. ν_{max} cm^{-1} 3260, 3125, 3086,

2937, 2218, 1756, 1660, 1540, 1463, 1156. ^{1}H NMR (300 MHz, DMSO-d_6): δ = 8.12 (br s, 1H), 7.80 (d, *J* = 8.2 Hz, 2H), 7.66 (d, *J* = 8.2 Hz, 2H), 7.60-7.48 (m, 4H), 7.22 (s, 1H), 7.16 (s, 1H), 4.32 (s, 2H), 4.02 (d, *J* = 4.4 Hz, 2H), 3.90 (s, 2H). ^{13}C NMR (75 MHz, DMSO-d_6): δ = 170.6, 166.4, 149.8, 140.5, 134.6, 132.8, 132.2, 132.1, 131.9, 131.2, 129.1, 124.2, 123.9, 119.4, 111.8, 110.4, 62.9, 39.8, 34.5. MS (ESI) m/z 511 $[M+H]^+$.

2-(((3-(4-Bromophenyl)imidazo[2,1-b]thiazol-5-yl)methyl)amino)-2-oxoethyl 2-(3-cyanophenyl)acetate, (7c).

White solid. Yield: 87%. Chromatography: PE/EtOAc 5/5. mp 161-163 °C. Found: C, 54.14; H 3.39; N, 11.12. $C_{23}H_{17}BrN_4O_3S$ requires C, 54.23; H, 3.36; N, 11.00. ν_{max} cm^{-1} 3274, 3062, 2922, 2229, 1735, 1650, 1541, 1452, 1176, 740. ^{1}H NMR (300 MHz, $CDCl_3$): δ = 7.59 (d, *J* = 7.7 Hz, 2H), 7.54-7.44 (m, 2H), 7.34 (d, *J* = 7.7 Hz, 2H), 7.29 (d, *J* = 7.3 Hz, 2H), 7.00 (s, 1H), 6.65 (s, 1H), 6.37 (br s, 1H), 4.39 (s, 2H), 4.18 (d, *J* = 4.0 Hz, 2H), 3.72 (s, 2H). ^{13}C NMR (75 MHz, DMSO-d_6): δ = 170.7, 166.5, 149.8, 136.4, 135.2, 134.6, 133.7, 132.2, 132.1, 131.9, 131.3, 130.0, 129.1, 124.2, 123.9 119.3, 111.9, 111.8, 62.9, 39.8, 34.5. MS (ESI) m/z 511 $[M+H]^+$.

2-(((3-(4-Bromophenyl)imidazo[2,1-b]thiazol-5-yl)methyl)amino)-2-oxoethyl 2-(4-hydroxyphenyl)acetate, (7d).

White solid. Yield: 76%. Chromatography: PE/EtOAc 5/5. mp 164-166 °C. Found: C, 52.99; H, 3.64; N, 8.33. $C_{22}H_{18}BrN_3O_4S$ requires C, 52.81; H, 3.63; N, 8.40. ν_{max} cm^{-1} 3256, 3111, 3035, 2937, 1750, 1645, 1516, 1455, 1145, 783. ^{1}H NMR (300 MHz, DMSO-d_6): δ = 9.35 (br s, 1H), 8.11 (br s, 1H), 7.67 (d, *J* 6.6 Hz, 2H), 7.54 (d, *J* = 6.6 Hz, 2H), 7.20 (s, 1H), 7.18 (s, 1H), 7.08 (d, *J* = 7.2 Hz, 2H), 6.72 (d, *J* = 7.2 Hz, 2H), 4.31 (s, 2H), 4.05 (s, 2H), 3.62 (s, 2H). ^{13}C NMR (75 MHz, DMSO-d_6): δ = 171.7, 166.6, 156.8, 156.7, 134.5, 132.2, 132.1, 131.9, 130.9, 129.1, 124.8, 124.2, 123.9, 115.7, 111.8, 62.7, 39.8, 34.5. MS (ESI) m/z 502 $[M+H]^+$.

2-(((3-(4-Bromophenyl)imidazo[2,1-b]thiazol-5-yl)methyl)amino)-2-oxoethyl 2-(3-hydroxyphenyl)acetate, (7e).

White solid. Yield: 84%. mp 211-213 °C. Found: C, 52.66; H, 3.57; N, 8.53. $C_{22}H_{18}BrN_3O_4S$ requires C, 52.81; H, 3.63; N, 8.40. ν_{max} cm^{-1} 3264, 3129, 3064, 2941, 1750, 1648, 1550, 1459, 1144, 770. ^{1}H NMR (300 MHz, DMSO-d_6): δ = 9.36 (br s, 1H), 8.06 (br s,1H), 7.67 (d, *J* = 8.3 Hz, 2H), 7.54 (d, *J* = 8.3 Hz, 2H), 7.25-7.05 (m, 3H), 6.75-6.62 (m, 3H), 4.28 (s, 2H), 4.03 (s, 2H), 3.64 (s, 2H). ^{13}C NMR (75 MHz, DMSO-d_6): δ = 171.3, 166.7, 155.9, 149.7, 134.5, 132.2, 132.1, 131.9, 131.6, 129.1, 128.7, 124.2, 123.9, 121.5, 119.4, 115.4, 111.7, 62.6, 35.3, 34.5. MS (ESI) m/z 502 $[M+H]^+$.

2-(((3-(4-Bromophenyl)imidazo[2,1-b]thiazol-5-yl)methyl)amino)-2-oxoethyl 2-(2-hydroxyphenyl)acetate, (7f).

White solid. Yield: 48%. mp 187-188 °C. Found: C, 52.63; H, 3.59; N, 8.46. $C_{22}H_{18}BrN_3O_4S$ requires C, 52.81; H, 3.63; N, 8.40. ν_{max} cm^{-1} 3341, 3125, 3043, 2929, 1735, 1665, 1535, 1457, 1251. ^{1}H NMR (300 MHz, $CDCl_3$): δ = 9.51 (br s,1H), 7.97 (br s, 1H), 7.66 (d, *J* = 8.3 Hz, 2H), 7.52 (d, *J* = 8.3 Hz, 2H), 7.27-7.01 (m, 4H), 6.82-6.68 (m, 2H), 4.27 (s, 2H), 4.03 (s, 2H), 3.63 (s, 2H). ^{13}C NMR (75 MHz, $CDCl_3$): δ = 171.3, 166.7, 155.9. 149.7, 134.5, 132.2, 132.1, 131.9, 131.6, 129.1, 128.7, 124.2, 123.9, 121.5, 119.4, 115.4, 111.7, 62.6, 35.3, 34.5. MS (ESI) m/z 502 $[M+H]^+$.

2-(((3-(4-Bromophenyl)imidazo[2,1-b]thiazol-5-yl)methyl)amino)-2-oxoethyl 2-(4-nitrophenyl)acetate, (7g).

White solid. Yield: 42%. Chromatography: PE/EtOAc 4/6. mp 200-202 °C. Found: C, 50.03; H, 3.31; N, 10.53. $C_{22}H_{17}BrN_4O_5S$ requires C, 49.92; H, 3.24; N, 10.58. ν_{max} cm^{-1} 3243, 3117, 3072, 2929, 1754, 1660, 1415, 1341, 1157, 724. ^{1}H NMR (300 MHz, DMSO-d_6): δ = 8.20 (d, *J* 7.7 Hz, 2H), 8.12 (br s, 1H), 7.76-7.51 (m, 6H), 7.22 (s, 1H), 7.16 (s, 1H), 4.33 (s, 2H), 4.06 (s, 2H), 3.96 (s, 2H). ^{13}C NMR (75 MHz,

DMSO-d_6): δ = 170.5, 166.4, 149.7, 147.1, 142.7, 134.5, 132.2, 132.1, 131.9, 131.5, 129.1, 124.2, 123.9, 123.8, 111.8, 62.9, 39.8, 34.5. MS (ESI) m/z 531 $[M+H]^+$.

2-(((3-(4-Bromophenyl)imidazo[2,1-b]thiazol-5-yl)methyl)amino)-2-oxoethyl 2-(3-nitrophenyl)acetate, (7h).

White solid. Yield: 35%. mp 98-100 °C. Found: C, 50.14; H, 3.27; N, 10.51. $C_{22}H_{17}BrN_4O_5S$ requires C, 49.92; H, 3.24; N, 10.58. ν_{max} cm^{-1} 3060, 2922, 2855, 1749, 1627, 1522, 1457, 1349, 1146, 727. ^{1}H NMR (300 MHz, DMSO-d_6): δ = 8.21 (br s, 1H), 8.14 (d, *J* = 8.3 Hz, 2H), 7.77 (d, *J* = 7.4 Hz, 1H), 7.75-7.65 (m, 3H), 7.55 (d, *J* = 8.3 Hz, 2H), 7.22 (s, 1H), 7.16 (s, 1H), 4.33 (s, 2H), 4.03 (d, *J* = 4.7 Hz, 2H), 3.98 (s, 2H). ^{13}C NMR (75 MHz, DMSO-d_6): δ = 170.8, 166.4, 149.7, 148.2, 137.1, 137.0, 134.5, 132.2, 132.1, 131.9, 130.3, 129.1, 124.9, 124.2, 123.9, 122.5, 111.8, 62.9, 39.8, 34.5. MS (ESI) m/z 531 $[M+H]^+$.

2-(((3-(4-Bromophenyl)imidazo[2,1-b]thiazol-5-yl)methyl)amino)-2-oxoethyl 2-(2-nitrophenyl)acetate, (7i).

White solid. Yield: 75%. Chromatography: $CHCl_3$. mp 162-164 °C dec. Found: C, 49.77; H, 3.19; N, 10.67. $C_{22}H_{17}BrN_4O_5S$ requires C, 49.92; H, 3.24; N, 10.58. ν_{max} cm^{-1} 3272, 3063, 2950, 1739, 1646, 1531, 1448, 1350, 1171, 721. ^{1}H NMR (300 MHz, DMSO-d_6): δ = 8.10 (d, *J* = 8.8 Hz, 2H), 8.08 (br s, 1H), 7.79-7.51 (m, 6H), 7.21 (s, 1H), 7.17 (s, 1H), 4.32 (s, 2H), 4.16 (s, 2H), 4.05 (d, *J* = 3.0 Hz, 2H). ^{13}C NMR (75 MHz, DMSO-d_6): δ = 170.2, 166.3, 150.0, 149.0, 134.6, 134.3, 132.2, 132.1 (2C), 131.9, 130.0, 129.5, 129.1, 125.4, 124.1, 123.9, 111.8, 62.9, 38.9, 34.5. MS (ESI) m/z 531 $[M+H]^+$.

2-(((3-(4-Bromophenyl)imidazo[2,1-b]thiazol-5-yl)methyl)amino)-2-oxoethyl 2-(4-chlorophenyl)acetate, (7j).

White solid. Yield: 66%. mp 182-183 °C. Found: C, 51.15; H, 3.34; N, 8.03. $C_{22}H_{17}BrClN_3O_3S$ requires C, 50.93; H, 3.30; N, 8.10. ν_{max} cm^{-1} 3268, 3125, 3080, 2912, 1754, 1661, 1540, 1463, 1157, 734. ^{1}H NMR (300 MHz, DMSO-d_6): δ = 8.10

(br s, 1H), 7.67 (d, *J* = 8.3 Hz, 2H), 7.54 (d, *J* = 8.3 Hz, 2H), 7.38 (d, *J* = 8.4 Hz, 2H), 7.31 (d, *J* = 8.4 Hz, 2H) 7.22 (s, 1H), 7.16 (s, 1H), 4.31 (s, 2H), 4.02 (d, *J* = 4.4 Hz, 2H), 3.77 (s, 2H). ^{13}C NMR (75 MHz, DMSO-d_6): δ = 171.0, 166.5, 149.8, 134.6, 133.7, 132.2, 132.1 (2C), 131.9 (2C), 129.1, 128.8, 124.2, 123.9, 111.8, 62.8, 39.8, 34.5. MS (ESI) m/z 520 $[M+H]^+$.

2-(((3-(4-Bromophenyl)imidazo[2,1-b]thiazol-5-yl)methyl)amino)-2-oxoethyl 2-(3-chlorophenyl)acetate, (7k).

White solid. Yield: 60%. mp 131-133 °C. Found: C, 51.08; H, 3.36; N, 8.06. $C_{22}H_{17}BrClN_3O_3S$ requires C, 50.93; H, 3.30; N, 8.10. ν_{max} cm^{-1} 3272, 3100, 3060, 2933, 1742, 1649, 1544, 1450, 1167, 726. ^{1}H NMR (300 MHz, DMSO-d_6): δ = 8.10 (br s, 1H), 7.67 (d, *J* = 8.2 Hz, 2H), 7.54 (d, *J* = 8.2 Hz, 2H), 7.41-7.32 (m, 4H), 7.22 (s, 1H), 7.16 (s, 1H), 4.32 (s, 2H), 4.03 (s, 2H), 3.80 (s, 2H). ^{13}C NMR (75 MHz, DMSO-d_6): δ = 170.9, 166.5, 149.8, 137.1, 134.5, 133.4, 132.2, 132.1, 131.9, 130.7, 130.0, 129.1, 128.8, 127.4, 124.2, 123.9, 111.8, 62.8, 39.8, 34.5. MS (ESI) m/z 520 $[M+H]^+$.

2-(((3-(4-Bromophenyl)imidazo[2,1-b]thiazol-5-yl)methyl)amino)-2-oxoethyl 2-(2-chlorophenyl)acetate, (7l).

White solid. Yield: 69%. mp 179-180 °C. Found: C, 50.77; H, 3.23; N, 8.18. $C_{22}H_{17}BrClN_3O_3S$ requires C, 50.93; H, 3.30; N, 8.10. ν_{max} cm^{-1} 3428, 3100, 2949, 2917, 1732, 1680, 1520, 1452, 1245, 750. ^{1}H NMR (300 MHz, DMSO-d_6): δ = 8.03 (br s, 1H), 7.67 (d, *J* = 8.2 Hz, 2H), 7.54 (d, *J* = 8.2 Hz, 2H), 7-50-7.40 (m, 2H), 7.37-7.28 (m, 2H), 7.22 (s, 1H), 7.16 (s, 1H), 4.32 (s, 2H), 4.03 (s, 2H), 3.89 (s, 2H). ^{13}C NMR (75 MHz, DMSO-d_6): δ = 170.2, 166.4, 149.8, 134.6, 134.3, 132.9, 132.7, 132.2, 132.1, 131.9 (2C), 129.7, 129.1, 127.8, 124.2, 123.9, 111.8, 62.9, 38.6, 34.5. MS (ESI) m/z 520 $[M+H]^+$.

Synthesis of N-((3-(4-Bromophenyl)imidazo[2,1-b]thiazol-5-yl)methyl)-2-hydroxyacetamide, (7m).

To a solution of 2-(((3-(4-bromophenyl)imidazo[2,1-b]thiazol-5-yl)methyl)amino)-2-oxoethyl 2-phenylacetate **7a** (1eq, 3.14 mmol) in water (1mL) and acetone (1mL) NaOH (2eq) was added. The resulting mixture was stirred overnight. The organic phase was washed with a saturated aqueous solution of $NaHCO_3$ (x 2), dried over sodium sulfate and evaporated. The crude product was purified by chromatography column using $CHCl_3$ as eluent. White solid. Yield: 70%. mp 198-200 °C. Found: C, 45.83; H, 3.25; N, 11.57. $C_{14}H_{12}BrN_3O_2S$ requires C, 45.91; H, 3.30; N, 11.47. ν_{max} cm^{-1} 3274, 2826, 1647, 1533, 1464, 1342, 1146, 1079, 820, 762. ^1H NMR (300 MHz, DMSO-d_6): δ = 7.69 (d, *J* = 8.4 Hz, 2H), 7.56 (d, *J* = 8.4 Hz, 2H), 7.19 (s, 1H), 7.09 (s, 1H), 5.22 (br s, 1H), 4.03 (d, *J* = 5.2Hz, 2H), 3.67 (s, 2H), 3.27 (br s, 1H). ^{13}C NMR (75 MHz, DMSO-d_6): δ = 172.0, 149.4, 134.1, 133.2, 132.1, 130.0, 129.2, 125.2, 125.1, 123.9, 61.8, 34.0. MS (ESI) m/z 368 $[M+H]^+$.

General procedure for the synthesis of compounds 8a-b.

To a solution of tritylamine (1 eq) in CH_3OH parafolmadehyde was added (1 eq). The mixture was stirred at 40 °C for 40 minutes. Then, BOC-protected amino acid (1eq) and isocyanide (1eq) were added and the mixture was stirred overnight at room temperature. When the reaction was finished, the solvent was evaporated. After dilution with EtOAc and washing with saturated aqueous solution of Na_2CO_3 (x 2), the organic phase was dried over sodium sulfate and evaporated to obtain a yellow solid which was used in the next step without further purification. The residue was dissolved in CH_2Cl_2 and CF_3COOH was added at 0 °C. After stirring for 30 minutes at 0 °C, a solution of NaOH 2M was added to adjust the pH to 10. The mixture was extracted with EtOAc (x 2) and the collected organic phases were dried over sodium sulfate and evaporated. The crude material was purified by chromatography column.

(S)-2-Amino-N-(2-(((3-(4-bromophenyl)imidazo[2,1-b]thiazol-5-yl)methyl)amino)-2-oxoethyl)-2-phenylacetamide, (8a).

Yellow solid. Yield: 17%. Chromatography: EtOAc. mp 56-58 °C. Found: C, 53.17; H, 4.11; N, 13.98. $C_{22}H_{20}BrN_5O_2S$ requires C, 53.02; H, 4.04; N, 14.05. ν_{max} cm^{-1} 3056, 2921, 2851, 1670, 1521, 1457, 1244, 1201, 1013, 813. ^{1}H NMR (300 MHz, $CDCl_3$, referred to the main rotamer): δ = 7.82 (br s, 1H), 7.60 (d, *J* = 8.5 Hz, 2H), 7.38-7.20 (m, 7H), 7.10 (s, 1H), 6.60 (s, 1H), 6.30 (br s, 1H), 4.56 (s, 1H), 4.15 (dd, J_s = 5.0, 15.7 Hz, 1H), 4.03 (dd, J_s = 5.0, 15.7 Hz, 1H), 3.76 (dd, J_s = 5.5, 16.3 Hz, 1H), 3.64 (dd, J_s = 5.5, 16.3 Hz, 1H). ^{13}C NMR (75 MHz, $CDCl_3$): δ = 173.6, 168.3, 150.5, 140.0, 134.6, 132.2, 132.0, 130.8, 128.9, 128.4, 128.3, 126.8, 124.6, 123.3, 110.7, 59.5, 42.8, 34.4. MS (ESI) m/z 500 $[M+H]^+$.

(S)-2-Amino-N-(2-(((3-(4-bromophenyl)imidazo[2,1-b]thiazol-5-yl)methyl)amino)-2-oxoethyl)-2-(4-hydroxyphenyl)acetamide, (8b).

Yellow solid. Yield: 30%. Chromatography: EtOAc. mp 160-162 °C. Found: C, 51.50; H, 3.96; N, 13.54. $C_{22}H_{20}BrN_5O_3S$ requires C, 51.37; H, 3.92; N, 13.61. ν_{max} cm^{-1} 3064, 2927, 2419, 1665, 1513, 1458, 1248, 1144, 1013, 838. ^{1}H NMR (300 MHz, CD_3OD): δ = 7.66 (d, *J* = 7.6 Hz, 2H), 7.44 (d, *J* = 8.2 Hz, 2H), 7.21 (d, *J* = 7.6 Hz, 2H), 7.03 (s, 1H), 6.97 (s, 1H), 6.71 (d, *J* = 8.2 Hz, 2H), 4.41 (s, 1H), 4.11 (d, *J* = 6.3 Hz, 2H), 3.70 (dd, J_s = 5.2, 16.7 Hz, 1H), 3.56 (dd, J_s = 5.2, 16.7 Hz, 1H). ^{13}C NMR (75 MHz, CD_3OD): δ = 169.4, 157.2, 133.6, 132.2, 131.8, 131.3, 131.1, 129.9, 129.3, 128.6, 128.1, 124.1, 123.6, 115.3, 111.3, 110.6, 58.4, 41.9. MS (ESI) m/z 516 $[M+H]^+$.

4.5.2. Appendix

^{1}H NMR (DMSO-d_6) of compound **7d**

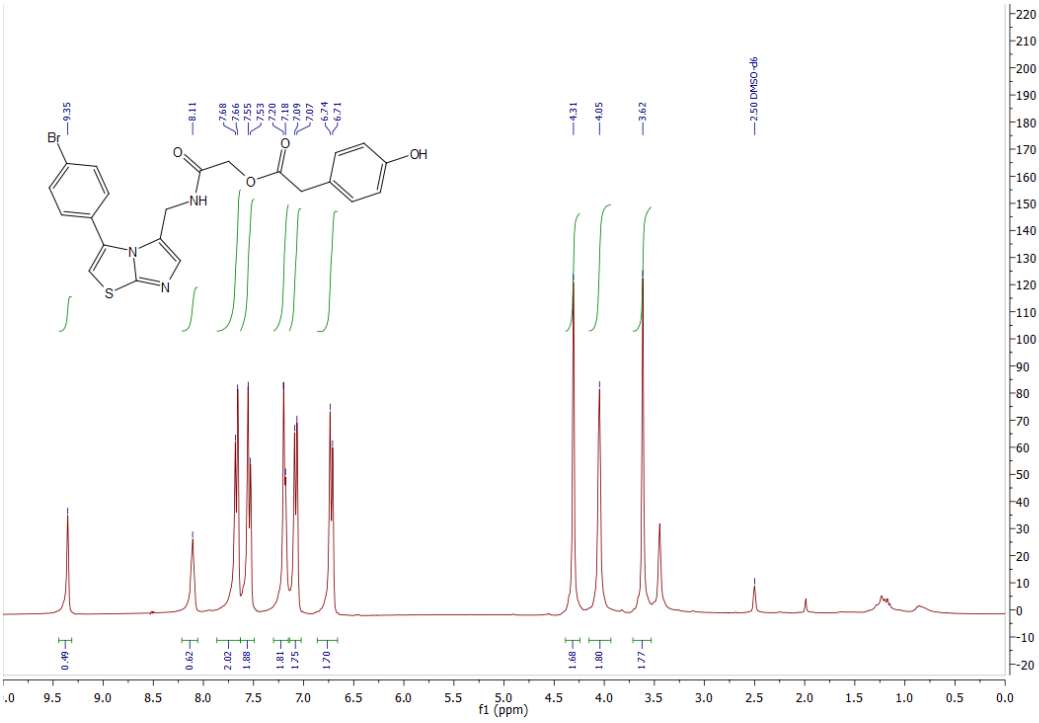

4.6. References

1. Prendergast, G.C.; Malachowski, W.P.; DuHadaway, J.B.; Muller, A.J. Discovery of IDO1 Inhibitors: From Bench to Bedside. *Cancer Res*. **2017**, *77*, 6795-6811.
2. Long, G.V.; Dummer, R.; Hamid, O.; Gajewski, T.; Caglevic, C.; Dalle, S.; Arance, A.; Carlino, M.S.; Grob, J-J.; Kim, T.M.; Demidov, L.V.; Robert, C.; Larkin, J.M.G.; Anderson, J.; Maleski, J.E.; Jones, M.M.; Diede, S.J.; Mitchell, T.C. Epacadostat (E) plus pembrolizumab (P) versus pembrolizumab alone in patients (pts) with unresectable or metastatic melanoma: Results of the phase 3 ECHO-301/KEYNOTE-252 study. *J. Clin. Oncol*. **2018,** *36*, (suppl 108-108).
3. Tojo, S.; Kohno, T.; Tanaka, T.; Kamioka, S.; Ota, Y.; Ishii, T.; Kamimoto, K.; Asano, S.; Isobe, Y. Crystal structures and structure–activity relationships of imidazothiazole derivatives as IDO1 inhibitors *ACS Med. Chem. Lett.* **2014**, *5*, 1119-1123.
4. a. Ugi, I.; Meyr, R.; Fetzer, U.; Steinbruckner, C. Versammlungsberichte. *Angew. Chem.* **1959**, *71*, 386.
   b. Dömling, A.; Ugi, I. Multicomponent Reactions with Isocyanides. Angew. *Chem. Int. Ed.* **2000**, *39*, 3168-3210.
   c. Dömling, A.; Wang, W.; Wang, K. Chemistry & biology Of multicomponent reactions. *Chem. Rev*. **2012**, *112*, 3083-3135.
   d. Zarganes-Tzizikas, T.; Dömling, A. Modern multicomponent reactions for better drug syntheses. *Org. Che. Front.* **2014**, *1*, 834-837.
5. Pick, R.; Bauer, M.; Kazmaier, U.; Hebach, C. Ammonia in Ugi reactions four-components -versus six-component coupling. *Synlett*. **2005**, *5*, 757-760.
6. Kazmaier, U.; Hebach, C. Peptide syntheses via Ugi reaction with ammonia. *Synlett*, **2003**, *11*, 1591-1594.
7. Thompson, M. J.; Chen, B. Versatile assembly of 5-aminothiazoles based on the Ugi four-component coupling. *Tetrahedron Lett.* **2008**, *49*, 5324-5327.
8. Patil, P.; de Haan, M.; Kurpiewska, K.; Kalinowska-Tluścik, J.; Dömling, A. Versatile protecting-group free tetrazolomethane amine synthesis by Ugi reaction. ACS Comb. Sci. **2016,** *18*, 170-175.
9. Zhao, T.; Boltjes, A.; Herdtweck, E.; Dömling, A. Tritylamine as an ammonia surrogate in the Ugi tetrazole synthesis. *Org. Lett.* **2013**, *15*, 639-64.
10. a. Passerini, M. *Gazz. Chim. Ital.* **1921**, *51*, 181-189;
    b. Banfi, L.; Riva, R. The Passerini Reaction. *Organic Reactions*, **2005** Vol. 65 L. E. Overman Ed. Wiley.
11. a. Brandsch, M. Transport of drugs by proton-coupled peptide transporters: pearls and pitfalls. *Expert Opin. Drug Metab. Toxicol.* **2009**, *5*, 887-905.

b. Rubio-Aliaga, I.; Daniel, H. Peptide transporters and their roles in physiological processes and drug disposition. *Xenobiotica.* **2008**, *38*, 1022-1042.

12. a. OMEGA, version 2.4.6, OpenEye Scientific Software, Santa Fe, NM, http://www.eyesopen.com.
    b. Hawkins, P. C. D.; Skillman, A. G.; Warren, G. L.; Ellingson, B. A.; Stahl, M. T. J. Conformer generation with OMEGA: algorithm and validation using high quality structures from the protein databank and cambridge structural database. *Chem. Inf. Model.* **2010**, *50*, 572–584.
    c. Hawkins, P. C. D.; Nicholls, *A. J.* Conformer generation with OMEGA: learning from the data set and the analysis of failures. *Chem. Inf. Model.* **2012**, *52*, 2919-2936.
13. a. FRED, version 3.0.0, OpenEye Scientific Software, Santa Fe, NM, http://www.eyesopen.com.
    b. McGann, M. J. FRED pose prediction and virtual screening accuracy. *Chem. Inf. Model.* **2011**, *51*, 578–596.

Chapter 5

Benzimidazole derivatives as indoleamine 2,3-dioxygenase 1 inhibitors: *in silico*-driven synthesis, biological evaluation and structure-activity relationship study

5.1. Introduction

In our ongoing effort to develop small molecules for targeting the tryptophan catabolism we have already discovered two different classes of IDO1 inhibitors, displaying the imidazole[1] and imidazothiazole[2] scaffold, respectively. In this context, I have personally worked on the latter project that has led to the identification of two compounds, **6n** and **7d** described in Chapter 4, endowed with a unique binding mode in the IDO1 active site: the long side-chain protrudes into an additional pocket that we named C, where a crucial hydrogen bond is formed with Lys238. Unfortunately, while the compounds displayed a good potency in the enzymatic assay and a full biocompatibility, they were not able to significantly permeate the cell membrane and inhibited IDO1 in a cell-based assay just to a small extent. This is the first time in which it was proven that pocket C can be exploited in the design of IDO1 inhibitors. This information was therefore integrated in a structure-based virtual screening performed by Dr. Massarotti. First of all, the virtual screening protocol was validated. To this aim, all the bioactivity data of known tested molecules extracted mainly from scientific literature were downloaded. The data were manually inspected and integrated with *in-house* information. The database chosen for our screening purpose was ZINC15,[3] a collection of commercially available molecules. We used the "in stock" "drug-like" subset (8.2 million molecules), containing readily purchasable compounds with drug like properties. The screening database was docked within IDO1 active site. After visual inspection of the top 500 molecules, 50 compounds were purchased for biological assays. Screening in cell-based assays (human melanoma A375 cell lines) for IDO1 inhibitory activity led to the discovery of three *hit compounds*. Among them, compound **1,** depicted in Figure 1A, is the most active against IDO1 with an IC_{50} of 16 nM (Figure 1C). Moreover, it does not display cytotoxicity up to 48 hours at 10 μM. Promisingly, this molecule is endowed with promising features: i) it is a novel chemotype; ii) it shows a peculiar binding

mode in the IDO1 active site (Figure 1B); iii) it displays synthetic feasibility and tractability.

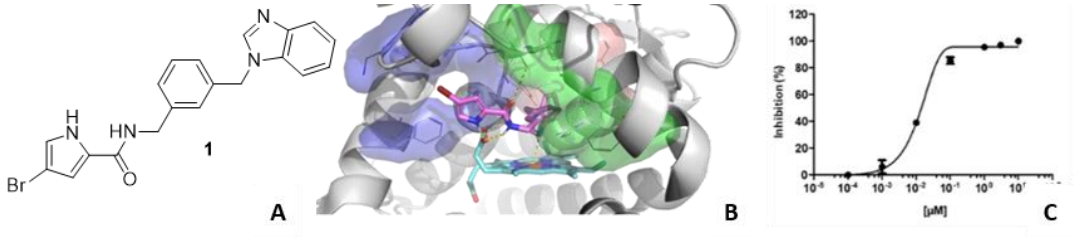

Figure 1. (**A**) Structure of the identified *hit compound* **1**; (**B**) Docking pose of **1**. Structure is depicted as pink sticks and heme is depicted as cyan sticks. Red shape: pocket A; green: pocket B; blue: pocket C; (**C**) Dose-response curve for **1**.

5.2. Aim of the work

The goal of the project was to re-synthesize the *hit* **1** in order to confirm its activity and *in silico*-design and synthesize a series of structural analogues. Moreover, the inhibitory activity against IDO1 of the related structural congeners is being evaluated in a cell-based assay carried out in Dr. Fallarini's laboratory and a preliminary structure-activity relationship study (SAR) is being performed. I have been involved in the synthesis and characterization of this class of benzimidazoles (See Chemistry section 5.5.1.).

5.3. Results and discussion

5.3.1. Chemistry

First of all, the *hit* was re-synthesized. To this aim, aniline **5** was prepared according to Scheme 1. The synthetic protocol afforded the desired compound in two steps: substitution and subsequent reduction of the aromatic nitrile **4**. Subsequent coupling between intermediate **5** and 4-bromo-1*H*-pyrrole-2-carboxylic acid easily provided **6** in good yield.

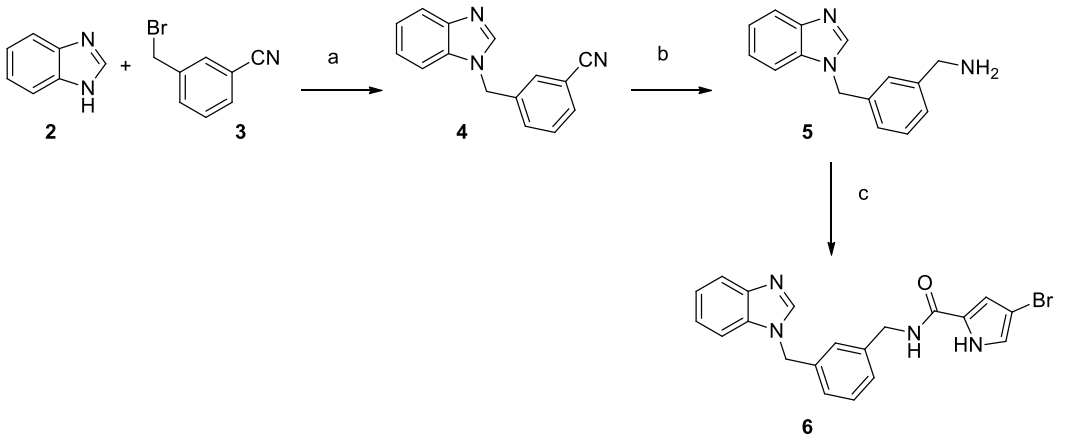

Scheme 1. Re-synthesis of the *hit compound***.**
(**a**) KOH, acetone, 60 °C, 4 h, 99%; (**b**) $LiAlH_4$, dry THF, 65 °C - rt, 18 h, 70%; (**c**) TEA, HOBt, EDCI, 4-bromo-1*H*-pyrrole-2-carboxylic acid, dry CH_2Cl_2, rt, 18 h, 50%.

Next, in order to examine the role of the 4-bromopirrole moiety, a series of analogues was *in silico*-designed and synthesized (**29**-**50**, **54**). In particular, synthetically feasible and purchasable carboxylic acids have been virtually combined and the resulted library of candidates has been screened in the IDO1 active site. Compounds have been ranked according to their binding energies in the two proteins, as well as their drug-like profiles, including predicted solubility and membrane permeability. The virtual candidates that displayed the highest score have been selected for the synthesis.

Picked compounds **29**-**50** were efficiently obtained by coupling aniline **5** with different carboxylic acids (**7**-**28**) (Scheme 2). The reaction provided the desired benzimidazoles in good (**29, 30, 32-41, 43, 44, 46-48, 50**) to excellent (**31, 42**) yields, while in some cases, the yields were poor (**45, 49**).

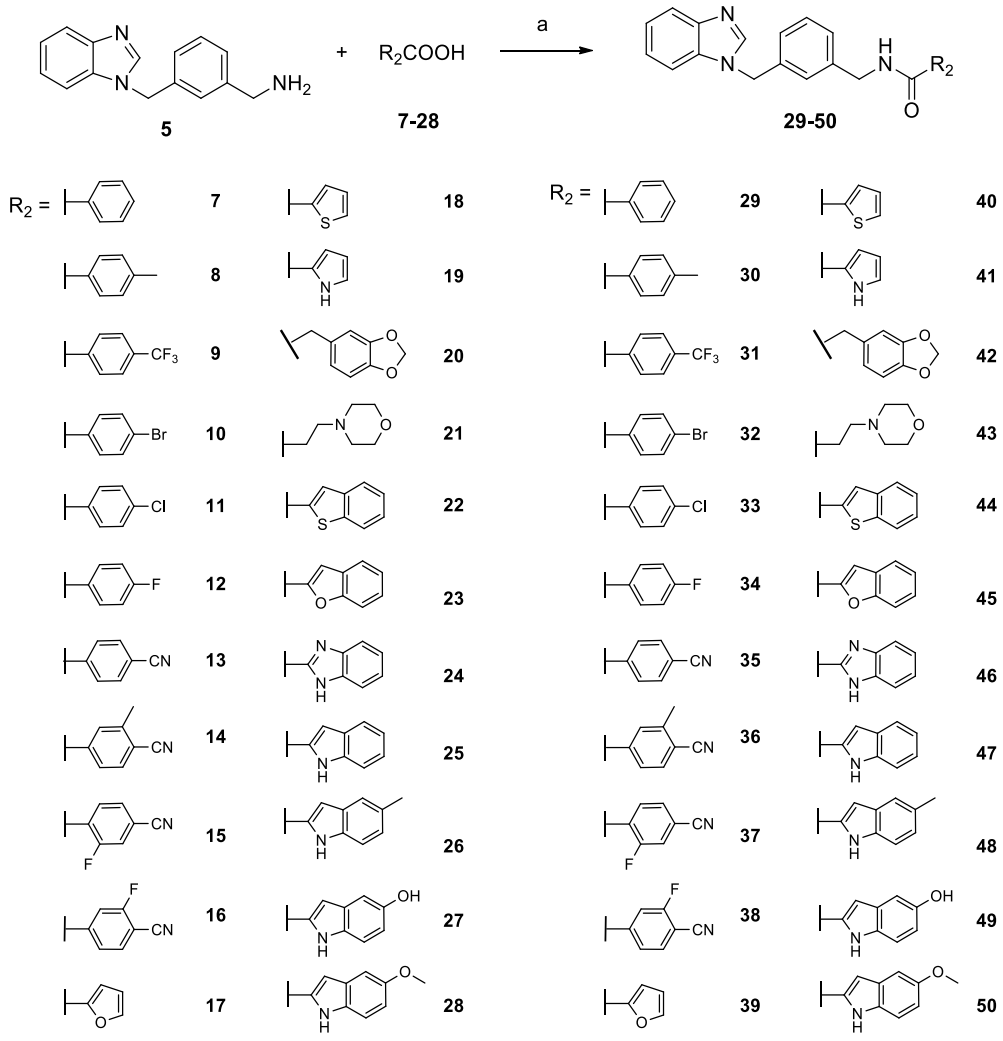

Scheme 2. Synthesis of compounds **29-50.**
(**a**) TEA, HOBt, EDCI, dry CH_2Cl_2, rt, 18 h, 13-86 %.

For the synthesis of compound **54** protection and deprotection of the additional amine group were necessary, according to Scheme 3.

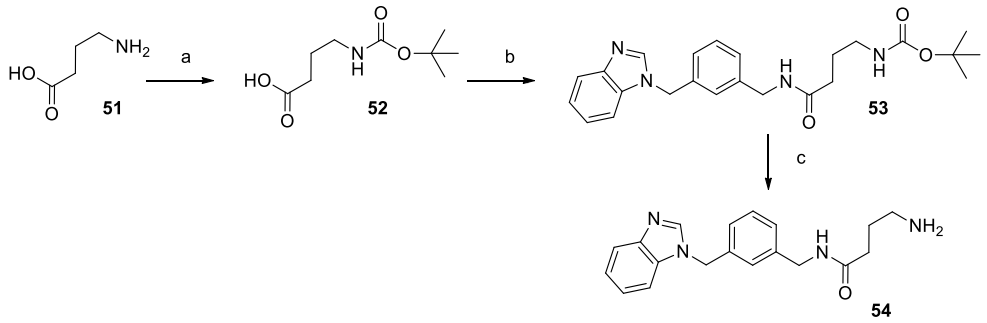

Scheme 3. Synthesis of compound **54**.
(**a**) 2 M aq. NaOH, Boc_2O, THF, 16 h, 86%; (**b**) compound **4**, TEA, HOBt, EDCI, dry CH_2Cl_2, rt, 18 h, 57%; (**c**) CF_3COOH, dry CH_2Cl_2, 0 °C, 30 min, 71%.

Then, docking studies revealed that the introduction of a bromine atom in the 6' position of the benzimidazole core might improve the affinity with pocket A in IDO1 active site. Taking advantage of this information, compound **60** has been synthesized by coupling reaction as described above (Scheme 4). Hence, the desired aniline **59** was prepared *via* a three-step procedure: substitution, cyclization and reduction of the nitrile group (Scheme 4).

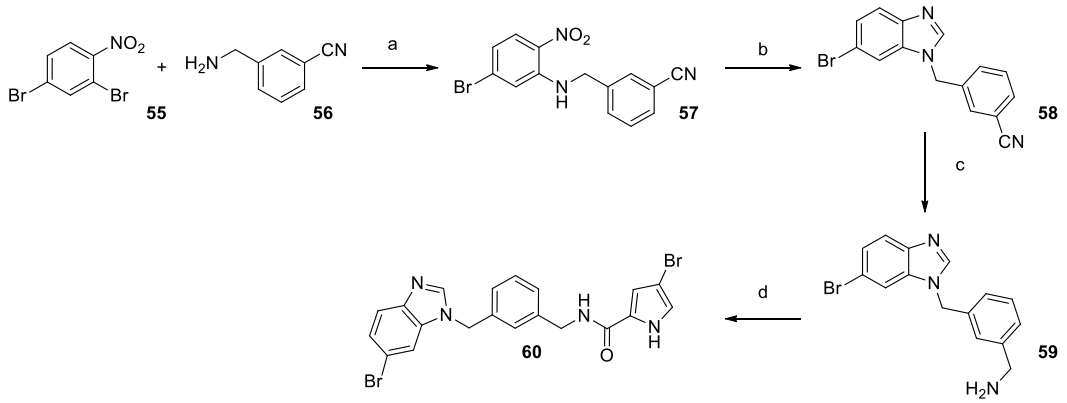

Scheme 4. (**a**) K_2CO_3, DMSO, 72 °C, 16 h, 13%; (**b**) formic acid, Fe, 85 °C, 16 h, 69%; (**c**) $LiAlH_4$, dry THF, rt, 16 h, 40%; (**d**) TEA, HOBt, EDCI, dry CH_2Cl_2, rt, 18 h, 39 %.

5.3.2. Biological evaluation

As already explained in Chapter 4.3.2., the measurement of cell viability is mandatory when reporting cellular IDO1 inhibitory activity, because the observed reduction of tryptophan degradation could simply be an effect of cytotoxicity. Thus, we decided to first investigate the cytotoxicity of all the synthesized compounds on A375 cell line. Cells were treated (48 h) with each compound (1 µM) and cell viability was measured by MTT assay. As shown in Table 1, compounds **44** and **50** displayed a cytotoxic effect, inducing a reduction of cell viability of -18% and -45%, respectively, while the other compounds resulted in being non-cytotoxic and biocompatible. The ability of the synthesized compounds to inhibit human IDO1 was analyzed in an *in vitro* cell-based assay, to evaluate their inhibitory effect together with their ability to permeate the cell membrane. IDO1 expression was induced in A375 cell line by IFN-γ and enzymatic activity was determined after 48 h by measuring the formation of the L-kynurenine (L-Kyn) product by high-performance liquid chromatography (HPLC). IC_{50} values were calculated for compounds that displayed an inhibition value greater than 80%. Biological evaluation is still ongoing and the results obtained so far are reported in the Table below.

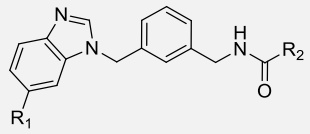

Cpd	R_1	R_2	Cell viability (%) @ 1 µM ± SD	IDO cellular assay inhibition (%) @ 1 µM	IC_{50}
6	H	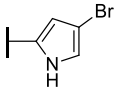	96 ± 2	98	16 nM
29	H		98 ± 2	32	-
30	H	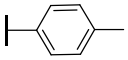	94 ± 3	88	BE

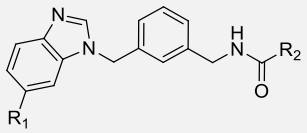

Cpd	R_1	R_2	Cell viability (%) @ 1 µM ± SD	IDO cellular assay inhibition (%) @ 1 µM	IC_{50}
31	H	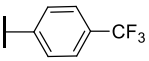	97 ± 3	81	BE
32	H	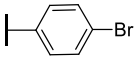	96 ± 4	98	BE
33	H	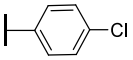	96 ± 4	99	BE
34	H	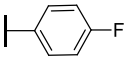	89 ± 7	88	BE
35	H	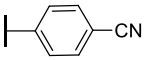	100 ± 1	88	90 nM
36	H	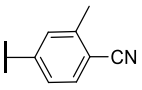	94 ± 1	44	-
37	H	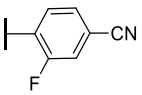	99 ± 1	37	-
38	H	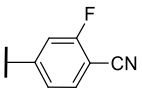	100 ± 0	32	-
39	H		100 ± 0	37	-
40	H		98 ± 1	62	-
41	H		94 ± 6	72	-
42	H	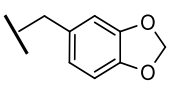	96 ± 3	5	-

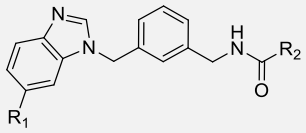

Cpd	R_1	R_2	Cell viability (%) @ 1 µM ± SD	IDO cellular assay inhibition (%) @ 1 µM	IC_{50}
43	H	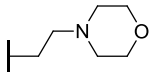	100 ± 1	0	-
44	H	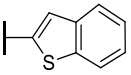	88 ± 1	77	-
45	H	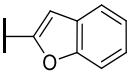	100 ± 0	87	413 nM
46	H	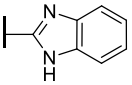	100 ± 0	81	407 nM
47	H	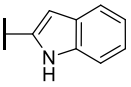	99 ± 4	94	72 nM
48	H	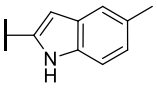	99 ± 1	90	636 nM
49	H	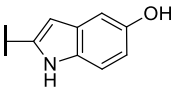	99 ± 1	82	781 nM
50	H	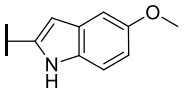	55 ± 11	-	-
54	H	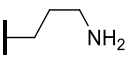	100 ± 0	0	-
60	Br	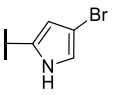	99 ± 1	99	19 nM

Table 1. Structure and biological profile of benzimidazole compounds. BE = being evaluated.

5.3.3. Preliminary SAR study

First, the presence of a phenyl ring at R_2 position and the effect of various substituents at different positions of the phenyl ring was investigated. While the inhibitory activity was low when a non-substituted phenyl ring was present (**29**, 32%), the addiction of a cyano group at position 4' produced a significative increase in activity (**35**, IC_{50} = 90 nM). However, the simultaneous presence of a cyano group at position 4' with a methyl group at 3' position (**36,** 44%) or, alternatively, a fluorine at 2' position (**37**, 37%) or at 3' position (**38,** 32%) produced a loss of activity. Electron-withdrawing groups such as chlorine, fluorine, bromine and trifluoromethyl at position 4' gave the compounds **31 – 34** displaying inhibitory activities between 88 and 99%. The same occurred when the methyl moiety was introduced at position 4' (**30**, 88%). Moreover, the introduction of a polar structure at R_2 position induced a loss of activity (**43**, 0%; **54**, 0%). The presence of a bromine group at 3' position on the pirrole ring of compound **6** seems to be crucial: indeed, when it was removed, a decrease in activity was observed (**41**, 72%). Similarly, different pentatomic heterocycles such as furan **39** and thiophene **40** produced a decrease in inhibitory activity (37 and 62%, respectively). Then, the influence of different fused heterocycles was studied. Nitrogenated heterocycles such as indole (**47**, 72 nM) and benzimidazole (**46**, 407 nM) showed a good activity, despite the IC_{50} values were higher compared to the *hit compound***.** The presence of a polar hydroxyl group at position 5' of the indole ring (**49,** 781 nM) or, alternatively, a methyl group at the same position was tolerated (**48**, 636 nM). Lastly, benzofuran **45** showed an IC_{50} value of 413 nM comparable to benzimidazole compound (**46**, 407 nM), while the presence of a benzodioxolane ring was not tolerated (**42**, 5%). Subsequently, we investigated whether the addiction of a bromine atom at R_1 position on the benzimidazole core might enhance the potency of the *hit*. Gratifyingly, compound **60** gave rise to the most active compound of this class of analogues with an IC_{50}

value of 19 nM. The preliminary results of this SAR study are summarized in Figure 2.

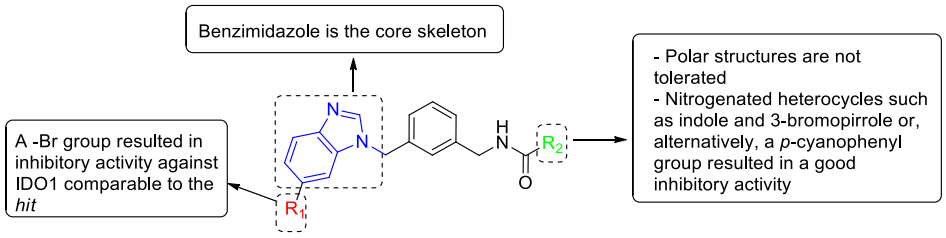

Figure 2. Preliminary SAR study of benzimidazoles.

Preliminary docking studies on **60** revealed that it can bind in the IDO catalytic pocket as *hit compound* **1** (Figure 1B). Nitrogen moiety of benzimidazole can interact with the heme group, while the Br substituent bind in the pocket A, near Cys129. The central aromatic ring is near pocket B, while the pyrrole end group is located in the pocket C. Its NH moiety, with NH of the amide linker, can give hydrogen bonding interaction with acid moiety of heme (Figure 3).

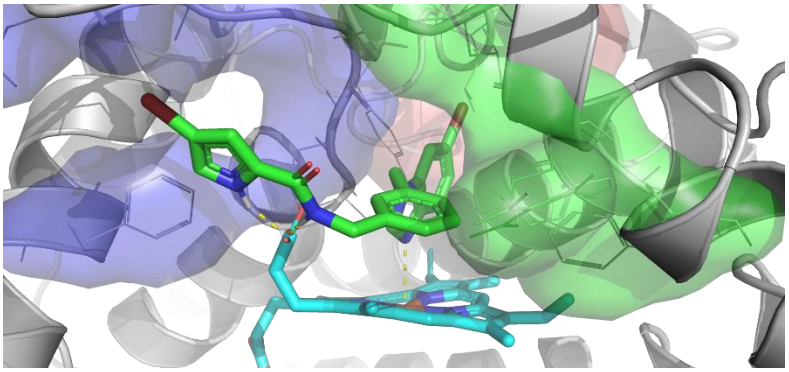

Figure 3. Docking pose of **60**. Structure is depicted as green sticks and heme is depicted as cyan sticks. Red shape: pocket A; green: pocket B; blue: pocket C. Hydrogen bond interactions are indicated as dashed yellow lines.

5.4. Conclusions

In conclusion, exploiting a structure-based virtual screening approach, we identified a promising *hit,* **1**, with an IC_{50} value against IDO1 in the nanomolar range. While a plethora of structural different molecules have been described in the literature as IDO1 inhibitors, to the best of our knowledge the benzimidazole scaffold has never been reported. The *hit* was re-synthesized by us and its biological activity was confirmed. Moreover, a preliminary SAR study of this class of compounds has been performed proving that at R_2 position: i) polar structures are not tolerated, ii) indole and 3-bromopirrole heterocycles show good inhibitory activities, iii) the removal of Br atom on the pirrole ring of the *hit compound* results in a decrease in inhibitory activity, iv) a cyano group in 4' position on the phenyl ring produces a significant increase in activity. We also demonstrated that the addiction of a bromine atom at R_1 significantly increased inhibitory potency.

In summary, together with the *hit* (**6**, IC_{50} = 16 nM), a potent compound has been identified, **60,** with an IC_{50} value against IDO1 of 19 nM.

Furthermore, docking studies suggest that this class of compounds might be accommodated also in the active site of IDO2 and TDO, as a similar pocket C is also present on the active site of these two dioxygenases. In this context, since recent reports have suggested that the combinatorial targeting of the three enzymes might deepen efficacy, limit acquired resistance to IDO1 blockade and reduce autoimmune side effects of immunotherapy, we realized that development of a dual/pan inhibitor of IDO1, IDO2 and TDO would be a more effective strategy in cancer therapy.[4]

For these reasons, the selectivity profile over these two enzymes and the ADME properties will be investigated for compounds **6** and **30**; indeed, since they showed comparable inhibitory activities the determination of metabolic and selectivity profile will be pivotal. Finally, as soon as a promising candidate will be identified, after appropriate maximal tolerated dose (MTD) and pharmacokinetics (PK)

experiments the efficacy of the compounds in triple-negative breast (4T1) cancer and in hepatocellular carcinoma (Hep-55.1c) will be evaluated.

5.5. Experimental section

General Methods. Commercially available reagents and solvents were used as purchased without further purification. When needed, solvents were distilled and stored on molecular sieves. Column chromatography was performed on silica gel Merck Kieselgel 70-230 mesh ASTM. Thin layer chromatography (TLC) was carried out on 5 cm x 20 cm plates with a layer thickness of 0.25 mm (Merck silica gel 60 F254). The spots were visualized by ultraviolet light (wavelengths 254 and 366 nm) and, when necessary, with Dragendorff reagent, aqueous $KMnO_4$ or aqueous Pancaldi solution. Melting points were determined in open glass capillary with a Stuart scientific SMP3 apparatus. All the target compounds were checked by IR (FT-IR Thermo-Nicolet Avatar), ^{1}H and ^{13}C NMR (Jeol ECP 300 MHz), and mass spectrometry (Thermo Finningan LCQ-deca XP-plus) equipped with an ESI source and an ion trap detector. Chemical shifts are reported in parts per million (ppm).

5.5.1. Chemistry

3-((1H-benzo[d]imidazol-1-yl)methyl)benzonitrile, (4).

To a solution of benzimidazole (3.00 g, 25.39 mmol, 1 eq) in acetone (83 mL) KOH (2.90 g, 50.79 mmol, 2 eq) and 3-(bromomethyl)benzonitrile (4.98 g, 25.39 mmol, 1 eq) were added in order. The reaction mixture was heated at 60 °C for 4 hours. Then, acetone was removed in vacuo, water was added and the aqueous layer was extracted with EtOAc (x1). The organic extract was dried over Na_2SO_4, filtered and concentrated in vacuo. Purification by silica gel column chromatography using petroleum ether/ethyl acetate 3:7 provided the desired compound (5.86 g, 25.14 mmol, 99%) as a yellow solid. mp 110-112 °C. ^{1}H NMR (300 MHz, $CDCl_3$): δ = 7.98 (s, 1H), 7.83 (d, J = 7.7 Hz, 1H), 7.59 (d, J= 7.7 Hz, 1H), 7.76 (s, 1H), 7.43 (d,

J = 7.4 Hz, 1H), 7.33-7.25 (m, 3H), 7.22 (t, *J* = 7.4 Hz, 1H), 5.40 (s, 2H). ^{13}C NMR (75 MHz, CD_3OD): δ = 143.9, 143.3, 137.4, 133.6, 131.9, 131.4, 130.4, 130.0, 123.6, 122.7, 120.5, 118.4, 113.0, 110.0, 47.9. IR (KBr): $\tilde{\nu}$ = 3099, 3077, 3051, 2865, 2757, 2560, 1496, 1439, 743 cm^{-1}. MS (ESI): *m/z* 234 $[M + H]^+$.

(3-((1H-benzo[d]imidazol-1-yl)methyl)phenyl)methanamine, (5).

Compound **4** (1.50 g, 6.43 mmol, 1 eq) was solubilized in dry THF (49 mL). The solution was cooled to 0 °C and $LiAlH_4$ (0.49 g, 16.09 mmol, 2.5 eq) was slowly added. The mixture was stirred at rt overnight and then heated at 65 °C for 2 hours. Then, EtOAc was added and the organic layer was washed with aqueous saturated Na_2SO_4 solution (x1), with water (x1), dried over Na_2SO_4 and concentrated in vacuo. Purification by silica gel column chromatography using ethyl acetate/MeOH 7:3 provided the title compound (1.07 g, 4.50 mmol, 70%) as a yellow oil. ^{1}H NMR (300 MHz, CD_3OD): δ = 8.28 (s, 1H), 7.66 (t, *J* = 7.2 Hz, 1H), 7.43 (t, *J* = 7.2 Hz, 1H), 7.30-7.15 (m, 6H), 5.74 (s, 2H), 3.75 (s, 2H). ^{13}C NMR (75 MHz, CD_3OD): δ = 143.9, 143.2, 137.4, 133.6, 131.9, 131.4, 130.4, 130.0, 123.6, 122.7, 120.5, 118.4, 113.0, 110.0, 47.8. IR (KBr): $\tilde{\nu}$ = 3359, 3048, 2984, 1730, 1494, 1438, 1286, 1201, 741 cm^{-1}. MS (ESI): *m/z* 238 $[M + H]^+$.

General procedure for the synthesis of compounds 6, 29-50, 60.

To a solution of compound **5** (167.11 mg, 0.7 mmol, 1 eq) in dry CH_2Cl_2 (5 mL) TEA (220 µL, 1.54 mmol, 2.2 eq), EDCI (161.28 mg, 0.84 mmol, 1.2 eq), HOBt (113.51 mg, 0.84 mmol, 1.2 eq) and carboxylic acid (0.84 mmol, 1.2 eq) were added in order. The resulting mixture was stirred at room temperature for 16 h. CH_2Cl_2 was added and the organic phase was washed with aqueous saturated NH_4Cl solution (x1), dried over sodium sulfate and evaporated. Purification by silica gel column chromatography afforded compounds **6**, **29-50.**

N-(3-((1H-benzo[d]imidazol-1-yl)methyl)benzyl)-4-bromo-1H-pyrrole-2-carboxamide, (6).

The title compound was synthesized following the general procedure, starting from compound **5** (90 mg, 0.38 mmol) and 4-bromo-1H-pyrrole-2-carboxylic acid (86 mg, 0.46 mmol). The crude material was purified by column chromatography using petroleum ether/ethyl acetate 2:8 as eluent to afford compound **5** (77 mg, 0.19 mmol, 50%) as a white solid. Mp 212-214 °C. ^{1}H NMR (300 MHz, CD_3OD): δ = 8.21 (s, 1H), 7.65 (d, *J* = 7.4 Hz, 1H), 7.38 (d, *J* = 7.6 Hz, 1H), 7.31-7.12 (m, 6H), 6.90 (s, 1H), 6.73 (s, 1H), 5.44 (s, 2H), 4.44 (s, 2H). ^{13}C NMR (75 MHz, DMSO-d_6): δ = 160.2, 144.8, 144.1, 140.9, 137.5, 134.3, 129.3, 127.3 (2C), 127.2, 127.0, 126.9, 126.5, 123.0, 122.2, 121.9, 120.1, 95.6, 48.2, 40.6. IR (KBr): $\tilde{\nu}$ = 3285, 3118, 2913, 2850, 2446, 2360, 3242, 1945, 1722, 748 cm^{-1}. MS (ESI): *m/z* 409 $[M + H]^+$.

N-(3-((1H-benzo[d]imidazol-1-yl)methyl)benzyl)benzamide, (29).

The title compound was synthesized following the general procedure, starting from compound **5** (166 mg, 0.70 mmol) and benzoic acid (102 mg, 0.84 mmol). The crude material was purified by column chromatography using petroleum ether/ethyl acetate 3:7 as eluent to afford compound **29** (128 mg, 0.39 mmol, 54%) as a white solid. ^{1}H NMR (300 MHz, CD_3OD): δ = 8.24 (s, 1H), 7.75 (d, *J* = 8.2 Hz, 2H), 7.64 (d, *J* = 8.2 Hz, 1H), 7.55-7.49 (m, 1H), 7.43 (t, *J* = 7.7 Hz, 1H), 7.38 (d, *J* = 7.7 Hz, 1H), 7.31-7.15 (m, 7H), 5.45 (s, 2H), 4.51 8s, 2H. MS (ESI): *m/z* 342 $[M + H]^+$.

N-(3-((1H-benzo[d]imidazol-1-yl)methyl)benzyl)-4-methylbenzamide, (30).

The title compound was synthesized following the general procedure, starting from compound **5** (76 mg, 0.32 mmol) and 2-oxo-2-(p-tolyl)acetic acid (52 mg, 0.38 mmol). The crude material was purified by column chromatography using ether/ethyl acetate 3:7 as eluent to afford compound **30** (79 mg, 0.21 mmol, 69%) as a white solid. Mp 137 – 139 °C.^{1}H NMR (300 MHz, CD_3OD): δ = 8.22 (s, 1H), 7.81-

7.58 (m, 3H), 7.38 (d, *J* = 7.6 Hz, 1H), 7.36-7.06 (m, 8H), 5.43 (s, 2H), 4.90 (s, 2H), 2.36 (s, 3H). MS (ESI): 356 *m/z* $[M + H]^+$.

N-(3-((1H-benzo[d]imidazol-1-yl)methyl)benzyl)-4-(trifluoromethyl)benzamide, (31).

The title compound was synthesized following the general procedure, starting from compound **5** (60 mg, 0.25 mmol) and 4-(trifluoromethyl)benzoic acid (57 mg, 0.30 mmol). The crude material was purified by column chromatography using ether/ethyl acetate 3:7 as eluent to afford compound **31** (84 mg, 0.21 mmol, 82%) as a white solid. Mp 154 – 158 °C.^{1}H NMR (300 MHz, CD_3OD): δ = 8.27 (s, 1H), 7.89 (d, *J* = 8.2 Hz, 2H), 7.75 (d, *J* = 8.2 Hz, 2H), 7.64 (d, *J* = 7.4 Hz, 1H), 7.39 (d, *J* = 8.2 Hz, 1H), 7.33-7.12 (m, 6H), 5.49 (s, 2H), 4.52 (s, 2H). MS (ESI): 410 *m/z* $[M + H]^+$.

N-(3-((1H-benzo[d]imidazol-1-yl)methyl)benzyl)-4-bromobenzamide, (32).

The title compound was synthesized following the general procedure, starting from compound **5** (60 mg, 0.25 mmol) and 4-bromobenzoic acid (61 mg, 0.30 mmol). The crude material was purified by column chromatography using ether/ethyl acetate 3:7 as eluent to afford compound **32** (81 mg, 0.19 mmol, 77%) as a white solid. Mp 151 – 153 °C. ^{1}H NMR (300 MHz, CD_3OD): δ = 8.27 (s, 1H), 7.73-7.56 (m, 5H), 7.41 (d, *J* = 7.1 Hz, 1H), 7.35 (d, *J* = 7.4 Hz, 2H), 7.29-7.18 (m, 4H), 5.50 (s, 2H), 4.61 (s, 2H). MS (ESI): 420 *m/z* $[M + H]^+$.

N-(3-((1H-benzo[d]imidazol-1-yl)methyl)benzyl)-4-chlorobenzamide, (33).

The title compound was synthesized following the general procedure, starting from compound **5** (60 mg, 0.25 mmol) and 4-chlorobenzoic acid (47 mg, 0.30 mmol). The crude material was purified by column chromatography using ether/ethyl acetate 3:7 as eluent to afford compound **33** (57 mg, 0.15 mmol, 60%) as a white solid. Mp 125 – 127 °C. ^{1}H NMR (300 MHz, CD_3OD): δ = 8.25 (s, 1H), 7.73 (d, *J* = 8.5 Hz, 2H),

7.65 (d, *J* = 7.1 Hz, 1H), 7.49-7.37 (m, 3H), 7.33-7.09 (m, 6H), 5.48 (s, 2H), 4.50 (s, 2H). MS (ESI): 376 *m/z* $[M + H]^+$.

N-(3-((1H-benzo[d]imidazol-1-yl)methyl)benzyl)-4-fluorobenzamide, (34).

The title compound was synthesized following the general procedure, starting from compound **5** (60 mg, 0.25 mmol) and 4-fluorobenzoic acid (43 mg, 0.30 mmol). The crude material was purified by column chromatography using ether/ethyl acetate 3:7 as eluent to afford compound **34** (70 mg, 0.19 mmol, 78%) as a grey solid. Mp 116 – 118 °C. ^{1}H NMR (300 MHz, CD_3OD): δ = 8.26 (s, 1H), 7.87-7.78 (m, 2H), 7.65 (d, *J* = 6.8 Hz, 1H), 7.41 (d, *J* = 6.8 Hz, 1H), 7.35 (d, *J* = 8.0 Hz, 2H), 7.27-7.09 (m, 6H), 5.49 (s, 2H), 4.52 (s, 2H). MS (ESI): 360 *m/z* $[M + H]^+$.

N-(3-((1H-benzo[d]imidazol-1-yl)methyl)benzyl)-4-cyanobenzamide, (35).

The title compound was synthesized following the general procedure, starting from compound **5** (166 mg, 0.70 mmol) and 4-cyanobenzoic acid (123 mg, 0.84 mmol). The crude material was purified by column chromatography using ether/ethyl acetate 3:7 as eluent to afford compound **35** (197 mg, 0.54 mmol, 77%) as a white solid. Mp 192-194 °C. ^{1}H NMR (300 MHz, CD_3OD): δ = 8.25 (s, 1H), 7.90-7.79 (m, 4H), 7.64 (d, *J* = 6.8 Hz, 1H), 7.39 (d, *J* = 6.8 Hz, 1H), 7.35-7.16 (m, 6H), 5.49 (s, 2H), 4.52 (s, 2H). IR (KBr): $\tilde{\nu}$ 3553, 3414, 3348, 3082, 2923, 2358, 2227, 1638, 1546, 1492, 1443, 736, 742 cm^{-1}. MS (ESI): *m/z* 367 $[M + H]^+$.

N-(3-((1H-benzo[d]imidazol-1-yl)methyl)benzyl)-4-cyano-3-methylbenzamide, (36).

The title compound was synthesized following the general procedure, starting from compound **5** (60 mg, 0.25 mmol) and 4-cyano-3-methylbenzoic acid (49 mg, 0.30 mmol). The crude material was purified by column chromatography using ether/ethyl acetate 3:7 as eluent to afford compound **36** (48 mg, 0.13 mmol, 51%) as a yellow solid. Mp 178 – 180 °C. ^{1}H NMR (300 MHz, DMSO-d_6): δ = 9.21 (br s, 1H), 8.40 (s, 1H), 7.90 (d, *J* = 6.9 Hz, 2H), 7.78 (d, *J* = 8.0 Hz, 1H), 7.65 (d , *J* = 5.0

Hz, 1H), 7.51 (d , *J* = 5.0 Hz, 1H), 7.34-7.27 (m, 2H), 7.21-7.17 (m, 4H), 5.48 (s, 2H), 4.50 (s, 2H). MS (ESI): 381 *m/z* $[M + H]^+$.

N-(3-((1H-benzo[d]imidazol-1-yl)methyl)benzyl)-4-cyano-2-fluorobenzamide, (37).

The title compound was synthesized following the general procedure, starting from compound **5** (60 mg, 0.25 mmol) and 2-oxo-2-(p-tolyl)acetic acid (49 mg, 0.30 mmol). The crude material was purified by column chromatography using ether/ethyl acetate 3:7 as eluent to afford compound **37** (58 mg, 0.15 mmol, 60%) as a white solid. Mp 103 – 105 °C. ^{1}H NMR (300 MHz, CD_3OD): δ = 8.28 (s, 1H), 7-79-7.57 (m, 4H), 7.42 (d, *J* = 5.2 Hz, 1H), 7.34 (d, *J* = 8.5 Hz, 2H), 7.27-7.19 (m, 4H), 5.51 (s, 2H), 4.53 (s, 2H). MS (ESI): 385 *m/z* $[M + H]^+$.

N-(3-((1H-benzo[d]imidazol-1-yl)methyl)benzyl)-4-cyano-3-fluorobenzamide, (38).

The title compound was synthesized following the general procedure, starting from compound **5** (60 mg, 0.25 mmol) and 4-cyano-3-fluorobenzoic acid (50 mg, 0.30 mmol). The crude material was purified by column chromatography using ether/ethyl acetate 3:7 as eluent to afford compound **38** (46 mg, 0.11 mmol, 48%) as a yellow solid. Mp 192 – 194 °C. ^{1}H NMR (300 MHz, DMSO-d_6): δ = 9.37 (br s, 1H), 8.58 (s, 1H), 8.08 (t, *J* = 8.08 Hz, 1H), 7.95-7.80 (m, 2H), 7.65 (d, *J* = 7.6 Hz, 1H), 7.56 (d, *J* = 7.6 Hz, 1H), 7.43-7.16 (m, 6H), 5.53 (s, 2H), 4.45 (s, 2H). MS (ESI): 385 *m/z* $[M + H]^+$.

N-(3-((1H-benzo[d]imidazol-1-yl)methyl)benzyl)furan-2-carboxamide, (39).

The title compound was synthesized following the general procedure, starting from compound **5** (166 mg, 0.70 mmol) and furan-2-carboxylic acid (94 mg, 0.84 mmol). The crude material was purified by column chromatography using ether/ethyl acetate 4:6 as eluent to afford compound **39** (150 mg, 0.46 mmol, 65%) as a white solid. Mp 153-154 °C. ^{1}H NMR (300 MHz, CD_3OD): δ = 8.19 (s, 1H), 7.64-7.57 (m, 3H), 7.34

(d, *J* = 7.4 Hz, 1H), 7.35-7.04 (m, 7H), 5.36 (s, 2H), 4.44 (s, 2H). IR (KBr): $\tilde{\nu}$ = 3477, 3231, 3070, 2977, 2926, 1742, 1638, 1495, 1442, 1365, 1015, 769, 745cm^{-1}. MS (ESI): *m/z* 332 $[M + H]^+$.

N-(3-((1H-benzo[d]imidazol-1-yl)methyl)benzyl)thiophene-2-carboxamide, (40).

The title compound was synthesized following the general procedure, starting from compound **5** (160 mg, 0.67 mmol) and thiophene-2-carboxylic acid (103 mg, 0.81 mmol). The crude material was purified by column chromatography using ether/ethyl acetate 3:7 as eluent to afford compound **40** (182 mg, 0.52 mmol, 78%) as a yellow solid. Mp 171-173 °C. ^{1}H NMR (300 MHz, CD_3OD): δ = 8.19 (s, 1H), 7.64-7.57 (m, 3H), 7.34 (d, *J* = 7.4 Hz, 1H), 7.35-7.04 (m, 7H), 5.36 (s, 2H), 4.44 (s, 2H). IR (KBr): $\tilde{\nu}$ = 3555, 3414, 3263, 3070, 2892, 1636, 1618, 1498, 1365, 744 cm^{-1}. MS (ESI): *m/z* 348 $[M + H]^+$.

N-(3-((1H-benzo[d]imidazol-1-yl)methyl)benzyl)-1H-pyrrole-2-carboxamide, (41).

The title compound was synthesized following the general procedure, starting from compound **5** (166 mg, 0.70 mmol) and 1H-pyrrole-2-carboxylic acid (93 mg, 0.84 mmol). The crude material was purified by column chromatography using ether/ethyl acetate 2:8 as eluent to afford compound **41** (143 mg, 0.43 mmol, 62%) as a yellow solid. Mp 206-208 °C. ^{1}H NMR (300 MHz, CD_3OD): δ = 8.23 (s, 1H), 7.64 (dd, *Js* = 1.0, 8.3 Hz), 7.39 (d, *J* = 6.9 Hz, 1H), 7.26-7.13 (m, 7H), 7.76 (s, 1H), 6.16 (d, *J* = 2.5 Hz, 1H), 5.43 (s 2H), 5.36 (s, 2H). IR (KBr): $\tilde{\nu}$ = 3220, 3087, 2935, 2701, 2563, 1628, 1560, 1491, 1437, 1438, 776, 745 cm^{-1}. MS (ESI): *m/z* 331 $[M + H]^+$.

N-(3-((1H-benzo[d]imidazol-1-yl)methyl)benzyl)-2-(benzo[d][1,3]dioxol-5-yl)acetamide, (42).

The title compound was synthesized following the general procedure, starting from compound **5** (166 mg, 0.70 mmol) and 2-(benzo[d][1,3]dioxol-5-yl)acetic acid (151

mg, 0.84 mmol). The crude material was purified by column chromatography using ether/ethyl acetate 3:7 as eluent to afford compound **42** (235 mg, 0.59 mmol, 84%) as an amorphous yellow solid. ^{1}H NMR (300 MHz, CD_3OD): δ = 8.13 (s, 1H), 7.66 (d, *J* = 8.0 Hz, 1H), 7.29 (d, *J* = 8.0 Hz, 1H), 7.30-7.00 (m, 7H), 6.74 (s, 1H), 6.66 (s, 1H), 5.76 (s, 2H), 5.27 (s, 2H), 4.23 (s, 2H), 3.30 (s, 2H). IR (KBr): $\tilde{\nu}$ = 3735, 3629, 3255, 2887, 2790, 1845, 1654, 1500, 1442, 1260, 1190, 1040, 668 cm^{-1}. MS (ESI): *m/z* 400 $[M + H]^+$.

N-(3-((1H-benzo[d]imidazol-1-yl)methyl)benzyl)-3-morpholinopropanamide, (43).

The title compound was synthesized following the general procedure, starting from compound **5** (166 mg, 0.70 mmol) and 3-morpholinopropanoic acid (133 mg, 0.84 mmol). The crude material was purified by column chromatography using ethyl acetate/MeOH 9:1 as eluent to afford compound **43** (146 mg, 0.39 mmol, 55%) as an amorphous yellow solid. ^{1}H NMR (300 MHz, CD_3OD): δ = 8.25 (s, 1H), 7.68 (t, *J* = 3.0 Hz, 1H), 7.43 (t, *J* = 3.0 Hz, 1H), 7.34-7.24 (m, 5H), 7.18 (d, *J* = 6.9 Hz, 1H), 5.48 (s, 2H), 4.34 (s, 2H), 3.58-3.50 (m, 4H), 2.60 (t, *J* = 7.0 Hz, 2H), 2.42- 2.39 (m, 4H), 2.36 (t, *J* = 7.0 Hz, 2H). IR (neat): $\tilde{\nu}$ = 3268, 2062, 1649, 1550, 1495, 1457, 1287, 1114, 743 cm^{-1}. MS (ESI): *m/z* 379 $[M + H]^+$.

N-(3-((1H-benzo[d]imidazol-1-yl)methyl)benzyl)benzo[b]thiophene-2-carboxamide, (44).

The title compound was synthesized following the general procedure, starting from compound **5** (166 mg, 0.70 mmol) and benzo[b]thiophene-2-carboxylic acid (149 mg, 0.84 mmol). The crude material was purified by column chromatography using petroleum ether/ethyl acetate 5:5 as eluent to afford compound **44** (144 mg, 0.36 mmol, 52%) as a white solid. Mp 185-187 °C. ^{1}H NMR (300 MHz, acetone-d_6): δ = 8.48 (s, 1H), 8.23 (s, 1H), 8.00-7.98 (m, 2H), 7.89 (dd, J_S = 1.9, 7.1 Hz, 1H), 7.77-7.63 (m, 1H), 7.48-7.47 (m, 2H), 7.44-7.41 (m, 2H), 7.33-7.28 (d, *J* = 5.8 Hz, 2H),

7.21-7.11 (m, 2H), 5.50 (s, 2H), 4.59 (s, 2H). IR (KBr): $\tilde{\nu}$ = 3183, 3055, 1642, 1560, 1495, 1458, 1290, 742 cm^{-1}. MS (ESI): *m/z* 398 $[M + H]^+$.

N-(3-((1H-benzo[d]imidazol-1-yl)methyl)benzyl)benzofuran-2-carboxamide, (45).

The title compound was synthesized following the general procedure, starting from compound **5** (166 mg, 0.70 mmol) and benzofuran-2-carboxylic acid (136 mg, 0.84 mmol). The crude material was purified by column chromatography using ether/ethyl acetate 3:7 as eluent to afford compound **45** (98 mg, 0.26 mmol, 37%) as a yellow solid. Mp 161-163 °C. ^{1}H NMR (300 MHz, CD_3OD): δ = 8.26 (s, 1H), 7.65 (d, *J* = 7.9 Hz, 1H), 7.60-7.57 (s, 1H), 7.50 (d, *J* = 7.9 Hz, 1H), 7.41 (m, 2H), 7.36-7.31 (m, 2H), 7.25 (m, 3H), 7.13-7.10 (m, 3H), 5.43 (s, 2H), 4.52 (s, 2H). IR (KBr): $\tilde{\nu}$ = 3892, 3801, 3735, 2927, 2850, 1734, 1590, 1560, 1496, 1474, 747 cm^{-1}. MS (ESI): 382 *m/z* $[M + H]^+$.

N-(3-((1H-benzo[d]imidazol-1-yl)methyl)benzyl)-1H-benzo[d]imidazole-2-carboxamide, (46).

The title compound was synthesized following the general procedure, starting from compound **5** (166 mg, 0.70 mmol) and 1H-benzo[d]imidazole-2-carboxylic acid (136 mg, 0.84 mmol). The crude material was purified by column chromatography using ether/ethyl acetate 4:6 as eluent to afford compound **46** (229 mg, 0.60 mmol, 86%) as a white solid. Mp 226-227 °C. ^{1}H NMR (300 MHz, DMSO-d_6): δ = 9.40 (br s, 1H), 8.34 (s, 1H), 7.77-7.58 (m, 3H), 7.47 (d, *J* = 7.2 Hz,1H), 7.36 (s, 1H), 7.27-7.21 (m, 4H), 7.16-7.06 (m, 3H), 5.46 (s, 2H), 4.46 (s, 2H). IR (KBr): $\tilde{\nu}$ = 3418, 3047, 1666, 1507, 1494, 1436, 1330, 744 cm^{-1}. MS (ESI): *m/z* 382 $[M + H]^+$.

N-(3-((1H-benzo[d]imidazol-1-yl)methyl)benzyl)-1H-indole-2-carboxamide, (47).

The title compound was synthesized following the general procedure, starting from compound **5** (166 mg, 0.70 mmol) and 1H-indole-2-carboxylic acid (135 mg, 0.84 mmol). The crude material was purified by column chromatography using petroleum ether/ethyl acetate 4:6 as eluent to afford compound **47** (144 mg, 0.38 mmol, 54%)

as a yellow solid. Mp 231-233 °C. ^{1}H NMR (300 MHz, DMSO-d_6): δ = 11.53 (br s, 1H), 8.94 (br s, 1H), 8.37 (s, 1H), 7.68-7.55 (m, 2H), 7.53-7.40 (m, 2H), 7.37 (s, 1H), 7.31-7.26 (m, 2H), 7.21-7.15, (m, 5H), 7.04 (t, *J* = 7.9 Hz, 1H), 5.49 (s, 2H), 4.48 (s, 2H). IR (KBr): $\tilde{\nu}$ = 3218, 3053, 2926, 2853, 2721, 2648, 1638, 1564, 1495, 1310, 746 cm^{-1}. MS (ESI): *m/z* 381 $[M + H]^+$.

N-(3-((1H-benzo[d]imidazol-1-yl)methyl)benzyl)-5-methyl-1H-indole-2-carboxamide, (48).

The title compound was synthesized following the general procedure, starting from compound **5** (166 mg, 0.70 mmol) and 5-methyl-1H-indole-2-carboxylic acid (147 mg, 0.84 mmol). The crude material was purified by column chromatography using ether/ethyl acetate 3:7 as eluent to afford compound **48** (134 mg, 0.34 mmol, 49%) as a white solid. Mp 222-224 °C. ^{1}H NMR (300 MHz, CD_3OD): δ = 8.25 (s, 1H), 7.62 (dd, *Js* = 1.9, 7.7 Hz, 1H), 7.41-7.28 (m, 6H), 7.18-7.16 (m, 3H), 7.61 (d, *J* = 7.7 Hz, 1H), 6.93 (s, 1H), 5.48 (s, 2H),4.53 (s, 2H), 2.40 (s, 3H). IR (KBr): $\tilde{\nu}$ = 3232, 3090, 3061, 2922, 1637, 1560, 1496, 1419, 802, 736 cm^{-1}. MS (ESI): *m/z* 395 $[M + H]^+$.

N-(3-((1H-benzo[d]imidazol-1-yl)methyl)benzyl)-5-hydroxy-1H-indole-2-carboxamide, (49).

The title compound was synthesized following the general procedure, starting from compound **5** (166 mg, 0.70 mmol) and 5-hydroxy-1H-indole-2-carboxylic acid (148 mg, 0.84 mmol). The crude material was purified by column chromatography using ether/ethyl acetate 3:7 as eluent to afford compound **49** (35 mg, 0.09 mmol, 13%) as a yellow solid. Mp 210-212 °C. ^{1}H NMR (300 MHz, acetone-d_6): δ = 10.42 (br s, 1H), 8.32 (s, 1H), 7.52(dd, J_S = 1.7, 7.1 Hz, 1H), 7.32-7.20 (m, 6H), 7.18-7.15 (m, 3H), 7.59 (d, J = 7.7 Hz, 1H), 7.01 (s, 1H), 5.67 (br s, 1H), 5.50 (s, 2H), 4.58 (s, 2H), 3.31 (br s, 1H). IR (KBr): $\tilde{\nu}$ = 3745, 2359, 2342, 1742, 1557, 1496, 1362, 1257 cm^{-1}. MS (ESI): *m/z* 397 $[M + H]^+$.

N-(3-((1H-benzo[d]imidazol-1-yl)methyl)benzyl)-5-methoxy-1H-indole-2-carboxamide, (50).

The title compound was synthesized following the general procedure, starting from compound **5** (166 mg, 0.70 mmol) and 5-methoxy-1H-indole-2-carboxylic acid (160 mg, 0.84 mmol). The crude material was purified by column chromatography using ether/ethyl acetate 2:8 as eluent to afford compound **50** (160 mg, 0.39 mmol, 56%) as a yellow solid. Mp 225-227 °C. ^{1}H NMR (300 MHz, DMSO-d_6): δ = 11.43 (br s, 1H), 8.97 (s, 1H), 8.39 (s, 1H), 7.65 (d, *J* = 7.1 Hz, 1H), 7.50 (d, *J* = 7.1 Hz, 1H), 7.33 (t, *J* = 6.3 Hz, 1H), 7.27 (d, *J* = 6.3 Hz, 2H), 7.22-7.18 (m, 3H), 7.06 (d, *J* = 6.3 Hz, 2H), 6.83 (d, *J* = 8.5 Hz, 1H), 5.48 (s, 2H), 4.47 (s, 2H), 3.75 (s, 3H). IR (KBr): $\tilde{\nu}$ = 3246, 3087, 3004, 2926, 2803, 1637, 1559, 1497, 1359, 1269, 163, 742 cm^{-1}. MS (ESI): 411 *m/z* $[M + H]^+$.

4-((tert-butoxycarbonyl)amino)butanoic acid, (52).

To a solution of 4-aminobutanoic acid (200 mg, 1.94 mmol, 1 eq) in 2 M aq. NaOH (3 mL), a solution of BOC_2O (507.50 mg, 2.33 mmol, 1.2 eq) in THF (5 mL) was added dropwise and the reaction was stirred at rt overnight. The solvent was removed in vacuo. The aqueous layer was acidified with 2M aq. HCl until pH 4 and extracted with EtOAc (6x). Additionally, the aqueous layer was saturated with NaCl and extracted with THF (3x). The combined organic layers were dried over Na_2SO_4, filtrated and concentrate in vacuo yielding the desired compound (339 mg, 1.67 mmol, 86%) as a yellow oil, which was used directly in the next step without further purification. ^{1}H NMR (300 MHz, DMSO-d_6): δ = 6.77 (br s, 1H), 2.92 (t, *J* = 6.3 Hz, 2H), 2.16 (t, *J* = 6.3 Hz, 2H), 1.58 (quint, *J* = 6.9 Hz, 2H), 1.41 (s, 9H). MS (ESI): 204 *m/z* $[M + H]^+$.

N-(3-((1H-benzo[d]imidazol-1-yl)methyl)benzyl)-4-aminobutanamide, (54).

Step 1: To a solution of compound **5** (166.11 mg, 0.70 mmol, 1 eq) in dry CH_2Cl_2 (5 mL) TEA (220 µL, 1.54 mmol, 2.2 eq), EDCI (161.28 mg, 0.84 mmol, 1.2 eq),

HOBt (113.51 mg, 0.84 mmol, 1.2 eq) and compound **52** (170.71 mg, 0.84 mmol, 1.2 eq) were added in order. The resulting mixture was stirred at room temperature for 16 h. CH_2Cl_2 was added and the organic phase was washed with H_2O (x3), dried over sodium sulfate and evaporated. Purification by silica gel column chromatography using EtOAc as eluent afforded compound **53** (168 mg, 0.40 mmol, 57%) as a yellow solid.

Step 2: To a solution of compound **53 (**148 mg, 0.35 mmol, 1 eq) in CH_2Cl_2 (2.5 mL) at 0 °C CF_3COOH (1.23 mL) was added. The reaction mixture was stirred at the same temperature for 30 min and then for 3 hours at rt. 2 M aq. NaOH was added until pH 7 and the aqueous layer was extracted with EtOAc (x3). The collected organic layers were dried over Na_2SO_4, filtrated and concentrated in vacuo. Purification by silica gel column chromatography using CH_3CN/NH_3 9:1as eluent afforded compound **54** (80 mg, 0.25 mmol, 71%) as a yellow oil. ^{1}H NMR (300 MHz,CD_3OD): δ = 8.24 (s, 1H), 7.67 (d, *J* = 7.6 Hz, 1H), 7.36 (d, *J* = 7.6 Hz, 1H), 7.23-7.13 (m, 6H), 5.41 (s, 2H), 4.30 (s, 2H), 2.61 (t, *J* = 7.4 Hz, 2H), 2.19 (t, *J* = 7.4 Hz, 2H), 1.70 (quint, *J* = 6.8 Hz, 2H). IR (KBr): $\tilde{\nu}$ = 3478, 2621, 1617, 1521, 1540, 1456, 615 cm^{-1}. MS (ESI): 323 *m/z* $[M + H]^+$.

3-(((5-bromo-2-nitrophenyl)amino)methyl)benzonitrile, (57).

To a solution of 2,4-dibromo-1-nitrobenzene (100 mg, 0.36 mmol, 1 eq) in DMSO (1 mL), K_2CO_3 (73 mg, 0.53 mmol, 1.5 eq) and 3-(aminomethyl)benzonitrile (51 mg, 0.39 mg, 1.01 eq) were added in order. The reaction mixture was stirred at 72 °C overnight. EtOAc was added and the organic later was washed with $NaHCO_3$ (3x), dried over Na_2SO_4, filtrated and concentrated in vacuo. Purification by silica gel column chromatography using petroleum ether/ehyl acetate 95:5 as eluent afforded compound **57** (15 mg, 0.05 mmol, 13%) as a yellow solid. Mp 196-198 °C. ^{1}H NMR (300 MHz, $CDCl_3$): δ = 8.42 (s,1H), 8.08 (d, *J* = 7.8 Hz, 1H), 7.62-7.49 (m, 2H), 7.51 (d, *J* = 7.8 Hz, 1H), 6.88-6.83 (m, 2H), 4.57 (d, *J* = 4.7 Hz, 2H). IR (KBr): $\tilde{\nu}$ =

3390, 2921, 2229, 1962, 1890, 1520, 1408, 1257, 1049, 750, 618 cm^{-1}. MS (ESI): 332 *m/z* $[M + H]^+$.

3-((6-bromo-1H-benzo[d]imidazol-1-yl)methyl)benzonitrile, (58).

To a solution of compound **57** (0.93 g, 56.24 mmol, 1 eq) in formic acid (29 mL), Fe (3.14 g, 56.24 mmol, 20 eq) was added. The reaction mixture was heated to 85 °C for 16 hours. MeOH (29 mL) was added, the reaction was filtered and the filtrate concentrate in vacuo. The crude material was purified by silica gel column chromatography using petroleum ether/ehyl acetate 4:6 as eluent yielding a yellow solid (1.21 g, 38.81 mmol, 69%). Mp 123-125 °C. ^{1}H NMR (300 MHz, $CDCl_3$): δ = 8.00 (s, 1H), 7.62 (m, 2H), 7.42-7.26 (m, 5H), 5.35 (s, 2H). IR (KBr): $\tilde{\nu}$ = 3063, 2921, 2722, 2356, 2228, 1699, 1493, 1462, 1361, 1283, 767, 690 cm^{-1}. MS (ESI): 313 *m/z* $[M + H]^+$.

(3-((6-bromo-1H-benzo[d]imidazol-1-yl)methyl)phenyl)methanamine, (59).

Compound **59** was synthesized as previously reported for the preparation of compound **5**, starting from compound **58** (350 mg, 1.17 mmol) and compound **9** (290 mg, 0.97 mmol). The crude material was purified by column chromatography using ethyl acetate/MeOH 7:3 to obtain the desired compound **59** (147 mg, 0.47 mmol, 40%) as a yellow oil. ^{1}H NMR (300 MHz, CD_3OD): δ = 8.21 (s, 1H), 7.55 (t, J = 7.1 Hz, 1H), 7.36 (dd, J_s = 1.4, 7.4 Hz, 1H), 7.23-7.17 (m, 4H), 7.05 (s, 1H), 5.32 (s, 2H), 3.7 (s, 2H). IR (KBr): $\tilde{\nu}$ = 3521, 3444, 2922, 2855, 1496, 1562, 1458, 1367, 745 cm^{-1}. MS (ESI): 316 *m/z* $[M + H]^+$.

4-bromo-N-(3-((6-bromo-1H-benzo[d]imidazol-1-yl)methyl)benzyl)-1H-pyrrole-2-carboxamide, (60).

The title compound was synthesized following the general procedure, starting from compound **59** (100 mg, 0.32 mmol) and 4-bromo-1H-pyrrole-2-carboxylic acid (71 mg, 0.38 mmol). The crude material was purified by column chromatography using petroleum ether/ethyl acetate 3:7 as eluent to afford compound **60** (61 mg, 0.12

mmol, 39%) as a white solid. Mp 200-202 °C.^{1}H NMR (300 MHz, CD_3OD): δ = 8.26 (s, 1H), 7.65 (d, *J* = 7.7 Hz, 1H), 7.55 (d, *J* = 7.7 Hz, 1H) 7.31-7.13 (m, 5H), 6.91 (s, 1H), 6.73 (s, 1H), 7.15 (s, 2H), 4.45 (s,2H). IR (KBr): $\tilde{v}$ = 3484, 3407, 3224, 3119, 3291, 2769, 1564, 1525, 1459, 749 cm^{-1}. MS (ESI): 489 *m/z* $[M + H]^+$.

5.5.2. Appendix

^{1}H NMR (CD_3OD) of compound **6**

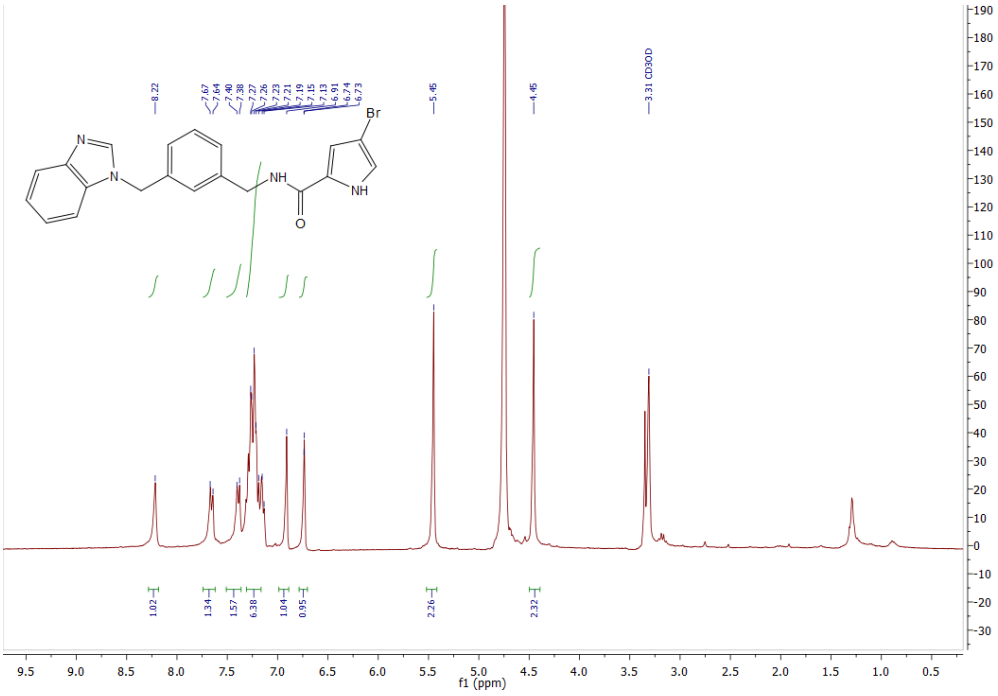

5.6. References

1. Fallarini, S.; Massarotti, A.; Gesù, A.; Giovarruscio, S.; Coda Zabetta, G.; Bergo, R.; Giannelli, B.; Brunco, A.; Lombardi, G.; Sorba, G.; Pirali, T. *In silico*-driven multicomponent synthesis of 4,5- and 1,5-disubstituted imidazoles as indoleamine 2,3-dioxygenase inhibitors. *MedChemComm.* **2016**, *7*, 409-419.
2. Griglio, A.; Torre, E.; Serafini, M.; Bianchi, A.; Schmid, R.; Coda Zabetta, G.; Massarotti, A.; Sorba, G.; Pirali, T.; Fallarini, S. A multicomponent approach in the discovery of indoleamine 2,3 dioxygenase 1 inhibitors: synthesis, biological investigation and docking studies. *Bioorg. Med. Chem. Lett.* **2018,** *28*, 651-657**.**
3. Sterling, T.; Irwin, J.J. ZINC 15 – ligand discovery for everyone. *J. Chem. Inf. Model.* **2015**, *55*, 2324–2337.
4. (a) Muller, A.; Manfredi, M.G.; Zakharia, Y.; Prednergast, G.C. Inhibiting IDO pathways to treat cancer: lessons from the ECHO-301 trial and beyond. *Semin. Immunopathol*. **2018**, 1-8.
   (b) Badawy, A.A-B. Targeting tryptophan availability to tumors: the answer to immune escape? *Immunol. Cell. Biol*. **2018**, 1-9.

Chapter 6

Design, synthesis and evaluation of *N*-aryl-2-aminothiazole derivatives as potential leads for the treatment of hereditary multiple exostoses

6.1. Introduction

As described above, heterozygous mutations in *Ext1* or *Ext2* genes cause HME, which results in decrease in HS levels. The current available therapy consists of surgical removal of exostoses and palliative drugs for pain control. Unfortunately, no pharmacological treatment is available for treating HME.

Consequently, the discovery of small molecules able to increase the HS expression could be of considerable clinical benefit.

In this context, Esko and co-workers developed a phenotypic screening assay based on binding of fluorescent derivative of fibroblast growth factor 2 (FGF2) to HS. They screened for molecules that increase HS levels on the plasma membrane of Chinese hamster ovary (CHO) cells. In detail 57,471 compounds were purchased and, after removal of the cytotoxic agents, the remaining 57,342 compounds were tested at 10 μM in a primary screen. Hits were then reconfirmed at a screening concentration in triplicate. After dose-response analysis and further studies *N*-aryl-2-aminothiazoles were identified as a promising class of molecules. Secondary assays confirmed that the effect of these molecules is due to specific interaction with a biological target and does not result from common non-specific mechanism or assay interference. Among this class of compounds was a promising *hit*, named **415**, that displayed an EC_{50} value of ~ 5 μM in the cell-based assays and had no cytotoxicity (Figure 1).

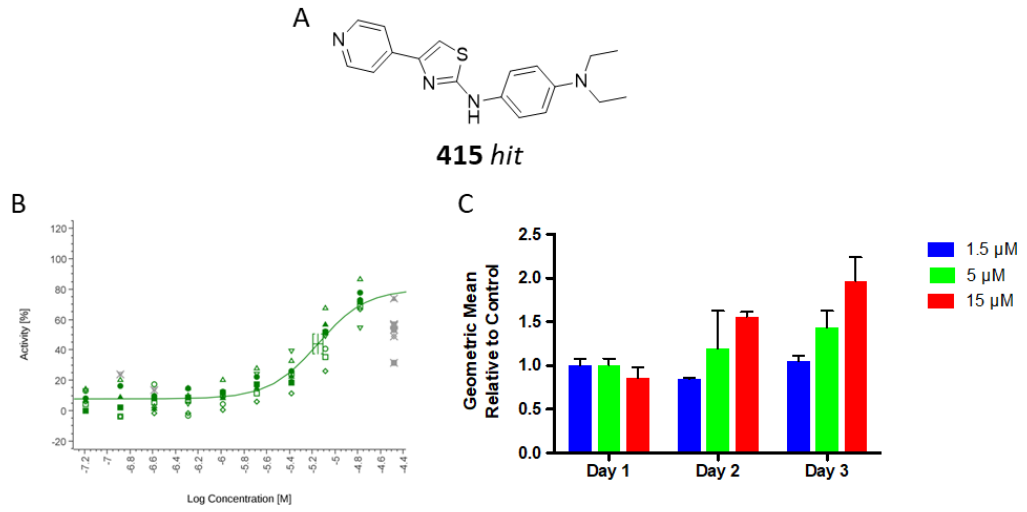

Figure 1. (**A**) Chemical structure of *hit compound* **415**. (**B)** Dose response profile using the optical high throughput assay for compound **415** in CHO cells using FGF-streptavidin as probe. (**C)** Compound **415** enhances heparan sulfate expression on A375 cells in a dose and time dependent manner.

6.2. Aim of the work

The goals of this project were to re-synthesize the representative *hit compound* **415** in order to confirm its activity and to design and synthesize a series of related structural analogues to enable a first assessment of structure activity relationship (SAR). Moreover, physicochemical properties of the most promising compounds including acidity (pKa), lipophilicity ($logD_{7.4}$) and aqueous solubility was determined. As a visiting PhD student of Prof. C. Ballatore's research group I participated in the synthesis and characterization of this class of compounds (See sections 6.5.1.and 6.5.3.).

6.3. Results and discussion

6.3.1. Chemistry

First of all the *hit compound* **415** was re-synthesized using two different synthetic strategies (Scheme 1A, 1B). The first one explored consists of condensation of bromoketone **4**, easily obtained by bromination of ketone **3**, with thiourea **2**. The latter was synthesized by conversion of aniline **1** first to isothiocyanate[1] and then to the desired thiourea. In the second procedure, **415** synthesis was accomplished in three steps: bromination, condensation and subsequent coupling of 2-aminothiazole **5.**[2] The exploited procedures gave an 60% and 46% overall yields, respectively, suggesting that the convergent synthesis resulted more efficient to obtain the *hit* (**6**).

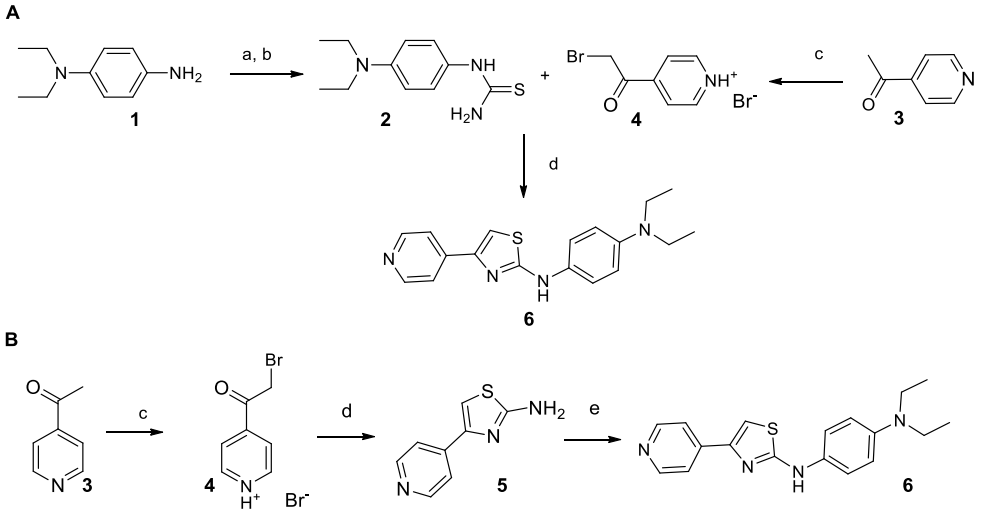

Scheme 1. Convergent (**A**) vs sequential (**B**) synthesis of *hit compound*, **415**.
(**a**) i) H_2O, CS_2, rt, 16 h ii) 2,4,6-trichloro-1,3,5-triazine, DCM, 50 min, rt, 91%; (**b**) 7 N NH_3 in MeOH, rt, 1 h, 63%; (**c**) HOAc/HBr, Br_2, 15 °C to 75 °C, 1 h, 100%; (**d**) thiourea, EtOH, microwaves, 110 °C, 30 min, 60-80%; (**e**) 4-bromo-*N*,*N*-diethylaniline, $Pd(OAc)_2$, tBuBrettPhos, K_2CO_3, degassed H_2O, *t*-BuOH, 110 °C, 58%.

Of notice, recrystallization from CH_2Cl_2/DMSO of compound **6** resulted in crystals that were suitable for single crystal X-ray diffraction analysis (Figure 2).

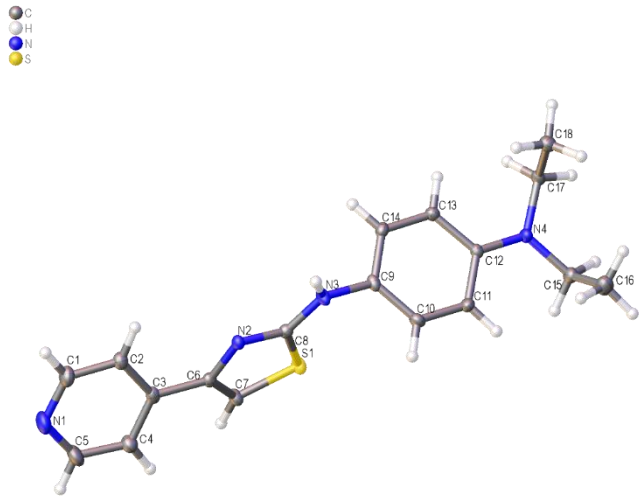

Figure 2. X-ray structure determination of compound **6**.

Then, in order to conduct SAR investigation a first series of analogues was synthesized by varying the diethyl amino group of the *p*-phenyl ring. To this aim, *N*-aryl-2-aminothiazoles **26-29** and **33-39** were synthesized according to the Hantzsch thiazole synthesis, by condensing α-bromoketones with thioureas in refluxing EtOH under microwave irradiation. Thioureas **23-25** were commercially available, while thioureas **15-22** were rapidly obtained in moderate to good yields by treating the appropriate aniline and NH_4SCN in acidic condition. Hydrolysis of the methyl ester of compound **26** gives the corresponding carboxylic acid **30**, while reduction of the nitroaniline **27** provided aminoaniline **31**. Azide **32** was prepared from the corresponding aryl bromide **28** under extremely mild conditions (Scheme 2).[3]

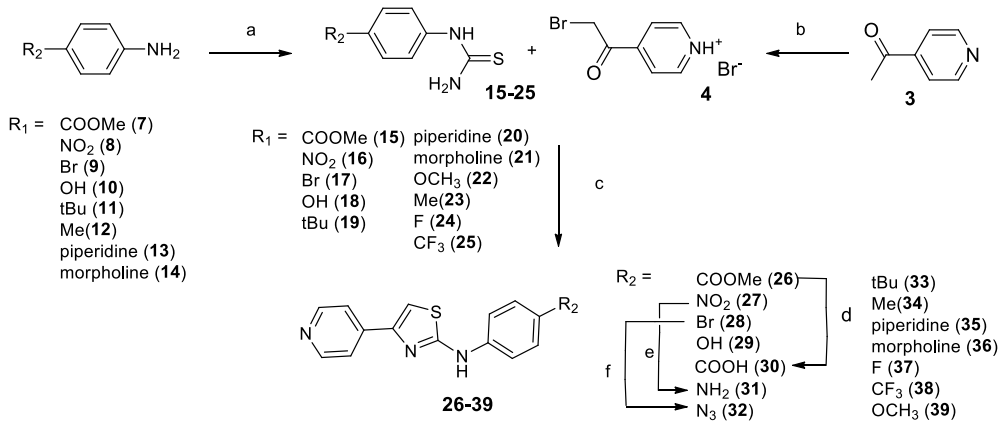

Scheme 2. Synthesis of the first series of analogues.
(**a**) NH_4SCN, aqueous HCl, 100 °C, 16 h, 37-66%; (**b**) HOAc/HBr, Br_2, 15 °C to 75 °C, 1 h, 100%; (**c**) EtOH, microwaves, 110 °C, 30 min, 30-93%; (**d**) 2 M aqueous NaOH, MeOH, reflux, 1h, 98%; (**e**) hydrazine monohydrate, Pd/C, dry MeOH, 60 °C, 16 h, 65%; (**f**) sodium ascorbate, CuI, N^1,N^2-dimethylethane-1,2-diamine, EtOH/H_2O, reflux, 40 min, 55%.

Next, to investigate the role of the pyridine ring a second series of derivatives (**47-53**) was designed and synthesized (Scheme 3). In this case, the thiourea **2** was reacted with the appropriate bromoketone (**40**-**46**) as described above. Bromoketones were commercially available except for compound **40** which was synthesized from the corresponding ketone.

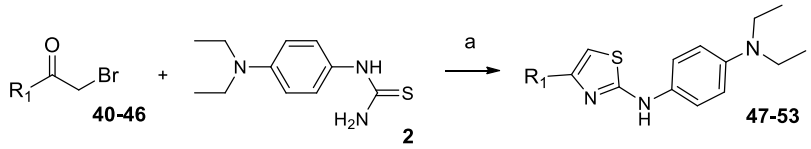

R_1 = 4-chlorophenyl (**40**)
4-fluorophenyl (**41**)
phenyl (**42**)
4-cyanophenyl (**43**)
4-methoxyphenyl (**44**)
pyridin-3-yl (**45**)
pyridin-2-yl (**46**)

R_1 = 4-chlorophenyl (**47**)
4-fluorophenyl (**48**)
phenyl (**49**)
4-cyanophenyl (**50**)
4-methoxyphenyl (**51**)
pyridin-3-yl (**52**)
pyridin-2-yl (**53**)

Scheme 3. Synthesis of the second series of analogues.
(**a**) EtOH, microwaves, 110 °C, 30 min, 26-98%.

Finally, in order to evaluate the SAR of the central 5-membered ring heterocycle, two **415** analogs bearing a central thiadiazole and oxadiazole were synthesized (**56-57**) as highlighted in Scheme 4. In both cases, the common thiosemicarbazide (**55**) intermediate was prepared by treating isothiocyanate **54** with hydrazine in EtOH. Then, condensation of **55** with isonicotinic acid in the presence of the dehydrating agent, $POCl_3$, led to thiadiazole **56**, while the corresponding oxadiazole derivative, **57**, could be accessed by reacting **55** and isonicotinic acid in the presence of coupling agent, EDCI.[4]

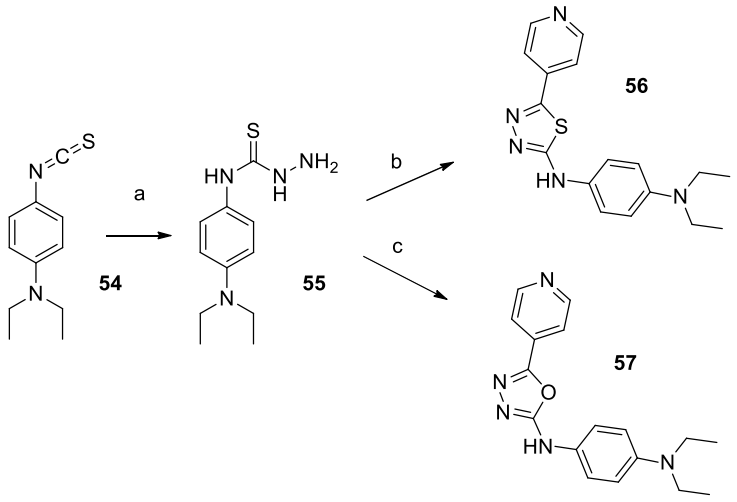

Scheme 4. Synthesis of thiadiazole and oxadiazole compounds.
(**a**) hydrazine hydrate, EtOH, 30 min, rt, 87%; (**b**) isonicotinic acid, $POCl_3$, dry dioxane, 90 °C, 3 h; (**c**) isonicotinic acid, EDCI, TEA, CH_2Cl_2, rt, 12 h.

6.3.2. Biological evaluation

The biological evaluation was carried out thanks to the collaboration with Prof. Esko's laboratory. The ability of the synthesized compounds to enhance HS levels was quantified *in vitro* on wild-type CHO cells using flow cytometry technique. Briefly, the ability of compounds to modulate HS levels was monitored by measuring the increase in fibroblast growth factor 2 (FGF2) binding to HS on the cell surface. FGF2 has been shown to bind HS with strong affinity and therefore represent a surrogate marker for HS expression. Thus, after incubation of CHO cells with test compounds, biotinylated FGF2 was added and bound biotinylated protein was quantified by using fluorescent-tagged streptavidin and flow cytometry. The results are shown in the table below. Compound **53** was not evaluated since it appeared cytotoxic while compound **33** displays a negligible cytotoxicity.

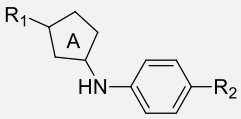

Cpd	R_1	R_2	A	Activity @10 µM VS untreated¥	Activity @10 µM VS **415**
Untreated	-	-	-	1	-
415	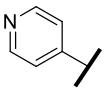	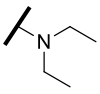	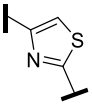	1.635	1
26	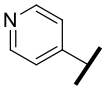	COOMe	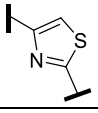	1.364	0.836
27	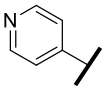	NO_2	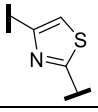	0.948	0.576
28	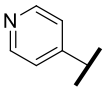	Br	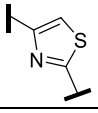	1.104	0.677
29	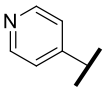	OH	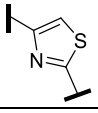	1.257	0.738
30	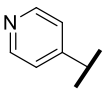	COOH	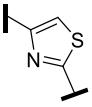	1.195	0.732
31	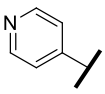	NH_2	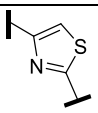	1.345	0.824
32	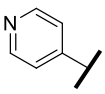	N_3	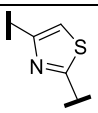	1.120	0.686
33	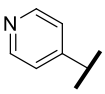	*t*-Bu	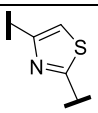	1.859	1.131
34	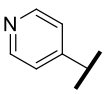	Me	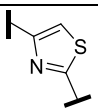	1.077	0.660
35	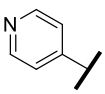	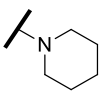	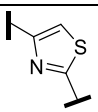	1.728	0.991

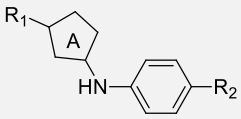

Cpd	R_1	R_2	A	Activity @10 µM VS untreated¥	Activity @10 µM VS **415**
36	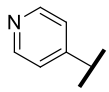	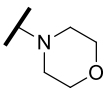	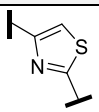	0.990	0.607
37	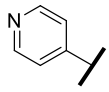	F	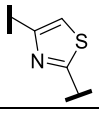	1.130	0.693
38	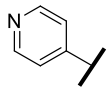	CF_3	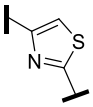	1.114	0.683
39	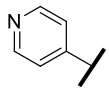	OMe	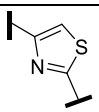	1.276	0.782
47	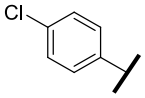	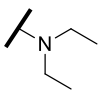	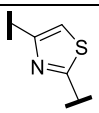	0.976	0.564
48	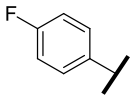	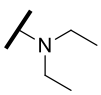	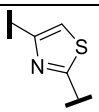	0.992	0.835
49	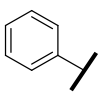	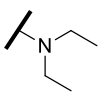	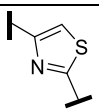	1.248	0.721
50	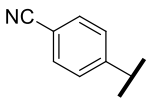	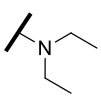	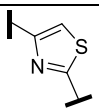	0.953	0.801
51	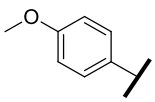	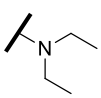	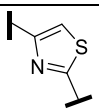	1.103	0.558
52	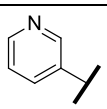	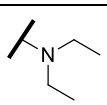	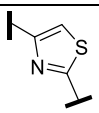	1.539	0.778
53	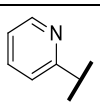	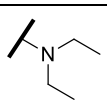	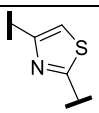	ND*	ND*
56	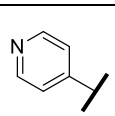	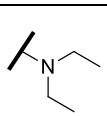	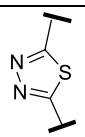	0.986	0.570

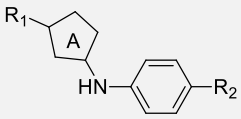

Cpd	R_1	R_2	A	Activity @10 µM VS untreated[¥]	Activity @10 µM VS **415**
57	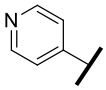	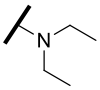	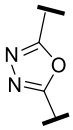	1.061	0.645

Table 1. Values of **415** and its analogues activity.
[¥] The ability of test compounds to enhance HS levels on the surface of CHO cells was determined at 10 µM compound concentration, relative to untreated cells; [#] The ability of test compounds to enhance HS levels on the surface of CHO cells was determined at 10 µM compound concentration, relative to treated with 10µM of **415**; * not determined

The primary outcomes of this preliminary SAR studies can be summarized as follows: (1) compounds bearing substituents at the R_2 position that are relatively large, lipophilic and electron donating appear to be preferred (cf., **35** and **36**, **33** and **34**); (2) replacement of the central thiazole ring with other 5-membered ring heterocycles reduces biological activity in the *in vitro* assay (e.g., see **56** and **57**); (3) with respect to the R1 fragment, a pyridine ring substitutent in the 3- or 4-position appears to be generally preferred (cf., **415, 52, 53**, and **49**) (Figure 2). Finally, although these studies did not result in the identification of compounds with significantly improved potency in the *in vitro* assay relative to **415**, the data presented in Table 1 suggest the existence of a rather discontinuous SAR, small changes in structure often produce significant changes in biological activity. This observation indicates that the interaction of **415** with its target is specific.

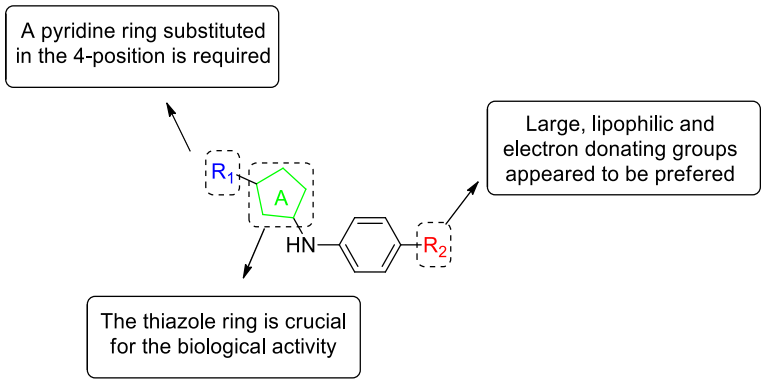

Figure 2. Summary of preliminary SAR.

6.3.3. Physicochemical evaluation

The most active compounds **33** and **35** were selected together with **415** for physicochemical properties evaluation (pKa, $logD_{7.4}$, aqueous solubility). The results, reported in Table 2, showed a good agreement between experimentally obtained pKa, and $logD_{7.4}$ and calculated values.

Cpd	Calculated pKa [a]	Measured $pKa_{n=6}$ [b]	Calculated $logD_{7.4}$ [a]	Measured $logD_{7.4}$ [c]	Thermodynamic solubility [d]	Kinetic solubility [d]
415 (6)	3.94 6.75	5.16 ± 0.06 6.97 ± 0.09	4.39	4.54 ± 0.01	2.60 µM [§]	23.86 µM
33	3.94	5.09 ± 0.08	5.12	ND*	ND*	ND*
35	3.94 6.48	4.90 ± 0.07 5.77 ± 0.04	4.53	3.76 ± 0.01	3.003 µM	55.03 µM

Table 2. [a]Calculated properties using MarvinSketch. [b]pKa values determined by potentiometric titration using Sirius T3 system. [c] Distribution coefficient between *n*-octanol and aqueous buffer (pH 7.4) determined by potentiometric titration using a Sirius T3 titrator according to manufacturer instructions. [d] Solubility value measured using a Sirius T3 titrator according to manufacturer instructions. [§] intrinsic solubility value calculated from General Solubility Equation (GSE) [*] not determinable.

As shown in Table 2, the test compounds appear to be rather lipophilic as revealed by the logD values between 3-5, as well as sparingly soluble with equilibrium solubility values in the low µM range. Although these characteristics suggest that further optimization is likely necessary, compounds of this type appear to be potentially viable starting points for probe/drug development plans.

6.4. Conclusions

In summary, the representative *hit* has been synthesized using both sequential and convergent synthetic procedures. Moreover, a small library of analogues was synthesized and a preliminary SAR study was performed proving that: i) the pyridine ring at the 5-position of the thiazole ring seems to be required; ii) bulky, lipophilic and electron-donating groups at position 4 of the phenyl ring appeared to be

preferred; iii) the substitution of thiazole ring with different heterocycle appeared to be detrimental. Further characterization of selected physicochemical properties, such as pKa, $logD_{7.4}$ and water solubility, of the most promising compounds identified in these studies suggests that compounds of this type may be suitable for *in vivo* testing.

6.5. Experimental section

General Methods. All solvents were reagent grade. All reagents were purchased from Aldrich or Acros and used as received. Thin layer chromatography (TLC) was performed with 0.25 mm E. Merck precoated silica gel plates. Silica gel column chromatography was performed with silica gel 60 (particle size 0.040-0.062 mm) supplied by Silicyte and Sorbent Technologies. TLC spots were detected by viewing under a UV light, or using $KMnO_4$. Chemical shifts were reported relative to the residual solvent's peak. Infrared spectra were recorded on a Nicolet 380 FTIR instrument using the neat thin film technique. High Resolution Mass Spectra (HRMS) were acquired on an Agilent 6230 High Resolution time-of-flight mass spectrometer and reported as m/z for the molecular ion $[M+Na]^+$, $[M+H]^+$, $[M-H]^+$. Proton (^1H) and carbon (^{13}C) NMR spectra were recorded on a Bruker AMX-500 spectrometer. The single crystal X-ray diffraction studies were carried out on a Bruker Kappa APEX-II CCD diffractometer equipped with Mo K_α radiation (λ = 0.71073) at University of California San Diego.

6.5.1. Chemistry

N,N-diethyl-4-isothiocyanatoaniline, (54).

To a stirred solution of commercially available N^1,N^1 -diethylbenzene-1,4-diamine (4.00 g, 24.40 mmol, 1.00 equiv) in H_2O (24.32 mL), CS_2 (5.84 mL, 97.40 mmol, 4.00 equiv) was added dropwise. The solution was stirred at r.t. for 16 h (formation of a yellow precipitate). Then, the reaction was cooled to 0 °C and a solution of 2.25 g of 2,4,6-trichloro-1,3,5-triazine in 18.42 mL of dichloromethane was added

dropwise. After stirring for 50 min, 6 N NaOH was added until pH > 11 and the aqueous layer was extracted with dichloromethane (x1). The organic layer was washed with H_2O (x8), dried over Na_2SO_4, filtered and concentrated. Purification by silica gel column column chromatography (100% hexanes) provided the desired compound (4.57 g, 22.20 mmol, 91%) as a yellow oil. ^{1}H NMR (600 MHz, $CDCl_3$) δ = 7.08 (d, *J* = 9.1 Hz, 2H), 6.55 (d, *J* = 9.1 Hz, 2H), 3.35 (q, *J* = 7.1 Hz, 4H), 1.16 (t, *J* = 7.1 Hz, 6H).^{13}C NMR (151 MHz, $CDCl_3$) δ 146.71, 131.55, 126.89, 117.20, 111.54, 44.45, 12.46. HRMS (ES^+) calculated for $C_{11}H_{15}N_2S$ $[M + H]^+$ 207.0950, found 207.0950.

1-(4-(diethylamino)phenyl)thiourea, (2).

N,*N*-diethyl-4-isothiocyanatoaniline (4.00 g, 19.40 mmol, 1.00 equiv) was solubilized in a 7 N solution of NH_3 in MeOH (4.12 mL) and the mixture was stirred for 1 h at r.t. The mixture was concentrated to give a solid, which was filtered and washed with Et_2O to give the desired compound (2.72 g, 12.19 mmol, 63%) as a white solid without further purification. ^{1}H NMR (600 MHz, $CDCl_3$) δ = 6.80 (br s, 1H), 6.59 (d, *J* = 8.5 Hz, 2H), 6.17 (d, *J* = 8.5 Hz, 2H), 2.89 (q, *J* = 7.1 Hz, 4H), 0.70 (t, J = 7.1 Hz, 6H). ^{13}C NMR (151 MHz, $CDCl_3$) δ 181.97, 147.42, 127.37, 123.34, 112.06, 44.44, 12.42. HRMS (ES^+) calculated for $C_{11}H_{17}N_3SNa$ $[M+ Na]^+$ 246.1035, found 246.1035.

4-(2-bromoacetyl)pyridin-1-ium bromide, (4).

To a stirred solution of 1-(pyridin-4-yl)ethan-1-one (2.00 g, 16.50 mmol, 1.00 equiv) in HBr (48 wt %, 8.12 mL) at 15 °C under N_2, Br_2 (0.851 mL, 16.50 mmol, 1.00 equiv) was added dropwise. The solution was stirred at 40 °C for 1 h, then at 75 °C for 1 h. After cooling to r.t, Et_2O (80.00 mL) was added, and the reaction was stirred at 20 °C for 30 min, during which a white precipitate was formed. Filtration afforded the title compound (4.62 g, 16.5 mmol, 100%) a pale rose solid, which was used in the next step without further purification. ^{1}H NMR (600 MHz, DMSO-d_6) δ = 8.95

(d, *J* = 6.7 Hz, 2H), 8.14 (d, *J* = 6.7 Hz, 2H), 5.04 (s, 2H). ^{13}C NMR (151 MHz, DMSO-d_6) δ = 187.30 162.57, 141.71, 125.08, 93.50

4-(pyridin-4-yl)thiazol-2-amine, (5).

Thiourea (0.56 g, 7.87 mmol, 1.00 equiv), 4-(2-bromoacetyl)pyridin-1-ium bromide (2.21 g, 7.87 mmol, 1.00 equiv) and EtOH (10.80 mL) were added to a microwave vial. The vial was sealed, warmed to 100 °C and stirred under microwave irradiation (Biotage Initiator) for 30 min. After cooling to r.t., the solid was filtered, washed with EtOH and with saturated satd. aq. $NaHCO_3$ and concentrated in vacuo to give the desired compound (1.12 g, 6.32 mmol, 80%) as a pale rose solid without further purification. ^{1}H NMR (600 MHz, DMSO-d_6) δ = 8.54 (d, *J* = 5.9 Hz, 2H), 7.72 (d, *J* = 5.9 Hz, 2H), 7.40 (s, 1H), 7.22 (s, 2H).

N^1,N^1-diethyl-N^4-(4-(pyridin-4-yl)thiazol-2-yl)benzene-1,4-diamine, (6).

Method A: 1-(4-(diethylamino)phenyl)thiourea (0.50 g, 2.24 mmol, 1.00 equiv), 4-(2-bromoacetyl)pyridin-1-ium bromide (0.63 g, 2.24 mmol, 1.00 equiv) and EtOH (2.50 mL) were added to a microwave vial. The vial was sealed, warmed to 100 °C and stirred under microwave irradiation (Biotage Initiator) for 30 min. After cooling to r.t., EtOAc was added and the organic extract was washed with satd. aq. $NaHCO_3$ (x1), with brine (x1), dried over Na_2SO_4, filtered and concentrated in vacuo. Purification by silica gel column chromatography (30% EtOAc in dichloromethane) provided the desired compound as a pale grey solid (0.43 g, 1.33 mmol, 59%). *Method B*: An oven-dried test tube was charged with $Pd(OAc)_2$ (0.8 mg, 1.5 mol%) and tBuBrettPhos (3.6 mg, 3.3 mol %). The vessel was evacuated and backfilled with argon (this sequence was carried out a total of three times). To this vessel was added tBuOH (904 µL) and degassed H_2O (0.3 µL, 6 mol %) via syringe, and the solution was placed in an oil bath at 110 °C for 1.5 min. A second oven-dried test tube equipped with a magnetic stir bar was charged with compound **5** (40 mg, 0.23 mmol, 1 eq), K_2CO_3 (4.4 mg, 0.32 mmol, 1.4 mmol), and 4-bromo-*N*,*N*-diethylaniline (51 mg, 0.23 mmol, 1 eq). The tube was then sealed, evacuated, and backfilled with

argon (this sequence was carried out a total of three times). The hot catalyst solution was then cannulated into the second tube containing the substrates and the second tube was then placed into an oil bath at 110 °C for 3 h. The reaction mixture was then cooled to r.t., diluted with ethyl acetate, and washed once each with water and brine, dried over Mg_2SO_4, filtered, and concentrated in vacuo. Purification by silica gel column chromatography (30% EtOAc in dichloromethane) provided the desired compound as a pale grey solid (43 mg, 0.13 mmol, 58%). X-ray quality crystals were obtained by slow evaporation from a CH_2Cl_2/DMSO solution. M.p. 179-180 °C. ^{1}H NMR (600 MHz, DMSO-d_6) δ = 9.92 (br s, 1H), 8.59 (d, *J* = 6.1 Hz, 2H), 7.82 (d, *J* = 6.1 Hz, 2H), 7.57 (s, 1H), 7.46 (d, *J* = 9.0 Hz, 2H), 6.70 (d, *J* = 9.0 Hz, 2H), 3.30 (q, *J* = 7.0 Hz, 4H), 1.07 (t, *J* = 7.0 Hz, 6H). ^{13}C NMR (151 MHz, DMSO-d_6) δ = 165.03, 150.15, 147.77, 143.49, 141.28, 130.32, 119.95, 119.93, 112.68, 106.13, 43.91, 12.46. HRMS (ES^+) calculated for $C_{18}H_{21}N_4S$ $[M + H]^+$ 325.1481, found 325.1482. IR $\tilde{\nu}$ = 3178.1, 3094.2, 2967.0, 1598.7, 1574.6, 1514.8 cm^{-1}.

Methyl 4-thioureidobenzoate, (15).

To a stirred solution of methyl 4-aminobenzoate (4.00 g, 26.46 mol, 1.00 equiv) in 1 M HCl (28.00 mL) at 100 °C, ammonium thiocyanate (2.01 g, 26.46 mmol, 1.00 equiv) was added, and the solution was stirred at 100 °C for 16 h. After cooling to r.t, the reaction was diluited with H_2O (32.00 mL), and the resulting solution was stirred at 5 °C for 2 h, during which a yellow precipitate was formed. The yellow solid was filtered and dried. Purification by silica gel column chromatography (40-90% EtOAc in hexanes) afforded the title compound (2.03 g, 9.68 mmol, 45%) as a white solid. ^{1}H NMR (600 MHz, DMSO-d_6) δ = 10.01 (br s, 1H), 7.89 (d, *J* = 8.7 Hz, 2H), 7.67 (d, *J* = 8.7 Hz, 2H), 3.82 (s, 3H). ^{13}C NMR (151 MHz, DMSO-d_6) δ = 181.15, 165.85, 143.98, 129.89, 124.28, 121.13, 51.94. HRMS (ES^+) calculated for $C_9H_{11}N_2O_2S$ $[M + H]^+$ 211.0536, found 211.0537.

1-(4-nitrophenyl)thiourea, (16).

To a stirred solution of 4-nitroaniline (1.00 g, 7.20 mmol, 1.00 equiv) in 1 M HCl at 100 °C, ammonium thiocyanate (0.55 g, 7.20 mmol, 1.00 equiv) was added, and the solution was stirred at 100 °C for 16 h. After cooling to r.t, the reaction was diluited with H_2O (8.60 mL), and the resulting solution was stirred at 5 °C for 2 h, during which a yellow precipitate was formed. The yellow solid was filtered and dried. Purification by silica gel column chromatography (50-90% EtOAc in hexanes) afforded the title compound (0.63 g, 3.20 mmol, 55%) as a yellow solid. ^{1}H NMR (600 MHz, DMSO-*d*$_6$) δ = 10.27 (br s, 1H), 8.18 (d, *J* = 9.2 Hz, 2H), 7.85 (d, *J* = 9.2 Hz, 2H); ^{13}C NMR (151 MHz, DMSO-*d*$_6$) δ = 181.41, 146.18, 142.29, 124.59, 120.97. HRMS (ES$^-$) calculated for $C_7H_6N_3O_2S$ [M - H]$^-$ 196.0186, found 196.0186.

1-(4-bromophenyl)thiourea, (17).

To a stirred solution of 4-bromoaniline (2.00 g, 11.60 mmol, 1.00 equiv) in 1 M HCl (14.40 mL) at 100 °C, ammonium thiocyanate (0.89 g, 11.60 mmol, 1.00 equiv) was added, and the resulting solution was stirred at 100 °C for 16 h. After cooling to r.t, the reaction was diluited with H_2O (13.90 mL), and the resulting solution was stirred at 5 °C for 2h, during which a white precipitate was formed. The white solid was filtered and dried. Purification by gel column chromatography (50-90% EtOAc in hexanes) afforded the title compound (0.77 g, 3.33 mmol, 37%) as a white solid. ^{1}H NMR (600 MHz, DMSO-*d*$_6$) δ = 9.75 (br s, 1H), 7.49 (d, *J* = 8.6 Hz, 2H), 7.40 (d, *J* = 8.6 Hz, 2H); ^{13}C NMR (151 MHz, DMSO-*d*$_6$) δ = 181.22, 138.79, 131.54, 125.01, 116.36; HRMS (ES$^+$) calculated for $C_7H_8BrN_2S$ [M + H]$^+$ 230.9586, found 230.9588.

1-(4-hydroxyphenyl)thiourea, (18).

To a stirred solution of 4-aminophenol (1.50 g, 13.70 mmol, 1.00 equiv) in 1 M HCl (10.8 mL) at 100 °C, ammonium thiocyanate (1.05 g, 13.70 mmol, 1.00 equiv) was added, and the resulting solution was stirred at 100 °C for 16 h. After cooling to r.t,

the reaction was diluited with H_2O (12.90 mL), and the resulting solution was stirred at 5 °C for 2h, during which dark brown precipitate was formed. Filtration afforded the title compound (0.79 g, 4.70 mmol, 43%) as a dark brown solid, which was used in the next step without further purification.^{1}H NMR (600 MHz, DMSO-d_6) δ = 9.40 (br s, 1H), 9.37 (br s, 1H), 7.05 (d, *J* = 8.5 Hz, 2H), 6.71 (d, *J* = 8.5 Hz, 2H). ^{13}C NMR (151 MHz, DMSO-d_6) δ =180.27, 155.16, 130.79, 126.11, 115.51. HRMS (ES^+) calculated for $C_7H_9N_2OS$ $[M + H]^+$ 169.0430, found 169.0429.

1-(4-(tert-butyl)phenyl)thiourea, (19).

To a stirred solution of 4-(tert-butyl)aniline (1.50 g, 10.10 mmol, 1.00 equiv), in 1 M HCl (10.80 mL) at 100 °C, ammonium thiocyanate (0.77 g, 10.10 mmol, 1.00 equiv) was added, and the resulting solution was stirred at 100 °C for 16 h. After cooling to r.t, the reaction was diluited with H_2O (12.90 mL), and the resulting solution was stirred at 5 °C for 2h, during which a white precipitate was formed. The white solid was filtered and dried. Purification by silica gel column chromatography (50% EtOAc in hexanes) afforded the title compound **19** (0.80 g, 3.82 mmol, 51%) as white solid.^{1}H NMR (600 MHz, DMSO-d_6) δ = 9.61 (br s, 1H), 7.34 (d, *J* = 8.6 Hz, 2H), 7.28 (d, *J* = 8.6 Hz, 2H), 1.27 (s, 9H); ^{13}C NMR (151 MHz, DMSO-d_6) δ = 180.85, 146.80, 136.44, 125.46, 122.88, 34.15, 31.21. HRMS (ES^+) calculated for $C_{11}H_{17}N_2S$ $[M + H]^+$ 209.1107, found 209.1105.

1-(4-(piperidin-1-yl)phenyl)thiourea, (20).

To a stirred solution of 4-(piperidin-1-yl)aniline (0.26 g, 1.49 mmol, 1.00 equiv), in 1 M HCl (1.88 mL) at 100 °C, ammonium thiocyanate (0.11 g, 1.49 mmol, 1.00 equiv) was added, and the resulting solution was stirred at 100 °C for 16 h. After cooling to r.t, the reaction was diluited with H_2O (12.90 mL), and the resulting solution was stirred at 5 °C for 2h. Basification of the reaction mixture with satd. aq. $NaHCO_3$ (until pH 6) caused precipitation of the title compound, which was filtered and dried. Purification by silica gel column chromatography (66% EtOAc in hexanes) afforded the title compound **20** as a white solid. ^{1}H NMR (600 MHz,

DMSO-d_6) δ = 9.40 (br s, 1H), 7.10 (d, *J* = 7.7 Hz, 2H), 6.88 (d, *J* = 7.7 Hz, 2H), 3.09 (t, *J* = 6 Hz, 4H), 1.63 – 1.57 (m, 4H), 1.54 – 1.48 (m, 2H). ^{13}C NMR (151 MHz, DMSO-d_6) δ = 180.76, 149.19 (2C), 124.96, 116.03, 49.77, 25.29, 23.90. HRMS (ES^+) calculated for $C_{12}H_{18}N_3S$ $[M + H]^+$ 236.1216, found 236.1215.

1-(4-morpholinophenyl)thiourea, (21).

To a stirred solution of 4-morpholinoaniline (0.50 g, 2.81 mmol, 1.00 equiv) in 1 M HCl (3.60 mL) at 100 °C, ammonium thiocyanate (0.21 g, 2.81 mmol, 1.00 equiv) was added, and the resulting solution was stirred at 100 °C for 16 h. After cooling to r.t, the reaction was diluited with H_2O (3.40 mL), and the resulting solution was stirred at 5 °C for 2h. The mixture was basified with satd. aq. $NaHCO_3$ (until pH 6), extracted with EtOAc (x1), dried over sodium sulfate and evaporated to give a violet solid (0.26 g, 1.08 mmol, 45%), which was in the next step without further purification. ^{1}H NMR (600 MHz, DMSO-d_6) δ =9.44 (br s, 1H), 7.21 – 7.10 (m, 2H), 6.90 (d, *J* = 7.5 Hz, 2H), 3.78 – 3.67 (m, 4H), 3.14 – 3.02 (m, 4H). ^{13}C NMR (151 MHz, DMSO-d_6) δ = 180.83, 163.53, 148.49, 124.93, 115.32, 66.13, 48.64. HRMS (ES^-) calculated for $C_{11}H_{14}N_3OS$ $[M - H]^-$ 236.0863, found 236.0862.

1-(4-methoxyphenyl)thiourea, (22).

To a stirred solution of 4-methoxyaniline (1.00 g, 8.12 mmol, 1.00 equiv) in 1 M HCl (7.20 mL) at 100 °C, ammonium thiocyanate (0.62 g, 8.12 mmol, 1.00 equiv) was added, and the resulting solution was stirred at 100 °C for 16 h. After cooling to r.t, the reaction was diluited with H_2O (8.60 mL), and the resulting solution was stirred at 5 °C for 2h, during which a purple precipitate was formed. Filtration afforded the title compound (0.53 g, 2.92 mmol, 47%) as a purple solid, which was used in the next step without further purification. ^{1}H NMR (600 MHz, DMSO-d_6) δ = 9.48 (br s, 1H), 7.21 (d, *J* = 8.5 Hz, 2H), 6.89 (d, *J* = 8.5 Hz, 2H), 3.73 (s, 3H); ^{13}C NMR (151 MHz, DMSO-d_6) δ = 181.47, 156.99, 132.09, 125.99, 114.40, 55.67. HRMS (ES^+) calculated for $C_8H_{11}N_2OS$ $[M + H]^+$ 183.0587, found 183.0587.

Methyl 4-((4-(pyridin-4-yl)thiazol-2-yl)amino)benzoate, (26).

4-thioureidobenzoate (0.074 g, 0.36 mmol, 1.00 equiv), 4-(2-bromoacetyl)pyridin-1-ium bromide (0.100 g, 0.36 mmol, 1.00 equiv) and EtOH (0.49 mL) were added to a microwave vial. The vial was sealed, warmed to 100 °C and stirred under microwave irradiation (Biotage Initiator) for 30 min. After cooling to r.t., the solid was filtered, washed with EtOH and with saturated satd. aq. $NaHCO_3$ and concentrated in vacuo to give the desired compound **26** (0.074 g, 0.24 mmol, 67%) as a yellow solid without further purification. ^{1}H NMR (600 MHz, DMSO-d_6) δ = 10.97 (br s, 1H), 8.78 (d, *J* = 5.6 Hz, 2H), 8.22 (d, *J* = 5.6 Hz, 2H), 8.15 (s, 1H), 7.97 (d, *J* = 8.5 Hz, 2H), 7.88 (d, *J* = 8.5 Hz, 2H), 3.82 (s, 3H). ^{13}C NMR (151 MHz, DMSO-d_6) δ = 166.20, 163.23, 146.88, 146.43, 145.13, 131.05, 122.35, 121.58, 116.70, 113.30, 52.15. HRMS (ES$^+$) calculated for $C_{16}H_{14}N_3O_2S$ $[M + H]^+$ 312.0807, found 312.0802. IR $\tilde{\nu}$ = 2957.3, 2917.8, 2848.4, 1712.5, 1284.4 cm^{-1}.

N-(4-nitrophenyl)-4-(pyridin-4-yl)thiazol-2-amine, (27).

1-(4-nitrophenyl)thiourea (0.100 g, 0.36 mmol, 1.00 equiv), 4-(2-bromoacetyl)pyridin-1-ium bromide (0.070 g, 0.36 mmol, 1.00 equiv), and EtOH (0.49 mL) were added to a microwave vial. The vial was sealed, warmed to 100 °C and stirred under microwave irradiation (Biotage Initiator) for 30 min. After cooling to r.t., the solid was filtered, washed with EtOH and with saturated satd. aq. $NaHCO_3$ and concentrated in vacuo to give the desired compound (0.088 g , 0.29 mmol, 83%) as a yellow solid without further purification. ^{1}H NMR (600 MHz, DMSO-d_6) δ = 8.63 (d, *J* = 5.3 Hz, 2H), 8.23 (d, *J* = 8.7 Hz, 2H), 7.91 (d, *J* = 5.3 Hz, 2H), 7.90 – 7.87 (m, 3H). ^{13}C NMR (151 MHz, DMSO-d_6) δ = 162.11, 149.07, 147.42, 146.52, 141.60, 140.27, 125.46, 120.27, 116.32, 110.81. HRMS (ES$^+$) calculated for $C_{14}H_{11}N_4O_2S$ $[M + H]^+$ 299.0597, found 299.0600. IR $\tilde{\nu}$ = 1539.9, 1327.8 cm^{-1}.

N-(4-bromophenyl)-4-(pyridin-4-yl)thiazol-2-amine, (28).

1-(4-bromophenyl)thiourea (0.49 g, 2.14 mmol, 1.00 equiv), 4-(2-bromoacetyl)pyridin-1-ium bromide (0.60 g, 2.14 mmol, 1.00 equiv), and EtOH (2.93 mL) were added to a microwave vial. The vial was sealed, warmed to 100 °C and stirred under microwave irradiation (Biotage Initiator) for 30 min. After cooling to r.t., the solid was filtered, washed with EtOH and with saturated satd. aq. $NaHCO_3$ and concentrated in vacuo to give the desired compound (0.66 g , 1.99 mmol, 93%) as an orange solid without further purification. ^{1}H NMR (600 MHz, DMSO-d_6) δ= 10.73 (br s, 1H), 8.85 (d, *J* = 5.7 Hz, 2H), 8.34 (d, *J* = 5.7 Hz, 2H), 8.24 (s, 1H), 7.74 (d, *J* = 8.5 Hz, 2H), 7.53 (d, *J* = 8.5 Hz, 2H). ^{13}C NMR (151 MHz, DMSO-d_6) δ = 163.76, 147.20, 146.19, 144.34, 140.26, 132.10, 122.08, 119.39, 114.62, 113.25. HRMS (ES^+) calculated for $C_{14}H_{11}BrN_3S$ $[M + H]^+$ 331.9852, found 331.9851. IR $\tilde{\nu}$ = 2597.3, 2171.8, 1549.5 cm^{-1}

4-((4-(pyridin-4-yl)thiazol-2-yl)amino)phenol, (29).

Methyl 1-(4-hydroxyphenyl)thiourea (0.10 g, 0.59 mmol, 1.00 equiv), 4-(2-bromoacetyl)pyridin-1-ium bromide (0.17 g, 0.59 mmol, 1.00 equiv) and EtOH (0.81 mL) were added to a microwave vial. The vial was sealed, warmed to 100 °C and stirred under microwave irradiation (Biotage Initiator) for 30 min. After cooling to r.t., the solid was filtered, washed with EtOH and with saturated satd. aq. $NaHCO_3$ and concentrated in vacuo to give the desired compound (0.14 g, 0.52 mmol, 88%) as a brown solid without further purification. ^{1}H NMR (600 MHz, DMSO-d_6) δ = 10.03 (br s, 1H), 9.21 (br s, 1H), 8.59 (d, *J* = 5.2 Hz, 2H), 7.82 (d, *J* = 5.2 Hz, 2H), 7.60 (s, 1H), 7.48 (d, *J* = 8.6 Hz, 2H), 6.76 (d, *J* = 8.6 Hz, 2H). ^{13}C NMR (151 MHz, DMSO-d_6) δ = 164.92, 152.87, 150.45, 148.00, 141.51, 133.34, 120.24, 119.71, 115.86, 106.80. HRMS (ES^+) calculated for $C_{14}H_{12}N_3OS$ $[M + H]^+$ 270.0696, found 270.0697. IR $\tilde{\nu}$ = 3444.2, 1579.4, 1514.8, 1411.6, 1235.2 cm^{-1}.

4-((4-(pyridin-4-yl)thiazol-2-yl)amino)benzoic acid, (30).

To a suspension of compound **26** (0.050 g, 0.16 mmol, 1.00 equiv) in MeOH (0.80 mL), 2 M aq. NaOH (0.40 mL) was added. The reaction was stirred at reflux for 1 h. After cooling to r.t., the reaction mixture was concentrated in vacuo. 1 M aq. HCl was added until pH = 4 and resulting the precipitate was filtered and washed with H_2O and concentrated in vacuo to give the desired compound (0.048 g, 0.16 mmol, 98%) as a yellow solid without further purification. ^{1}H NMR (600 MHz, DMSO-d_6) δ = 11.32 (br s, 1H), 8.90 (d, *J* = 6.3 Hz, 2H), 8.50 (d, *J* = 6.3 Hz, 2H), 8.43 (s, 1H), 7.95 (d, *J* = 8.7 Hz, 2H), 7.90 (d, *J* = 8.7 Hz, 2H). ^{13}C NMR (151 MHz, DMSO-d_6) δ = 167.43, 163.72, 148.89, 145.86, 144.86, 142.54, 131.24, 123.82, 122.84, 116.94, 116.85. HRMS (ES$^+$) calculated for $C_{15}H_{12}N_3O_2S$ $[M + H]^+$ 298.0645, found 298.0645. IR $\tilde{\nu}$ =3370.0, 3074.9, 2927.4, 1603.5, 1544.7 cm^{-1}.

N^1-(4-(pyridin-4-yl)thiazol-2-yl)benzene-1,4-diamine, (31).

To a stirred solution of compound **27** (0.23 g, 0.75 mmol, 1.00 equiv) in degassed MeOH (0.80 mL) under N_2, Pd/C (10 wt % (wet), 0.040 g, 0.05 equiv) and hydrazine monohydrate (0.37 mL, 7.54 mmol, 10.00 equiv) were added. The resulting mixture was stirred at 60 °C for 16 hours. After cooling to r.t., the reaction mixture was filtered through a pad of Celite, washed with MeOH. Evaporation of the solvent in vacuo provided the title compound **31** (0.13 g, 0.48 mmol, 65%) as a beige solid without further purification. ^{1}H NMR (600 MHz, DMSO-d_6) δ = 9.80 (br s, 1H), 8.58 (d, *J* = 5.3 Hz, 2H), 7.80 (d, *J* = 5.3 Hz, 2H), 7.54 (s, 1H), 7.28 (d, *J* = 8.2 Hz, 2H), 6.58 (d, *J* = 8.2 Hz, 2H), 4.89 (br s, 2H). ^{13}C NMR (151 MHz, DMSO-d_6) δ = 165.62, 150.13, 147.76, 144.44, 141.30, 130.54, 120.31, 119.91, 114.39, 105.97. HRMS (ES$^+$) calculated for $C_{14}H_{13}N_4S$ $[M + H]^+$ 269.0855, found 269.0855. IR $\tilde{\nu}$ = 2927.4, 1736.6, 1598.7, 1514.8 cm^{-1}.

N-(4-azidophenyl)-4-(pyridin-4-yl)thiazol-2-amine, (32).

Compound **28** (0.100 g, 0.30 mmol, 1.00 equiv), sodium ascorbate (2.98 mg, 0.015 mmol, 0.05 equiv), copper iodide (5.73 mg, 0.030 mmol, 0.10 equiv), N^1,N^2-dimethylethane-1,2-diamine (5.00 µL, 0.045 mmol, 0.15 equiv) and EtOH/H_2O (7:3, 0.60 mL) were added in order in a round-bottom flask. The mixture was degassed and then introduced under a N_2 atmosphere. The reaction was stirred at reflux for 40 min. Then, EtOAc was added and the organic layer was washed with H_2O (x2), brine (x1), dried over $MgSO_4$, filtered and evaporated in vacuo to give the desired compound (49.00 mg, 0.17 mmol, 55%) as a beige solid without further purification. ^{1}H NMR (600 MHz, DMSO-d_6) δ = 10.54 (br s, 1H), 8.67 – 8.60 (m, 2H), 7.87 (d, *J* = 5.3 Hz, 2H), 7.78 (s, 1H), 7.73 (d, *J* = 8.9 Hz, 2H), 7.53 (d, *J* = 8.8 Hz, 2H). ^{13}C NMR (151 MHz, DMSO-d_6) δ = 163.5, 150.7, 148.2, 141.3, 140.7, 132.2 (2C), 119.3, 113.0, 108.5. HRMS (ES$^+$) calculated for $C_{14}H_{11}N_6S$ $[M + H]^+$ 295.2760, found 295.0766. IR $\tilde{\nu}$ =2922.6, 2853.2, 1706.7, 1603.5 cm^{-1}.

N-(4-(tert-butyl)phenyl)-4-(pyridin-4-yl)thiazol-2-amine, (33).

1-(4-(tert-butyl)phenyl)thiourea (0.11 g, 0.53 mmol, 1.00 equiv), 4-(2-bromoacetyl)pyridin-1-ium bromide (0.15 g, 0.53 mmol, 1.00 equiv) and EtOH (0.80 mL) were added to a microwave vial. The vial was sealed, warmed to 100 °C and stirred under microwave irradiation (Biotage Initiator) for 30 min. After cooling to r.t., the solid was filtered, washed with EtOH and with saturated satd. aq. $NaHCO_3$ and concentrated in vacuo to give the desired compound (0.85 g, 0.27 mmol, 51%) as a beige solid without further purification. ^{1}H NMR (600 MHz, DMSO-d_6) δ = 10.31 (br s, 1H), 8.61 (d, *J* = 5.6 Hz, 2H), 7.86 (d, *J* = 5.6 Hz, 2H), 7.69 (s, 1H), 7.64 (d, *J* = 8.5 Hz, 2H), 7.38 (d, *J* = 8.5 Hz, 2H), 1.28 (s, 9H). ^{13}C NMR (151 MHz, DMSO-d_6) δ = 163.64, 150.20, 147.70, 143.82, 141.11, 138.53, 125.71, 119.96, 116.83, 107.24, 33.99, 31.32. HRMS (ES$^+$) calculated for $C_{18}H_{20}N_3S$ $[M + H]^+$ 310.1372, found 310.1373. IR $\tilde{\nu}$ = 3035.4, 2962.1, 1063.5, 1514.8 cm^{-1}.

4-(pyridin-4-yl)-N-(p-tolyl)thiazol-2-amine, (34).

Commercially available 1-(p-tolyl)thiourea (0.059 g, 0.36 mmol, 1.00 equiv), 4-(2-bromoacetyl)pyridin-1-ium bromide (0.100 g, 0.36 mmol, 1.00 equiv) and EtOH (0.50 mL) were added to a microwave vial. The vial was sealed, warmed to 100 °C and stirred under microwave irradiation (Biotage Initiator) for 30 min. After cooling to r.t., the solid was filtered, washed with EtOH and with saturated satd. aq. $NaHCO_3$ and concentrated in vacuo to give the desired compound (0.077 g, 0.29 mmol, 81%) as an orange solid without further purification. ^{1}H NMR (600 MHz, DMSO- d_6) δ = 10.30 (br s, 1H), 8.64 (d, J = 5.7 Hz, 2H), 7.91 (d, J = 5.7 Hz, 2H), 7.75 (s, 1H), 7.60 (d, J = 8.3 Hz, 2H), 7.17 (d, J = 8.3 Hz, 2H), 2.27 (s, 3H). ^{13}C NMR (151 MHz, DMSO- d_6) δ = 164.19, 149.73, 147.86, 142.37, 138.97, 130.86, 129.90, 120.61, 117.60, 108.54, 20.85. HRMS (ES$^+$) calculated for $C_{15}H_{14}N_3S$ $[M + H]^+$ 268.0903, found 268.0905.IR $\tilde{\nu}$ = 3198.4, 2971.8, 1731.8, 1598.7, 1549.5, 1416.5 cm^{-1}.

N-(4-(piperidin-1-yl)phenyl)-4-(pyridin-4-yl)thiazol-2-amine, (35).

1-(4-(piperidin-1-yl)phenyl)thiourea (20.00 mg, 0.085 mmol, 1.00 equiv), 4-(2-bromoacetyl)pyridin-1-ium bromide (24.00 mg, 0.085 mmol, 1.00 equiv) and EtOH (0.20 mL) were added to a microwave vial. The vial was sealed, warmed to 100 °C and stirred under microwave irradiation (Biotage Initiator) for 30 min. After cooling to r.t., the solid was filtered, washed with EtOH and with saturated satd. aq. $NaHCO_3$ and concentrated in vacuo to give the desired compound (12.00 mg, 0.036 mmol, 42%) as a pink solid without further purification. ^{1}H NMR (600 MHz, DMSO-d_6) δ = 10.09 (br s, 1H), 8.60 (d, J = 4.5 Hz, 2H), 7.83 (d, J = 4.5 Hz, 2H), 7.62 (s, 1H), 7.53 (d, J = 8.5 Hz, 2H), 6.95 (d, J = 8.5 Hz, 2H), 3.05 (t, J = 5.6 Hz, 4H), 1.62 (p, J = 5.6 Hz, 4H), 1.51 (p, J = 5.6 Hz, 2H). ^{13}C NMR (151 MHz, DMSO- d_6) δ = 164.30, 150.16, 147.71, 147.19, 141.20, 133.20, 119.94, 118.63, 116.96, 106.60, 50.42, 25.45, 23.91. HRMS (ES$^+$) calculated for $C_{19}H_{21}N_4S$ $[M + H]^+$ 337.1481, found 337.1482. IR $\tilde{\nu}$ = 2932.2, 1731.8, 1598.7, 1510.0, 1229.4 cm^{-1}.

N-(4-morpholinophenyl)-4-(pyridin-4-yl)thiazol-2-amine, (36).

1-(4-morpholinophenyl)thiourea (84.50 mg, 0.36 mmol, 1.00 equiv), 4-(2-bromoacetyl)pyridin-1-ium bromide (100.00 mg, 0.36 mmol, 1.00 equiv) and EtOH (0.50 mL) were added to a microwave vial. The vial was sealed, warmed to 100 °C and stirred under microwave irradiation (Biotage Initiator) for 30 min. After cooling to r.t., the solid was filtered, washed with EtOH and with saturated satd. aq. $NaHCO_3$ and concentrated in vacuo to give the desired compound (36.00 mg, 0.11 mmol, 30%) as a pink solid without further purification. ^{1}H NMR (600 MHz, DMSO-d_6) δ = 10.13 (br s, 1H), 8.60 (d, *J* = 5.3 Hz, 2H), 7.83 (d, *J* = 5.3 Hz, 2H), 7.70-7.47 (m, 3H), 6.97 (d, *J* = 8.2 Hz, 2H), 3.91 – 3.56 (m, 4H), 3.18 – 2.88 (m, 4H). ^{13}C NMR (151 MHz, DMSO-d_6) δ = 164.59, 150.57, 148.11, 146.72, 141.59, 134.13, 120.34, 118.96, 116.53, 107.12, 66.60, 49.60. HRMS (ES^+) calculated for $C_{18}H_{19}N_4OS$ $[M + H]^+$ 339.1274, found 339.1275. IR $\tilde{\nu}$ = 2967.0, 1736.6, 1598.7, 1510.0, 1235.2 cm^{-1}.

N-(4-fluorophenyl)-4-(pyridin-4-yl)thiazol-2-amine, (37).

Commercially available 1-(4-fluorophenyl)thiourea (0.10 g, 0.59 mmol, 1.00 equiv), 4-(2-bromoacetyl)pyridin-1-ium bromide (0.17 g, 0.59 mmol, 1.00 equiv) and EtOH (0.81 mL) were added to a microwave vial. The vial was sealed, warmed to 100 °C and stirred under microwave irradiation (Biotage Initiator) for 30 min. After cooling to r.t., the solid was filtered, washed with EtOH and with saturated satd. aq. $NaHCO_3$ and concentrated in vacuo to give the desired compound (0.14 g, 0.52 mmol, 88%) as a brown solid without further purification.^{1}H NMR (600 MHz, DMSO-d_6) δ = 10.61 (br s, 1H), 8.85 (d, *J* = 5.9 Hz, 2H), 8.33 (d, *J* = 5.9 Hz, 2H), 8.21 (s, 1H), 7.78 (dd, *J* = 8.8, 4.7 Hz, 2H), 7.26 – 7.15 (m, 2H). ^{13}C NMR (151 MHz, DMSO-d_6) δ = 164.16, 157.42 (d, *J* = 238.2 Hz), 147.51, 146.03, 144.13, 137.50, 122.12 (d, *J* = 22.1 Hz), 119.02, 115.94 (d, *J* = 5.3 Hz). HRMS (ES^+) calculated for $C_{14}H_{11}FN_3S$ $[M + H]^+$ 272.0652, found 272.0654. IR $\tilde{\nu}$ = 3000.7, 2967.0, 1736.6, 1549.5, 1505.2, 1214.9 cm^{-1}.

4-(pyridin-4-yl)-N-(4-(trifluoromethyl)phenyl)thiazol-2-amine, (38).

Commercially available 1-(4-(trifluoromethyl)phenyl)thiourea (78.40 mg, 0.36 mmol, 1,00 equiv), 4-(2-bromoacetyl)pyridin-1-ium bromide (100.00 mg, 0.36 mmol, 1.00 equiv) and EtOH (3.00 mL) were added to a microwave vial. The vial was sealed, warmed to 100 °C and stirred under microwave irradiation (Biotage Initiator) for 30 min. After cooling to r.t., the solid was filtered, washed with EtOH and with saturated satd. aq. $NaHCO_3$ and concentrated in vacuo to give the desired compound (65.00 mg, 0.20 mmol, 57%) as a yellow solid without further purification. ^{1}H NMR (600 MHz, DMSO-d_6) δ = 10.84 (br s, 1H), 8.64 (d, *J* = 8.6 Hz, 2H), 8.07 – 7.80 (m, 5H), 7.72 (d, *J* = 8.6 Hz, 2H). ^{13}C NMR (151 MHz, DMSO-d_6) δ = 163.07, 150.49, 148.05, 144.48, 141.18, 126.71, 125.54 (d, J = 265.5 Hz), 121.04 (d, *J* = 32.2 Hz), 120.32, 116.97, 109.15. HRMS (ES$^+$) calculated for $C_{15}H_{11}F_3N_3S$ $[M + H]^+$ 322.0620, found 322.0622. IR $\tilde{\nu}$ = 2932.2, 1736.6, 1603.5, 1535.1 cm^{-1}.

N-(4-methoxyphenyl)-4-(pyridin-4-yl)thiazol-2-amine, (39).

1-(4-methoxyphenyl)thiourea (0.060 g, 0.36 mmol, 1.00 equiv), 4-(2-bromoacetyl)pyridin-1-ium bromide (0.100 g, 0.36 mmol, 1.00 equiv) and EtOH (0.49 mL) were added to a microwave vial. The vial was sealed, warmed to 100 °C and stirred under microwave irradiation (Biotage Initiator) for 30 min. After cooling to r.t., the solid was filtered, washed with EtOH and with saturated satd. aq. $NaHCO_3$ and concentrated in vacuo to give the desired compound (0.050 g, 0.19 mmol, 54%) as a brown solid without further purification.^{1}H NMR (600 MHz, DMSO-d_6) δ = 10.29 (br s, 1H), 8.74 (d, *J* = 6.0 Hz, 2H), 8.13 (d, *J* = 6.0 Hz, 2H), 7.95 (s, 1H), 7.65 (d, *J* = 8.5 Hz, 2H), 6.96 (d, *J* = 8.5 Hz, 2H), 3.74 (s, 3H). ^{13}C NMR (151 MHz, DMSO-d_6) δ = 164.56, 154.65, 146.87, 146.72, 145.03, 134.58, 121.29, 119.20, 114.59, 111.03, 55.52. HRMS (ES$^+$) calculated for $C_{15}H_{14}N_3OS$ $[M + H]^+$ 284.0852, found 284.0853. IR $\tilde{\nu}$ = 3266.8, 2946.7, 1593.9, 1229.4 cm^{-1}.

2-bromo-1-(4-chlorophenyl)ethanone, (40).

To a stirred solution of 1-(4-chlorophenyl)ethan-1-one (0.754 g, 4.88 mmol, 1.00 equiv) in EtOAc (70.00 mL), $CuBr_2$ was added (1.31 g, 5.85 mmol, 1.20 equiv). The solution was stirred at reflux for 18 h. After cooling to r.t, the mixture was filtered. The filtrate was washed with satd. aq. $Na_2S_2O_3$, dried over Na_2SO_4, filtrate and concentrated in vacuo. Purification by silica gel column chromatography (100% hexanes) afford the desired compound (0.323 g, 1.38 mmol, 28%) as a white solid. ^{1}H NMR (600 MHz, $CDCl_3$) δ = 7.94 (d, *J* = 8.6 Hz, 2H), 7.48 (d, *J* = 8.6 Hz, 2H), 4.41 (s, 2H). ^{1}H NMR (600 MHz, $CDCl_3$) δ = 7.94 (d, *J* = 8.6 Hz, 2H), 7.48 (d, *J* = 8.6 Hz, 2H), 4.41 (s, 2H).

N^1-(4-(4-chlorophenyl)thiazol-2-yl)- N^4, N^4-diethylbenzene-1,4-diamine, (47).

1-(4-(diethylamino)phenyl)thiourea (0.106 g, 0.48 mmol, 1.00 equiv), 2-bromo-1-(4-chlorophenyl)ethan-1-one (0.111 g, 0.48 mmol, 1.00 equiv) and EtOH (0.50 mL) were added to a microwave vial. The vial was sealed, warmed to 100 °C and stirred under microwave irradiation (Biotage Initiator) for 30 min. After cooling to r.t., EtOAc was added and the organic extract was washed with satd. aq. $NaHCO_3$ (x1), with brine (x1), dried over Na_2SO_4, filtered and concentrated in vacuo to afford the desired compound (0.113 mg, 0.32 mmol, 66%) as a white solid.^{1}H NMR (600 MHz, DMSO-d_6) δ = 9.84 (br s, 1H), 7.90 (d, *J* = 8.7 Hz, 2H), 7.49 – 7.42 (m, 4H), 7.26 (s, 1H), 6.69 (d, *J* = 8.7 Hz, 2H), 3.29 (q, *J* = 7.0 Hz, 4H), 1.07 (t, *J* = 7.0 Hz, 6H). ^{13}C NMR (151 MHz, DMSO-d_6) δ = 164.78, 148.87, 143.39, 133.63, 131.81, 130.52, 128.63, 127.35, 119.82, 112.74, 102.37, 43.95, 9.52, 12.49. HRMS (ES^+) calculated for $C_{19}H_{21}ClN_3S$ $[M + H]^+$ 358.1139, found 358.1137. IR $\tilde{\nu}$ = 3187.8, 2971.8, 1741.4, 1613.2, 1559.2, 1514.8 cm^{-1}.

N^1,N^1-diethyl- N^4-(4-(4-fluorophenyl)thiazol-2-yl)benzene-1,4-diamine, (48).

1-(4-(diethylamino)phenyl)thiourea (0.103 g, 0.46 mmol, 1.00 equiv), commercially available 2-bromo-1-(4-fluorophenyl)ethan-1-one (0.100 mg, 0.46 mmol, 1.00

equiv) and EtOH (0.50 mL) were added to a microwave vial. The vial was sealed, warmed to 100 °C and stirred under microwave irradiation (Biotage Initiator) for 30 min. After cooling to r.t., EtOAc was added and the organic extract was washed with satd. aq. $NaHCO_3$ (x1), with brine (x1), dried over Na_2SO_4, filtered and concentrated to afford the desired compound (0.060 mg, 0.17 mmol, 38%) as a grey solid without further purification. ^{1}H NMR (600 MHz, CD_3OD) δ = 7.87 (dd, J_S = 5.8, 2.2 Hz, 2H), 7.42 (d, J = 8.8 Hz, 2H), 7.13 – 7.09 (m, 2H), 6.87 (s, 1H), 6.80 (d, J = 8.7 Hz, 2H), 3.34 (q, J = 7.5 Hz, 4H), 1.14 (t, J = 7.1 Hz, 6H). ^{13}C NMR (151 MHz, DMSO-d_6) δ = 163.54 (d, J = 353.4 Hz), 160.76, 149.05, 143.33, 131.40, 130.59, 127.60 (d, J = 8.1 Hz), 119.76, 115.43 (d, J = 21.4 Hz), 112.73, 101.24, 43.94, 12.47. HRMS (ES^+) calculated for $C_{19}H_{21}FN_3S$ $[M + H]^+$ 342.1435, found 342.1433. IR $\tilde{\nu}$ = 3198.4, 2976.6, 1741.4, 1608.3, 1520.6, 1210.1 cm^{-1}.

N^1,N^1-diethyl- N^4-(4-phenylthiazol-2-yl)benzene-1,4-diamine, (49).

1-(4-(diethylamino)phenyl)thiourea (0.141 g, 0.63 mmol, 1.00 equiv), commercially available 2-bromo-1-phenylethan-1-one (0.126 g, 0.63 mmol, 1.00 equiv) and EtOH (0.6 mL) were added to a microwave vial. The vial was sealed, warmed to 100 °C and stirred under microwave irradiation (Biotage Initiator) for 30 min. After cooling to r.t., EtOAc was added and the organic extract was washed with satd. aq. $NaHCO_3$ (x1), with brine (x1), dried over Na_2SO_4, filtered and concentrated in vacuo to afford the desired compound (0.077 mg, 0.24 mmol, 38%) as a white solid. ^{1}H NMR (600 MHz, DMSO-d_6) δ = 9.82 (br s, 1H), 7.89 (d, J = 8.3 Hz, 2H), 7.47 (d, J = 8.3 Hz, 2H), 7.41 (t, J = 7.3 Hz, 2H), 7.29 (t, J = 7.3 Hz, 1H), 7.18 (s, 1H), 6.69 (d, J = 7.3 Hz, 2H), 3.28 (q, J = 6.8 Hz, 4H), 1.06 (d, J = 7.3 Hz, 6H). ^{13}C NMR (151 MHz, DMSO-d_6) δ = 165.00, 150.50, 143.71, 135.17, 131.05, 129.00, 127.85, 126.04, 120.13, 113.16, 101.90, 44.34, 12.87. HRMS (ES^+) calculated for $C_{19}H_{22}N_3S$ $[M + H]^+$ 324.1529, found 324.1528. IR $\tilde{\nu}$ = 3173.3, 2971.8, 2932.2, 1741.4, 1510.0, 1264.1 cm^{-1}.

4-(2-((4-(diethylamino)phenyl)amino)thiazol-4-yl)benzonitrile, (50).

1-(4-(diethylamino)phenyl)thiourea (0.100 g, 0.45 mmol, 1.00 equiv), commercially available 4-(2-bromoacetyl)benzonitrile (0.100 g, 0.45 mmol, 1.00 equiv) and EtOH (0.50 mL) were added to a microwave vial. The vial was sealed, warmed to 100 °C and stirred under microwave irradiation (Biotage Initiator) for 30 min. After cooling to r.t., EtOAc was added and the organic extract was washed with satd. aq. $NaHCO_3$ (x1), with brine (x1), dried over Na_2SO_4, filtered and concentrated to afford the desired compound (0.154 mg, 0.44 mmol, 98%) as a pale orange solid. ^{1}H NMR (600 MHz, DMSO-d_6) δ = 8.13 (d, *J* = 8.1 Hz, 2H), 8.01 (d, *J* = 8.5 Hz, 2H), 7.90 (d, *J* = 8.1 Hz, 2H), 7.83 (d, *J* = 8.5 Hz, 2H), 7.75 (s, 1H), 3.58 – 3.44 (m, 4H), 1.05 (t, *J* = 7.0 Hz, 6H). ^{13}C NMR (151 MHz, DMSO-d_6) δ 162.85, 148.17, 141.92, 138.47, 132.82, 130.30, 126.33, 123.75, 119.10, 117.48, 109.62, 107.96, 52.37, 9.96. HRMS (ES^+) calculated for $C_{20}H_{21}N_4S$ $[M + H]^+$ 349.1481, found 349.1484. IR $\tilde{\nu}$ = 3050.8, 2632.4, 2218.7, 1741.4, 1608.3, 1510.0 cm^{-1}.

N^1,N^1-diethyl- N^4-(4-(4-methoxyphenyl)thiazol-2-yl)benzene-1,4-diamine, (51).

1-(4-(diethylamino)phenyl)thiourea (0.146 g, 0.66 mmol, 1.00 equiv), commercially available 2-bromo-1-(4-methoxyphenyl)ethan-1-one (0.150 g, 0.66 mmol, 1.00 equiv) and EtOH (0.80 mL) were added to a microwave vial. The vial was sealed, warmed to 100 °C and stirred under microwave irradiation (Biotage Initiator) for 30 min. After cooling to r.t., the solid was filtered, washed with EtOH and with H_2O and concentrated in vacuo to give the desired compound (0.060 g, 0.17 mmol, 26%) as a white solid without further purification. ^{1}H NMR (600 MHz, CD_3OD) δ = 7.78 (d, *J* = 8.6 Hz, 2H), 7.48 – 7.40 (m, 2H), 6.94 (d, *J* = 8.6 Hz, 2H), 6.88 – 6.80 (m, 2H), 6.75 (s, 1H), 3.82 (s, 3H), 3.37 – 3.33 (m, 4H), 1.14 (t, J = 7.0 Hz, 6H).^{13}C NMR (151 MHz, DMSO-d_6) δ = 164.51, 158.71, 149.92, 143.26, 130.74, 127.69, 126.97, 119.69, 113.94, 112.78, 99.34, 55.15, 12.48. HRMS (ES^+) calculated for $C_{20}H_{24}N_3OS$ $[M + H]^+$ 354.1635, found 354.1633. IR $\tilde{\nu}$ = 3173.3, 2971.8, 2932.2, 1736.6, 1608.3, 1514.8, 1249.7 cm^{-1}.

N^1,N^1-diethyl- N^4-(4-(pyridin-2-yl)thiazol-2-yl)benzene-1,4-diamine, (52).

1-(4-(diethylamino)phenyl)thiourea (0.119 g, 0.53 mmol, 1.00 equiv), commercially available 2-bromo-1-(pyridin-2-yl)ethan-1-one hydrobromide (0.150 g, 0.53 mmol, 1.00 equiv) and EtOH (0.80 mL) were added to a microwave vial. The vial was sealed, warmed to 100 °C and stirred under microwave irradiation (Biotage Initiator) for 30 min. After cooling to r.t., Et_2O was added and the resulting precipitate was filtered, washed with Et_2O and with satd. aq. $NaHCO_3$ and concentrated in vacuo to give the desired compound (0.130 g, 0.40 mmol, 75%) as a brown solid without further purification. ^{1}H NMR (600 MHz, CD_3OD) δ = 8.55 (d, J = 4.3 Hz, 1H), 8.13 (d, J = 7.8 Hz, 2H), 8.00 – 7.89 (m, 3H), 7.53 (s, 1H), 7.48 – 7.39 (m, 1H), 7.36 (d, J = 4.3 Hz, 1H), 3.71 – 3.55 (m, 4H), 1.17 (t, J = 7.1 Hz, 6H). ^{13}C NMR (151 MHz, DMSO-d_6) δ = 177.07, 162.93, 151.30, 149.46, 148.78, 138.23, 129.45, 123.62, 123.04, 120.82, 117.69, 52.64, 10.15. HRMS (ES^+) calculated for $C_{18}H_{21}N_4S$ $[M + H]^+$ 325.1481, found 325.1482. IR $\tilde{\nu}$ = 3242.7, 3045.1, 2971.8, 1593.9, 1514.8, 1338.4 cm^{-1}.

N^1,N^1-diethyl-N^4-(4-(pyridin-3-yl)thiazol-2-yl)benzene-1,4-diamine, (53).

1-(4-(diethylamino)phenyl)thiourea (79.50 mg, 0.36 mmol, 1.00 equiv), commercially available 2-bromo-1-(pyridin-3-yl)ethan-1-one hydrobromide (100.00 mg, 0.36 mmol, 1.00 equiv) and EtOH (0.50 mL) were added to a microwave vial. The vial was sealed, warmed to 100 °C and stirred under microwave irradiation (Biotage Initiator) for 30 min. After cooling to r.t., satd. aq. $NaHCO_3$ was added and the mixture was extracted with EtOAc (x2). The combined organic extracts were washed with brine (x1), dried over Na_2SO_4, filtered and concentrated to give the desired compound (40.00 mg, 0.12 mmol, 35%) as a light brown solid without further purification. ^{1}H NMR (600 MHz, DMSO-d_6) δ = 9.87 (br s, 1H), 9.10 (s, 1H), 8.49 (d, *J* = 4.6 Hz, 1H), 8.22 (d, *J* = 8.0 Hz, 1H), 7.48 – 7.42 (m, 3H), 7.36 (s, 1H), 6.70 (d, *J* = 8.9 Hz, 2H), 3.30 (q, *J* = 6.8 Hz, 4H), 1.07 (t, *J* = 7.0 Hz, 6H). ^{13}C NMR (151 MHz, DMSO-d_6) δ = 165.16, 148.29, 147.22, 146.97, 143.44, 132.73, 130.41,

130.35, 123.74, 119.93, 112.70, 103.11, 43.92, 12.46. HRMS (ES^+) calculated for $C_{18}H_{21}N_4S$ $[M + H]^+$ 325.1481, found 325.1484. IR $\tilde{\nu}$ = 2967.0, 2922.6, 1736.6, 1549.5, 1514.8, 1264.1 cm^{-1}.

N-(4-(diethylamino)phenyl)hydrazinecarbothioamide, (55).

To a stirred solution of compound **54** (0.30 g, 1.45 mmol, 1.00 equiv) in EtOH (1.90 mL), hydrazine hydrate (0.09 mL, 1.45 mmol, 1.00 equiv) was added. The solution became warm (a precipitate formed during the addition). The solution was stirred for 30 min at r.t. Then, the precipitate was filtered, washed EtOH and concentrated in vacuo to give the desired compound (0.30 g, 1.27 mmol, 87%) as a white solid without further purification. ^{1}H NMR (600 MHz, DMSO-d_6) δ = 9.32 (brs, 1H), 8.84 (br s, 1H), 7.23 (d, J = 8.7 Hz, 2H), 6.58 (d, J = 8.7 Hz, 2H), 4.67 (br s, 2H), 3.30 (q, J = 7.0 Hz, 4H), 1.07 (t, J = 7.0 Hz, 6H). ^{13}C NMR (151 MHz, DMSO-d_6) δ = 172.81, 145.11, 127.48, 126.06, 111.29, 43.93, 12.59. HRMS (ES^+) calculated for $C_{11}H_{18}N_4SNa$ $[M + Na]^+$ 261.1144, found 261.1146.

N^1,N^1-diethyl-N^4-(5-(pyridin-4-yl)-1,3,4-thiadiazol-2-yl)benzene-1,4-diamine, (56).

To a solution of compound **55** (0.15 mg, 0.63 mmol, 1.00 equiv) in dry dioxane (3.50 mL), isonicotinic acid (0.076 g, 0.63 mmol, 1.00 equiv) was added. The solution was heated at 90 °C and at this temperature $POCl_3$ was added dropwise. After 3 h stirring the reaction was cooling to r.t. Then, satd. aq. $NaHCO_3$ was added until pH = 7 and the mixture was extracted with EtOAc (x2). The combined organic extracts were washed with brine (x1), dried over Na_2SO_4, filtered and concentrated in vacuo. Purification by preparative TLC (70% EtOAc in hexanes) provided the desired compound as a brown solid. ^{1}H NMR (600 MHz, DMSO-d_6) δ = 10.32 (s, 1H), 8.66 (d, J = 5.9 Hz, 2H), 7.76 (d, J = 5.9 Hz, 2H), 7.37 (d, J = 8.0 Hz, 2H), 6.69 (d, J = 8.0 Hz, 2H), 3.31 (q, J = 5.9 Hz, 4H), 1.07 (t, J = 7.0 Hz, 6H). ^{13}C NMR (151 MHz, DMSO- d_6) δ = 167.36, 153.69, 150.66, 144.34, 137.57, 129.38, 121.07, 120.45,

112.42, 43.91, 12.51. HRMS (ES^+) calculated for $C_{17}H_{19}N_5SNa$ $[M + Na]^+$ 348.1253, found 348.1255. IR $\tilde{\nu}$ = 2917.8, 1736.6, 1520.6 cm^{-1}.

N^1,N^1-diethyl-N^4-(5-(pyridin-4-yl)-1,3,4-oxadiazol-2-yl)benzene-1,4-diamine, (57).

To a stirring solution of compound **55** (0.080 g, 0.34 mmol, 1.00 equiv) in dichloromethane (3.50 mL) isonicotinic acid (0.041 g, 0.34 mmol, 1.00 equiv), EDCI hydrochloride (0.190 g, 1.00 mmol, 3.00 equiv) and TEA (0.28 mL, 2.00 mmol, 6.00 equiv) were added in order. The solution was stirred for 12 h at r.t. The mixture was diluited with dichloromethane and the organic extract was washed with H_2O, dried over Na_2SO_4, filtered and concentrated in vacuo. Purification by preparative TLC (70% EtOAc in hexanes) provided the desired compound as a pale yellow solid. ^1H NMR (600 MHz, DMSO-d_6) δ = 10.39 (br s, 1H), 8.76 (d, *J* = 4.5 Hz, 2H), 7.78 (d, *J* = 4.5 Hz, 2H), 7.38 (d, *J* = 8.6 Hz, 2H), 6.70 (d, *J* = 8.6 Hz, 2H), 3.29 (q, *J* = 6.8 Hz, 4H), 1.06 (t, *J* = 6.9 Hz, 6H). ^{13}C NMR (151 MHz, DMSO-d_6) δ = 161.24, 155.91, 150.92, 143.81, 131.06, 127.17, 119.66, 119.19, 112.72, 43.99, 12.53. HRMS (ES^+) calculated for $C_{17}H_{20}N_5O$ $[M + H]^+$ 310.1662, found 310.1664. IR $\tilde{\nu}$ = 2971.8, 2932.2, 1741.4, 1628.6, 1514.8 cm^{-1}.

6.5.2. X-ray crystallography

The single crystal X-ray diffraction studies were carried out on a Bruker Kappa APEX-II CCD diffractometer equipped with Mo K_α radiation (λ = 0.71073). Crystals of the subject compound were grown by dissolving approximately 5mg of sample in 3 drops of dimethyl sulfoxide, which was then vapor diffused with dichloromethane over one week. A 0.480 x 0.150 x 0.160 mm piece of a green block was mounted on a Cryoloop with Paratone oil. Data were collected in a nitrogen gas stream at 100.0 K using ϕ and ϖ scans. Crystal-to-detector distance was 40 mm using variable exposure time (4s) with a scan width of 0.70°. Data collection was 100% complete to 53° in θ. A total of 10847 reflections were collected covering the indices,

$-9 \leq h \leq 11$, $-12 \leq k \leq 12$, $-13 \leq l \leq 13$. 3483 reflections were found to be symmetry independent, with a R_{int} of 0.0290. Indexing and unit cell refinement indicated a primitive, triclinic lattice. The space group was found to be P-1. The data were integrated using the Bruker SAINT software program and scaled using the SADABS software program. Solution by direct methods (SHELXL) produced a complete phasing model consistent with the proposed structure. A summary of the crystal data and structure refinement is presented in the tables below.

Table 1. Crystal data and structure refinement for compound 6.

Identification code	415
Empirical formula	$C_{18}H_{20}N_4S$
Formula weight	324.44
Temperature/K	100.0
Crystal system	Triclinic
Space group	P-1
a/Å	9.2551(13)
b/Å	10.2414(15)
c/Å	10.4509(14)
α/°	82.199(4)
β/°	66.091(4)
γ/°	64.841(4)
Volume/Å^3	818.9(2)
Z	2
ρ_{calc}g/cm^3	1.316
μ/mm^{-1}	0.203
F(000)	344.0
Crystal size/mm^3	0.48 × 0.16 × 0.15
Radiation	MoKα (λ = 0.71073)
2Θ range for data collection/°	4.268 to 53.474
Index ranges	$-9 \leq h \leq 11$, $-12 \leq k \leq 12$, $-13 \leq l \leq 13$
Reflections collected	10847
Independent reflections	3483 [R_{int} = 0.0290, R_{sigma} = 0.0301]
Data/restraints/parameters	3483/0/210
Goodness-of-fit on F^2	1.034
Final R indexes [I>=2σ (I)]	R_1 = 0.0361, wR_2 = 0.0872
Final R indexes [all data]	R_1 = 0.0439, wR_2 = 0.0924
Largest diff. peak/hole / e Å^{-3}	0.46/-0.28

Table 2. Fractional Atomic Coordinates (×10^4) and Equivalent Isotropic Displacement Parameters (Å^2×10^3) for compound 6. U_{eq} is defined as 1/3 of of the trace of the orthogonalised U_{IJ} tensor.

Atom	*X*	*y*	*z*	U(eq)
S1	6273.8(5)	4890.4(4)	6007.8(4)	16.20(11)
N1	13152.6(19)	988.7(16)	7766.9(16)	28.8(3)
N2	6900.8(16)	4172.5(12)	8270.7(12)	12.7(3)
N3	3948.0(16)	5466.9(14)	8694.9(13)	16.6(3)
N4	-1734.8(16)	8195.4(13)	7067.6(13)	15.4(3)
C1	11591(2)	1147.0(17)	8729.7(18)	23.7(4)
C2	10040(2)	2008.4(16)	8582.3(16)	17.6(3)
C3	10079.0(19)	2767.8(15)	7365.4(15)	14.9(3)
C4	11696(2)	2627.9(17)	6364.0(17)	20.4(3)
C5	13166(2)	1740.2(19)	6612.7(19)	28.0(4)
C6	8477.1(19)	3659.0(15)	7130.6(15)	13.5(3)
C7	8399(2)	3954.6(16)	5849.7(16)	16.6(3)
C8	5626.3(19)	4841.6(15)	7833.2(15)	13.1(3)
C9	2564.7(19)	6141.2(16)	8212.8(15)	14.5(3)
C10	2268(2)	7470.6(16)	7586.9(16)	16.8(3)
C11	852.4(19)	8159.4(16)	7211.8(15)	16.2(3)
C12	-347.3(18)	7547.3(15)	7471.4(14)	12.6(3)
C13	-25.8(19)	6206.3(15)	8113.7(15)	14.6(3)
C14	1412.2(19)	5515.4(15)	8455.6(15)	15.1(3)
C15	-1993(2)	9528.1(16)	6310.9(16)	18.7(3)
C16	-2848(2)	10894.7(17)	7228.1(19)	26.1(4)
C17	-3128.7(19)	7696.6(16)	7580.0(16)	15.6(3)
C18	-4264(2)	8028.3(17)	9130.5(16)	19.9(3)

Table 3. Anisotropic Displacement Parameters (Å^2×10^3) for compound 6. The Anisotropic displacement factor exponent takes the form: -2π^2[h^{2}a*^{2}U$_{11}$+2hka*b*U$_{12}$+…].

Atom	U_{11}	U_{22}	U_{33}	U_{23}	U_{13}	U_{12}
S1	14.0(2)	21.7(2)	12.44(18)	0.47(13)	-7.10(14)	-4.86(15)
N1	18.6(8)	29.1(8)	35.5(8)	3.4(6)	-15.3(7)	-2.9(6)
N2	11.6(6)	13.4(6)	13.7(6)	1.1(4)	-6.5(5)	-4.2(5)
N3	11.4(6)	24.1(7)	11.3(6)	1.1(5)	-5.4(5)	-3.8(5)
N4	13.4(6)	15.6(6)	20.0(6)	5.3(5)	-9.5(5)	-6.9(5)
C1	22.3(9)	22.2(8)	25.2(8)	3.4(6)	-13.5(7)	-4.4(7)
C2	15.7(8)	16.8(7)	18.5(7)	-1.0(6)	-7.2(6)	-4.0(6)
C3	14.3(7)	12.9(7)	18.0(7)	-3.3(5)	-7.6(6)	-3.5(6)
C4	16.5(8)	22.1(8)	19.2(8)	0.8(6)	-5.8(6)	-5.9(6)

C5	13.2(8)	31.8(9)	31.7(9)	-0.1(7)	-7.1(7)	-3.7(7)
C6	13.4(7)	12.2(6)	15.2(7)	-0.9(5)	-5.8(6)	-4.8(5)
C7	12.2(7)	20.1(7)	15.1(7)	-1.1(6)	-5.0(6)	-4.2(6)
C8	14.5(7)	13.3(7)	13.1(7)	0.6(5)	-6.2(6)	-6.2(6)
C9	11.1(7)	18.3(7)	11.4(7)	-1.4(5)	-5.1(6)	-2.5(6)
C10	13.3(7)	19.9(7)	19.0(7)	1.7(6)	-6.3(6)	-8.6(6)
C11	14.3(7)	15.0(7)	18.9(7)	4.7(6)	-6.6(6)	-6.6(6)
C12	10.9(7)	13.8(7)	12.1(6)	-0.2(5)	-4.4(6)	-3.9(5)
C13	13.6(7)	15.0(7)	16.7(7)	1.2(5)	-6.3(6)	-7.0(6)
C14	15.0(7)	13.4(7)	14.7(7)	2.4(5)	-5.9(6)	-4.3(6)
C15	17.0(8)	18.5(7)	21.9(8)	6.6(6)	-10.6(6)	-7.2(6)
C16	24.1(9)	19.9(8)	36.8(10)	1.9(7)	-14.8(8)	-8.6(7)
C17	12.8(7)	15.5(7)	21.3(7)	1.6(6)	-8.8(6)	-6.3(6)
C18	16.0(8)	19.7(8)	21.8(8)	0.6(6)	-5.3(6)	-7.3(6)

Table 4. Bond Lengths for compound 6.

Atom	Atom	Length/Å	Atom	Atom	Length/Å
S1	C7	1.7292(16)	C3	C4	1.394(2)
S1	C8	1.7532(14)	C3	C6	1.475(2)
N1	C1	1.339(2)	C4	C5	1.384(2)
N1	C5	1.338(2)	C6	C7	1.356(2)
N2	C6	1.3905(19)	C9	C10	1.394(2)
N2	C8	1.3171(18)	C9	C14	1.390(2)
N3	C8	1.3457(19)	C10	C11	1.387(2)
N3	C9	1.4305(18)	C11	C12	1.414(2)
N4	C12	1.3807(19)	C12	C13	1.4105(19)
N4	C15	1.4588(18)	C13	C14	1.384(2)
N4	C17	1.4622(19)	C15	C16	1.520(2)
C1	C2	1.389(2)	C17	C18	1.520(2)
C2	C3	1.393(2)			

Table 5. Bond Angles for compound 6.

Atom	Atom	Atom	Angle/°	Atom	Atom	Atom	Angle/°
C7	S1	C8	88.67(7)	C6	C7	S1	110.57(11)
C5	N1	C1	116.11(14)	N2	C8	S1	114.83(11)
C8	N2	C6	110.01(12)	N2	C8	N3	123.84(13)
C8	N3	C9	123.52(12)	N3	C8	S1	121.33(11)
C12	N4	C15	120.99(12)	C10	C9	N3	121.45(14)

C12	N4	C17	120.55(12)	C14	C9	N3	119.69(13)
C15	N4	C17	117.75(12)	C14	C9	C10	118.71(13)
N1	C1	C2	124.13(15)	C11	C10	C9	120.85(14)
C1	C2	C3	119.00(15)	C10	C11	C12	121.14(13)
C2	C3	C4	117.39(14)	N4	C12	C11	121.95(13)
C2	C3	C6	121.36(14)	N4	C12	C13	121.04(13)
C4	C3	C6	121.24(14)	C13	C12	C11	116.96(13)
C5	C4	C3	119.07(15)	C14	C13	C12	121.33(14)
N1	C5	C4	124.28(16)	C13	C14	C9	120.99(13)
N2	C6	C3	119.58(12)	N4	C15	C16	114.74(13)
C7	C6	N2	115.91(13)	N4	C17	C18	114.70(12)
C7	C6	C3	124.38(14)				

Table 6. Hydrogen Atom Coordinates (Å×10^4) and Isotropic Displacement Parameters (Å^2×10^3) for compound 6.

Atom	*X*	*y*	*z*	U(eq)
H3	3687.4	5460.66	9603.74	20
H1	11541.46	637.75	9566.28	28
H2	8968.36	2079	9300.33	21
H4	11787.51	3134.77	5522.93	24
H5	14256.06	1659.08	5918.71	34
H7	9375.16	3685.05	4985.68	20
H10	3046.27	7910.61	7414.94	20
H11	685.49	9057.64	6772.95	19
H13	-812.14	5768.5	8315.68	18
H14	1614.27	4599.54	8862.42	18
H15A	-2714.56	9607.42	5793.12	22
H15B	-853.94	9464.7	5611.57	22
H16A	-2925.54	11730.95	6636.8	39
H16B	-2155.33	10825.11	7757.86	39
H16C	-4013.26	11009.04	7880.64	39
H17A	-2611.22	6639.08	7396.44	19
H17B	-3870.01	8147.76	7037.58	19
H18A	-4903.72	9075.78	9306.12	30
H18B	-3536.23	7647.78	9677.16	30
H18C	-5084.32	7575.09	9407.72	30

Refinement model description

Number of restraints - 0, number of constraints - unknown.
Details:
1. Fixed Uiso
At 1.2 times of:
All C(H) groups, All C(H,H) groups, All N(H) groups
At 1.5 times of:
All C(H,H,H) groups
2.a Secondary CH2 refined with riding coordinates:
C15(H15A,H15B), C17(H17A,H17B)
2.b Aromatic/amide H refined with riding coordinates:
N3(H3), C1(H1), C2(H2), C4(H4), C5(H5), C7(H7), C10(H10), C11(H11), C13(H13), C14(H14)
2.c Idealised Me refined as rotating group:
C16(H16A,H16B,H16C), C18(H18A,H18B,H18C)

This report has been created with Olex2, compiled on 2018.04.26 svn.r3504 for OlexSys.

6.5.3. Physicochemical properties determination

pKa -value determination by potentiometric titration

In this approach, an automated potentiometric titration technique using the Sirius T3 system is applied. Typically, 3 titration experiments are performed with a varying mixture of aqueous to organic media (typical mixtures contain approx. 45, 50 and 55% of organic solvent). As the amount of organic solvent affects the measured pK-values only so called apparent pKa-values (psKa) are obtained. The pure aqueous pKa can be deduced by extrapolation of the psKa values to 0% organic solvent using the so called Yasuda & Shedlovsky extrapolation. Standard deviation for this type of pKa-value determination is in the range of ± 0.1 log unit for all measured compounds.

pH-dependent lipophilicity profile determination by potentiometric titration

For compounds with ionisable groups the partition coefficient between an organic solvent and an aqueous phase depends strongly on the pH of the aqueous media. A full pH-dependent lipophilicity profile can be measured using also the Sirius T3 equipment. Prerequisite for this technique is the knowledge of the ionization behaviour (pKa -values) of the respective compound, e.g. measured ideally also

using the Sirius T3 equipment. In this approach the apparent partition coeffcient is determined by performing potentiometric titrations experiments similarly to the ones described above except that an organic solvent is used which is immiscible with the aqueous phase. The partition coeffcient between *n*-octanol and aqueous media is collected. The pH-dependent partition coeffcient can be deduced from the observed shifts of the apparent psKa-values in comparison to the pure aqueous pKa-values. Standard deviation for this type of log P – value determination is in the range of ± 0.1 log unit for all measured compounds.

Solubility determination by Chasing Equilibrium Solubility method

The kinetic and thermodynamic solubilities were measured by the potentiometric Chasing Equilibrium Solubility method.[5] The substance was dissolved and titrated until a precipitate of neutral species was formed. Under this condition, the compound is supersaturated with respect to the neutral species solubility. The solution was then back titrated until the substance started dissolving again. The state with dissolving substance is denoted as subsaturation. The change between the subsaturated and supersaturated state was repeated several times to determine the substance thermodynamic solubility by interpolation. The intrinsic solubility was calculated using the principles of mass and charge balance at the pH where the equilibrium of the system was reached.

6.5.4. Biological assay

Compound Treatment and FGF2 Binding

Wild-type CHO cells (ATCC CCL-61) were grown in F12 growth medium supplemented with 10% (v/v) fetal bovine serum (FBS), 100 μg mL−1 of streptomycin sulfate, and 100 units per mL of penicillin G. Cells were plated at 30,000 cells/well in 6-well plates and let adhere overnight. The media was replaced with specific concentrations of each compound (0, 5, 10, or 15 μM) diluted in complete F12 media and incubated for 3 days at 37°C. Next, the media was removed,

cells were lifted with Cell Dissociation Buffer (Gibco) and washed twice with cold PBS buffer (+ 0.1% BSA). Biotinylated FGF2 (1.25 nM, Peprotech) was added and incubated for 30 min on ice. Cells were washed, and bound biotinylated protein was detected by using streptavidin-PE-Cy5 (1:1000, BD Biosciences) and flow cytometry (FacsCalibur, BD Biosciences). Raw data was interpreted using FlowJo Analytical Software (Tree Star Inc.). Protein binding was quantified by the geometric mean of the fluorescence intensity. These values were plotted and further analyzed using GraphPad Prism v5.0.

Stock solutions were made for each compound in DMSO (10 mM). For each experiment, the stock solutions were diluted first to 10 mM DMSO, then the appropriate serial dilutions were made in complete F12 media. Stock solutions were made and stored in glass containers at −20 °C.

$^{35}S0_4$ Radiolabeling Experiments

Wild-type CHO cells were plated at 30,000 cells/well in 6-well plates and let adhere overnight. The media was replaced with 10 µM of each compound diluted in F12 media (+10% FBS, 100 units/mL penicillin G) and radiolabeled for 3 days by supplementing the media also with 10 µCi/ml Na[^{35}S]O_4 (PerkinElmer Life Science). The media was collected to analyze secreted GAGs and cells were washed in PBS and incubated in 0.05% trypsin-EDTA to lift the cells and release cell surface proteoglycans. Cell pellets were lysed in 0.1N NaOH and used to measure protein concentration by BCA assay. Secreted GAG chains were extracted from the collected media and from cell surface GAGs through exhaustive digestion with Pronase (Sigma-Aldrich) in phosphate-buffered saline at 37 °C for 16 h followed by anion-exchange chromatography (DEAE-Sephacel, GE Healthcare). All preparations were desalted by gel filtration (PD-10, GE Healthcare). Total GAG amount was quantified from the media and cell surface fractions by taking an aliquot and measuring radioactivity by scintillation counting.

Heparan sulfate (HS) and chondroitin sulfate (CS) in the secreted media and on the cell surface were quantified by digestion with 2 milliunits of heparin lyases I, II, and III for 16 h at 37 °C in 240 µl of buffer containing 40 mM ammonium acetate and 3.3 mM calcium acetate, pH 7.0, or for 16 h at 37 °C with 20 milliunits of chondroitinase ABC (AMSBio) in 100 µl of buffer containing 50 mM Tris and 50 mM sodium chloride, pH 8.0. Following digestion, GAGs were purified by an additional anion-exchange chromatography (DEAE-Sephacel) and desalting (PD-10) step prior to quantification of radioactivity by scintillation counting. Results are expressed as [^{35}S]O_4 counts per microgram of protein quantified by Pierce BCA protein assay (Thermo Fisher).

6.5.5. Appendix

^{1}H NMR (DMSO-d_6) of compound **6**

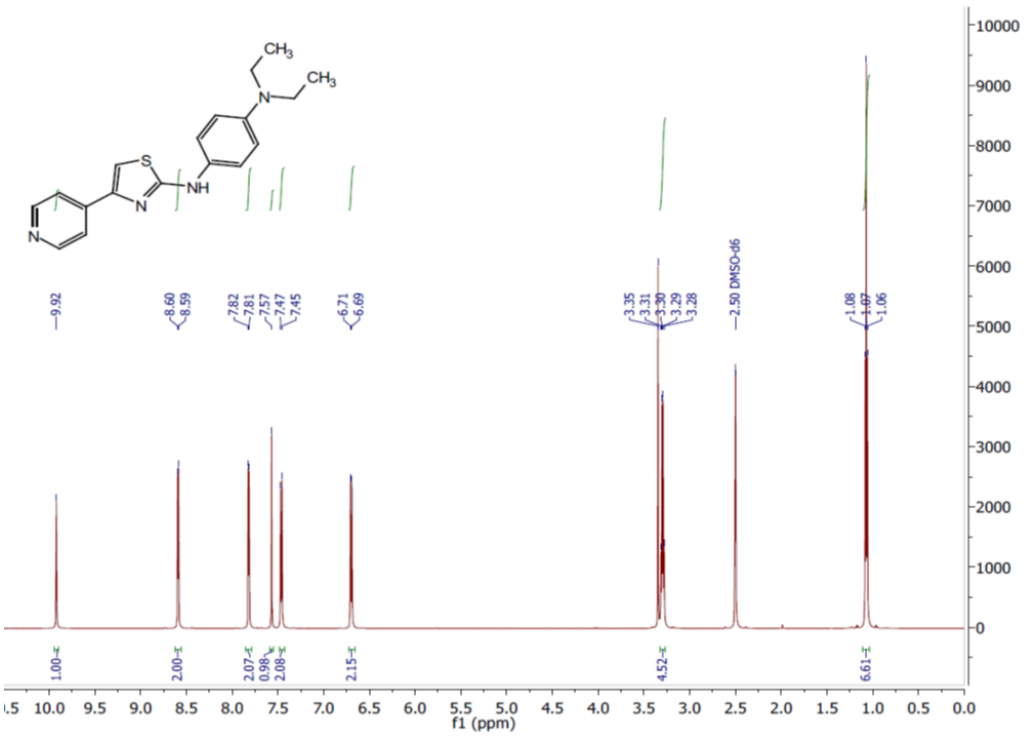

Report for multiset pKa determination of compound **6**

Yasuda-Shedlovsky Result

Multiset name:
Instrument ID: **T317135**
Analyst: **CB**
Quality: **Good**
Filename: **C:\Users\labuser\Box Sync\Carlo-previous backup\Multiset_pKa_BL-0533_(KO-II-217).t3r**

Yasuda-Shedlovsky result

Extrapolation type	pKa 0%	SD	Intercept	Slope	R^2	Ionic strength	Temperature
Yasuda-Shedlovsky	5.16	±0.06	9.44	-198.8300	0.9813	0.169 M	25.0°C
Yasuda-Shedlovsky	6.97	±0.09	11.25	-198.8890	0.9579	0.169 M	25.0°C

Warnings and errors

Errors None
Warnings None

Graphs

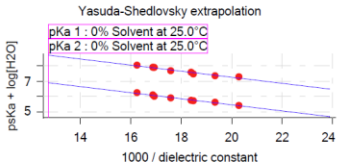

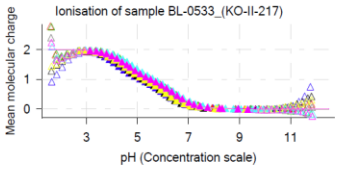

pH-metric Result

RMSD 0.083

Warnings and errors

Errors None
Warnings None

Graphs

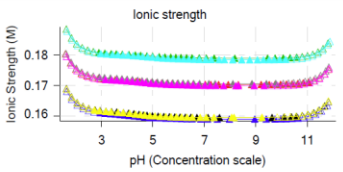

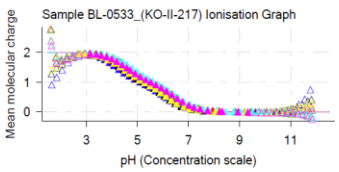

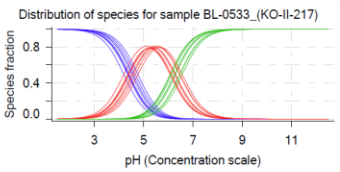

Multiset assays

Assay 1 of 3

Sample name	pKa-BL-0533_assay_3
Assay name	pH-metric psKa
Assay ID	18A-05006
Instrument ID	T317135
Imported from	C:\Users\SIRIUS\Desktop\Carlo\18A-05006_BL-0533_(KO-II-217)_pKa-BL-0533_assay_3.t3r
Imported on	1/5/2018 5:12:09 PM
Analyst name	CB
Experiment start time	1/5/2018 4:08:44 PM

Assay 2 of 3

Sample name	pKa-BL-0533_assay_2
Assay name	pH-metric psKa
Assay ID	18A-05005

Report for multiset pH-metric logP determination of compound **6**

pH-metric Result

Sample name: **BL-0533** Experiment start time: **5/8/2018 2:01:47 PM**
Assay name: **pH-metric high logP** Analyst:
Assay ID: **18E-08002** Instrument ID: **T317135**
Filename: **C:\SiriusData\2018\March\18E-08002_BL-0533_pH-metric high logP.t3r**

pH-metric Result

logP (neutral X) 4.54 ±0.01 (n=49)
RMSD 1.579

Warnings and errors

Errors None
Warnings None

Sample logD values

pH	BL-0533 logD	Comment
1.000	-5.59	
1.200	-5.19	Stomach pH
2.000	-3.59	
3.000	-1.60	
4.000	0.38	
5.000	2.18	
6.000	3.47	
6.500	3.93	
7.000	4.25	
7.400	4.40	Blood pH
8.000	4.50	
9.000	4.53	
10.000	4.54	
11.000	4.54	
12.000	4.54	

Graphs

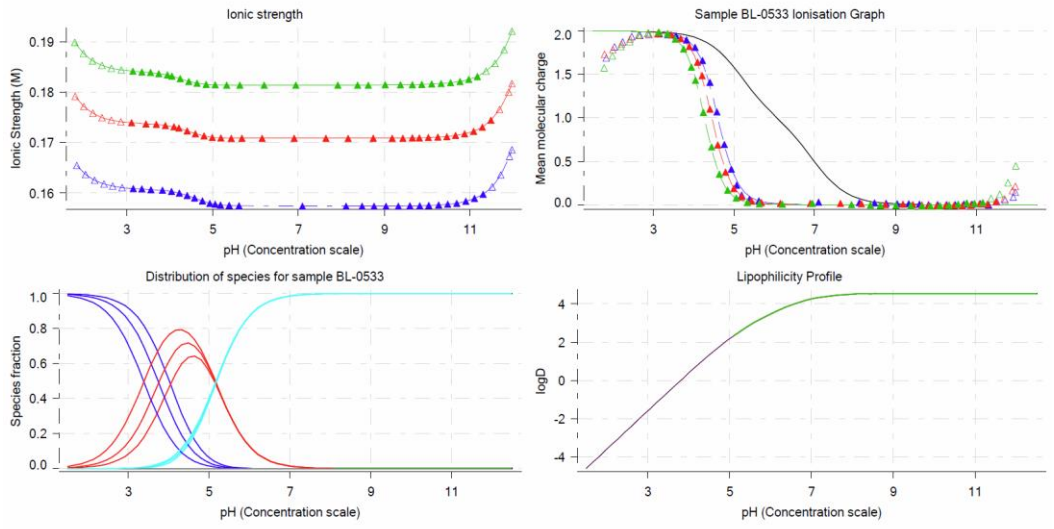

Report for solubility determination of compound **6**

Solubility

Sample name: **BL-0533-(KO-II-217)**
Assay name: **CheqSol**
Assay ID: **18F-01005**
Filename: **C:\SiriusData\2018\March\18F-01005_BL-0533-(KO-II-217)_Solubility.t3r**

Experiment start time: **6/1/2018 12:29:32 PM**
Analyst:
Instrument ID: **T317135**

Overall Result

Refinement method	**Curve fitting**
Molarity	**10.09 µM**
logS	**-4.996**
log(1/S)	**4.996**
Weight/mL	
Ionic Strength	**0.158 M**
Temperature	**24.6°C**
Kinetic solubility	**28.45 µM**
Natural solubility	**11.33 µM**
Natural pH	**7.881**

Warnings and errors

Errors None
Warnings None

Solubility Versus pH Table (calculated)

pH	Molarity	logS	log(1/S)	Weight/mL	Comment
1.000					
1.200					Stomach pH
2.000					
3.000					
4.000	145.6 mM	-0.837	0.837		
5.000	2.313 mM	-2.636	2.636		
6.000	117.9 µM	-3.929	3.929		
6.500	41.24 µM	-4.385	4.385		
7.000	19.65 µM	-4.707	4.707		
7.400	13.86 µM	-4.858	4.858		Blood pH
8.000	11.03 µM	-4.957	4.957		
9.000	10.19 µM	-4.992	4.992		
10.000	10.1 µM	-4.996	4.996		
11.000	10.09 µM	-4.996	4.996		
12.000	10.09 µM	-4.996	4.996		

Individual Results

	Molarity	logS	log(1/S)	Weight/mL	Ionic strength	Temperature	Time	Change
☑	917.7 nM	-6.037	6.037		0.159 M	23.4°C	49:32.1	-ve
☑	933.1 nM	-6.03	6.03		0.158 M	23.5°C	57:31.8	-ve
☑	951.4 nM	-6.022	6.022		0.158 M	23.5°C	53:31.9	-ve
☑	981.6 nM	-6.008	6.008		0.159 M	24.8°C	41:12.8	-ve
☑	994 nM	-6.003	6.003		0.159 M	23.7°C	45:12.4	-ve
☑	1.09 µM	-5.962	5.962		0.158 M	23.5°C	51:37.0	+ve
☑	1.101 µM	-5.958	5.958		0.158 M	23.5°C	59:42.7	+ve
☑	1.12 µM	-5.951	5.951		0.158 M	23.5°C	55:36.8	+ve
☑	1.162 µM	-5.935	5.935		0.159 M	23.6°C	47:17.1	+ve
☑	1.166 µM	-5.933	5.933		0.159 M	24.0°C	43:17.5	+ve
☑	1.175 µM	-5.93	5.93		0.159 M	25.0°C	37:13.3	-ve
☑	1.305 µM	-5.885	5.885		0.159 M	25.0°C	39:17.9	+ve
☑	1.358 µM	-5.867	5.867		0.159 M	25.0°C	35:18.7	+ve
☑	1.376 µM	-5.862	5.862		0.159 M	25.0°C	33:14.1	-ve
☑	1.522 µM	-5.818	5.818		0.159 M	25.0°C	31:19.3	+ve
☑	1.865 µM	-5.729	5.729		0.159 M	25.0°C	29:14.8	-ve
☑	1.904 µM	-5.72	5.72		0.159 M	25.0°C	27:20.1	+ve
☑	2.732 µM	-5.563	5.563		0.159 M	25.0°C	25:15.6	-ve
☑	3.237 µM	-5.49	5.49		0.159 M	25.0°C	23:17.9	+ve
☑	3.351 µM	-5.475	5.475		0.159 M	25.0°C	22:34.7	-ve

Solubility

Sample name: **BL-0533-(KO-II-217)**
Assay name: **CheqSol**
Assay ID: **18F-01005**
Filename: **C:\SiriusData\2018\March\18F-01005_BL-0533-(KO-II-217)_Solubility.t3r**

Experiment start time: **6/1/2018 12:29:32 PM**
Analyst:
Instrument ID: **T317135**

Individual Results (continued)

	Molarity	logS	log(1/S)	Weight/mL	Ionic strength	Temperature	Time	Change
☑	4.177 µM	-5.379	5.379		0.159 M	25.0°C	21:50.6	+ve
☑	16.98 µM	-4.77	4.77		0.158 M	25.0°C	19:26.6	-ve
☑	24.41 µM	-4.612	4.612		0.158 M	25.0°C	18:42.5	+ve

Sample graphs

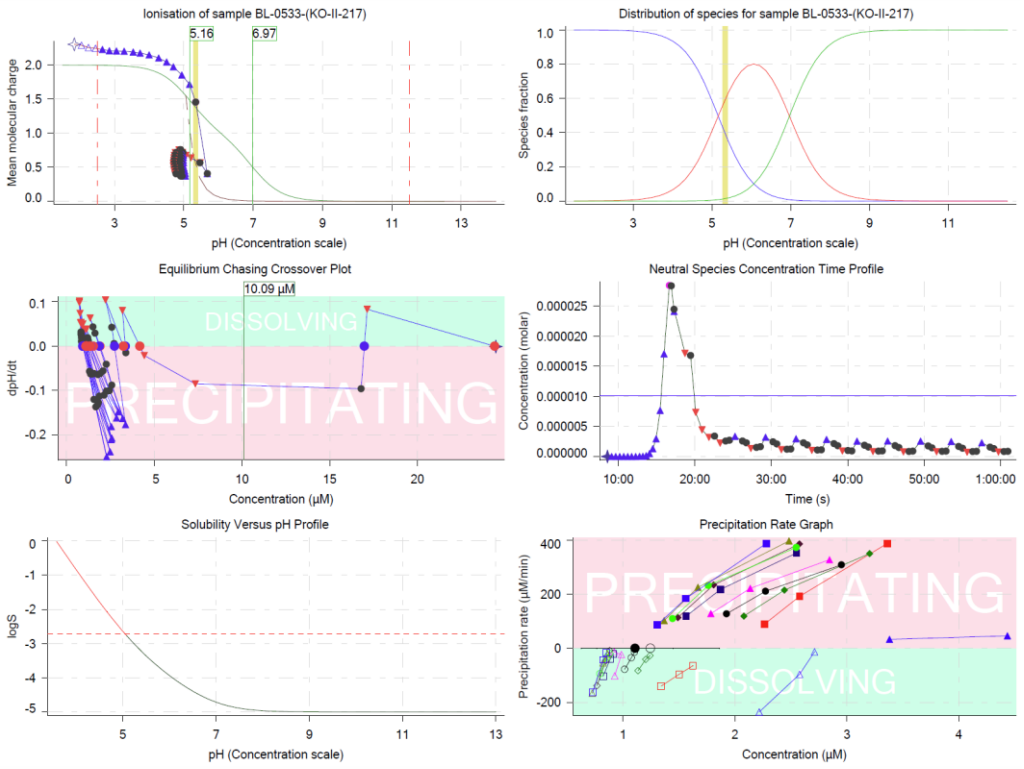

Solubility

Sample name:	**BL-0533-(KO-II-217)**	Experiment start time:	**6/1/2018 12:29:32 PM**
Assay name:	**CheqSol**	Analyst:	
Assay ID:	**18F-01005**	Instrument ID:	**T317135**
Filename:	**C:\SiriusData\2018\March\18F-01005_BL-0533-(KO-II-217)_Solubility.t3r**		

Other graphs

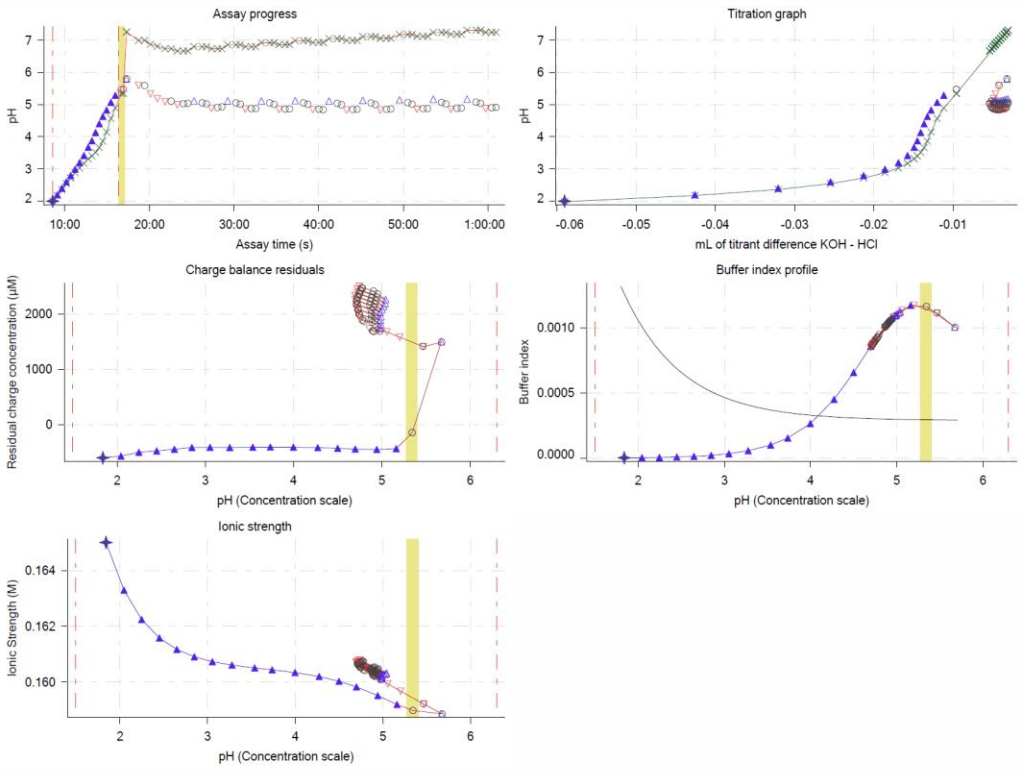

pH-metric

Sample name: **BL-0533-(KO-II-217)**
Assay name: **CheqSol**
Assay ID: **18F-01005**
Filename: **C:\SiriusData\2018\March\18F-01005_BL-0533-(KO-II-217)_Solubility.t3r**

Experiment start time: **6/1/2018 12:29:32 PM**
Analyst:
Instrument ID: **T317135**

Overall results

RMSD	0.439
Average ionic strength	0.161 M
Average temperature	25.0°C
Analyte concentration range	1898.9 µM to 1976.9 µM
Total points considered	16 of 83

Warnings and errors

Errors None
Warnings Turbidity threshold has been exceeded

Four-Plus parameters

Alpha	0.162	6/1/2018 12:29:32 PM	C:\SiriusData\2018\March\18F-01002_Blank standardisation.t3r
S	0.9927	6/1/2018 12:29:32 PM	C:\SiriusData\2018\March\18F-01002_Blank standardisation.t3r
jH	0.6	6/1/2018 12:29:32 PM	C:\SiriusData\2018\March\18F-01002_Blank standardisation.t3r
jOH	-0.5	6/1/2018 12:29:32 PM	C:\SiriusData\2018\March\18F-01002_Blank standardisation.t3r

Titrants

0.50 M HCl	1.004100	6/1/2018 12:29:32 PM	C:\SiriusData\2018\March\18F-01002_Blank standardisation.t3r
0.50 M KOH	1.016270	6/1/2018 12:29:32 PM	C:\SiriusData\2018\May\KOH standardisation 25May2018.t3r

Sample

BL-0533-(KO-II-217) concentration factor	1.000
Base pKa 1	5.16
Base pKa 2	6.97

Sample graphs

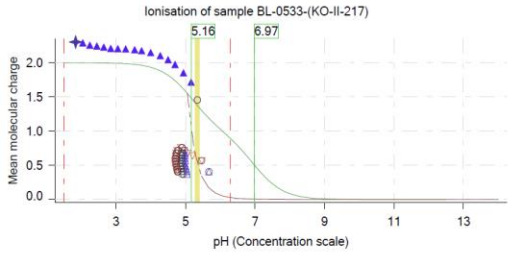

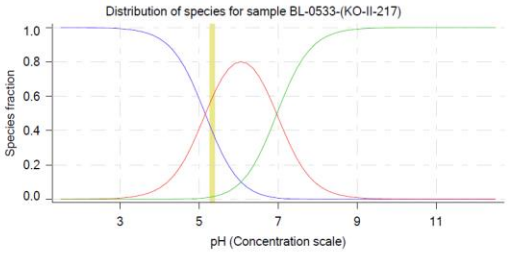

Carbonate and acidity

Carbonate	0.000 mM
Acidity error	0.000 mM

6.6. References

1. Sun, N.; Li, B.; Shao, J.; Mo, W.; Hu, B.; Shen, Z.; Hu, X. A general and facile one-pot process of isothiocyanates from amines under aqueous conditions. *Beilstein J. Org. Chem.* **2012**, *8*, 61–70.
2. McGowan, M.A.; Henderson, J.L.; Buchwald, S.L. Palladium-catalyzed *N*-arylation of 2-aminothiazoles. *Org. Lett*. **2014**, *14*, 1432-1435.
3. Andersen, J.; Madsen, U.; Björkling, F.; Liang, X. Rapid synthesis of aryl azides from aryl halides under mild conditions. *Synlett*. **2005**, *14*, 2209-2213.
4. a. Piatnitski Chekler, E.L.; Elokdah, H.M.; Butera, J. Efficient one-pot synthesis of substituted 2-amino-1,3,4-oxadiazoles. *Tetrahedron Lett.***2008**, *49*, 6709,6711.
   b. Verma, S.; Srivastava, A.K.; Pandey, O.P. A facile, rapid, one-pot synthesis and biological evaluation of some thiadiazole derivatives. *Research Journal of Chemical Sciences*. **2016,** *6*, 22-31.
5. Stuart, M.; Box, K. Chasing equilibrium: measuring the intrinsic solubility of weak acids and bases. *Anal. Chem.* **2005,** *77*, 983-990.

Chapter 7

Conclusions and outlook

7.1. Conclusions and outlook

During my PhD program, I have exploited various methods of organic synthesis (*i.e.* click chemistry, multicomponent reactions and traditional chemistry) for the discovery of small molecules of therapeutic relevance. In particular, several ambitious medicinal chemistry programs for targeting unconventional and not yet drugged targets and diseases have been undertaken and presented in this thesis.

Primarily, in Chapter 3, a novel class of compounds able to finely tune the SOCE mechanism that include both positive and negative modulators have been developed using a click chemistry approach. In addition, a SAR study focused on a selected inhibitor led to the identification of two promising molecules, **23** and **31** (Figure 1), that (a) do not display cytotoxicity up to 100 µM, (b) are able to reduce SOCE in the low micromolar range, (c) do not display activity on voltage-operated calcium channels (VOCC), TRPV1 and TRPM8 channels, (d) are more hydrolytically and metabolically stable in respect to the parent compound **1S**.

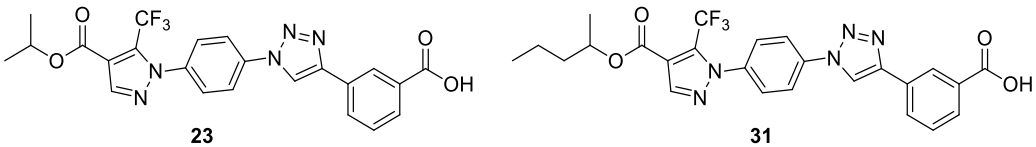

Figure 1. Chemical structures of Pyrtriazoles **23** and **31**.

Promisingly, compounds **23** and **31** were shown to be effective in restoring calcium entry to control levels *ex vivo* in myotubes of muscle biopsies from patients affected by TAM, while compound **31** proved to be effective in an animal model of acute pancreatitis. Administration of **31** showed a reduction of edema and inflammation in pancreatic tissues. Moreover, a transgenic mouse model displaying one of the mutations behind TAM disease is being characterized and a Pyrtriazole compound will be selected for *in vivo* studies. Overall, these results pave the way for the treatment of human disorders characterized by aberrant SOCE activity. Ongoing

studies in our laboratory are aimed at proving the reliability of this kind of approach, demonstrating that the isosteric replacement of the arylamide substructure with the a 1,4-disubstituted 1,2,3-triazole ring can be applied to other classes of SOCE inhibitors reported in the literature and, at the same time, can lead to the identification of compounds that do not display the ester moiety.

Regarding the development of IDO1 inhibitors for cancer immunotherapy, described in Chapter 4, starting from a common isocyanide intermediate, we exploited the Passerini and the Ugi multicomponent reactions to develop a small library of inhibitors that target IDO1. Unfortunately, despite the most active compounds (**6n** and **7g**, Figure 2) display activities at the sub-micromolar level and a full biocompatibility, a significant discrepancy between the enzymatic and the cellular inhibition was observed, suggesting that the low cell permeability might be related to imidazothiazole scaffold owned by this class of compounds.

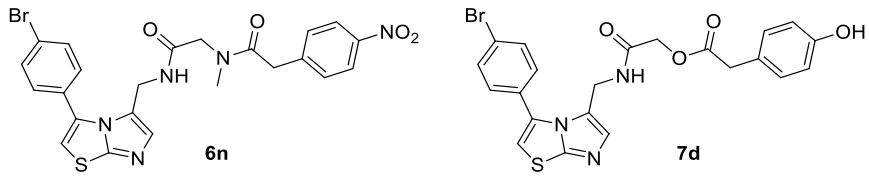

Figure 2. Chemical structures of imidazothiazole compounds **6n** and **7d**.

Nevertheless, molecular docking studies suggest that the presence of an additional pocket, that we named C, in the active site of the enzyme might be exploited in the design of IDO1 inhibitors. This discovery provides a new direction for future developments. Indeed, this information was integrated in a structure-based virtual screening that has allowed us to identify a promising *hit* **1**, bearing a benzimidazole scaffold, with an IC_{50} value against IDO1 in a cell-based assay of 16 nM (Figure 3).

From the SAR study performed by synthesizing a small library of 24 analogues, compound **60** emerged with an inhibitory activity against IDO1 in a cell-based assay comparable to the *hit* (Figure 3).

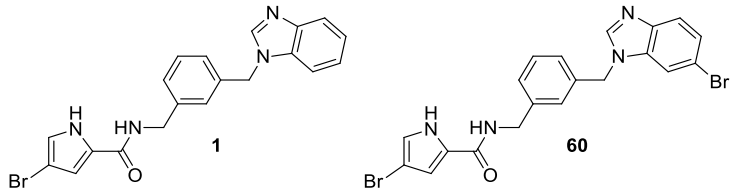

Figure 3. Chemical structure of the *hit* **1** and structural analogue **60.**

Promisingly, a computational analysis showed that that pocket C is also present in the active site of IDO2 and TDO and that this class of molecules might be accommodated in all these three dioxygenases active site. This is of high significance, as the development of dual/pan IDO1/IDO2/TDO inhibitors might deepen efficacy, limit acquired resistance to IDO1 blockade and reduce autoimmune side effects of immunotherapy. Therefore, studies addressed to evaluate the selectivity of the selected compounds, depicted in Figure 3, over IDO2 and TDO are ongoing in our laboratory. Yet, their metabolic profile will be investigated, with the aim of selecting the most promising compound and evaluating it in *in vivo* proof-of-concept studies.

Lastly, a project aimed at identifying compounds that enhance HS formation as a therapeutic strategy to prevent initiation or retard the growth of exostoses in HME disease has been performed. In particular, a screening of a compound library of ~57,000 molecules in a phenotypic assay that monitors HS levels on the plasma membrane of CHO cells identified a promising *hit* from the *N*-aryl-2-aminothiazoles class. Preliminary SAR and SPR studies have been conducted to (a) confirm/validate the biological activity; (b) identify new biologically active analogues; and (c) determine key physicochemical properties of representative compounds of interest. The SAR study, which was based on the synthesis and evaluation of a focused library of 23 derivatives, identified two analogues, **33** and **35** (Figure 4), with comparable activity as the primary *hit*. Characterization of selected physicochemical properties, such as pKa, $logD_{7.4}$, and water solubility of the most promising compounds suggests

that compounds of this type may be considered promising starting points towards the development of probes suitable for *in vivo* testing. Ongoing studies are directed towards the expansion of the SAR studies and the identification of a preferred candidate compound for *in vivo* proof-of-concept studies. In addition, future studies will be focused on the identification of the biological target(s) of **415** and related compounds.

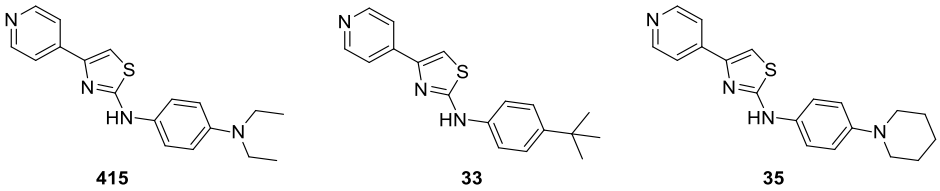

Figure 4. Chemical structure of the *hit compound* **415** and structural analogues **33** and **35.**

Chapter 8

Publications

Research publications from thesis

- Riva, B. [#]; **Griglio, A.** [#]; Serafini, M.; Sanchez, C.; Aprile, S.; Di Paola, R.; Gugliandolo, E.; Alansary, D.; Biocotino, I.; Lim, D.; Grosa, G.; Galli, U.; Niemeyer, B.; Sorba, G.; Canonico, P.L.; Cuzzocrea, S.; Genazzani, A.; Pirali, T. Pyrtriazoles, a novel class of Store-Operated Calcium Entry modulators: discovery, biological profiling and in vivo proof-of-concept efficacy in acute pancreatitis. *J. Med. Chem.* **2018**, *61*, 9756-9783. DOI: 10.1021/acs.jmedchem.8b01512.

- **Griglio, A**.; Torre, E.; Serafini, M.; Bianchi, A.; Schmid, R.; Coda Zabetta, G.; Massarotti, A.; Sorba, G.; Pirali, T.; Fallarini, S. A multicomponent approach in the discovery of indoleamine 2,3-dioxygenase 1 inhibitors: synthesis, biological investigation and docking studies. *Bioorg. Med. Chem. Lett.* **2018**, *28*, 651-657. DOI: 10.1016/j.bmcl.2018.01.032

Research publications from allied project

- Serafini, M.; **Griglio, A**.; Aprile, S.; Seiti,F.; Travelli,C.; Pattarino,F.; Grosa, G.; Sorba, G.; Genazzani, A.A.; Gonzales-Rodriguez, S; Butron, L.; Devesa, I.; Fernández-Carvajal, A.; Pirali, T.; Ferrer-Montiel, A. Targeting TRPV1 softly: the discovery of Passerini adducts as a topical treatment for inflammatory skin disorders *J. Med. Chem*. **2018**, *61*, 4436-4455. DOI: 10.1021/acs.jmedchem.8b00109

- Serafini, M.; **Griglio, A**.; Oberto, E.; Pirali, T.; Tron, G.C. The use of 2-hydroxymethyl benzoic acid as an effective water surrogate in the Passerini reaction: A straightforward access to α-hydroxyamides. *Tetrahedron Lett.* **2017**, *58*, 4786-4789. DOI: 10.1016/j.tetlet.2017.11.021

- Serafini, M.; **Griglio, A**.; Viarengo, S.; Aprile, S.; Pirali, T. An aryne-based three-component access to α-aroylamino amides. *Org. Biomol. Chem.* **2017**, *15*, 6604-6612. DOI: 10.1039/C7OB01715D

- Pirali, T.; Ciraolo, E.; Aprile, S.; Massarotti, A.; Berndt, A.; **Griglio, A**.; Serafini, M.; Mercalli, V.; Landoni, C.; Campa, C.; Margaria, J.C.; Silva, R.L.; Grosa, G.; Sorba, G.; Williams, R.; Hirsch E.; Tron, G.C. Identification of a potent phosphoinositide 3-kinase (PI3K) pan inhibitor displaying a strategic carboxylic acid group and development of its prodrugs. *ChemMedChem.* **2017**, *12*, 1542-1554. DOI: 10.1002/cmdc.201700340

Book Chapters

- Pirali, T.; Galli, U.; Serafini, M.; **Griglio A**.; Tron, G.C. Drug discovery for soft drugs on TRPV1 and TRPM8 channels using the Passerini reaction. submitted (on invitation) to Methods in Molecular Biology (Springer Nature).

Curriculum vitae

Alessia Griglio

Personal information

Date/Place of birth:19/03/1990, Pinerolo (TO)
Nationality: Italian
Phone +39 3407324952
e-mail: alessia.griglio@uniupo.it

Education and training

November 2015 – October 2018
PhD student in "Chemistry & Biology"
Università del Piemonte Orientale, Novara. Supervisor: Prof. Tracey Pirali.

January 2018 - July 2018
Visiting PhD student
Skaggs School of Pharmacy and Pharmaceutical Science, University of California San Diego (UCSD). Supervisor: Prof. Carlo Ballatore.

June 2015
Qualification to practice as Pharmacist
Università del Piemonte Orientale, Novara.

October 2009 – March 2015
Master's Degree in Pharmacy
Thesis: Synthesis of soft TRPV1 modulators via Passerini reaction
Università del Piemonte Orientale, Novara. Supervisor: Prof. Tracey Pirali.

September 2009 – June 2014

High School Student: Liceo Scientifico "Maria Curie", Pinerolo, Italy.

Teaching experience

March 2017 – April 2018

Co-supervisor of three Master's degree experimental thesis: "Synta 66 analogues as negative modulators of Store-Operated Calcium Entry", candidate Lisa Rovetti; "A preliminary structure-activity relationship study for the negative modulation of Store-Operated Calcium Entry in gain-of-function mutations", candidate Veronica Barillaro; IDO1 inhibitors with imidazothiazole scaffold: design, synthesis and SAR study, candidate Roberta Schmid.

Università del Piemonte Orientale (Dipartimento di Scienze del Famaco), Novara.

April 2017

Assistant educator for Biotechnology master's student in Medicinal Chemistry

Università del Piemonte Orientale (Dipartimento di Scienze del Famaco), Novara.

March 2016 and March 2017

Tutoring Biotechnology master's students during General and Inorganic chemistry laboratory

Università del Piemonte Orientale (Dipartimento di Scienze del Famaco), Novara.

November 2015 and November 2016

Tutoring Medicinal Chemistry and Pharmaceutical Technology (CTF) master's students during extractive and synthetic preparation of drugs (PESF) laboratory

Università del Piemonte Orientale (Dipartimento di Scienze del Famaco), Novara.

Publications

Riva, B. [#]; **Griglio, A.** [#]; Serafini, M.; Sanchez, C.; Aprile, S.; Di Paola, R.; Gugliandolo, E.; Alansary, D.; Biocotino, I.; Lim, D.; Grosa, G.; Galli, U.; Niemeyer, B.; Sorba, G.; Canonico, P.L.; Cuzzocrea, S.; Genazzani, A.; Pirali, T. Pyrtriazoles, a novel class of Store-Operated Calcium Entry modulators: discovery, biological profiling and in vivo proof-of-concept efficacy in acute pancreatitis. *J. Med. Chem.* **2018**, *61*, 9756-9783. DOI: 10.1021/acs.jmedchem.8b01512, accepted for publication.

Serafini, M.; **Griglio, A**.; Aprile, S.; Seiti,F.; Travelli,C.; Pattarino,F.; Grosa, G.; Sorba, G.; Genazzani, A.A.; Gonzales-Rodriguez, S; Butron, L.; Devesa, I.; Fernández-Carvajal, A.; Pirali, T.; Ferrer-Montiel, A. Targeting TRPV1 softly: the discovery of Passerini adducts as a topical treatment for inflammatory skin disorders *J. Med. Chem*. **2018**, *61*, 4436-4455. DOI: 10.1021/acs.jmedchem.8b00109

Griglio, A.; Torre, E.; Serafini, M.; Bianchi, A.; Schmid, R.; Coda Zabetta, G.; Massarotti, A.; Sorba, G.; Pirali, T.; Fallarini, S. A multicomponent approach in the discovery of indoleamine 2,3-dioxygenase 1 inhibitors: synthesis, biological investigation and docking studies. *Bioorg. Med. Chem. Lett*. **2018**, *28*, 651-657. DOI: 10.1016/j.bmcl.2018.01.032

Serafini, M.; **Griglio, A.;** Oberto, E.; Pirali, T.; Tron, G.C. The use of 2-hydroxymethyl benzoic acid as an effective water surrogate in the Passerini reaction: A straightforward access to α-hydroxyamides. *Tetrahedron Lett*. **2017**, *58*, 4786-4789. DOI: 10.1016/j.tetlet.2017.11.021

Serafini, M.; **Griglio, A**.; Viarengo, S.; Aprile, S.; Pirali, T. An aryne-based three-component access to α-aroylamino amides. *Org. Biomol. Chem*. **2017**, *15*, 6604-6612. DOI: 10.1039/C7OB01715D

Pirali, T.; Ciraolo, E.; Aprile, S.; Massarotti, A.; Berndt, A.; **Griglio, A**.; Serafini, M.; Mercalli, V.; Landoni, C.; Campa, C.; Margaria, J.C.; Silva, R.L.; Grosa, G.; Sorba, G.; Williams, R.; Hirsch E.; Tron, G.C. Identification of a potent phosphoinositide 3-kinase (PI3K) pan inhibitor displaying a strategic carboxylic acid group and development of its prodrugs. *ChemMedChem.* **2017**, *12*, 1542-1554. DOI: 10.1002/cmdc.201700340

Conferences

26th National Meeting of the Italian Chemistry Society - Paestum (Italy) 10-14 September 2017

Poster Communication: "*Discovery of Store-Operated Calcium Entry modulators as an effective treatment for calcium-related rare genetic diseases*" Alessia Griglio, Marta Serafini, Beatrice Riva, Armando Genazzani and Tracey Pirali

42nd Edition of the "A.Corbella" International Summer School on Organic Synthesis (ISOS 2017) - Gargnano (Italy) 18-22 June 2017

Poster Communication: "*A mild one-pot synthesis of α-hydroxyamides via a Passerini modified reaction*" Alessia Griglio, Marta Serafini, Gian Cesare Tron and Tracey Pirali

XXIV NMMC - National Meeting in Medicinal Chemistry - Perugia (Italy) 11-14 September 2015

Poster Communication: "*Synthesis of IDO1 inhibitors via click chemistry and four-component Ugi reaction*" Alessia Griglio, Marta Serafini, Silvia Fallarini and Tracey Pirali.

Awards

Best student award at University of Oriental Piedmont, Department of Pharmaceutical Sciences academic year 2013/2014